EFFECT OF AGEING ON THE MICROSTRUCTURE AND MECHANICAL PROPERTIES OF Al-Si ALLOYS WITH COPPER ADDITIONS

Thesis

Submitted in partial fulfilment of the requirements for the degree of

DOCTOR OF PHILOSOPHY

by

SHIVAPRASAD CHANNAPPAGOUDAR

DEPARTMENT OF MECHANICAL ENGINEERING

NATIONAL INSTITUTE OF TECHNOLOGY KARNATAKA

SURATHKAL, MANGALORE-575025

December, 2016

D E C L A R A TIO N

I hereby *declare* that the Research Thesis entitled **"Effect of Ageing on the Microstructure and Mechanical Properties of Al-Si Alloys with Copper Additions"** which is being submitted to the **National Institute of Technology Karnataka, Surathkal** in partial fulfillment of the requirements for the award of the Degree of **Doctor of Philosophy** in Mechanical Engineering is a *bonafide report of the research Work carried out by me*. The material contained in this **Research Thesis** has not been submitted to any University or Institution for the award of any degree.

Register Number:**102009ME10P06**

Name of the Research Scholar: **SHIVAPRASAD CHANNAPPAGOUDAR**

Signature of the Research Scholar:

Department of Mechanical Engineering

Place: NITK-Surathkal

Date

C E R T I F I C A T E

This is to *certify* that the Research Thesis entitled **"Effect of Ageing on the Microstructure and Mechanical Properties of Al-Si Alloys with Copper Additions"** submitted by **SHIVAPRASAD CHANNAPPAGOUDAR** (Register Number: **102009ME10P06)** as the record of the research work carried out by him, is accepted as the *Research Thesis submission* in partial fulfillment of the requirements for the award of degree of **Doctor of Philosophy**.

Research Guide(s)

Dr. Narendranath S
Professor and Research Guide
Department of Mechanical Engineering

Dr. Vijay Desai
Professor and Research Guide
Department of Mechanical Engineering

Chairman–DRPC

Dedicated to my mother for her ongoing love and support
and to my father who could not see this thesis completed.

ACKNOWLEDGEMENTS

First of all, I would like to thank my guides **Dr. Vijay Desai,** Professor, Department of Mechanical Engineering and **Dr. Narendranath S**, Professor, Department of Mechanical Engineering, for accepting me willingly as their Ph.D. student. I am forever indebted to them for their guidance and unrelenting support from the initial to the final stages of this study. Their enthusiasm, encouragement, and faith in me throughout have been extremely helpful. They were always available for guidance, most of the times beyond office hours. This thesis would not have the spirit that it has without their patient reading and meticulous corrections.

I thank Dr. Gangadharan K.V, Head, Mechanical Department and also former Head Dr. Prasad Krishna for their kind support throughout my PhD course.

For me, it is a proud privilege and a matter of honour to offer my over whelming gratitude to Prof. Mukunda, Retd. Professor, IIT Kharagpur, (currently working at NMIT, Bangalore) for sharing his over fifty years of experience in metallurgy and helping me understand both fundamentals and intricacies of Al-Si-Cu alloy systems.

My sincere thanks to Dr. K Venkateswarlu, Principal Scientist, NAL, Bangalore, one of the nicest and most helpful people imaginable. I am indebted to him for is invaluable technical and psychological support. A very good critic of my all actions, he provided me the necessary inputs that helped me at all stages.

I would like to express the deepest appreciation to Dr. Kiran Aithal, HOD (Mech), NMIT and to the management of NMIT, for sharing their R&D facilities for most of my experimental work. I thank faculty members of NMIT for their help and suggestions at all stages.

I express my sincere thanks for helpful suggestions from my committee members Dr. Ramachandra and Dr. Ravishankar and to all the faculty members of

Department of Mechanical Engineering, of N.I.T.K Surathkal for their support all through this research work.

This would not materialize without the support of management of Hindustan Aeronautics Ltd. I would like to recognize the important roles of Sri. M.P Singh, Sri. Shrikantha Sharma, AGM, Sri. P. S Roy, Offg. Executive Director, Sri. A.K Tyagi, ED (HR) and Sri. V.M Chamola, Director (HR) of Hindustan Aeronautics Ltd. My special thanks to my colleagues of HAL Management Academy for their support and encouragement.

I would like to thank Dr. Veeresh Basalalli, Director, Sir MVIT and Smt. Indira, Principal, Sir MVIT for encouraging me to take up this research work. My special thanks to my friends Dr. M.S Ganesh Prasad, Dr. Manjaiah and Prof. Sangamesh for their suggestions and timely help.

I am eternally grateful to my wife Veena and son Rahul for their ongoing and unwavering support, patience and understanding. I would like to acknowledge with gratitude, the support and love of my brother Prakash in every sphere of my life and this work would not have been possible without him. Lastly, thanks to my parents and sister for the unconditional love and support they have given me over the years.

ABSTRACT

Aluminum has a density approximately one-third that of cast-iron or steel and have proved effective alternatives for many engineering applications. The good strength to weight ratio offered by Al-Si and Al-Si-Cu alloys has made these alloys popular as they present opportunities for weight reduction in automotive applications. The mechanical properties of aluminum can be enhanced by adding alloying elements such as silicon, copper, magnesium, zinc etc. Silicon as an alloying element has the ability of to reduce density and coefficient of thermal expansion, improve hardness, mechanical properties such as modulus and strength, thermal stability, wear resistance and corrosion resistance of aluminum. Further it also improves castability of aluminum also. This has created considerable interest among the materials and manufacturing engineers to explore the Al–Si family of alloys for possible applications in automotive, electrical and aerospace industries. Based on Si content Al-Si alloys are generally classified as hypoeutectic (up to 11%), eutectic (11 to 13 %) and hypereutectic (13 to 19 %) alloys. Grain refinement and modification of the alloy using suitable refiner and modifier improves the mechanical properties further. Addition of copper to Al-Si alloys induces precipitation of $CuAl_2$ particles and depending on cooling rate and modifier level, this phase appears as blocky $CuAl_2$ or fine eutectic colonies at the grain boundaries. Hence, an addition of Cu to Al-Si alloys improves the tensile strength. Solution heat treatment and ageing in Al-Si-Cu alloys, forms variants of $CuAl_2$ leading to still better hardness and mechanical properties.

The present work is carried out to investigate the influence of addition of copper (4.5 wt.%), combined modification and grain refinement, effect of T6 heat treatment process on hypoeutectic (7% Si), eutectic (12% Si) and hypereutectic Al-Si (15% Si) alloys. Al-1Ti-3B is used as grain refiner while Sr and P are used as modifiers. The effect of these processes on microstructure of Al-Si alloys, mechanical properties and tribological properties are investigated.

Al-1Ti-3B grain refiner showed a markedly positive effect on the refinement of α-Al phase. Addition of Al-10Sr modifier was responsible for the modification of Si.

The micro structural changes due to modification and grain refinement led to an improvement in UTS and % elongation of all the three types of alloys considered in this work. For Al-7Si the UTS increased from 154 MPa to 171 MPa (11%) while % elongation showed marked improvement increasing from 7.6 to 11.9 (56.6%). The corresponding improvement in UTS values for Al-12Si and Al-15Si were 18% and 22% and % improvement in elongation were 57 and 28, respectively. Addition of 4.5 wt.% Cu to Al-Si alloys was responsible for improved tensile strength and also resulted in improved sliding wear properties. This is attributed to the presence of $CuAl_2$ as particle or eutectic in the Al interdendritic region. A combined addition of Al-1Ti-3B and Al-10Sr to hypoeutectic and eutectic alloys resulted in conversion of large α-Al grains in to equiaxed grains, plate like eutectic Si in to fine particles and changed the coarse $CuAl_2$ morphology to fine eutectic colonies of Cu + $CuAl_2$. A combined addition of Al-1Ti-3B grain refiner and AlP and Al-10Sr modifier to Al-15Si-4.5Cu alloy provided a favorable microstructural change that led to superior mechanical and sliding wear properties.

The heat treatment schedule applied in this study consisted of solution heat treatment at a temperature of 500°C for 6h; quenching in water at room temperature; ageing at a temperature of 200°C for varying time periods. Experimental results showed that heat treatment influenced the mechanical properties to a good extent in both the as-cast as well as combined modified and refined alloy. The Al-7Si-4.5Cu alloy showed a peak hardness of 126 BHN in as-cast condition where as the modified alloy showed 138 BHN. The UTS of melt treated Al-7Si-4.5Cu alloy increased from 208 MPa to 262 MPa (26% improvement), Similar trends were also observed for the other two alloys. The refinement during solution treatment and subsequent precipitation of fine $CuAl_2$ particles may be the main reason for this improvement. The increase in strength due to Cu addition and age hardening of the alloy is balanced out by corresponding decrease in ductility. For 7Si alloy the ductility reduced by 22%

on adding Cu and further reduced by 22% on ageing for 20 h. However, the ductility is improved to a certain extent by grain refinement and modification.

During dry sliding wear test, melt treatment reduced the wear volume loss of as-cast Al-7Si alloy by 25% and with Cu addition and melt treatment, the loss reduced by 40%. The solution treatment and ageing for 20 h improved the wear resistance substantially, with wear volume loss reducing by 79% as compared to as-cast Al-7Si alloy. Similar results were also observed for 12Si and 15Si alloys.

Keywords: Al-Si-Cu alloy; Modification; Grain refinement; Ageing; Sliding wear

CONTENTS

LIST OF FIGURES

LIST OF TABLES

NOMENCLATURE

Al	: Aluminum
Si	: Silicon
Cu	: Copper
Sr	: Strontium
Ti	: Titanium
B	: Boron
AlP	: Aluminium Phosphide
Mg	: Magnesium
SEM	: Scanning electron microscopy
Wt.	: Weight
BHN	: Brinell Hardness Number
% EL	: Percentage of Elongation
YS	: Yield Strength
UTS	: Ultimate tensile strength
Al_2O_3	: Aluminum Oxide
DAS	: Dendritic Arm Spacing
GP Zones	: Guinier–Preston zones

Chapter 1

Introduction

1.1 General Background

Aluminium is considered one of the most important engineering materials and has been substituted for ferrous alloys in automobile, marine, and other engineering applications. Aluminium alloys have a density approximately one-third that of cast-iron or steel and have proved effective alternatives for many engineering applications. Silicon is one of the less expensive alloying additions used in aluminium, The ability of silicon to reduce the density and coefficient of thermal expansion and to improve the hardness, ambient temperature mechanical properties such as modulus and strength, thermal stability and wear resistance of aluminium had been catalytic in engendering considerable interest in the materials science community to explore the Al–Si family of alloys for possible applications in automotive, electrical and aerospace industries (Gupta and Ling 1999).

1.2 Aluminium-Silicon alloys

Aluminium-Silicon (Al-Si) alloys occupy an important position in the family of cast Al alloys owing to high specific strength and excellent corrosion resistance. In addition, the low coefficient of thermal expansion and good wear resistance of these alloys make them more suitable for automobile, aerospace, marine and electrical applications (Gruzleski and Closset 1990). Typical automotive components made of Al-Si alloys are cylinder blocks, heads, liners, pistons, axels and wheels. (Liao et al. 2002; Jigajinni et al. 2013; Zeren et al. 2011). In view of large applications in automotive sector, it is desired to study Al-Si alloys in detail.

The industrial applications of Al-Si alloys are governed by mechanical and tribological properties offered by Al-Si castings which in turn depend on the composition and microstructural features of the alloy. The predominant features include the size and shape of eutectic Si, the morphology of α-Al dendrite and intermetallics (Mohamed et al. 2009). A refined grain size represents better mechanical and tribological properties. Use of additional alloying elements and appropriate casting process parameters help in solidification of alloys to form equiaxed α-Al (in the case of hypoeutectic alloy), fine primary Si particles of size 25-30 μm (hypereutectic) and fibrous eutectic Si.

1.3 Addition of alloying elements

The properties of Al-Si alloys are also dependent on the amount of alloying elements such as Cu, Mg, Fe, Zn and others. Variations in the amount of these alloying elements have shown significant influence on the mechanical properties of base Al-Si alloy. Copper is a major alloying element used in Al-Si alloy system in order to impart better heat treatability to the castings on account of its large solid solubility in Al matrix (Wang et al. 2011). Al-Si-Cu alloys present sufficient opportunities for weight reduction in automotive applications, besides other high-technology applications. This is partly due to enhanced mechanical properties induced by Si and Cu. Copper additions up to 5% impart high strength and toughness especially after ageing treatment (Zeren and Karakulak 2009). An addition of copper to Al-Si alloys induces precipitation of $CuAl_2$ particles and depending on cooling rate and modifier level, this phase appears as blocky $CuAl_2$ or fine eutectic colonies of Al-$CuAl_2$ at the grain boundaries. Hence, an addition of Cu to Al-Si alloys improves the tensile strength.

1.4 Grain refinement and modification

Grain refinement can be obtained by rapid cooling, mould vibration, agitation of the melt during solidification and also by the addition of grain refiners to liquid metal. Generally, for Al alloys, Al-Ti and Al-Ti-B master alloys are used for grain

refinement (Kashyap and Chandrashekar 2001; McCartney 1989; Flemings 1974; Hamid 1989). The Al-Si alloys are invariably subjected to modification to produce fine eutectic silicon in Al matrix. The modification also results in decreased dendritic arm spacing (DAS). Modification using sodium or strontium has resulted in fibrous eutectic phase showing improved mechanical properties (Spittle et al. 1997). The combined addition of grain refiner (Al-1Ti-3B) master alloy and strontium (Sr) modifier to Al-Si alloys results in more uniform distribution of α-Al grains and also fine eutectic Si throughout the Al matrix as compared to the microstructure obtained with individual additions of grain refiner and modifier (Kori et al. 2000).

1.5 Heat treatment of Al-Si-Cu alloys

The strength of Al-Si-Cu alloys can be considerably increased after heat treatment due to precipitation hardening, wherein precipitates are formed in the matrix. The heat treatment cycle comprising of solution treatment, quenching and ageing, generally results in a good combination of strength and ductility (Zeren 2005). During solution treatment, Al-Si-Cu alloy is heated above the solvus temperature of the secondary phases in the matrix, for relatively longer periods to get homogeneity of alloying elements and to modify the acicular eutectic Si to spherical particles (Prasad 1994). Subsequent to solution treatment, the Al-Si-Cu alloys are quenched in water at room temperature in order to preserve the $CuAl_2$ precipitates in the solid solution.

1.6 Microstructural features and Mechanical properties

Earlier studies on Al-Si-Cu have reported that alloys, with the same chemical composition can have different microstructures due to variations in the solidification, the use of modifier and grain refiner, and also due to heat treatment parameters. Effect of variation of Si content on mechanical and tribological properties of Al-Si alloys reported in past studies are not comparable and few of the findings appear to be contradictory. Some of the investigations have suggested that the optimum Si content is around the eutectic region (Sarkar 1975; Pramila Bai and Biswas 1987), while, Shivnath et al. (1977) have suggested that it is in the hypereutectic region. One of the

studies has also claimed that Si has little effect on wear resistance (Andrews et al. 1985). Contradictory findings in these studies can probably be attributed to their attempt to correlate material behavior with only composition without considering microstructure and morphology of the Al-Si-Cu alloy.

In the present work, an attempt has been made to understand the effect of the addition of Cu (4.5 wt. %) on Al-7Si, Al-12Si and Al-15Si alloys on microstructure by keeping all other experimental conditions and other alloying elements same with an objective of clearly understanding the effect of Cu addition on hypoeutectic, eutectic and hypereutectic Al-Si alloys. Further, the effect of combined addition of grain refiner and modifier and also the influence of T6 heat treatment on Al-7Si-4.5Cu, Al-12Si-4.5Cu and Al-15Si-4.5Cu under identical experimental conditions are also studied. It is appropriate to perform characterization of all Al-Si, Al-Si-Cu experimental alloys produced under various processing conditions in order to realize the influence of (i) Addition of 4.5 wt. % Cu (ii) Combined addition of modifier and grain refiner, and (iii) T6 heat treatment.

1.7 Organization of the thesis

The thesis is organized in seven chapters. Chapter 1 provides a brief introduction to Al-Si alloys and their processing. Elaborate review of the available literature is carried out and presented in Chapter 2. Following a thorough literature review, the methodology for conducting the current research work is defined and adopted.

The details of the experimental work conducted are presented in Chapter 3. The procedure adopted for the preparation and characterization of Al-7Si, Al-12Si, Al-15Si and Al-7Si-4.5Cu, Al-12Si-4.5Cu, Al-15Si-4.5Cu alloys in the as-cast condition and the addition of both refiner and modifier to alter the microstructures is discussed in detail. The experimental work on ageing and mechanical studies (hardness and tensile) and dry sliding wear properties are also presented.

Chapter 4 provides information on of Al-7Si, Al-7Si-4.5Cu, Al-12Si, Al-12Si-4.5Cu, Al-15Si and Al-15Si-4.5Cu alloys. The microstructural details of as-cast alloys, the changed microstructures after combined addition of modifier and grain refiner are presented and discussed. The influence of solutionizing on microstructure of Al-7Si-4.5Cu, Al-12Si-4.5Cu and Al-15Si-4.5Cu alloys are presented. Also, the effect of ageing treatment on the hardness of the alloys are studied and presented as ageing time vs. hardness (BHN). The microstructural changes observed at peak hardness points obtained from the ageing time vs. hardness are also reported.

Results and discussion on mechanical properties of Al-7Si, Al-7Si-4.5Cu, Al-12Si, Al-12Si-4.5Cu, Al-15Si and Al-15Si-4.5Cu alloys are given in chapter 5. The effect of combined addition of modifier and grain refiner on mechanical properties are studied and correlated with microstructures. The changes in mechanical properties after the addition of 4.5% Cu to Al-7Si, Al-12Si and Al-15Si alloys are studied correlated with changes in corresponding microstructures. Further, an effect of ageing treatment and its influence on the mechanical properties of as-cast Al-7Si-4.5Cu, Al-12Si-4.5Cu and Al-15Si-4.5Cu alloys and grain refined and modified Al-7Si-4.5Cu, Al-12Si-4.5Cu and Al-15Si-4.5Cu alloys is discussed.

The investigations on sliding wear properties of Al-7Si, Al-7Si-4.5Cu, Al-12Si, Al-12Si-4.5Cu, Al-15Si and Al-15Si-4.5Cu alloys and of the effect of ageing on sliding wear properties of as-cast Al-7Si-4.5Cu, Al-12Si-4.5Cu and Al-15Si-4.5Cu alloys and grain refined and modified Al-7Si-4.5Cu, Al-12Si-4.5Cu and Al-15Si-4.5Cu alloys are presented and discussed in chapter 6.

Chapter 7 provides the conclusions drawn from the present work and also future scope of work of Al-Si alloys is listed.

Chapter 2

Literature Review

2.1 Introduction

Aluminium is the second most abundant metal available in the earth's crust. The unique properties offered by aluminium have made this metal a good alternate for materials such as wood, copper and steel. Aluminium finds wide range of applications for structural components in the sectors of aerospace, transport and in constructing buildings, where lightweight, durability and strength are desired. Some of the other applications also include electrical transmission lines and in packaging industry (cans, foil, etc.). Commercial production of Al usually involves melting and casting. Aluminium and its alloys generally exhibit a coarse columnar grain structure. Better mechanical properties of aluminium are obtained by forming desirable intermetallic compounds, alloying elements and refiners are added in the Al system. Aluminium and its alloys thus form a group of materials with excellent properties, fatigue and fracture resistance, lightweight, high strength etc.

Aluminium-Silicon (Al-Si) alloys are promising material for several applications in automotive, aerospace and defense industries, mainly due their thermal expansion coefficient, as well as high wear and corrosion resistance in addition to their high strength-to-weight ratio and superior castability (Spada 2002; Palazzo 1977). The fact that the ability to absorb the energy of impact for Al is twice that of steel has made them more popular.

The casting properties of Al-Si alloys mainly depend on Si content as it imparts low shrinkage characteristics. Silicon also improves the casting characteristics, such as improved fluidity, resistance to hot tear, and feeding. The improved fluidity facilitates easy filling of thin walls and intricate designs and shapes

(Rooy 1992; Polmear 2006). Silicon has a low density (2.34 g/cm^3), which is an added advantage in reducing the overall weight of the casting. Further, silicon has a diamond crystal structure with very high hardness. It has a very low solubility and hence precipitates as pure silicon thereby improving the tribological properties of these alloys (Mondolfo 1976). Thus it is a very potential alloy for applications requiring lower weight and higher wear resistance.

For quite some time, binary Al-Si alloys were used for manufacture of automobile parts subjected to friction and wear but these alloys were not meeting the strength requirements in such components. As a result, Mg, Cu, Ni etc are added as alloying elements. The additional alloying elements made the Al-Si alloys heat treatable wherein the morphology of the silicon particles and other constituents could be changed leading to the attainment of required physical and mechanical properties. A large number of Al-Si alloys containing specified amounts of Cu, Mg, Ni and other alloying elements are now available for industrial applications (Jigajinni et al. 2013). Components such as manifolds, engine blocks and cylinder heads require high strength at elevated temperatures necessitating the addition of alloying elements such as Mg and Cu. (Grosselle et al. 2010). Further higher strength is achieved through heat treatment to alloys with Cu and Mg causing microstructural changes due to temperature and time. T6 heat treatment cycle is most popular thermal treatment process applied for Al-Si-Cu and Al-Si-Mg alloys for meeting industrial needs (Mohamed and Samuel 2012).

Over the last few years, significant research has been done on Al-Si alloys. The structured literature survey on Al-Si alloys helps in realizing and planning the further research work. The current chapter includes details on review of Al-Si cast alloys and their properties in relation to a number of processing parameters. The parameters include the composition of the alloy, casting process and post-solidification heat treatment.

The existing literature in the field is reviewed under the following sections:

- Classification of Al-Si alloys
    - Hypoeutectic
    - Eutectic
    - Hypereutectic composition
- The Relation between Microstructure and its properties
    - Alloy composition
    - Casting process and
    - Post solidification heat treatment
- Effect of Cu additions on Al-Si alloys
- Effect of grain refiners and modifiers on Al-Si and Al-Si-Cu alloys
- Effect of T6 Heat treatment on Al-Si alloys with Cu additions
    - Solution Treatment
    - Quenching
    - Age hardening
- Characterization of Al-Si and Al-Si-Cu alloys
    - Tensile strength
    - Hardness
    - Wear
- Summary
- Objectives
- Problem statement
- Scope

2.2 Classification of Al-Si alloys

As shown in Figure 2.1, the Al-Si binary system forms eutectic structure at 577 °C and 12.6% Si. It is also visible that Al can dissolve a maximum of 1.65% Si into solid solution.

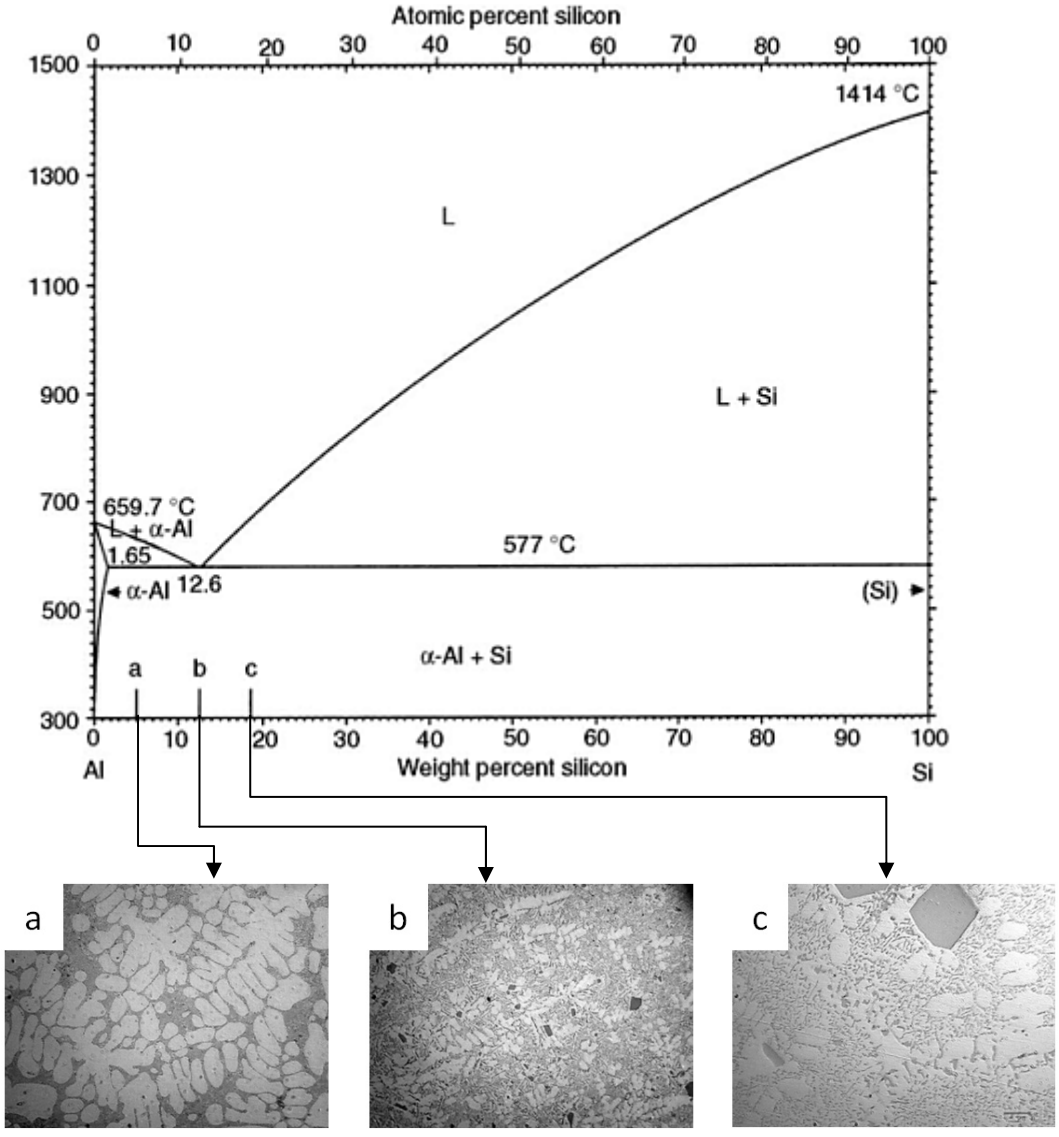

Figure 2.1: Al-Si binary system and microstructures of (a) hypoeutectic alloys; (b) eutectic alloys; (c) hypereutectic alloys.

Al-Si alloys are categorized into three groups based on % Si content as hypoeutectic (<10% Si), eutectic (10-13% Si) and hypereutectic (>13% Si) alloys

(Backerud et al. 1990). The constituents in all these group of alloys are same. However, only relative volume, size and distribution of the constituents differ from case to case. Representative microstructures are shown in Figure 2.1a-c, respectively. Microstructural features, applications and the research findings of these alloys are discussed in subsequent sections.

2.2.1 Hypoeutectic Al-Si alloys

Hypoeutectic Al-Si alloys with Si content generally less than 10%, occupies an important position in industrial applications. Hypoeutectic Al-Si alloys have a microstructure with matrix consisting of large fraction of primary Al dendrites and eutectic Si in the matrix. Due to acicular structure of eutectic Si, these alloys generally are not ductile. Hence hypoeutectic alloys are treated with Na, Sr or Ba modifiers to increase the ductility (Zhang et al. 2010). Grain refinement of hypoeutectic Al-Si alloys is conducted by the addition of Al-Ti-B master alloys with different Ti and B ratios to improve the quality of casting (Kori et al. 2000). The process of grain refinement involves conversion of columnar grains to equiaxed ones throughout the casting.

Hypoeutectic Al-Si alloys find extensive applications in the marine, electrical, automobile and aircraft industries where it is used for cylinder blocks, heads and other engine body castings (Lozano et al. 2006). LM-16 (5.0% Si) alloy is used to make military and aerospace parts that meet the MIL-A-21180 specification for “premium strength / quality” castings. They are used in aircraft crankcases, gearboxes, housings and supports, as well as in impellers for superchargers. LM-21 alloy with 6% Si is used for making cylinder heads and intake manifolds and LM-24 alloy with 8.5% Si is used as high pressure die casting alloy. These alloys offer moderate strength at low cost as they do not require heat treatment. Generally Mg content in these alloys is kept very low to reduce oxidation. However, addition of about 0.2-0.4% Mg can drastically improve machinability and strength (Apelian 2009).

LM-25 alloy (7.0% Si) finds extensive applications in electrical components and hardware used in marine industry. LM-25 alloys are popular in automotive industry and finds applications in manufacture of chassis and suspension systems. LM-25 alloy cast in sand and permanent moulds have excellent castability, pressure tightness and corrosion resistance, hence these alloys are very attractive for many automotive and aircraft part applications (Mondolfo 1976).

2.2.2 Eutectic Al-Si alloys

In Al-Si alloys, the eutectic point is reported to vary from 11.7-14.5 wt.% Si and most likely at 11.7 wt.% Si (Murray 1992). The eutectic composition in binary Al-Si system shifts depending on the alloying elements and the casting processes. Extensive research has been done regarding the microstructure and mechanical properties of eutectic alloys with varying Si % in the range defined above (Liao et al. 2002; Basavakumar et al. 2008; Hegde and Prabhu 2008; Djurdjevic et al. 1999).

Eutectic and near-eutectic alloys offer superior castability and low shrinkage properties and are required for complex castings. They are widely used in the manufacturing of pistons and are popularly known as piston alloys (Haque and Sharif 2004). These alloys are used in manufacture of marine castings, engine castings and switch boxes. LM-series alloys possess eutectic composition and offer good castability due to their low melting point. Hence these alloys are used for manufacture of thin walled castings with intricate shapes. They provide moderate strength but better elongation. They are popular for excellent weldability.

LM-6 (12 % Si) is the Al-Si eutectic alloy and solidifies over the narrowest range of casting alloys. For high pressure die casting alloy, LM-6 (12% Si) has better castability than LM-18 (5.25% Si). LM-6 (12% Si) and LM-20 (10-13% Si) offer excellent ductility due to low Si content but they have a tendency to drag during machining and cause rapid tool wear (Mondolfo 1976).

The microstructure of Al-12Si alloy contains columnar α-Al dendrites along with eutectic Si. The mechanical properties of these alloys are improved by adding Al-Ti-B grain refiner and Na or Sr modifier. Grain refinement results in fine equiaxed α-Al dendrites and fine fibrous eutectic Si leading to improved strength, toughness and machinability (Chandrashekharaiah et al. 2009). Additions of 0.5 wt.% Sr results in full modification with completely fibrous microstructure. However, it has been observed that the microstructure of eutectic alloy is similar to hypoeutectic alloy (Faraji and Katgerman 2009; Lim 2009; Liao et al. 2007) as it contains unrefined coarse columnar α-Al dendrites.

2.2.3 Hypereutectic Al-Si alloys

Hypereutectic Al-Si alloys contain coarsely segregated hard primary particles of non-metallic silicon dispersed in Al-Si eutectic matrix. Hence, these alloys are understood to offer very high wear resistance properties and are good for tribological applications (Chirita et al. 2009). However, the presence of primary silicon content has an adverse influence on strength and ductility of these alloys (Zuo et al. 2009, Srivastava et al. 2004). The primary silicon in hypereutectic alloys exhibit irregular platelet and polygon shapes which are required to be refined and modified to avoid detrimental effects on mechanical properties as reported by Zuo et al. (2013). Refinement in primary Si is generally obtained by adding phosphorous. Phosphorous reacts with the liquid Al to form aluminium phosphide (AlP). This has a crystal structure similar to that of Si, and acts as an effective heterogenous nucleant (Chen et al. 1981). The Si morphology is highly dependent on the solidification parameters such as freezing rate, temperature gradient in the liquid and liquid composition. Higher Si present in hypereutectic alloy reduces the thermal coefficient of expansion and improves the wear resistance. These alloys are used in the production of pistons, cylinder liners, cylinder blocks, rocker arms, and cylinder heads etc (Miller et al. 2000).

Alloys such as LM-30 containing 17% Si and LM-29 is containing 22% Si possess low coefficient of thermal expansion and also have good wear characteristics.

The outstanding wear and strength characteristics offered by LM-30 alloys make them suitable for pumps, pulleys, brake shoes, and air compressors.

The coarse primary Si particles and needle-like eutectic Si present in hypereutectic alloy affect the tensile and wear characteristics of the alloy. The coarse primary Si particles lead to early crack initiation during tensile load and adversely affect the strength and ductility (Ying et al. 2007). Mechanical and wear characteristics of hypereutectic alloys are enhanced by achieving refinement of Si by addition of modifiers (Mahanti et al. 1993), faster cooling rate (Dasgupta 1997), spray forming and electromagnetic stirring (Radjai et al. 1998). Among these methods, the addition of chemical modifiers such as phosphorous to hypereutectic melt is found to be effective and economical.

2.3 Microstructure and Mechanical Properties

The mechanical properties of the Al-Si castings primarily depend on their microstructures. The microstructure of Al-Si alloys consists of Al-Si eutectic constituent, the primary phase α-Al in hypoeutectic and primary Si in hypereutectic alloy. For enhanced mechanical properties, grain refinement of hypoeutectic alloys is carried out for obtaining the equiaxed α-Al and modification is carried out for obtaining fine eutectic Si and refined primary Si (Gruzleski and Closset 1990). The mechanical properties also depend on the type, shape, size and distribution of Si particles in the matrix (Basavakumar et al. 2008). Other popular methods of controlling the features of microstructures are heat treatment and plastic deformation. During solidification of the melt stirring also helps in achieving required features. However these methods require more time and added energy requirement. Addition of alloying elements (Gruzleski and Closset 1990; Zhang et al. 2010), modifiers (Mohamed et al. 2009), grain refiners (Metan and Eigenfeld 2013, Basavakumar et al. 2007, Jigajinni et al. 2013) to liquid melt is a good option to obtain better control on microstructure and hence, these are responsible for improved mechanical properties.

Following three are the main factors that influence the mechanical properties of Al-Si casting alloys to a large extent:

- Composition of the alloy,
- Solidification and
- Heat treatment.

2.3.1 Composition of alloy

Principally, castings of pure aluminium are used because of their very high ductility, electrical conductivity and excellent corrosion resistance but exhibit low strength, hardness and poor machinability. The mechanical properties in the as-cast condition of commercial pure Al are in the order of 68 MPa tensile strength, 41 MPa yield strength, 30% elongation and a hardness of about 22 BHN. Therefore, several alloying elements like Si, Cu, Mg and Zn are added to improve the mechanical properties (Hatch 1988). Table 2.1 shows the composition of LM series Al-Si alloys.

The alloying elements such as Si, Cu, Mg and Zn are added to increase the fluidity, machinability, strength and hardness of the aluminium alloys lowering their ductility, conductivity, impact resistance and corrosion resistance. The addition of Cu, Mg or Ni improves the strength of Al-Si alloys (Garcia et al. 2003; Yang et al. 2011). Cu is commonly added to Al-Si alloys because of its observable solubility and marked strengthening effect (Ma et al. 2010). Commercially available die-cast alloys contain 2-4.5 wt.% Cu with 7-12 wt.% Si. However, they have limited fluidity and require careful gating and generous riser feeding during solidification to ensure casting soundness. Pressure-tight parts of the intricate design are difficult to obtain and its resistance to hot cracking is relatively poor. Copper additions (up to 12%) to Al imparts strength and hardness. It also improves the machinability, creep resistance and increases the fluidity of Al-Si alloys. Hot tearing is a common and severe defect encountered in aluminium alloy castings. However, copper additions above 5%, increase the resistance to hot tearing and reduce the susceptibility to hot cracking (Sigworth 1983).

Table 2.1 Compositions of common LM-Series Al-Si casting alloys
(Gruzleski and Closset 1999)

Alloy code	Casting Process	Element (wt.%)					Others
		Si	Cu	Mg	Fe	Zn	
LM-16	S, P	5.0	1.25	0.5	<0.06	<0.35	-
LM-18	S, P	5.25	<0.3	<0.05	<0.8	<0.5	-
LM-21	S, P	6.0	3.5	<0.10	<1.0	<1.0	-
LM-25	S, P	7.0	<0.20	0.35	<0.2	<0.1	-
LM-24	D	8.5	3.5	<0.1	<1.3	<3.0	-
LM-13	P	9.5	3.5	1.0	1.2	1.0	-
LM-20	D	11.0	2.0	<0.3	<1.3	<3.0	0.35Sn
LM-6	D	12.0	<0.1	<0.10	<2.0	-	-
LM-30	D	17.0	4.5	0.55	<1.3	<0.1	<0.1Mg

S; Sand casting, P; Permanent mould casting and D; High pressure die casting

Aluminium-copper alloys are high strength-ductility cast alloys. They are commonly used for components such as bearings, particularly under heavy loads and slow speed conditions. Apart from this, they have high hardness and can operate at high temperatures. An addition of Mg imparts bright surface finish and enhances machinability. It also provides good impact resistance, ductility and largely maintains their properties at elevated temperatures. When silicon is present along with magnesium (0.25 - 0.5%) the compound magnesium silicide (Mg_2Si) is formed. If the precipitation of this phase is uniformly dispersed, then hardness and strength increases but ductility of the alloy reduces. Piston alloys are manufactured with magnesium content ranging from 0.5-1.5%. With trace alloying of Cu and Mg, Al-Si alloys can be strengthened by solid solution of alloying elements and by precipitation of intermetallics, but often at the expense of ductility (Tao Lu et al. 2014)

Zinc is generally added along with magnesium. With increased zinc content, the fluidity of the molten alloys increases but shrinkage problems may be experienced (Rooy, 1992). Zinc increases the machinability when combined with copper. Generally, a maximum of 0.8 or 1% of Fe is added to Al-Si alloys as higher contents impair feeding ability and ductility. Impurities like manganese are common in Al-Si alloys in which the concentration usually ranges from 5 to 50 ppm. It increases the strength either in solid solution or as a finely precipitated intermetallic phase. It has no adverse effect on corrosion resistance. The addition of manganese increases the strength and controls the grain structure. The effect of manganese is to increase the recrystallization temperature and to promote fine fibrous structure upon hot working (Kaufman and Rooy, 2004). Iron is restricted to a maximum of 0.8 or 1% in permanent mould castings as at higher contents impair feeding ability and mechanical properties, especially ductility. A maximum of 0.2% iron is stipulated for Al-Si-Mg or Al-Si-Mg-Cu alloys to allow attainment of the required ductility and toughness, which otherwise combines other elements and forms insoluble embrittling constituents, that act as severe stress risers and reduces the ductility (Wang et al., 2003). The solid solubility of nickel in Al is less than 0.04%. Over this amount, it is present as an insoluble intermetallic, usually in combination with iron. The addition of Ni in Al-Si alloy improves strength and hardness at higher temperatures and reduces the thermal expansion coefficient. Tin improves the anti-frictional characteristics and machinability of aluminium and its alloys when the concentration is below 0.3%. Titanium is added to aluminium alloys for obtaining the grain refinement. It is generally added along with a small quantity of boron. It is also added at a higher quantity to minimize cracking tendencies (Basavakumar et al. 2008). Free machining alloys are made by adding low melting point metals like lead, tin, bismuth and cadmium. These elements have a restricted solubility in solid aluminium and form a soft, low melting phase that promotes chip breaking and helps to lubricate the cutting edge.

Table 2.2 summarizes the typical applications of LM series alloys. These alloys are selected based on their casting characteristics like fluidity, resistance to heat treatment, physical properties, machinability, resistance to corrosion etc.

Table 2.2 Applications of LM-Series Al-Si casting alloys (Campbell 1991)

Alloy code	% of Si	Applications
LM-16	4.5-5.5	High mechanical properties are required in fairly intricate casts
LM-18	4.5-6.0	Good foundry characteristics, corrosion resistance, pressure tightness and ductility
LM-21	5.0-7.0	Sand and permanent mould castings, has very good casting characteristics, better machinability
LM-25	6.5-7.5	Where good corrosion with high strength is needed.
LM-24	7.5-9.5	All types of die castings
LM-13	9.5-12	Pistons
LM-20	10-13	Large, intricate and thin walled castings with machinability and hardness
LM-6	10-13	Large, intricate and thin walled castings

2.3.2 Solidification

Solidification of liquid metal depends on the type of casting process and its processing parameters. The rate of solidification, in turn, influences the grain size, the size of intermetallics and their distribution. In case of aluminium alloys, solidification begins with the separation of primary α-Al phase from the melt. As the temperature of the melt reduces, the α-Al phase forms the dendritic shape. Once the temperature of the melt reaches the eutectic point, the solidification proceeds with the formation of the eutectic solid phase in space between dendritic arms. It has been studied experimentally that the size of the dendrites is influenced by both the heat transfer rate during solidification and chemical composition of the alloy. (Whisler and Kattamis 1972; Feurer 1977).

Influence of the cooling rate on the microstructure of Al-9Si-Cu alloy was investigated by Dobrzanski et al. (2007). It is reported that the solidification was affected by the cooling rate. The formation temperatures of various phases changed with an increasing cooling rate. It is also revealed that increasing the cooling rate, increases significantly the Al nucleate temperature and leading to an increased number of the nuclei that affect the Secondary Dendrite Arm Spacing (SDAS) size of the grains. SDAS is used to describe the solidification rate; thus, a smaller SDAS is an indication of a rapid cooling rate while a larger SDAS refers to a slower solidification rate. Boileau et al. (1977), investigated the effect of cooling rates on the microstructure and mechanical properties of LM-25 alloys. They have reported that, by applying higher cooling rates, UTS, fatigue strength and ductility could be improved significantly.

2.3.3 Heat treatment

Heat treatment is generally used to improve the mechanical properties of Al-Si alloys. Different heat treatment processes are available depending on the composition of the alloy. A T6 heat treatment cycle; consisting of solution treatment, quenching and artificial ageing is often used to achieve an increase in strength. (Sigworth and Kuhn 2007).

2.4 Effect of Cu additions on Al-Si alloys

Cu is the major additional element added to Al-Si alloy system. Addition of Cu improves the strength, hardness and other mechanical properties of Al-Si alloy. Strength and ductility are dependent on the distribution of copper in the alloy. Al-Si alloys with copper dissolved in the matrix show increased strength while retaining ductility. `

Al-Si-Cu system has a great importance in the industry as Cu acts as precipitation strengthening agent. Cu additions up to ~ 5% impart high strength and toughness especially after ageing treatment (Zeren and Karakulak 2009). The

enhanced mechanical properties and wear resistance is governed by the shape, size and distribution of second phase particles and the microstructure of the matrix. Hardness is generally considered as a wear controlling property (Torabian et al. 1994). The presence of Cu in Al-Si alloys enables them to be heat-treated and can consequently improve the strength significantly by means of a precipitation hardening mechanism. The copper strengthens Al-Si alloy via the precipitation hardening of θ-$CuAl_2$ precursor and modification of the brittle Al-Fe-Si phases (Sjolander and Seifeddine 2010). Al-Si-Cu alloys are extensively used in high pressure die casting applications for producing thin wall components (Ji et al. 2012).

Yang et al. (2015) investigated the influence of heat treatment on Al-9Si-3.5Cu die cast alloy. The as-cast alloys provided a yield strength of 140 MPa, UTS of 320 MPa and 3% elongation. The alloy is solution treated at 510 °C for 30 minutes and aged at 170 °C for 24 h. The solution treatment resulted in the dissolution of $CuAl_2$ intermetallics into the primary α-Al phase and rounding of the eutectic Si phase. Post heat treatment, the alloy exhibited yield strength of 320 MPa, UTS of 400 MPa and 2.5-4% elongation. Researchers have found that the $CuAl_2$ phase can exist as dense blocky particles or lamellar eutectic (Al–$CuAl_2$) phase, or as a mixture of both, in the as-cast microstructure (Samuel et al. 1996; Djurdjevic et al. 1999).

Studies on Al-9Si alloy with an addition of 1%-4% Cu addition have showed that the microstructure and mechanical properties depends on the change in morphology of eutectic Si particles from coarse to flake-like form. It is observed that the increase in Cu content caused change in morphology of the eutectic Si from a coarse flake like form to a fine fibrous one leading to improved mechanical properties with increase in Cu content. However, the alloys with 2% Cu addition displayed higher ultimate compression strength compared to the alloys with 1% and 4% of Cu additions (Dobrzanski et al. 2007).

Wu C.T et al. (2010) studied the influence of 0.52 wt.% and 4.65 wt.% of Cu additions on Al-14.5Si-0.5Mg alloy. Experimental studies indicated a relatively higher tensile strength (334 MPa) in low Cu alloy (0.52 wt.% of Cu) that contains

$Al_4Mg_3FeSi_6$ as compared to the strength of 374 MPa in the case of high Cu alloys (4.65 wt.% of Cu) that showed acicular β-Al_5FeSi phase. Moreover, as the Cu % in Al-14.5Si material is increased, it promotes solution and precipitation hardening condition leading to improved hardness from 68 HRB to 80 HRB. Experimental investigations on the influence of Cu content on near-eutectic alloys have inferred that Cu content improve the mechanical properties and heat treatment of these alloys plays an important role in further improvement of properties. Increased Cu content from 2% to 5% found to improve hardness from 55HB to 115HB (Zeren and Karakulak 2009).

Basavakumar et al. (2007) have demonstrated that melt treatments such as grain refinement and modifications are responsible for the microstructural change in Al-7Si alloys. Work hardening is noticed in Al-7Si-2.5Cu alloys largely as compared to base Al-7Si alloy. The influence of grain refinement and modification has resulted in the reduction in coefficient of friction and the temperature rise at higher wear load. Coefficient of friction reduced from 0.45 to 0.35 when wear test is conducted on modified and grain refined Al-7Si-2.5Cu alloy with 50 N load and 4.0 m/s sliding speed. In their studies, the influence of 2.5% Cu content to Al-7Si alloys is clearly observed. Further, these researchers have also studied the microstructure and properties of Al-7Si-0.5Cu and Al-7Si-1Cu alloys in modified and unmodified condition using 0.02 wt.% Sr. The investigators have concluded that the addition of Cu as alloying element complemented by the modification by Sr is an excellent method to get better microstructure and mechanical properties (Garcia-Hinojosa et al. 2003).

The Al-Si-Cu alloys exhibit improved strength at high temperature compared with Al-Si-Mg alloys, but intergranular corrosion is observed in Al-Si-Cu alloys (Grosselle et al. 2010). However, the studies conducted by Wislei et al. concluded that refined microstructures with fine SDAS (5-15 μm) having needle-like Si particles with homogenously distributed $CuAl_2$ intermetallics provide better galvanic protection to both $CuAl_2$ and Si phases and reduce the corrosion resistance of the alloy (Wislei et al. 2011).

Tao Lu et al. (2014) investigated the effect of Cu on tensile properties of Al-11Si-0.3Mg alloy both in as-cast condition and after solution treatment. They observed the following; the addition of copper resulted in the coarsening of α-Al dendrites, the addition of 1.88% Cu resulted in increase of UTS from 229 MPa to 247 MPa but the elongation reduced from 5.4% to 3.6%. After solution heat treatment at 500 °C for 8 h, UTS of the Al-11S-0.3Mg-1.88Cu alloy increased to 290 MPa with 5.1% elongation. It was observed that the strengthening by copper additions depends on the weight ratio of Cu and Mg. Optimized UTS of 383 MPa and 430 MPa are obtained for Al-11Si-0.3Mg alloy with the weight ratio of Cu/Mg of 5:1.

Investigations on the effect of combined alloying of Cu and Fe on mechanical properties of Al-Si alloys are carried out by preparing alloys with composition of 13.0 Si, 3.0-5.0 Cu, 0.3-0.8 Fe. It was found that Cu and Fe rich phases are precipitated in the form of blocky α-Fe and $CuAl_2$ along the grain boundaries of α-Al dendrites. The UTS and elongation of the alloy with 3.0% Cu and 0.3% Fe are reported as 310 MPa and 3.2%, respectively. The UTS of the alloy increased further to 336 MPa with Cu content increasing to 5.0% and Fe to 0.8%. The fracture surfaces showed mixed failure mode showing quasi-cleavage and ductile fracture morphology (Wang et al. 2010).

2.5 Effect of grain refiners and modifiers on Al-Si and Al-Si-Cu alloys

Generally, aluminium foundries add master alloys to aluminium melt for refinement. Properties of Al-Si castings are significantly enhanced by grain refinement. A fine equiaxed microstructure leads to improved mechanical properties, reduced shrinkage porosity and improved surface finish. Grain refinement ensures high toughness, high yield strength, good castability, extrudability, sheet formabilty, and improved machinability (Kumar 1972). Titanium (Ti) is popularly used for grain refinement purpose, generally along with smaller amounts of boron (Rooy 1992).

Addition of 1 wt.% Al-1Ti-3B master alloy is suggested for hypoeutectic and eutectic Al-Si alloys to refine the coarse columnar primary α-Al grains to fine

equiaxed α-Al grains due to the presence of Al_3Ti and TiB_2 particles acting as nucleants during solidification of hypoeutectic and eutectic alloys (Basavakumar et al. 2008). Other refiners include Al-5Ti, Al-3B, Al-5Ti-1B containing Al_3Ti, AlB_2, TiB_2, Al/TiB_2 as nucleating particles which are responsible for grain refinement during solidification.

The modification of eutectic Si results in conversion of needle like to fine fibrous microstructures enhances the ductility and strength of the alloy (Shabestari and Shahri 2004). Calcium, sodium, strontium, and antimony are used for modification of Al-Si. Modification is carried out using potassium, lithium and cesium at reasonable concentrations. The lanthanide and rubidium fade quickly and are expensive. Calcium and barium show mild modification while improving the melt flow characteristics and have a tendency for increased loss from the melt by oxidation. Phosphorous, sulfur, zinc, bismuth and lead are not effective in modifying the microstructure of hypoeutectic Al-Si alloys (McCartney 1989). Strontium is a very popular alloying element usually added as a chemical modifier to Al-Si alloys to transform coarse acicular morphology of eutectic silicon particles into a fine fibrous form. (Sigworth 2008; Hegde and Prabhu 2008; Paray and Gruzleski 1994).

In case of hypereutectic Al-Si alloys, refinement of primary Si is usually achieved by the addition of phosphorous to the melt. Addition of phosphorous can be carried out in many forms such as Al-P (Wang et al. 2013), Cu-P (Hernándeza and Sokolowski 2006) and Al-Zr-P (Zuo et al. 2010) master alloys. Zuo et al. studied the effect of P and Sr addition on Si phase in Al-30Si alloys and observed that a significant refinement of primary Si takes place with an average particle size decreasing from 203.8 μm to ~ 32.8 μm. It was found that by controlling the melt temperature at 770 °C, the reaction between P and Sr can be avoided and excellent modification effect could be realized (Zuo et al. 2013).

Al-10Sr, an environmental friendly master alloy is widely accepted by most of the industries for the modification purposes that contain Al_4Sr particles for the

modification. This process involves addition of chips of grain refiner and modifier to the melt.

Glasson and Emely (1968), have investigated the combined effect of grain refiner and modifier in LM-25 alloy and reported improved hardness, elongation and tensile strength. Cupini et al. (1980) experimented with different ratios of Al-Sr-B master alloys and reported that by the addition of these master alloys to LM-25 and LM-21, the grain refining effectiveness increases at short holding times. Chandrashekharaiah and Kori have reported that the addition of grain refiner Al-1Ti-3B master alloy along with strontium (Sr) modifier to the hypoeutectic and eutectic Al-Si alloys show more uniformly distributed α-Al grains and fine eutectic silicon throughout the matrix compared with the microstructure obtained with individual additions of grain refiner and modifier (Chandrashekharaiah and Kori 2009). The combined addition of Al-5Ti-B grain refiner and Al-10Sr modifier to Al-7.5Si-4Cu resulted in the increase in tensile strength to 246 MPa from 226 MPa (as-cast), the increase in yield strength to 190 MPa from 178 MPa. Also, % elongation is increased from 2.3% to 2.9% after combined addition of modifier and grain refiner (Du et al. 2014).

Morphology of eutectic Si and intermetallic phases present in the Al-Si system determines the mechanical properties. Several studies have confirmed that, mechanical properties of the cast Al-Si alloys largely depend on the size, morphology and distribution of eutectic Si (Elsebaie et al. 2010; Hu et al. 2012). In order to improve the strength, Al-Si alloys are usually melt treated by adding modifiers and grain refiners.

Studies on the effect of combined addition of Al-3Ti-4B and Al-10Sr on the microstructure of Al7Si4Cu alloy have revealed that the addition of 0.02% Ti and 0.026% B refined the grains to 100-120 μm and does not have any effect on modification of the eutectic Si (Li et al. 2002). The studies on the effect of combined addition of 0.04% Sr and 0.02% B in near-eutectic Al-Si alloys showed greater reduction in eutectic grain size, when Sr and B were added together than the addition

of Sr alone. The addition of boron resulted in 10% -15% reductions in eutectic size. The results showed noticeable effect of cooling rate on the eutectic size. For the same additions of Sr and B, a high cooling rate is responsible for finer grains (Liao et al. 2007). Liao et al. (2002) studied the correlation between the quantities of dendritic α-Al phase and UTS of Al-11.6Si alloys. Different morphology of dendritic α-Al phase was obtained by varying the addition of Sr. The amount of dendritic α-Al phase is increased by 104% when Sr addition is increased from 0.015% to 0.02%. Compared to unmodified alloy, an addition of 0.0375% Sr resulted in 236.9% increase in α-Al phase. Tensile strength is increased by 33.8% from 162.8 to 218.1 MPa when Sr content is increased from 0 to 0.0375%. Experimental studies on the effect of Ti on hardness of Al-13Si alloy were performed by Zeren and Karakulak (2008). Improved hardness is obtained with the increase in Ti % because of the formation of relatively hard Al_3Ti intermetallic phase. The hardness of the alloy is found to increase from 841 to 1543 HV (83% increase) when Ti content is varied from 0.1% to 10%. The coarseness of the Ti, Al and Si particles is found to increase with increase in Ti. Mean area of the particle increased from 11.0 μm^2 to 116.4 μm^2 with increase in Ti from 0.1% to 10%. The experimental studies to investigate the effect of Ti and Sr on Al-12.5Si alloy reported a decrease in hardness after the addition of grain refiner and modifier. An addition of 0.04 wt.% Sr resulted in hardness reducing from 62 to 51 HRB and addition of 0.00123 wt.% Ti also reduced hardness from 62 to 55 HRB due to the change in morphology of β phase. (Rodriguez et al. 2011). Yudong Sui et al. studied the effect of Sr additions on the microstructure and mechanical properties of Al-12Si-4Cu-2Ni-0.8Mg alloys. An addition of 0.02 wt.% of Sr caused the SDAS to change from 18 μm to 13 μm. The microstructural changes resulted in the improvement of UTS from 196 MPa to 249 MPa, and the yield strength from 176 MPa to 207 MPa. As compared to the unmodified alloy, modified alloy showed 27% and 18% enhancement in UTS and YS, respectively. The SEM of the fracture surface of unmodified sample showed quasi cleavage fracture while modified sample exhibited fracture surface with dimples (Sui et al. 2015).

D. Apelian confirmed that the addition of 0.50 wt.% of Al-5Ti-0.2B master alloy to Al-7Si alloy resulted in the grain refinement of Al-7Si alloy, but interestingly,

it was also found that grain refinement of eutectic structure occurred (Apelian et al. 1989). In other words grain refining nucleants have confirmed the indirect effect on the morphology of eutectic structure. This is because, during solidification, there are numerous primary phase islands and the size of the interdendritic liquid pockets will become so much smaller, that even the volume of the interdendritic liquid remains the same. This causes an indirect modification of structure. Faraji and Katgerman conducted experiment on LM-25 (LM-25) alloy with the addition of 0.002% Ti and 0.02% Sr that resulted in a decreased effect of grain refinement. However, the addition of 0.02% of Sr alone resulted in slight grain refinement effect of α-Al. Also, introducing TiB_2 into the melt hinders the modification effect of eutectic Si particles. This could be due to the possibility of the interaction between TiB_2 with Al_4Sr particles to form SrB_6 particles. As a result, a decrease for strontium is expected to modify eutectic Si (Faraji and Katgerman 2009).

2.6 Effect of T6 Heat treatment on Al-Si-Cu alloys

The mechanical properties of cast Al-Si-Cu alloy depend on alloy composition and processing parameters. In order to obtain better mechanical properties and to achieve an optimum value of strength and ductility, these alloys are heat treated (Samuel et al. 2013). Various heat treatment cycles consisting of different combinations of temperature and time are used depending on the alloy composition and desired mechanical properties. The European Aluminium Association has standardized the definitions and nomenclature for heat treatment is given in Table 2.3.

T6 heat treatment is typically applied to sand and gravity die-cast Al-Si alloys. As described by Brooks in the ASM handbook, T6 cycle begins with solution treatment at ~ 505 °C (±6 °C) for a 12 h duration, water quenching at ~ 65-100 °C and aging treatment at 155 °C for ~ 2-5 h (Brooks 1991). The studies carried out by Mohamed and Samuel (2012), shows the improvement of tensile properties after heat treatment due to the development of non-equilibrium precipitates within primary dendrites during aging. They have also reported that Al-Si-Cu alloys have a slow and

low age-hardening response as determined by the fraction size, dispersion and consistency of precipitates formed.

Table 2.3 Definition and nomenclature of heat treatment

T1	Cooled from the fabrication temperature and naturally aged
T2	Cooled from the fabrication temperature, cold worked and naturally aged
T3	Solution treated, cold worked and naturally aged
T4	Solution treated and naturally aged
T5	Cooled from the fabrication temperature and naturally aged
T6	Solution treated and artificially aged
T7	Solution treated and stabilized by over-ageing

2.6.1 Solution Treatment

Al-Si alloy is subjected to solution treatment at appropriate temperature and for a specific period to enhance the microstructural features and mechanical properties. The temperature for solution treatment is selected near to the eutectic temperature, so as to dissolve the Cu and Mg rich intermetallic phases and spheroidoize the Si particles (Sjölander and Seifeddine 2010). During solution treatment, the alloy is heated to a sufficiently high degree (lower than liquidus temperature) and held for a period to ensure dissolution of Cu rich particles thereby producing a supersaturated solid solution of Cu rich α-Al.. The temperature and time duration should be enough to achieve a nearly homogeneous solid solution. The Cu rich eutectic phases are usually found along the grain boundaries due to non-equilibrium solidification.

For obtaining maximum solution of the constituents, solution heat treatment temperature has to be controlled at as close as possible to the liquidus temperature. Solution heat treatment at a higher temperature than the optimum can lead to the incipient melting of these phases at the grain boundaries affecting the mechanical properties adversely. The typical temperature range of the solution treatment of binary Al-Cu alloys is shown in Figure 2.2 (Hatch (Ed.) 1988).

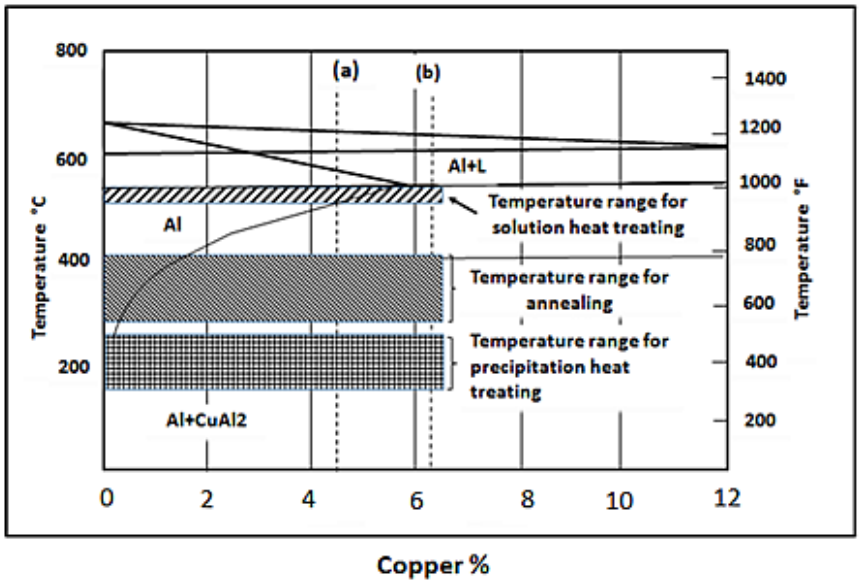

Figure 2.2: Partial equilibrium diagram for aluminium-copper alloys showing the temperature range of solution heat treatment

Researchers have reported that blocky $CuAl_2$ phase is difficult to dissolve during solution heat treatment in comparison with the eutectic (Al–$CuAl_2$) phase, and that fine $CuAl_2$ phase particles can dissolve within 2 h of solid solution heat treatment (Han et al. 2008). Eutectic (Al–$CuAl_2$) phase dissolves due to the $CuAl_2$ particles disintegrating into smaller fragments that can spheroidize, whereby the Cu atoms can dissolve by radial diffusion into the matrix. The reason for the difficulty in the dissolution of the blocky $CuAl_2$ phase is because of the lower interfacial area with the matrix (Chaudhury and Apelian 2006).

Several investigations have been performed by earlier researchers for correlating the influence of solutionizing parameters (time and temperature) on the microstructure and mechanical properties of Al-Si alloys. The amount of Cu and Mg

concentrations have been observed to be the limiting factors for deciding the solution treatment temperature as high temperature can lead to incipient melting (Sjolander and Seifeddine 2010). Hence, the selection of solution treatment temperature and solution treatment time is critical. Higher solution temperature leads to the formation of shrinkage cavities when samples are quenched, leading to reduced mechanical properties (Li et al. 2003). Researchers in the past have used different heating cycles to investigate age hardening process. Zeren and Karakulak found that 500 °C is a suitable solution treatment temperature for alloys with more than 2 wt.% Cu. (Zeren and Karakulak 2009). Al-Si-Mg alloys can be heat treated at 540-550 °C (Shivkumar et al. 1990), while Al-Si-Cu alloys must be solution treated at lower temperature to avoid local melting of Cu rich phases (Samuel 1998). Based on conventional solution treatment rules, the solution temperature of Al-Si-Cu-Mg alloys is restricted to 495 °C, in order to avoid incipient melting of the copper rich phase (Wang et al. 2003). Solidification of $CuAl_2$ phase in Al-Si-Cu are studied extensively (Sjolander and Seifeddine 2010). The $CuAl_2$ phase may be present in blocky phase or as eutectic phase or as a mixture of both types. Faster solidification facilitates the formation of eutectic $CuAl_2$ phase while Sr modification promotes formation of blocky $CuAl_2$ phase (Samuel et al. 1996). Sr modification and solution treatment together influence the morphology of eutectic Si and greatly improve the mechanical properties (Samuel et al. 2014). The experimental studies on LM-25 alloy (Al-7Si-0.35Mg) to assess the effect of modification and solution treatment showed significant improvement in UTS from 162 MPa to 262 MPa after 8 h solution treatment at 495 °C (Samuel et al. 2015). Elsebaie et al. studied the effect of solution treatment on the impact toughness of Al-11Si-2.7Cu-0.3Mg-0.45Fe alloy and have showed that solution treatment carried out for 8 h at 495 °C yields significantly improved impact energy of the alloy by 41% as compared to the 21% improvement obtained by Sr modification (Elsebaie et al. 2014). Experimental studies performed by Ma et al. on the effect of heat treatment on as-cast and Sr modified Al-11Si-2.5Cu-Mg alloys have reported that solution treatment is found to have different effects on as-cast and Sr modified alloys. Generally, solution treatment is found to render Si particles coarser in the non-modified sample. Also, solution treatment found to improve the particle roundness in the Sr modified samples and had no effect on particle roundness of unmodified alloys (Ma et al. 2010).

Researchers have also attempted a two stage solution treatment (Sokolowski et al. 1995). First stage solution heat treatment was performed at 495 °C for 8 h, to allow dissolving of the Cu-containing particles, and second stage solution treatment was performed at 520 °C for 2 h, to allow the alloying elements to homogenise. After two stage solution treatment, improved strength and ductility were observed. Solution treatment of Al-Si alloys resulted in improved microstructural characteristics, as well as enhanced mechanical properties. However, inappropriate solution treatment, results in incipient melting and surface blistering.

Studies have been carried out to understand the effect of solution heat treatment parameters on the microstructure and mechanical properties of LM-25 alloys (Shivkumar et al. 1990). It was found that solutionizing at 540 °C for 1-2 hours is optimum. The investigators concluded that further increase in solutionizing temperature would result in incipient melting of the eutectic structure.

2.6.2 Quenching

Subsequent to solution treatment, quenching of alloy is carried out by rapid cooling in water, oil, ambient air or any other quenching medium in order to preserve the structure existing at high temperature. (Apelian et al. 1989; Zhang and Zheng 1996). The prime objective of quenching is to prevent the precipitation of intermetallic phases such as $CuAl_2$ and Mg_2Si and also to achieve a supersaturated solid solution.

The quenching rate and the time delay in quenching are the important process control parameters and influence the mechanical properties of the alloy. These parameters must be balanced in order to retain the maximum secondary phases in the solid solution. By doing so, distortions and residual stresses can be minimized in the castings being quenched (Martin 1998; Staley 1987).

For optimizing the precipitation strengthening effect, it is essential to understand the quench sensitivity. The minimum precipitation time depends on the

amount of solute atoms. For alloys with higher percentage of solute atoms, the cooling rate must be high to avoid precipitate formation. Experimental investigations have revealed that quenching rate significantly affects the mechanical properties of Al-Si alloys with Mg and Cu additions (Seifeddine et al. 2007). It is recommended to increase the quenching rate to certain limits so as to avoid residual stresses and distortions of the castings that might accompany a very fast quenching rate (Apelian et al. 1989). The A354 samples quenched in water showed finer Si particles compared to coarse Si particles exhibited by samples subjected to lower quenching rate. The strength of the alloys showed a direct relation with the quenching rate. The increase in quenching rate led to increase in strength. However, it is recommended to increase the quenching rate carefully to avoid possible residual stresses and distortions of the castings which might accompany at very fast quenching rate (Kaufman and Rooy 2004; Hatch 1984; Apelian et al. 1989). An experimental study is performed with Al–Mg–Si–Cu alloy at different rates of quenching. It is found that changing the water quench temperature from 20 °C to 60 °C does not have any effect on crack propagation energy. However, when the samples are subjected to air cooling, a significant reduction in crack propagation is observed (Morgeneyer et al. 2008).

Experimental investigations to determine the influence of quenching rates on the mechanical properties of LM-21 alloys were carried out at five different quenching rates varying from 0.02 °C/s to 18.8 °C/s. The study indicated that, the hardness increased steadily in the quenching rate ranging from 0.5 °C/s to 18.8 °C/s while in the range of 0.02 °C/s to 0.5 °C/s there was no significant change observed in the hardness of the alloys. The UTS was observed to increase in the quenching rate ranging from 0.02 °C/s to 3.8 °C/s while no significant change in strength was observed at quenching rates higher than 3.8 °C/s. Elongation was observed to decrease with increasing the quenching rate due to the increase in the strength and hardness of the alloys (Byczynski et al. 1996).

Investigative studies on the effect of quenching rate have shown that faster quenching rates cause higher residual stresses and distortion, whereas a slow quenching rate produces less residual stresses and distortion; however, this causes

precipitation that have adverse effects like localized over-ageing, higher corrosion tendencies and a minimized response to ageing treatment (Staley 1987; Martin 1998).

2.6.3 Age hardening

During T6 heat treatment, aging treatment is carried out subsequent to the solution treatment and quenching process. During ageing, the castings are subjected to a specified temperature for a certain period of time. The aim of aging is to acquire uniform distribution of the strengthening precipitates. This leads to a better homogenous microstructure thus, leading to improved material properties. Ageing can be either carried out at room temperature called natural ageing or at an elevated temperature known as artificial ageing (Sjolander and Seifeddine 2010). Both ageing time and temperature control the characteristics of the phases precipitated during the aging treatment, and this affects the mechanical properties of the alloys. By controlling the ageing time and temperature, a wide range of mechanical properties are obtained. Microstructure can be stabilized and tensile strength can be increased. Figure 2.3 represents a scheme over the age hardening behaviour of an Al-4% copper alloy (William and Callister 2004).

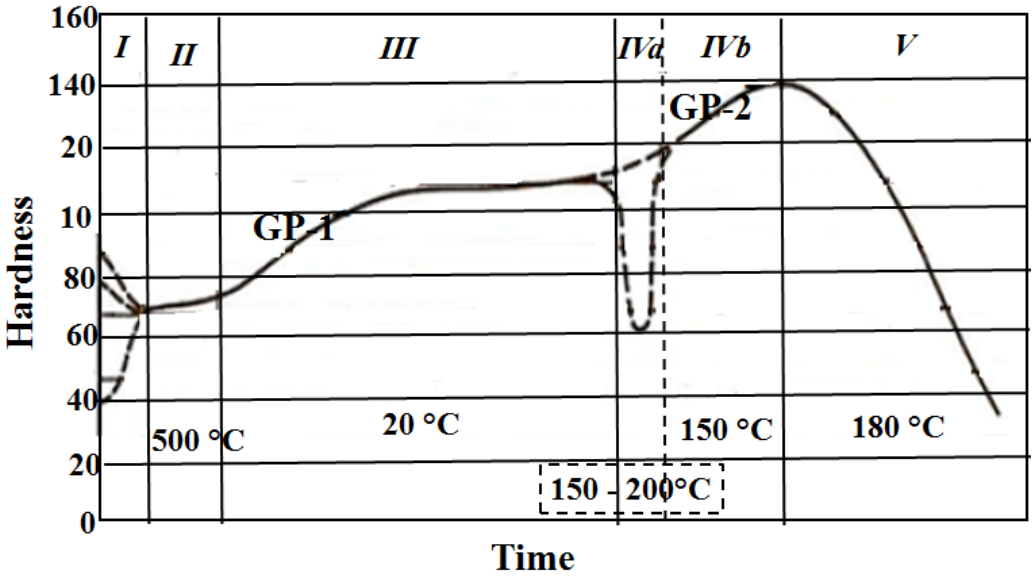

Figure 2.3: Correlation of ageing time and hardness for Al-4%Cu alloy

There are five stages of microstructural changes during heat treatment. The first stage is representing microstructure before solution heat treatment. In stage II, precipitated copper atoms are dissolved at 500 °C. After quenching the material to room temperature, stage III represents the natural aging sequence. In this stage copper-loaded coherent precipitation GP-1 zones (Guinier–Preston zones) are formed. The GP-1 zones, which are small, do not grow any further with subsequent artificial aging but are, instead, reversed into solution for a short while at 150-200 °C. The hardness also is momentarily decreased and is represented as stage IVa. Stage IVb refers the artificial aging at 150 °C which makes it possible to form GP-2 zones. Further aging at elevated temperature results in the formation of metastable phase θ′. The curve from the graph shows that maximum hardness is achieved when GP-2 zones are formed and when mixtures of GP-2 and θ′ occur. Over aging takes place when there are only θ′ precipitates in the structure and hence, hardness, strength and elongation decreases dramatically. Further aging at temperatures between 170-300° C forms coarse $CuAl_2$ precipitates that causes the aluminium alloy to be soft and therefore increases the toughness (William and Callister 2004).

The precipitation sequence of an Al-Cu alloy during the aging process is well documented (Eskin 2003; Son et al. 2005) and presented below:

Supersaturated α → GP1 zones → GP2 zones (θ″ phase) → θ′ phase → θ phase ($CuAl_2$).

The effects of aging treatment on the microstructure and mechanical properties of Al-Si casting alloys were examined and discussed in several studies. Drouzy et al. studied the influence of aging temperature and time on the tensile properties of Al-7Si-Mg casting alloy, and observed that in the under-aged condition the UTS increases while elongation decreases. In the over-aging conditions, it is found that the UTS and elongation reduces with increased aging time (Drouzy et al. 1980). Muzaffer Zeren studied the effect of heat treatment on different grades of piston alloys containing 11-23 wt.% Si, 0.5-5.5 wt.% Cu, 0.6-1.3 wt.% Mg and 0.5-3 wt.% Ni. The solution treatment of the specimens are conducted at 500 °C for 5 h, quenched in cold water and ageing treatment was carried out at 180 °C for 9 h. It is

found that the ageing treatment resulted in improved hardness due to formation of GP zones in the early stage of ageing. The highest UTS of 280 MPa is obtained after heat treatment while highest % elongation of 3.9% is found in as-cast condition (Zeren 2007). Yasmin and others studied the wear properties of 12Si-2Cu-0.14Mg after heat treatment. The specimens were subjected to heating at 535±5 °C for 8 h, water quenching and ageing for 8 h at 170±2 °C. The wear studies indicated the increase in wear with an increase in rotational speed, sliding distance and input weight for both as-cast and heat treated specimens. The volumetric wear rates and specific wear rates were also increased with increase in rotational speed of both specimens. However, with the increase in input weight and sliding distance both volumetric wear rates and specific wear rates showed a decreasing trend (Yasmin et al. 2004).

Kezhun et al. (2012) conducted characterization of precipitates of Al-17.5Si-4.5Cu-1Zn-0.7Mg-0.5Ni alloy by ageing the test samples for 4-6 h at different temperatures. Specimen aged at 150 °C for 16 h exhibited a peak UTS of 396 MPa. The study found that the peak strengthening of the alloy was due to the homogeneous distribution of fine plate shaped θ″ phase within the matrix. (Kezhun et al. 2012). In the review of optimization of solutionizing the cast Al–Si–Cu alloys, the authors have identified the need and importance of considering the entire treatment process to obtain the optimum material properties (Sjölander and Seifeddine 2010).

2.7 Characterization

Many researchers have carried out characterization studies to understand the effect of Si % in Al-Si alloys (Andrews et al. 1985; Okabayashi and Kawamoto 1968), the influence of Cu content in Al-Si-Cu alloys (Zeren 2005; Palta et al. 2012), the role of modifiers and grain refiners (Samuel et al. 2015; Sigworth 2008) and the effect of heat treatment on Al-Si-Cu alloys (Samuel 1998; Shabestari et al. 2004). Material characterization includes chemical analysis, metallography and mechanical testing including tensile strength and wear studies.

2.7.1 Tensile Strength

As the silicon % in the Al-Si alloy increases, the strength of the alloys also increases up to the eutectic composition, after which a decline in properties is observed due to crack propagation and this is due to primary Si particles. However, with increasing silicon content, the hardness increases and the elongation (%) decrease continuously. This is due to the size, shape and distribution of silicon particles in the cast structures up to the eutectic composition. Silicon is present as fine particles and is uniformly distributed in the structure up to 12.5% Si, and hence, the strength properties are increased (Torabian et al. 1994). Caceres et al. conducted a comparative study to examine the effects of Si, Cu, Mg, Fe and Mn, and solidification rate on Al-Si-Cu-Mg alloys to assess the strength and ductility of alloys. It is found that the strength increases proportionally with Cu and Mg content. The increase of Fe is also responsible for decreased strength and ductility of low-Si alloys (Caceres et al. 2003).

For Al-Si-Cu alloys, dense areas of Cu atoms with diameters between 3-5 nm constitute the GP zones formed at room temperature. Temperature above 100 °C causes dissolution of these GP zones, which is replaced by θ″ phases (also stated as GP2). Before the formation of the θ″ phase noticeable strength reductions are observed. Extended ageing causes the θ″ phase to change into the metastable θ′, which is partially coherent with the matrix. The formation of the stable incoherent equilibrium phase θ ($CuAl_2$) is formed during the last stage of ageing. Strength is proportional to the fraction of θ″ phase present in the matrix (Hatch 1984).

2.7.2 Wear

Wear of materials occurs by different mechanisms based on the operating conditions and the geometry of the wearing bodies. Accordingly, wear classification is based on the mechanical aspects and on the chemical factors. Wear of a material is controlled by the material characteristics as well as test parameters such as applied

pressure, sliding speed, environment and type of sliding interaction. Barwell (1957) classified wear into the following major groups:

- Adhesive wear
- Abrasive wear
- Corrosive wear
- Surface fatigue and
- Erosive wear

2.7.2.1 Adhesive Wear or Sliding Wear

Adhesive or sliding wear occurs as a result of relative sliding between two surfaces under the influence of an applied load. In general, at microscopic levels, machined surfaces are not perfectly flat but consists of sharp asperities. When two solid surfaces are brought in close proximity, the two surfaces would be touching only at a few points. They adhere strongly to each other and form asperity junctions. As the contact area is very small, the pressure exerted on each asperity is extremely high. This results in elastic and plastic deformation of the softer of the two materials in contact, until the area of the contact junctions is large enough to support the load. If the strength of the junction is more than the shear strength of the softer material, then during sliding action the tangential force will shear the softer junctions and leave clean surface at the softer asperity (Bowden and Tabor 1954). The consequences of the above process result in the transfer of softer material to the harder counterface (Burwell and Stang 1952). There is every possibility that the transferred material may remain adhered to the harder surface or in subsequent sliding may get knocked down resulting in loose wear debris. The possibility of the softer material either to adhering or getting knocked off from the harder surface has been explained with the help of an energy model as shown by Davies (Davies 1953). The energy model states that the adhered material will get detached from the harder surface only when the residual energy of the transferred material is more than the adhesional energy. The residual energy is accumulated by the way of repetitive collisions. The morphology of these transferred materials has been studied by Chen and Rigney. Their results indicate that

initial transfer events form discrete fragments and on prolonged sliding give rise to layer or patches, mainly consisting of finely mixed material on the surface (Chen and Rigney 1985).

Formation of oxide films on the tribo-surfaces during sliding wear has been the subject of many investigators (Kragelskii 1965). Such oxide films retard further material loss and alter the friction and wear behaviour of sliding materials. Balau (1981) has discussed various processes that may cause transition in the friction and wear behavior. Some of these processes are: (i) metal transfer, (ii) film formation, (iii) degrees generation and (iv) cyclic surface deterioration.

In addition to the above, the temperature and the nature of the sliding surfaces profoundly affect the quantity of transferred material. It has been pointed out that the high temperature of the sliding assembly increases and accelerates adhesive wear. The temperature of the sliding assembly may also be enhanced by way of frictional heating. It has been reported that during adhesive transfer, a material produces a spot on the surfaces which effectively increases the friction and then the rate of heating. This consequently raises the temperature and leads to heavy damage to the sliding materials. Santanam has made attempts to study the dependence of wear rate on temperature of the sliding surfaces. The microstructure of the material at or below the wear surface i.e. in the sub surface regions is reported to change due to sliding wear and the extent of this change in microstructure depends upon the sliding conditions and properties of the sliding materials (Santanam 1983).

2.7.2.2 Abrasive wear

Abrasive wear is caused by ploughing or cutting action of hard particles on a relatively softer surface of the material. The hard particles maybe either loosely held between two sliding surfaces as in three-body abrasive wear or part of the second surface as in two-body abrasive wear using abrasive papers. In some cases, the abrasive particle causes damage to the specimen through impact assisted abrasion. This mode of wear is known as gouging abrasion.

In abrasive wear, the surface of softer metal is ploughed by hard abrasive particles or wear particles or hard asperities of the counter face. In this type of wear, the harder the material the lesser will be the wear rate. The wear particles generated by the abrasive mechanism resembles metal chip generated by cutting action (Suh 1981).

2.7.2.3 Surface Fatigue Wear

Surface fatigue wear is caused by the removal of particles from the surface due to cyclic loading. This is associated with the surfaces in rolling contact, where the friction coefficient is negligible. Wear due to fatigue can also occur during sliding operation by way of cyclic crack growth (Kimura 1981). The wear mechanism is mainly governed by the formation of surface or sub surface cracks and fatigue crack propagation. The process of crack nucleation in rolling contact fatigue is similar to the fatigue wear due to sliding action. The main difference is that in sliding wear the plastic zone is extended to the surface, whereas in rolling contact, the plastic zone is surrounded by elastic regions.

2.7.2.4 Fretting Wear

In fretting wear, the interface undergoes a small oscillatory motion which results in wear of materials. The wear coefficient in this case depends on the amplitude of oscillation, when the relative displacement at the interface is less than a critical value. At large amplitudes of oscillation, the fretting wear coefficient approaches that of unidirectional sliding wear (Suh 1981). Although wear has been classified into the above distinct types, in real situations several types of wear can occur simultaneously. In fact, Rigney and Glaeser (1978) have stated that plastic deformation on a microstructural scale is prevalent in all wear processes and the understanding of debris formation requires a clear knowledge of all possible wear mechanisms. The development of a tribo-material would therefore require a systems

approach involving the materials characteristics and the types of wear a tribo-component is likely to experience in practice.

2.7.3 Factors Influencing the Wear

The concept of wear involves the presence of small particles between the contacting surfaces. It is possible that the abrading particles first penetrate the metal and then cause tearing of the surface introducing surface stress cracks, which lead to the ultimate break down of the surface. The main factors that influence wear and friction are listed below (Balu 1981):

- Variables connected with metallurgy:
  Hardness, Toughness, Constitution and Structure
- Variables connected with service:
  Contacting material, Normal pressure, Sliding speed and Temperature
- Other Factors:
  Lubrication and Corrosion

2.7.4 Wear Characteristics of Al-Si alloys

The wear characteristics of Al-Si alloy depends mainly on the microstructural features of the material such as shape, size and distribution of micro constituents in the matrix and operating conditions such as sliding speed, load, temperature and sliding distance. Based on surface and subsurface observations on the worn out samples of eutectic and hypereutectic Al-Si alloys, Clarke and Sarkar have reported the formation of craters (Clarke and Sarkar 1981; Sarkar and Clarke 1982). Two types of delamination process have been reported to be responsible for producing craters. These have been termed primary delamination and secondary delamination. Cracks that have nucleated in the sub surface regions terminated at the surface give rise to primary delamination wear. The authors have also reported the existence of cracks running parallel to the wear surface in the subsurface regions. Their observations on the surface of worn out samples have shown that the incipient delamination giving

rise to craters is associated with transverse cracks. Once initial fracture occurs by primary delamination the surface deterioration occurs on already weakened areas due to surface forces, which would result in the removal of material through a series of delamination.

Krishna Kanth et al. have investigated wear mechanisms in hypereutectic Al-17Si alloy (Krishna Kanth et al. 1990). It is mentioned that in this alloy also an initial compacted layer on the pin surface exists similar to the one reported (Suh 1978) in case of hypoeutectic Al-Si alloys. Delamination and abrasion are concluded to be the main mechanisms to contribute for the removal of material in the micro wear region. Torabian et al. have reported that the debris generated in the mild region contains mostly oxides such as alumina, silica and iron oxide. Based on the observations on worn out surfaces they have concluded that the oxide debris is produced by cracking of oxide surface layers (Torabian et al. 1994).

Wear rates in the severe wear region are many times higher than that in the mild wear region and metal to metal contact exists in the region. Shivnath et al. (1977) have reported that, when yield strength of the surface layer is exceeded then plastic deformation occurs with the transfer of material from the pin to the counter face. Oxide formation in this region is difficult because of the rate of material removal exceeding the rate at which oxide formation occurs.

Studies on dry sliding wear properties of Al-Si alloys have been conducted to optimize silicon content for maximum wear resistance, to determine wear transition loads of Al-Si alloys as a function of silicon content and to understand the mechanisms of material removal in these alloys during sliding (Torabian et al. 1994). Effects of silicon particle size on wear resistance have also been studied by varying the silicon particle size in 12.6% Si alloy (Okabayashi and Kowamoto 1968). The authors performed the unidirectional sliding experiments on four different Al-Si alloys with silicon content of 8.4%, 11.7%, 15% and 21.6%. All the alloys were tested in the as-cast condition. The studies revealed that the wear resistance of 21.6% Si alloy is maximum when compared to other three alloys. Further, it is noticed that Si

particle size in the range 26-73 μm does not influence the wear rate of Al-21.6% Si alloy. They have attributed low wear of 21.6% Si alloy to hardened high spots, which have been formed on the surfaces of the alloy due to the adhesion of debris. Another study by Stonebrook (1960) has revealed that it is the quantity rather than the size of the silicon particles which controls wear rate. He has further concluded that high silicon content is always desirable for improved wear resistance. Many authors have investigated the influence of alloying elements on tribological properties of Al-Si alloys (Dwivedi et al. 2004; Lozano et al. 2009). An addition of Al-1Ti-3B (grain refiner) and Al-10Sr (modifier) master alloys to eutectic Al-Si alloys and its influence on dry sliding wear behaviour has been studied (Chandrashekharaiah et al. 2009). The studies revealed that the wear resistance of eutectic Al-Si alloys improved after modification and grain refinement. The studies on wear behaviour of Al-12Si alloy reinforced with TiB_2 particles showed that these particles played a vital role in reducing the size of Si particles and minimizing the subsurface crack propagation resulting in improved wear resistance (Mandal et al. 2009).

Copper is another important alloying element in Al-Si alloys among the elements used in production. It imparts heat treatability to castings through the formation of $CuAl_2$ and enhances mechanical properties remarkably (Caceres et al. 2003). Al–Si–Cu alloys with up to 4.5% copper are satisfactory for ordinary conditions of service. An addition of 1% copper in these alloys increases the transition load by 3–4 times by increasing the strength and stability of protective surface layer (Das et al. 1989). Effect of adding 1, 2 and 4 wt.% Cu to Al-12 Si-20Mg cast alloys on its wear and corrosion properties have been studied (Palta et al. 2012). The studies showed that the addition of Cu led to the formation of $CuAl_2$ phase. Adding Cu to the Al-Si alloy exhibited increased hardness values. Wear behaviour of hypereutectic Al–Si–Cu–Mg casting alloys with 6 wt.% and 10 wt.% Mg using dry sand rubber wheel (Alireza et al. 2010). Alloys with high Mg content showed improved wear resistance. Microstructural investigations indicated that the intermetallic Mg_2Si particles in Al-Si alloys with 6% and 10% Mg addition are more solidly bonded to the matrix compared to the coarse primary silicon particles. The effect of addition of Cu on wear behaviour of Al-18Si-0.5Mg alloys has been

investigated (Dwivedi et al. 2004). The study showed that the wear rate is not appreciably affected with addition of Cu. However, the addition of copper increased the transition load at 2.0 m/s sliding speed. Addition of Cu more than 2%, did not show any effect on the transition load.

Chandra Sekhar Rao et al. investigated the effect of melt treatment by adding Al-1Ti-3B grain refiner, Sr and P modifiers to Al-15Si-4Cu cast alloys and concluded that the improvement in wear resistance of melt treated alloy is due to grain refinement and fine $CuAl_2$ particles found in interdendritic region (Chandra Sekhar Rao et al. 2012).

Prasad et al. (1998), investigated the role of shape and size of Al-Si particles on sliding wear behaviour of LM-13 and LM-29 alloys. Wear tests were conducted with varying speeds and loads. Studies revealed that the wear behaviour of test alloys was influenced by the presence of primary silicon particles and was a function of their size. Samples with identical micro constituents but with refined micro structures exhibited better wear characteristics.

2.8 Summary

Studies on the effect of grain refiner and modifier have been carried out to investigate the mechanical properties, but there appears to be ample scope for investigating on a comparison basis the microstructure, mechanical and tribological properties of hypoeutectic, eutectic and hypereutectic Al-Si alloys. It is also observed that extensive studies have not been devoted to systematically investigating the effect of addition of Cu on Al-Si alloys with varying quantity of Si representing hypoeutectic, eutectic and hypereutectic alloy.

Literature reveals that heat treatment is an important aspect for the improving mechanical properties of Al-Si-Cu alloys. The influence of melt treatment and heat treatment on the mechanical and tribological properties of Al-Si-Cu alloys considering the Si content and its distribution on ageing behaviour of Al-Cu alloys

has not been investigated in detail. Hence it is necessary that a comprehensive study comparing the effect of heat treatment on mechanical and wear properties of Al-Si-Cu alloys with varying quantity of Si in three different compositions i.e. hypoeutectic, eutectic and hypereutectic alloys is still important for industries.

As a result, the present work is focused on the melting and characterizing of hypoeutectic, eutectic and hypereutectic Al-Si alloys with and without the addition of copper. The present work is also aimed at studying the effect of combined modification and grain refinement and the effect of ageing on mechanical and tribological wear behaviour of these Al-Si-Cu alloys under various conditions.

2.9 Objectives of the Present Work

The objectives of the present research work are to investigate the microstructure and mechanical properties of as-cast, combined modified and grain refined and heat treated Al-Si alloys with and without copper additions and a comparison study will be made in detail. However, based on the literature survey the following specific objectives are designed:

1. To study the effect of 4.5 wt. % copper addition on microstructure, mechanical properties and wear behavior of hypoeutectic (7% Si), eutectic (12% Si) and hypereutectic (15% Si) Al-Si alloys.
2. To study the effect of combined addition of grain refiner (Al-1Ti-3B) and modifiers (Al-10Sr and Al-23P) on microstructural features, mechanical and wear properties of Al-Si and Al-Si-Cu alloys.
3. To study the microstructural changes caused due to T6 heat treatment of as-cast and modified and grain refined Al-Si-Cu alloys and its effect on their mechanical and wear properties.

2.10 Scope of the Present Work

The scope of the present work includes the preparation and characterization of Al-7Si, Al-12Si, Al-15Si, Al-7Si-4.5Cu, Al-12Si-4.5Cu and Al-15Si-4.5Cu alloys. A combined grain refinement and modification are carried out by the addition of 1 wt. % Al-1Ti-3B and 0.02 wt. % Sr to Al-7Si and Al-7Si-4.5Cu alloys and 1 wt. % Al-1Ti-3B and 0.04 wt. % Sr to Al-12Si and Al-12Si-4.5Cu alloys. In the case of Al-15Si and Al-15Si-4.5Cu alloys, in addition to the addition of 1 wt. % Al-1Ti-3B and 0.04 wt. % Sr, refinement of primary Si is achieved by the addition of 0.04 wt. % P.

The Al-Si-Cu alloys are subjected to T6 heat treatment as it offers the increase in hardness and other mechanical properties, which is often required for many applications. All of the experimental alloys are characterized by optical microscopy, SEM / EDX analysis. The influence of (i) combined grain refinement and modification, (ii) addition of 4.5 wt. % of Cu and (iii) heat treatment on hardness, strength and wear properties are also studied.

2.11 Problem Statement

In view of the scope defined above the present research work is defined as

'EFFECT OF AGEING ON THE MICROSTRUCTURE AND MECHANICAL PROPERTIES OF Al-Si ALLOYS WITH COPPER ADDITIONS'.

Chapter 3

Experimental Details

3.1 Introduction

This chapter, details the materials, experimental procedures and the heat treatment procedures adopted for this investigation. The following experimental work is planned and executed in the following sequence to fulfil the objectives of the present research work.

1. Selection of alloy and confirmation of chemical composition.

2. Preparation of castings of Al-7Si, Al-12Si, Al-15Si alloys with and without modification and grain refinement

3. Preparation of castings of Al-7Si-4.5Cu, Al-12Si-4.5Cu, Al-15Si-4.5Cu alloys with and without modification and grain refinement

4. T6 heat treatment of Al-7Si-4.5Cu, Al-12Si-4.5Cu and Al-15Si-4.5Cu cast alloys with and without modification and grain refinement.

5. Microstructural characterization of all the above alloy systems.

6. Mechanical property and dry sliding wear studies were carried out for alloy systems.

Material Processing Flow charts for the alloy systems are shown as Figure 3.1 and 3.2

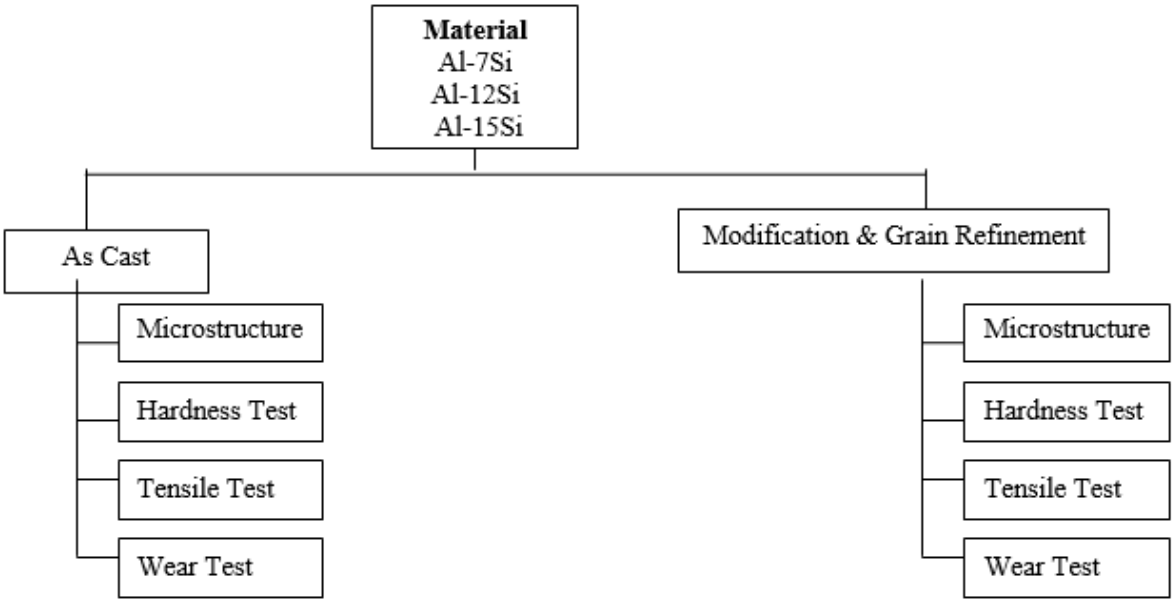

Figure 3.1 Processing flow chart for Al-7Si, Al-12Si, Al-15Si alloys

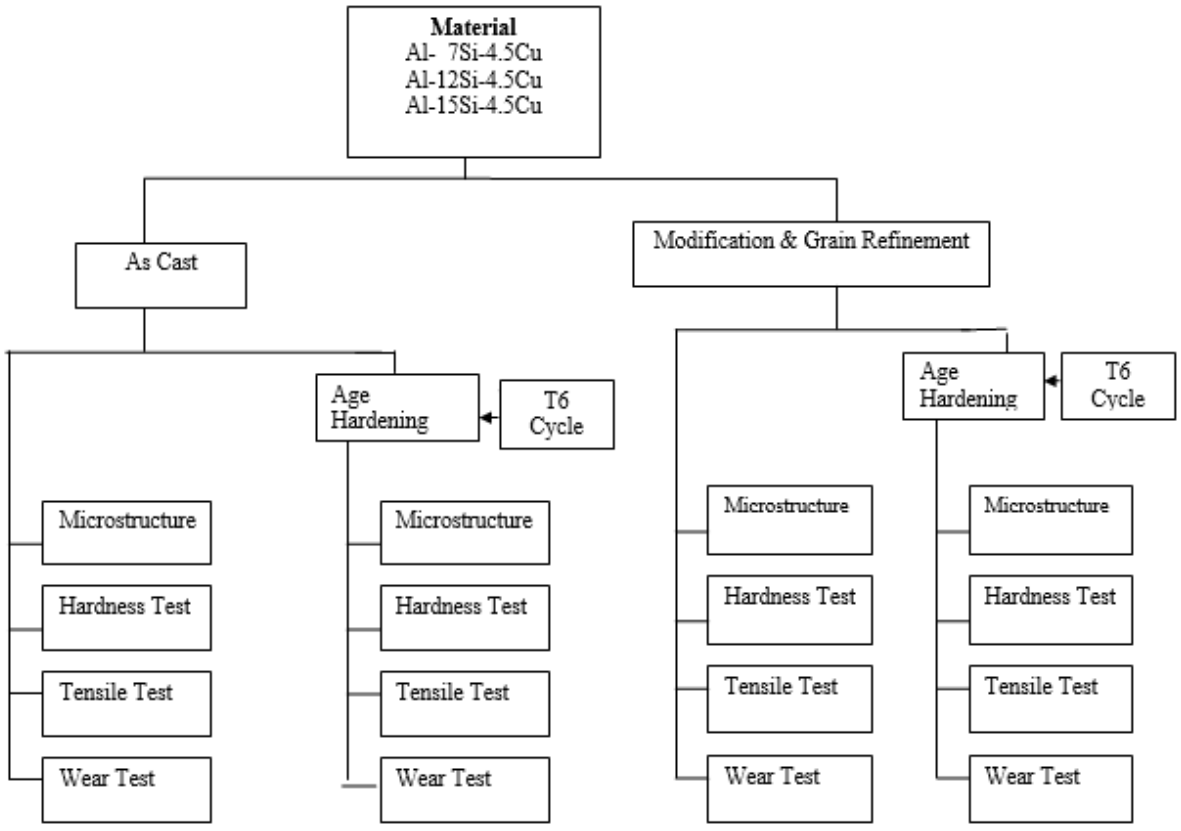

Figure 3.2 Material Processing flow chart for Al-7Si-4.5Cu, Al-12Si-4.5Cu and Al-15Si-4.5Cu alloys

3.2 Raw materials

The basic raw materials in the form Al-7Si, Al-12Si and Al-15Si alloys in ingot form and Al-10Sr master alloy (modifier) and Al-1Ti-3B master alloy (grain refiner) were procured from M/s Fen Fe Metallurgicals, Bangalore, India. Aluminium phosphide (grain refiner for hypereutectic Al-Si alloy) and pure copper was procured from M/s Leo Chem, Bangalore, India.

3.2.1 Chemical Analysis

The chemical analysis of modifier and grain refiner used for the studies are carried out using Flame Atomic Absorption Spectrometer (Model: AA 240 of Varian, Netherlands) and recorded composition in wt. % are given in Table 3.1, Table 3.2 and Table 3.3, respectively.

Table 3.1: Chemical composition of Al-1Ti-3B master alloy

Alloy Composition	**Composition (wt. %)**				
	Ti	**B**	**Fe**	**Si**	**Al**
Al-1Ti-3B	1.10	2.28	0.17	0.18	Balance

Table 3.2: Chemical composition of Al-10Sr master alloy

Alloy Composition	**Composition (wt. %)**			
	Sr	**Fe**	**Si**	**Al**
Al-10Sr	9.96	0.09	0.16	Balance

Table 3.3: Chemical composition of Al-23P

Alloy Composition	Composition (wt. %)			
	P	Fe	Si	Al
Al-23P	22.96	0.07	0.09	Balance

3.2.2 XRD and SEM studies on Al-1Ti-3B master alloy

X-ray diffraction studies were performed on Al-1Ti-3B master alloy in order to identify the phases present. For this purpose, the master alloys were cut in to 5 x 10 x 5 mm^3 in size and and metallographically polished. XRD studies were carried out using a JEOL X-ray diffractometer using CuK_α radiation. Figure 3.3 shows XRD of Al-1Ti-3B master alloy. Indexing of the XRD patterns on Al-1Ti-3B master alloy showed the presence of AlB_2 phase in addition to α-Al phase.

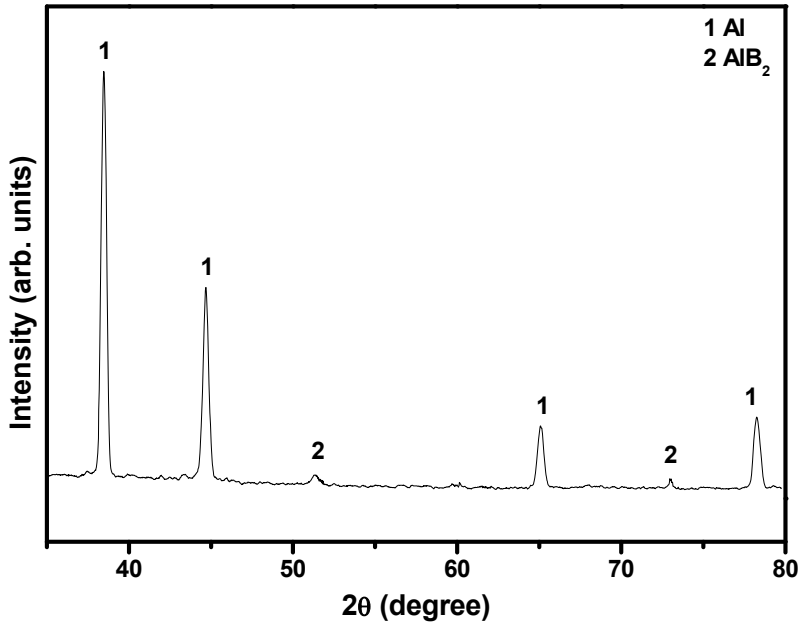

Figure 3.3: XRD patterns of Al-1Ti-3B master alloy

The 2θ range from 20-80° was selected such that all the major intense peaks of the phases expected were covered. However, the peaks of TiB_2 particles were not observed and the reason for this could be due to possibility of overlapping of the AlB_2

peaks with that of TiB_2 because of the similar crystal structures (hexagonal) and lattice parameters (for TiB_2 a = 0.3038 nm and c = 0.3292 nm and for AlB_2 a = 0.3009 nm and c = 0.3262 nm).

Figure 3.4 shows the SEM micrograph of Al-1Ti-3B master alloy featuring the distribution and morphology of aluminium boride particles in an aluminium matrix. Particles acquire a definite shape resembling hexagonal morphology of boride particles.

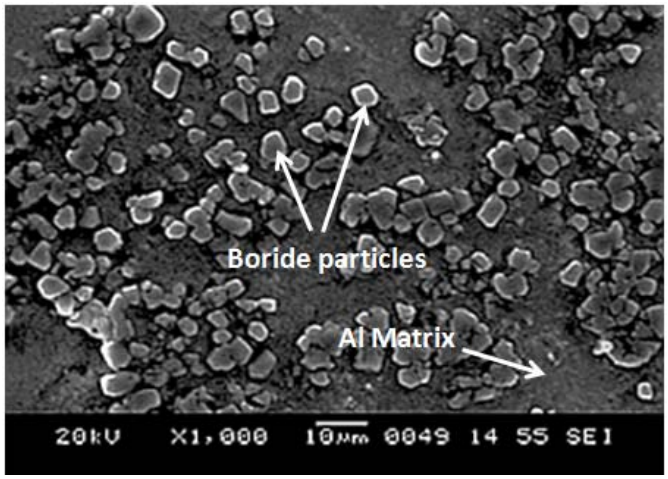

Figure 3.4: SEM micrograph of Al-1Ti-3B master alloy

Energy Dispersive X-Ray Spectroscopy (EDX) allows one to identify the elements present in the alloy and their relative proportions (Atomic % for example). Figure 3.5a and b show EDX spectra obtained from AlB_2 and TiB_2 particles present in Al-1Ti-3B master alloy. Figure 3.5a depicts the EDX spectrum obtained at the centre of a hexagonal particle and shows the presence of Al and B peaks, suggesting that these are AlB_2 particles. EDX spectrum presented as Figure 3.5b taken at the edge of the TiB_2 particle shows the presence of both Ti and B apart from Al. Absence of Ti in the centre of the particle rules out the possibility of forming a solid solution of AlB_2 and TiB_2. Presence of Ti at the edge of a particle suggests that possibly TiB_2 particle remain separately attached to the AlB_2 particles. In other words, both AlB_2 and TiB_2 co-exist and Ti:B ratio is less than 0.5, which should promote the formation of

Al/TiB_2. However, TiB_2 particle could not be identified separately which possibly means that a layer of Al_3Ti may surround the AlB_2 particles.

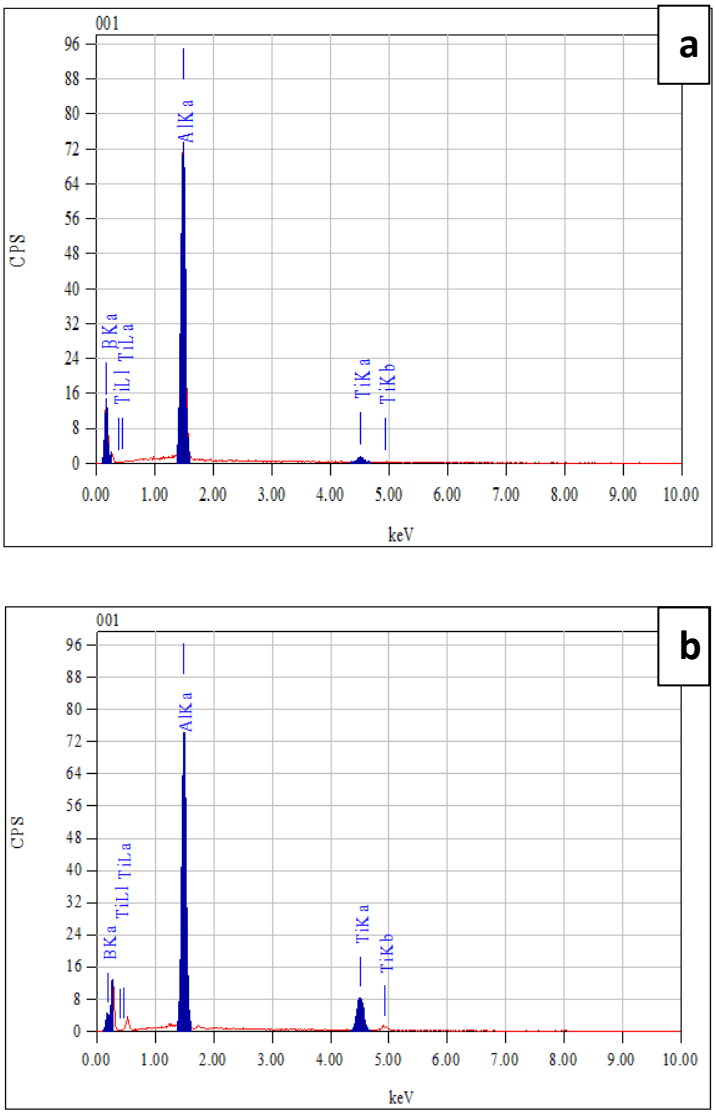

Figure 3.5: EDX spectrum of (a) AlB_2 particle and (b) TiB_2 particle of Al-1Ti-3B master alloy

3.2.3 XRD and SEM studies on Al-10Sr master alloy

Al-10Sr master alloy was subjected to XRD investigations. Figure 3.6 illustrates the XRD pattern of Al-10Sr master alloy. The presence of α-Al and Al_4Sr phases can be seen from the XRD results. The results are in confirmation with phase

diagram that the composition of Al-10Sr master alloy should contain Al_4Sr particle along with α-Al phase (Gruzleski 1999).

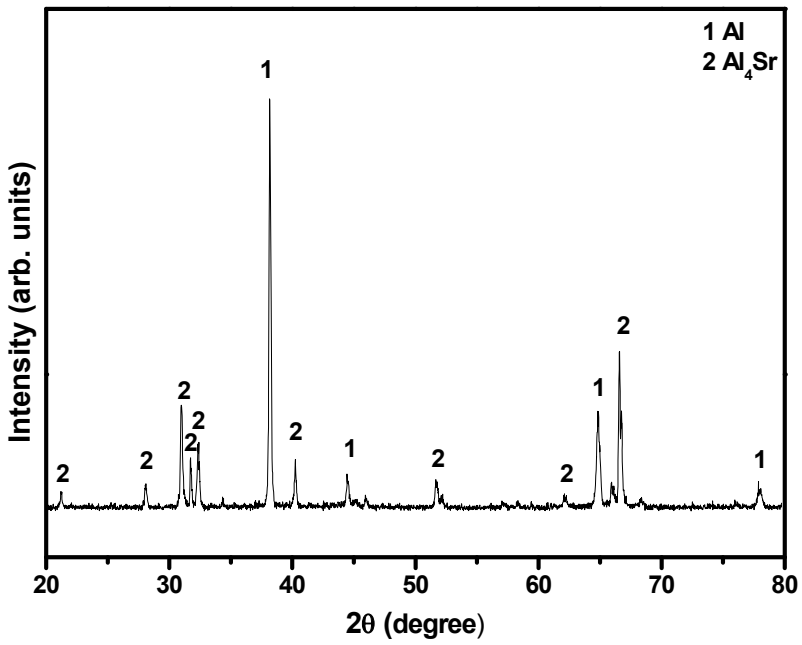

Figure 3.6: XRD patterns of Al-10Sr master alloy.

Figure 3.7 shows the metallographic morphology and size distribution of Al_4Sr particles in Al-10Sr alloy. The Al_4Sr particles exhibited shapes of rectangular stripes and plates. These particles are found to be homogenously distributed in α-Al matrix.

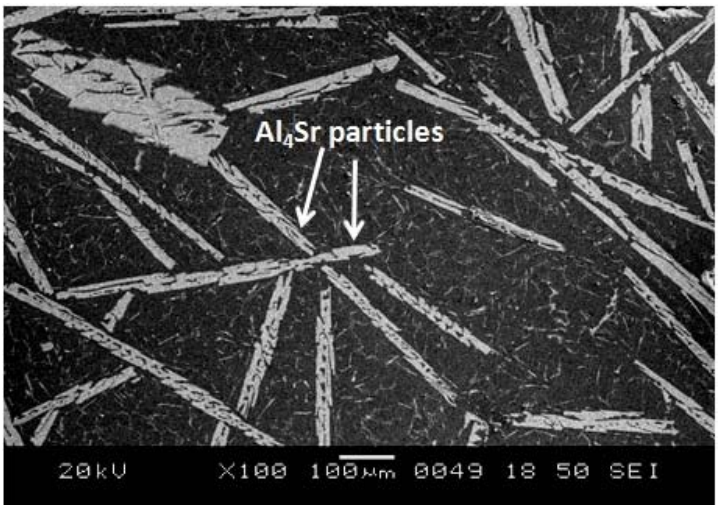

Figure 3.7: SEM micrograph of Al-10Sr master alloy

Figure 3.8 shows the EDX spectrum of Al-10Sr master alloy indicating the elemental composition of the material. Presence of Al and Sr peaks can be clearly seen from the EDX spectrum.

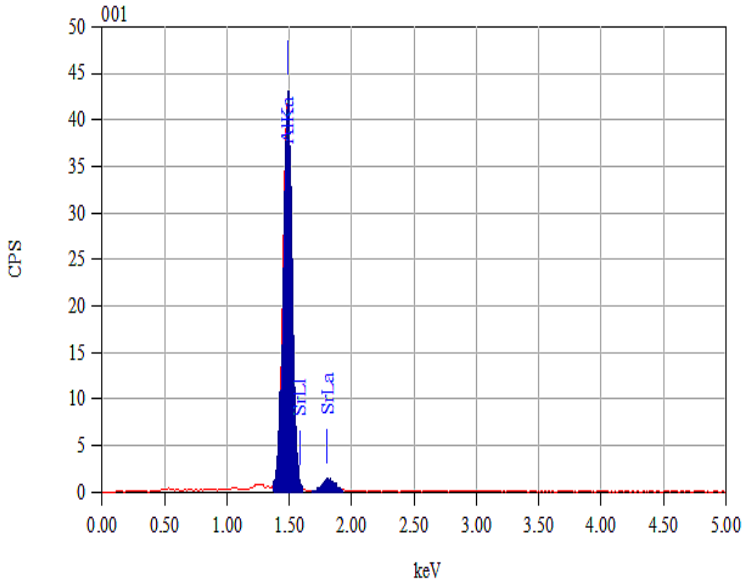

Figure 3.8: EDX spectrum of Al-10Sr master alloy

3.3 Preparation of as-cast (Al-Si / Al-Si-Cu) alloys

Al-7Si, Al-12Si and Al-15Si alloys were prepared by melting the respective ingots using clay graphite crucible in a resistance furnace shown in Figure 3.9a and b. The furnace can accommodate 0.5 Kg of melt and attain a maximum temperature of 1100 $^{\circ}$C. The furnace temperature was controlled with in an accuracy of ±5 $^{\circ}$C using a digital temperature controller with a thermocouple. The melt was held at 720 $^{\circ}$C for Al-7Si and Al-12Si alloys, and at 780 $^{\circ}$C for Al-15Si alloy. The melt was degassed with 1% solid hexachloroethane (C_2Cl_6) degasser before pouring into a split type preheated cast iron mould shown in Figure 3.9c. Similar melting practices are followed for preparing Al-7Si-4.5Cu, Al-12Si-4.5Cu and Al-15Si-4.5Cu as-cast alloys. Pieces of commercially available 99.9% pure copper wire were added to the melt so as to yield 4.5 wt.% of Cu in respective experimental alloy. Castings are prepared as per the experimental requirements and are shown in Figure 3.9d. These

castings are further machined to different test pieces as per the standard for carrying out microstructural studies, tensile, wear and ageing studies.

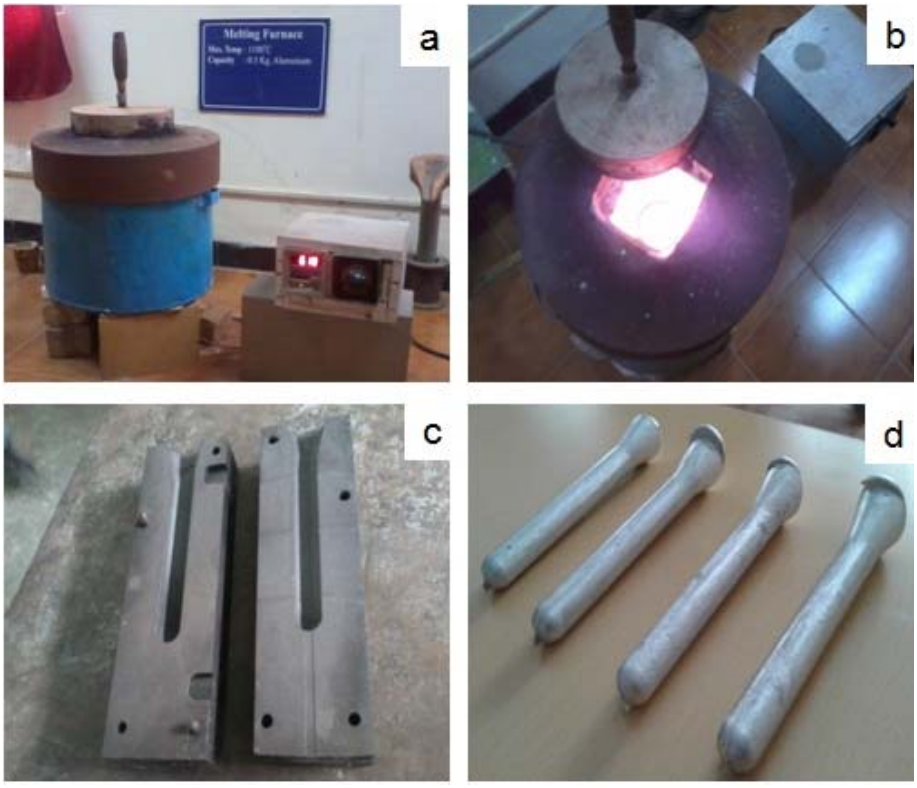

Figure 3.9: (a) Furnace with closed condition (b) Liquid melt inside the furnace (c) Cast iron mould (d) Castings produced after solidification

3.4 Combined grain refinement and modification

Grain refinement and modification of experimental alloys were carried out by the addition of appropriate quantity of Al-10Sr, AlP and Al-1Ti-3B as shown in Table 3.4. The melt was stirred for 30 s after the addition of grain refiner and modifier to ensure a homogenous reaction. Melt was held for additional 5 minutes before pouring into a split type preheated cast iron cylindrical mould. Hypereutectic Al-15Si alloys consisting of primary Si are effectively refined by the addition phosphorous. Hence, Al-23P was added as modifier to Al-15Si and Al-15Si-4.5Cu alloys. The chemical composition of these alloys is presented in Table 3.5.

Table 3.4-Additional levels of grain refiner and modifier

Alloy	Addition level of grain refiner (wt.%)	Addition level of modifier (wt.%)	
	Al-1Ti-3B	Al-23P	Al-10Sr
Al-7Si	1.0	--	0.2
Al-Si-4.5Cu	1.0	--	0.2
Al-12Si	1.0	--	0.4
Al-12Si-4.5Cu	1.0	--	0.4
Al-15Si	1.0	0.17	0.4
Al-15Si-4.5Cu	1.0	0.17	0.4

Table 3.5 - Chemical composition of experimental master alloys

Alloy	Composition									
	Si	Cu	Fe	Mn	Mg	Ti	B	Sr	P	Al
Al-7Si	7.06	.02	0.15	0.02	0.01	-	-	-	-	Balance
Al-7Si *	7.01	0.02	0.11	0.04	0.02	0.01	0.04	0.02	-	Balance
Al-7Si-4.5Cu	7.13	4.46	0.13	0.03	0.03	-	-	-	-	Balance
Al-7Si-4.5Cu*	7.09	4.53	0.14	0.04	0.03	0.01	0.03	0.02	-	Balance
Al-12Si	12.09	0.04	0.16	0.02	0.01	-	-	-	-	Balance
Al-12Si*	12.06	0.03	0.18	0.04	0.03	0.01	0.04	0.04	-	Balance
Al-12Si-4.5Cu	12.14	4.48	0.18	0.05	0.08	-	-	-	-	Balance
Al-12Si-4.5Cu*	12.11	4.56	0.14	0.03	0.06	0.01	0.03	0.04	-	Balance
Al-15Si	15.39	0.05	0.18	0.06	0.01	-	-	-	-	Balance
Al-15Si*	15.09	0.06	0.15	0.07	0.08	0.01	0.03	0.04	0.04	Balance
Al-15Si-4.5Cu	15.09	4.57	0.18	0.06	0.02	-	-	-	-	Balance
Al-15Si-4.5Cu*	15.8	4.56	0.18	0.05	0.01	0.01	0.03	0.05	0.04	Balance

*Modified and grain refined

3.5 Heat Treatment of Al-Si-Cu alloys

Al-Si-Cu alloys are subjected to T6 heat treatment to obtain improved mechanical properties. Figure 3.10 depicts the steps followed in T6 heat treatment for the precipitation hardening studies. For conducting heat treatment studies on Al-7Si-4.5Cu, Al-12Si-4.5Cu and Al-15Si-4.5Cu alloys, 25 mm Φ x 15 mm samples were prepared from each of the castings.

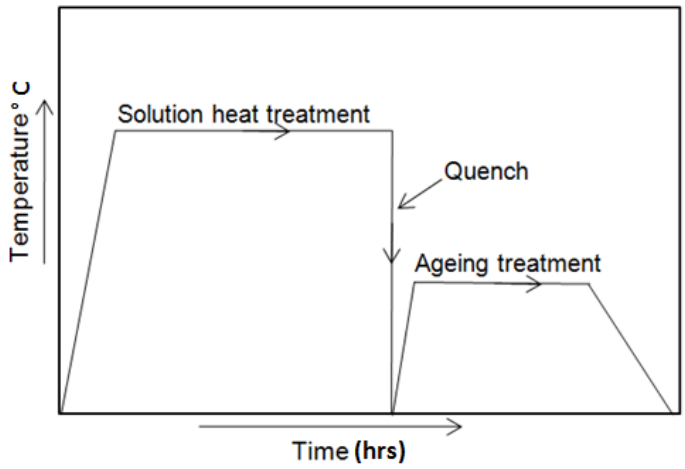

Figure 3.10 – Temperature Vs Time diagram showing T6 heat treatment cycle

Aging studies were carried out in order to obtain the peak hardness time. Specimen were solutionized for 6 h at 500 °C, quenched in water at room temperature and aged at 200 °C for various intervals of time. In this study, a calibrated electric resistance furnace with a variation of ± 5 °C was used for heat treatment of the alloys. Test specimens were subjected to solutionizing and ageing with specified parameters mentioned in Table 3.6 for obtaining precipitation hardening. The solutionizing and ageing parameters are selected based on the studies carried out by other researchers on Al-Si-Cu alloys (Tao Lu et al. 2014; Zeren and Karakulak 2009). Initially, solutionizing was carried at 500±5 °C for a period of 6 h. After solution treatment, samples from the furnace were taken out and dipped in water maintained at room temperature (~30 °C). The ageing treatment was carried out at 200±5 °C. After specified time interval, samples were taken out and hardness measurements were performed.

Table 3.6 – Solutionizing and ageing parameters

Heat Treatment	Temperature (° C)	Time (Hours)	Cooling medium
Solutionizing	500±5	6	Water (at room temperature)
Ageing	200±5	1, 2, 4, 6, 8, 12, 16, 20, 24, 28, 32, 36, 40, 44 and 48	Natural air

3.6 Characterization of Al-Si, Al-Si-Cu alloys

Characterizations of all experimental alloys are carried out for microstructural features, tensile and sliding wear properties. Test specimens of all alloy systems in as-cast condition, and after combined addition of modifier and grain refiner and finally after heat treatment are subjected to optical microscopy, grain size measurement, and microstructural characterization by SEM / EDX microanalysis. The specimens were also examined for hardness, tensile and wear properties. These are discussed in detail in following subsequent sections.

3.7 Microscopic studies

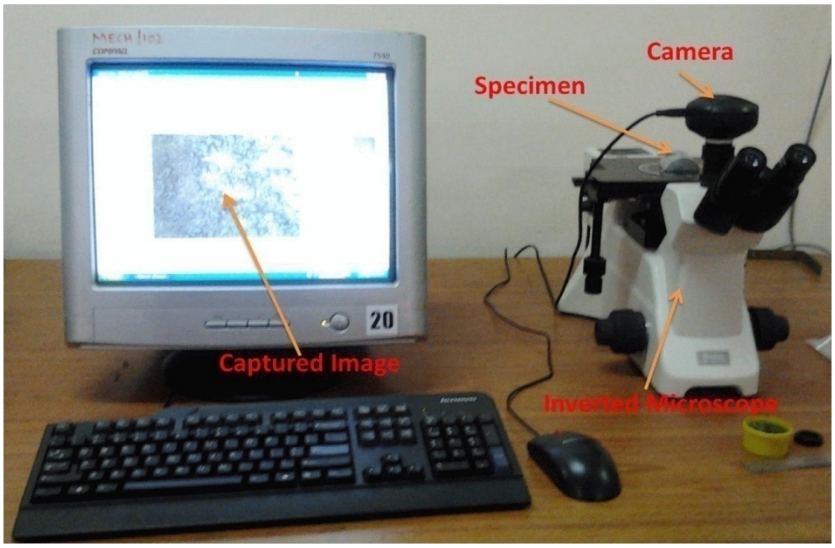

Figure 3.11: Inverted microscope interfaced with metalife software

The optical microscope used for microscopic studies is shown in Figure 3.11. An inverted microscope of Dewinter make interfaced with Metalife image analyzer software is used for microscopic studies. The experimental alloys were sectioned at a height of 25 mm from bottom and were taken for microstructural studies as shown in Figure 3.12.

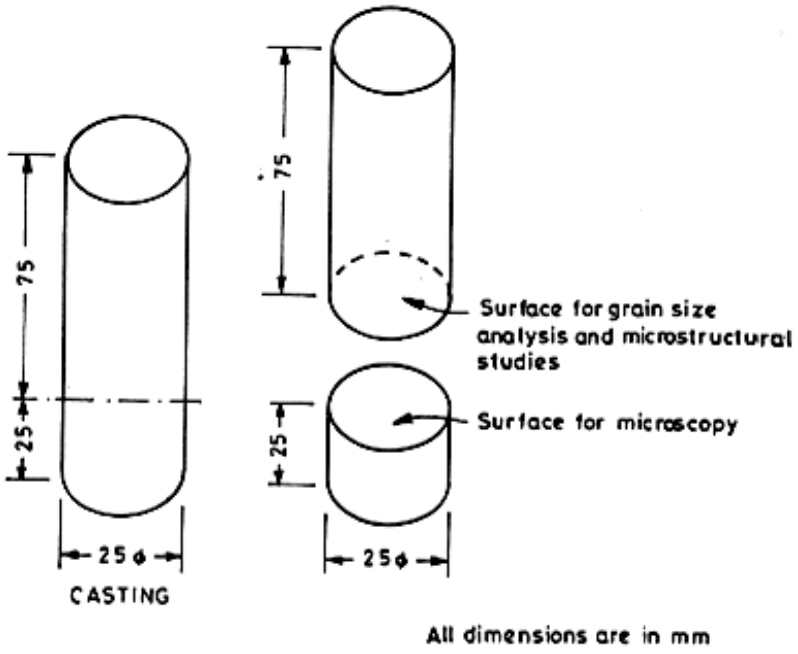

Figure 3.12: Sections selected for characterization by microscopy.

The sectioned surfaces were initially polished on a belt grinder and further on a series of SiC water proof emery papers with increasing grit size. Final stages of polishing was performed on a disc polisher using 7.5 μm Al_2O_3 paste with water until a scratch free mirror surface was obtained. The polished samples were then thoroughly cleaned with soap solution and ethyl alcohol followed by drying. The polished samples were etched with Keller's reagent (2.5% HNO_3 + 1.5% HCl + 1% HF + 95% H_2O by volume) for about 30-40s. The sample surface was cleaned with alcohol after etching. The samples were observed under an optical microscope. The standard linear intercept method was used to measure the grain size. Standard micron bars available with the microscope have been used to measure the number of grain boundaries intersecting the vertical and horizontal lines of the standard micron bar. In

order to obtain average grain size of each sample, over 100 readings per sample have been taken. Sufficient care has been taken to cover the various regions of the sample.

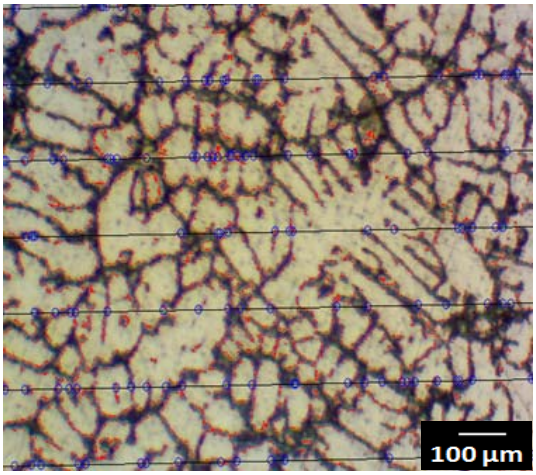

Grain Size Analysis: Results Summary

Fields measured	1
Analysed Area	0.086
Standard Area	ASTME112

Linear Intercept Procedure	
ASTM Grain Size	4.5
Intercepts	103
Mean intercept length (µm)	109

Figure 3.13 – Grain size measurement

3.8 Scanning Electron Microscopy/Energy Dispersive X-Ray analysis

A detailed microstructural examination of the as-cast, modified and grain refined and followed by heat treated samples were examined by using SEM (FEI Netherlands make Quanta−200). For SEM studies, the samples were polished in the similar manner to that for optical microscopic sample preparation. The samples were electrolytically polished and etched using an electrolytic polisher. The electrolytic bath consists of 39% orthophosphoric acid, 37% ethanol and 24% H_2O. The electro polishing was carried out for 5 min. at 50V and at room temperature. Polished samples were cleaned with soap solution, distilled water and ethyl alcohol followed with drying. The samples thus prepared were taken for SEM and EDX microanalysis. Microstructural and EDX analysis was carried out in order to identify the presence of intermetallics.

3.9 X-ray diffraction studies

X-ray diffraction studies were performed on Al-1Ti-3B and Al-10Sr master alloys in order to identify the phases present in these master alloys. XRD studies were carried out using a JEOL X-ray diffractometer using CuK_{α} radiation. The details of XRD studies are presented in section 3.1.2 and 3.1.3.

3.10 Mechanical Testing (Tensile and Hardness)

UTS, 0.2% proof stress and % of elongation of all alloy systems were evaluated. The tensile tests were conducted at room temperature using computer controlled tensometer, KIPL make, Pune, India, as shown in Figure 3.14. The machine is provided with load cells for high precision load measurements. 0.2 mm/s cross head speed is applied during the tensile test. All the tests were recorded and results were extracted through the built in software which automatically generates peak load and UTS.

Figure 3.14: Tensometer setup

An average of three readings was taken and average value is reported for each test condition. The dimensions of the tensile specimen used for testing are shown in Figure 3.15.

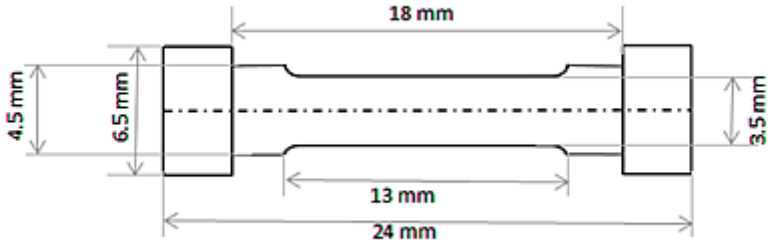

Figure 3.15: Schematic of the test specimen

Three specimens were obtained along the longitudinal directions from every casting. The specimens were machined to the dimensions as per ASTM E8M-91.

Hardness test is performed using Brinell hardness tester, as per ASTM E-10.In the Brinell hardness test, a hard spherical indenter is pressed under a fixed normal load onto the smooth surface of a material. When the equilibrium is reached, the load and the indenter are withdrawn, and the diameter of the indentation formed on the surface is measured using a microscope with a built-in millimeter scale. The Brinell hardness is expressed as the ratio of the indenter load to the area of the concave (i.e., contact) surface of the spherical indentation that is assumed to support the load and is given as Brinell Hardness Number (BHN) as shown in Eq 3.1

$$BHN = \frac{2F}{\pi D\left[D - \sqrt{\left(D^{2} - d^{2}\right)}\right]} \qquad 3.1$$

Where F is the constant load in kilograms, D is the diameter of the indenter in millimeters and d is the diameter of the indentation in millimeters which is the average value of d_1 and d_2 respectively. The schematic representation of the hardness test is shown in Figure 3.16.

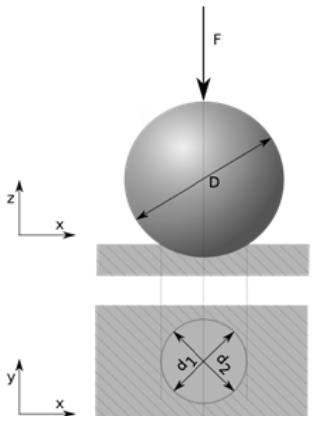

Figure 3.16: Schematic representation of indentation process

In the present work Brinell hardness Tester (model BV-120) is used which confirms to IS-Specification 1754. The specimen is cleaned from dirt and oil on the surface. In this test a ball indenter of diameter 5mm and a normal load of 15.625 kg are selected in accordance with ASTM E-10. Once the load actuation button is pushed the indenter swings due to its own weight and penetrates into the specimen. The load adjusted by means of push button becomes effective and forms the impression. The impression formed is lighted and displayed on the focusing screen.

3.11 Dry Sliding Wear Tests

Dry sliding wear tests were carried out at room temperature as per ASTM G99, using Pin-On-Disc type tribo meter (Model TR-20LE, Ducom, Bangalore, India). Schematic diagram of experimental set up is shown in Figure 3.17. Load was applied on a pin through pulley string arrangement. The system has maximum loading capacity of 200 N. The rpm and the sliding speed of the disc were 0-2000 rpm and 0-10 m/s respectively. The disc is made of En-32 steel (0.14%C, 0.18% Si, 0.52% Mn, 0.015% S, 0.019% P, 0.13% Ni, 0.05% Cr, 0.06% Mo, balance Fe), having dimensions of 160 mm diameter and 8 mm thickness with a hardness value of HRC65. During the test, recording of change in height of the specimen was recorded using a Linear Variable Differential Transformer (LVDT). Frictional force and

coefficient of friction were also recorded. The data acquired is processed using the Winducom software.

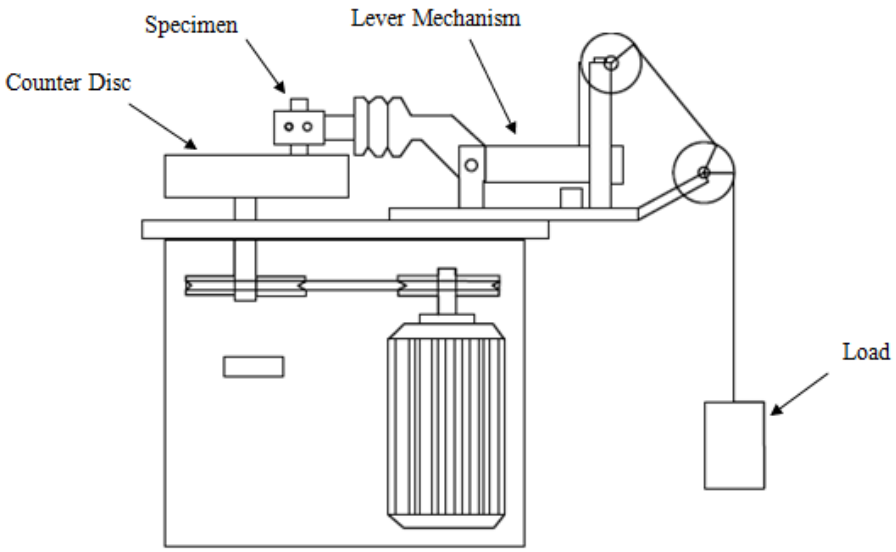

Figure 3.17: Experimental setup of dry sliding wear test

The sliding wear tests were conducted under varying loads (10, 20, 30 and 40 N) at a constant sliding speed of 2.0 m/sec for a constant sliding distance of 1500 m. The change in height of the specimen due to sliding wear and the coefficient of friction were measured continuously by electronic sensors. The LVDT used is capable of measuring with an accuracy of ± 1 µm. The load cell provided in the machine is capable of measuring a maximum load of 200 N and measures the frictional load with an accuracy of ± 0.1 N. Frictional force (N) and reduction in height of the specimen (µm) were measured as a function of sliding time. The volume loss and wear rates of the specimens were calculated from the wear data.

Chapter 4

Microstructural studies on Al-Si and Al-Si-Cu alloys

4.1 Introduction

The strength and wear resistance of Al-Si alloy castings is primarily a function of its microstructural features. The morphology, volume fraction, size and distribution of the primary phase and the eutectic constituent in the microstructure depend on the alloy composition and the solidification / casting process involved. For obtaining better performance characteristics, it is desired that these alloys solidify with fine equiaxed α-Al in hypoeutectic, primary Si in hypereutectic alloy and fine eutectic silicon. These features can be achieved by suitable grain refinement treatment (Cook et al. 1996) and modification (Massalsski 1990). A fine grain size ensures improved mechanical properties, improved feeding during solidification, reduced and more evenly distributed shrinkage porosity and good tribological properties (Collins 1972). Morphology of the eutectic silicon also plays an important role on the mechanical properties of Al-Si alloys. Silicon is a faceted phase and makes the Al-Si eutectic an irregular eutectic. The brittleness of silicon particles is the major reason for lowering mechanical properties of Al-Si alloys since the large eutectic silicon particles lead to premature crack initiation and fracture in tension conditions (Faraji and Katgerman 2009). Therefore, the objective is to achieve grain refinement as well as modification of eutectic silicon so that Al-Si alloys solidify with the fine primary grains and fine eutectic silicon.

There are industrial applications of Al-Si alloy such as engine blocks, cylinder heads and manifolds in which high material strength is predominant over its ductility. The addition of alloying elements such as copper and magnesium to Al-Si alloys is highly beneficial for such applications (Grosselle et al. 2010). Thermal treatments such as solutionizing, quenching and ageing play a vital role in improving the strength

of Al-Si-Cu alloy system. The strengthening of these alloys is achieved by the precipitation of copper rich phases during ageing heat treatment (Tash et al. 2007).

The influence of combined modification and refinement on as-cast Al-Si alloys, and the influence of Cu addition to Al-Si alloys in both as-cast and modified and refined condition are discussed in this chapter. Further, the effect of heat treatment on Al-Si-Cu is presented. Solutionizing is carried out at 500 °C to avoid risk of incipient melting of low temperature eutectic aggregates (Campbell 1991).

4.2 Al-7Si and Al-7Si-4.5Cu Alloys

4.2.1 Combined modification and grain refinement of Al-7Si alloy

Al-7Si alloys show α-Al with a coarse columnar grain structure as the major constituent with randomly dispersed elongated plates or lamellae of silicon in it. The microstructure evolution of hypoeutectic Al–Si alloys during solidification takes place in two stages: Formation of primary dendrite Al–phase (α–matrix) and the subsequent transformation of eutectic (eutectic Si particles in α–matrix). The eutectic silicon shows divorced morphology and this may be due to high interfacial energy between the two component phases (Gupta and Ling 1999). The eutectic silicon in untreated alloy exhibits coarse acicular or plate type shape with sharp edge and these flaked brittle particles are responsible for poor ductility and also for commencement and propagation of fracture resulting in the lowering of tensile strength, elongation and tribological properties of these alloys (discussed in next two chapters). To overcome this, the melt is treated with 0.2 wt.% Al-10Sr modifier and 1 wt.% Al-1Ti-3B grain refiner to achieve fine grain size and globular Si. Figure 4.1 shows the SEM micrographs of the alloy in as-cast condition and with combined addition of modifier and grain refiner. Microstructural details in Figure 4.1a shows the eutectic Si is in the form of needles. As seen in Figure 4.1b, with the combined addition of modifier and refiner the alloy shows refined α-Al and modified Si particles as globules. It is reported that apart from refinement of grain size, the refinement by treating the melt with grain refiners like Al-3Ti-1B provides a number of technical and economic

advantages such as reduced ingot cracking, better ingot homogeneity and reduction in susceptibility to hot cracking (Patel and Prajapathi 2012).

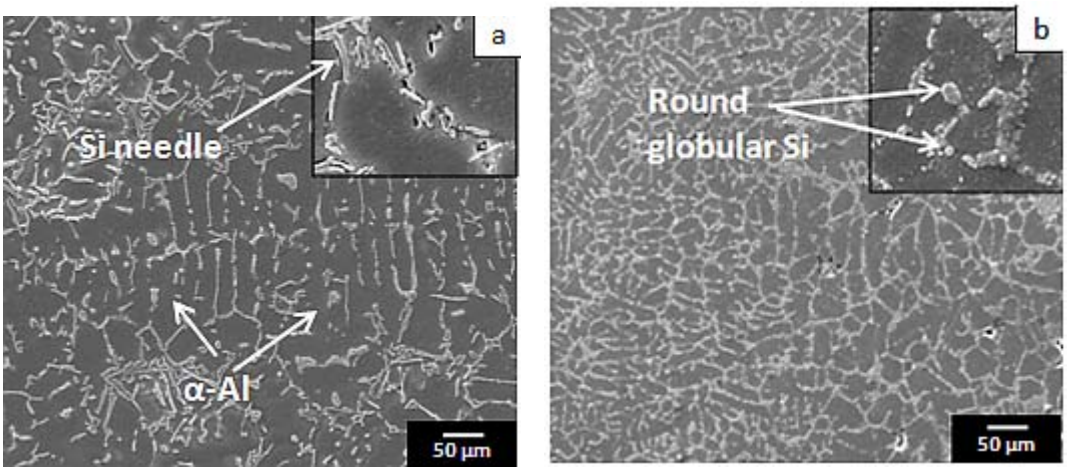

Figure 4.1: SEM micrograph of Al-7Si alloy (a) As-cast (b) Modified and grain refined

Similar observations can be made from the optical microstructure depicted in Figure 4.2a and b.

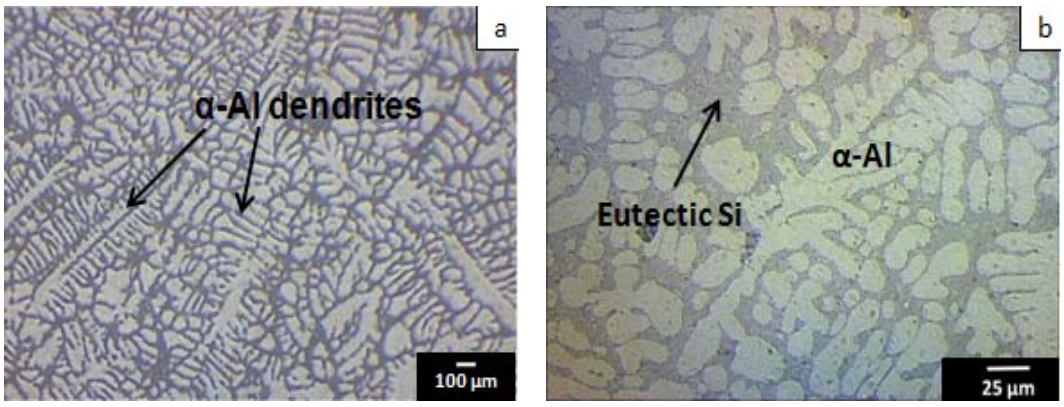

Figure 4.2: Optical microstructure of Al-7Si alloy (a) As-cast (b) Modified and grain refined

The microstructural details in Figure 4.2a clearly shows large primary α-Al grains as dendritic structure and plate like eutectic Si in as-cast Al-7Si alloy. Figure 4.2b depicts microstructural transition with the columnar dendritic structure with large

eutectic Si needles / flakes at the grain boundaries changing to equiaxed fine grain structure and fine particles of eutectic Si.

The grain size is measured using the method explained in 3.6. A reduction in size of Al grains from 105 μm to 68 μm (average size) is achieved. In general, there are two factors that contribute to the formation of grains. First, there must be the presence of suitable substrates in sufficient amount to act as heterogeneous nucleation sites. The Al_3Ti particles formed in the melt due to addition of Al-3Ti-1B act as heterogeneous nucleation sites to promote formation of large number of small size α-Al grains. Secondly sufficient under cooling could also be reason to facilitate the survival and growth of the nuclei.

The as-cast Al-7Si alloy exhibited a hardness of 45 BHN, whereas the alloy with combined addition of grain refiner and modifier exhibited a hardness of 54 BHN. This improvement in melt treated casting results from finer grains and well dispersed tiny Si particles. These further influences the wear performance of the alloy discussed in later sections.

4.2.2 Al-7Si alloy with Copper addition

The presence of additional elements in the Al-Si alloys allows many complex intermetallic phases to form and significantly contribute in developing aluminium alloys for desired purposes. Different minor alloying elements such as copper, silicon, magnesium and zinc are added to Al-Si alloys in order to improve mechanical and tribological properties. Copper additions are one among the few prominent alloying elements. Earlier studies have shown that 3-5 wt% copper addition is useful for precipitation-strengthening agent in aluminium (Yasir and Abdul 2014). It is an important precipitation-hardening agent in aluminium (Mohamed et al. 2009). This is due to formation of extremely small particles of second phase dispersed uniformly within the matrix which further aid the strengthening mechanism during heat treatment. Cu additions up to about 5% have indicated high strength and good toughness when subjected to natural or artificial aging (Belov et al. 2002).

The addition of Cu increases the strength of Al–Si alloys due to precipitation and dispersion of θ′ and θ′ phases during aging. The strengthening contribution from precipitation is typically a function of both precipitate size distribution and volume fraction. In addition, copper improves machinability and thermal conductivity, but at the expense of ductility and corrosion resistance (Davis 2001).

The SEM micrograph of as-cast Cu added Al-7Si alloy shown in Figure 4.3 indicates microstructural changes undergone by the as-cast Al-7Si alloy (Figure 4.2a) due to copper addition. The copper additions have given rise to $CuAl_2$ particles at the interdendritic regions and the α-Al also has been refined from columnar to equiaxed type. Copper phase is seen mainly as small pockets of the blocky $CuAl_2$ phase nucleating on coarse Si particles. A similar observation is reported by Mohamed et al. (2009).

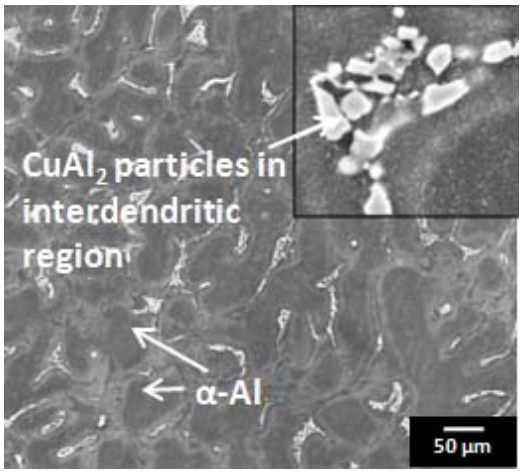

Figure 4.3: SEM micrograph of Al-7Si-4.5Cu alloy (as-cast)

These microstructural changes have resulted in the increase in hardness of as-cast Al-7Si-4.5Cu alloy to 65 BHN as compared to 45 BHN of as-cast Al-7Si alloy showing 44.4% improvement. This is higher than the % increase in hardness of Al-7Si alloy subjected to combined addition of grain refiner and modifier to Al-7Si alloy which is measured as 54 BHN.

4.2.3 Combined modification and grain refinement of Al-7Si-4.5Cu alloy

Acicular eutectic Si and $CuAl_2$ precipitates of Al-7Si-4.5Cu alloy on the interdendritic region can be apparently seen in Figure 4.3 presented in earlier section. Combined addition of modifier and grain refiner to cast alloy has changed the morphology of acicular eutectic Si and large blocks of $CuAl_2$ phases to fine colonies of eutectic and $CuAl_2$ particles, as shown in Figure 4.4. Addition of Cu makes the microstructure finer mainly due to under cooling effect and the addition of Ti provides the finer α-Al formation which helps to restrict the growth of primary Si and intermetallic phases.

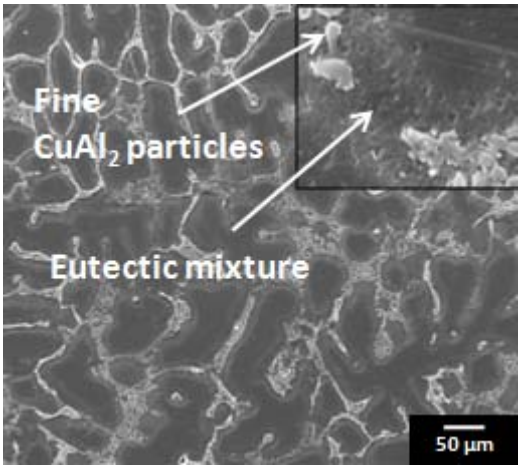

Figure 4.4: SEM micrograph of Al-7Si-4.5Cu alloy (Modified and grain refined)

The microstructure of as-cast alloy consisting of large primary α-Al grains and plate like eutectic Si is shown in Figure 4.5a. In as-cast condition, the addition of Cu is responsible for slight coarsening of α-Al dendrite but insignificant effect on the size and morphology of eutectic Si particles. Similar conclusions have been made by Lu et al. (2015). The effect of combined addition of 1 wt.% of Al-1Ti-3B grain refiner and 0.2 wt.% of Al-10Sr modifier is shown in Figure 4.5b. Acicular and plate like Si has transformed to small Si particles and refined α-Al grains can be explicitly seen. As reported by Mohamed et al. (2009), the Sr addition leads to the segregation of $CuAl_2$ particles in regions away from the growing Al-Si eutectic colonies as can be seen in the Figure 4.5.

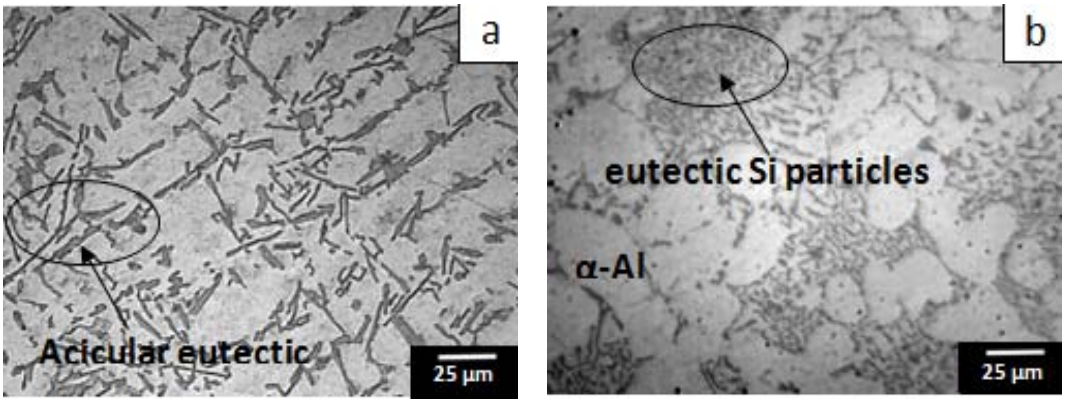

Figure 4.5: Optical image of Al-7Si-4.5Cu alloy (a) As-cast (b) Modified and grain refined

Figure 4.6 displays the EDX spectrum of modified and refined Al-7Si-4.5Cu alloy. The EDX spectrum shows the Al and Si peaks. Small peak intensities of Cu, Ti and Sr are also observed.

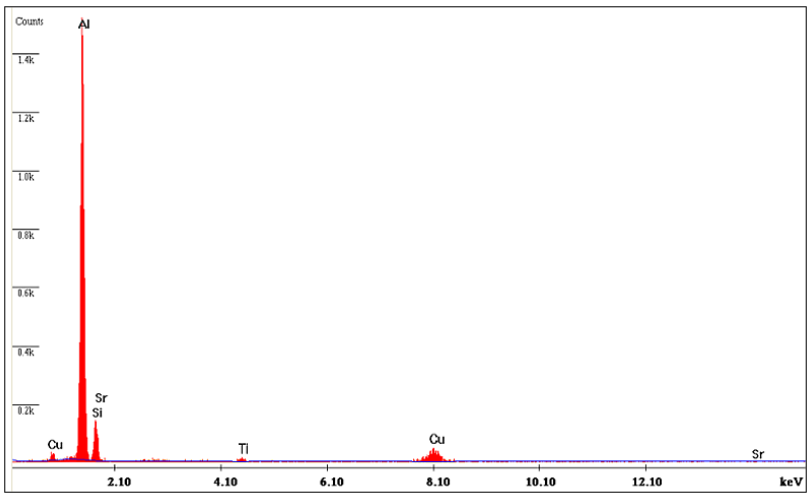

Figure 4.6: EDX Spectrum of melt treated Al-7Si -4.5Cu alloy

The nucleating particles such as Al_3Ti, AlB_2 and TiB_2 present in Al-1Ti-3B grain refiner and Al_4Sr particle present in Al-10Sr modifier are responsible for grain refinement and modification of Al-7Si and Al-7Si-4.5Cu alloys. Similar reference on the use of Al-1Ti-3B and Al-10Sr has been reported by Basavakumar et al. (2008).

Figure 4.7a shows microstructural features of Al_4Sr particle present in Al-10Sr master alloy at high magnification. The EDX spectrum shown in Figure 4.7b obtained on the Al_4Sr particle shows the presence of Al and Sr peaks in proportional limits that clearly demonstrates that particle is Al_4Sr.

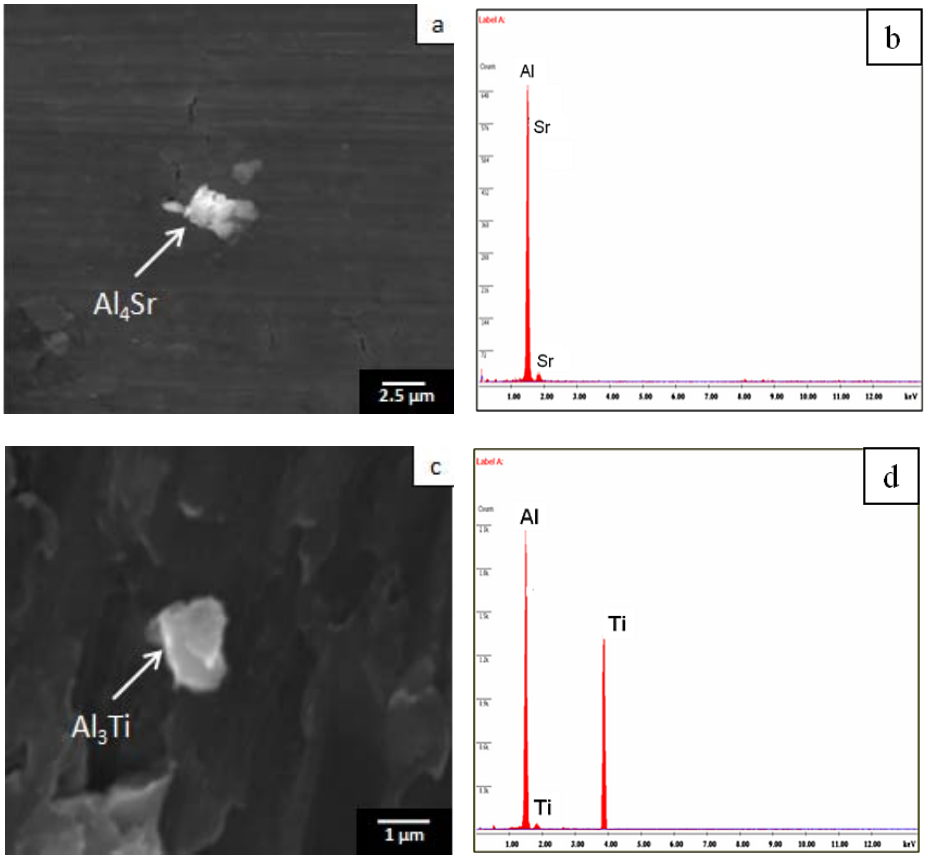

Figure 4.7: Nucleating particles present in grain refiner and modifier: (a) Al_4Sr in Al-10Sr, (b) EDX on Al_4Sr particle, (c) Al_3Ti in Al-1Ti-3B and (d) EDX on Al_3Ti particle

Figure 4.7c shows SEM micrograph of Al_3Ti particle in Al-1T-3B grain refiner at high magnification. Figure 4.7d shows the EDX spectrum to confirm the composition of Al_3Ti. Since the EDX is focussed on the Al_3Ti particle the concentration of Ti peak is relatively higher. Boron peaks are not identified due to lower composition. The $Al_3Ti + TiB_2$ particles released from grain refiner show both nucleant and solute effect for grain refinement (Vijeesh and Narayan Prabhu 2014).

4.2.4 T6 heat treatment of as-cast Al-7Si-4.5Cu alloy - Influence on microstructure and hardness

The Al-7Si-4.5Cu alloy is solution treated at 500 °C for 6 h and quenched in water (Sjolander and Seifeddine, 2010). Further, ageing is carried out on 16 samples up to a maximum of 48 h. Samples are drawn from the furnace at different time intervals cooled to near room temperature and hardness is measured . The influence of solutionizing and ageing on Al-7Si-4.5Cu alloy is discussed in following paragraph. Changes in the size and shape of eutectic Si particles before and after solution treatment are shown in Figure 4.8a and b. The microstructural details of as-cast alloy in Figure 4.8a shows the presence of $CuAl_2$ particles at the interdendritic regions. Observation in Figure 4.8b of solutionized alloy depicts modified grain structure of as-cast alloy. There is a significant refinement in the eutectic with most of the precipitates dissolved in the aluminium matrix. Apart from using modifier, modification of the silicon particles can also be achieved thermally, through solution heat treatment, where the silicon particles are initially broken down into smaller fragments that are then gradually get spherodized and coarsened. Spheroidization (globularization) and coarsening process of the silicon particles is due to the growth of larger particles at the expense of smaller ones and is known as Ostwald ripening (Khaled Ragab 2012). This could be due to an effort to reduce the surface energy (Mulazimoglu 1988). The rate of spherodization and coarsening also increases with solution temperature. In addition, the solution treatment is responsible for fragmentized smaller spherical eutectic Si particles. These microstructural changes along with dissolution of $CuAl_2$ phase may lead to strengthening by solid solution formation. As a result of this, 20% increase in hardness from 65 BHN to 78 BHN is obtained the as cast and solution treated alloy. Similar effect of eutectic silicon morphology, viz., particle size and shape in the improvement of mechanical properties is discussed in chapter 5.

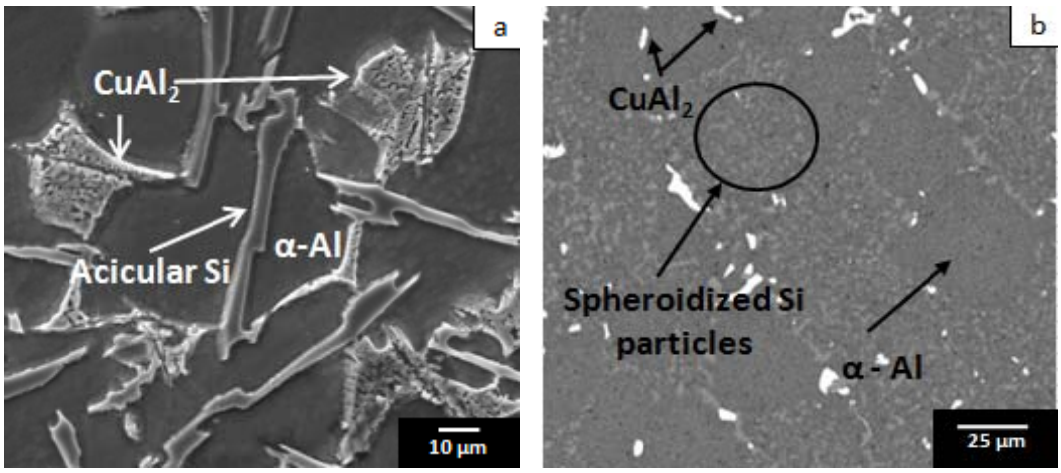

Figure 4.8: Effect of solution treatment on morphology of eutectic Si. (a) Al-7Si-4.5Cu (as-cast) (b) Al-7Si-4.5Cu (solutionized)

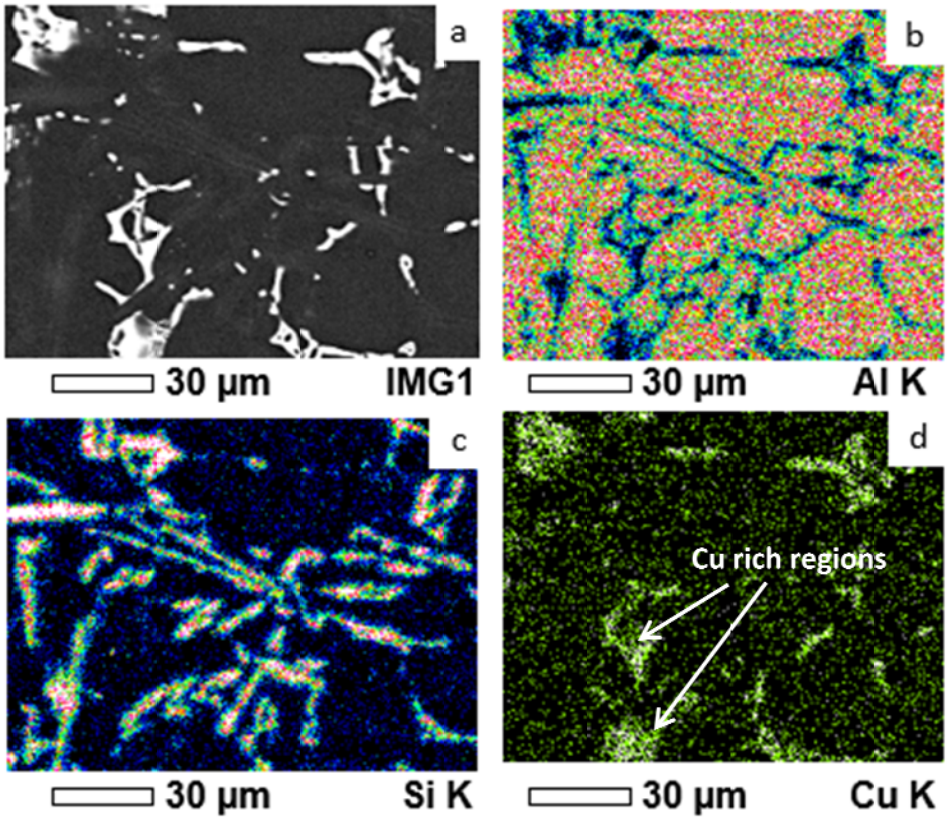

Figure 4.9: (a) Backscattered image of Al-7Si-4.5Cu alloy (solutionized condition) and corresponding X-ray mapping of (b) Al (c) Si and (d) Cu

Figure 4.9a shows the SEM backscattered image exhibiting few blocky $CuAl_2$ particles in Al matrix indicating that precipitates are not fully dissolved. In the X-ray mapping (Figure 4.9b-d), the presence of Si is seen at the interdendritic regions. In addition, the presence of sufficient amount of Cu is evident in the α-Al matrix. Peng et al. (2011) studied the influence of solution treatment on A356 alloys and suggested that the primary α-Al dendrites are less distinct and the eutectic silicon has been spheroidized. The solution heat treatment of Al-7Si-4.5Cu alloy in the present study has also shown similar results. With the rapid cooling of the alloy from homogenization temperature precipitation of $CuAl_2$ is prevented on reheating or ageing. Precipitation occurs because of super saturation and rejection of solute from the alloy. In the above alloy Cu is rejected.

The mechanism of precipitation hardening suggested by Khaled Ragab (2012) indicated that precipitation occurs with the formation of GP zones (Guinier–Preston zones). The precipitation of $CuAl_2$ occurs in different forms. GP zones are first precipitates formed from the supersaturated solid solution (α_{sss}) due to clustering of Cu atoms. These GP (also called $GP_{(1)}$) zones are coherent in nature that is they have one to one lattice matching with the solvent crystal lattice. After some time these GP zones starts forming θ″ $GP_{(2)}$ providing hardness to the alloy. On further ageing θ′ $CuAl_2$, semi-coherant precipitates form to further harden the sample. Further θ forms with drop in hardness.

The Al-7Si-4.5Cu alloy is subjected to ageing at 200 °C and hardness of the alloy is noted with ageing time. During ageing finely dispersed precipitates are formed due to controlled decomposition of the supersaturated solid solution. The variation in hardness of Al-7Si-4.5Cu alloy against ageing time is shown in Figure 4.10. The hardness of the Al-7Si-4.5Cu alloy increases with ageing time due to the initial formation of solute enriched GP zones. Further increase in the duration time of the aging treatment results in the formation of coherent and semi coherent precipitates (θ′ phase) at the sites of the GP zones until it reached a first peak hardness level of 111 BHN. Further increase in ageing showed a decreasing trend in hardness. After 20 h of ageing, the hardness is increased to 126 BHN due to the formation of transition θ′ semi-coherent phase which may provide hardening of the matrix. In this alloy the

first peak is seen at 4 h, second peak is seen at 20 h and with further aging, over aging sets in with the formation of incoherent equilibrium phase θ precipitate. Broadly similar observations are reported for Al-Cu alloys aged at 190 °C (Khaled Ragab 2012).

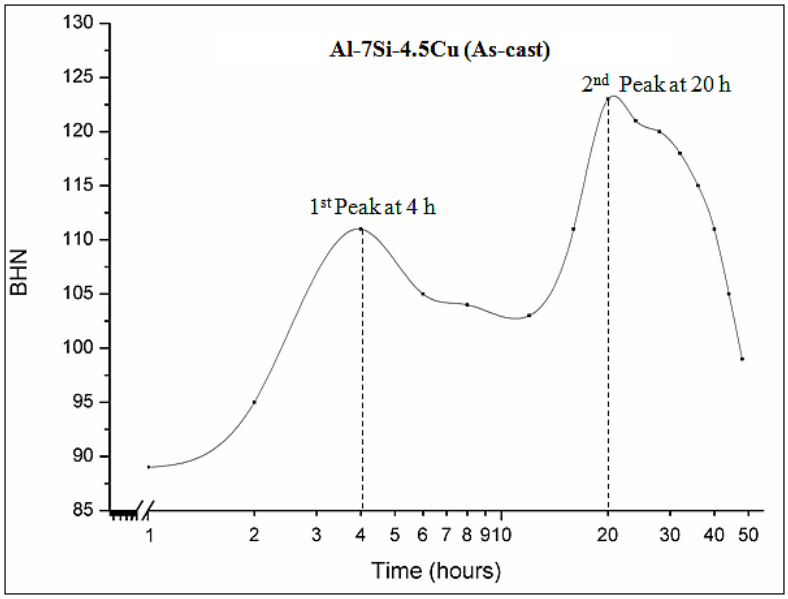

Figure 4.10: Ageing characteristics of as-cast Al-7Si-4.5Cu alloy

4.2.5 T6 heat treatment of combined modified and grain refined Al-7Si-4.5Cu alloy - Influence on microstructure and hardness

Al-7Si-4.5Cu alloy subjected to combined melt treatment with modifier and grain refiner is solution treated for 6 h at 500 °C and quenched in water at room temperature. The enlarged microstructure in Figure 4.11a shows fine fibrous particles of eutectic Si. After solution treatment the fragmented eutectic Si has been spheroidized as shown in Figure 4.11b. In this case also the silicon is coarsened and it can be observed that $CuAl_2$ is dissolved after solution treatment.

Juan (2003), has observed that the solution heat treatment time of modified and grain refined Al-Si-Cu alloy can be reduced, due to the positive effect that strontium exerts on the silicon morphology. However, a homogeneous soaking is mandatory during the solution heat treatment of large castings to achieve time

reduction. Further, combined modified and grain refined alloy is subjected to ageing at 200 °C, temperature selected based on the literature, (William and Callister 2004). Hardness of the alloys is noted after different ageing times as detailed in Table 3.6.

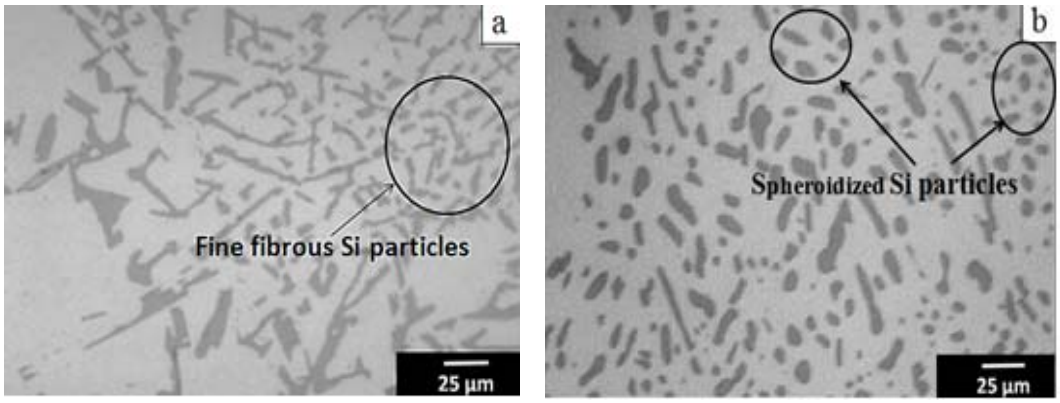

Figure 4.11: Effect of solution treatment on morphology of eutectic Si. (a) Al-7Si-4.5Cu (modified and refined) (b) Al-7Si-4.5Cu (modified & refined, solutionized)

Figure 4.12 exhibits the variation in hardness with ageing time. The Cu bearing Al alloys on ageing at a temperature in the lower range (200 °C in the present work) typically showed two peaks.

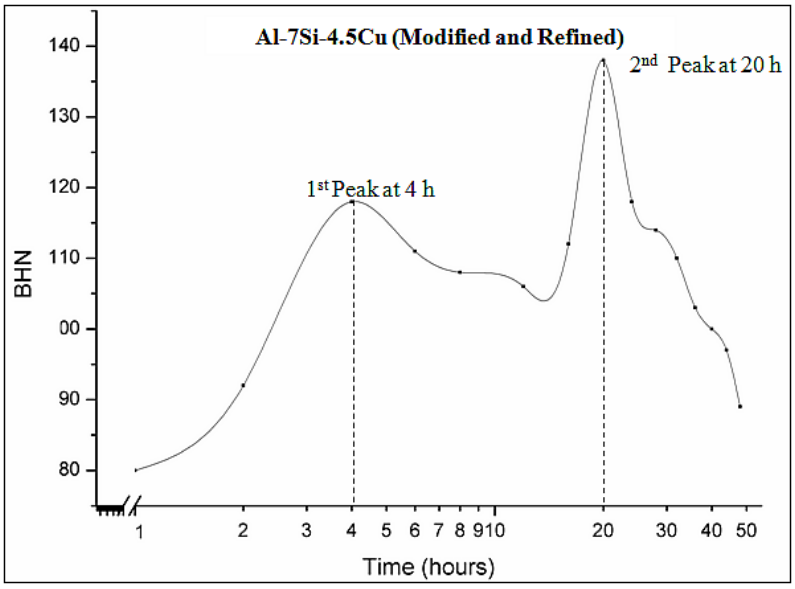

Figure 4.12: Ageing characteristics of modified and grain refined Al-7Si-4.5Cu alloy

The first peak hardness of 118 BHN is obtained at 4 h of ageing and the increase in hardness attributed to formation of $GP_{(1)}$, $GP_{(2)}$ zones. The second peak hardness of 138 BHN at 20 h may arise from θ′ precipitates along with θ″. Further increase in ageing resulted in reduction in hardness and after 20 h of ageing, increase in peak hardness of 138 BHN is observed. After 20 hours, over aging takes place due to only θ precipitates formation in the structure. Traces of remaining eutectic phase are detected by the presence of the fine Si particles that co-precipitated along with the eutectic during its formation.

Figure 4.13 shows SEM micrograph of the alloy subjected to ageing for 4 h. It can be clearly seen that the eutectic Si is refined in the Al matrix. Elemental mapping in Figure 4.9d shows distribution of Cu in the solid solution. The refined eutectic Si along with uniform distribution of second copper containing zone or phase also improves the mechanical properties of these alloys as discussed in chapter 5.

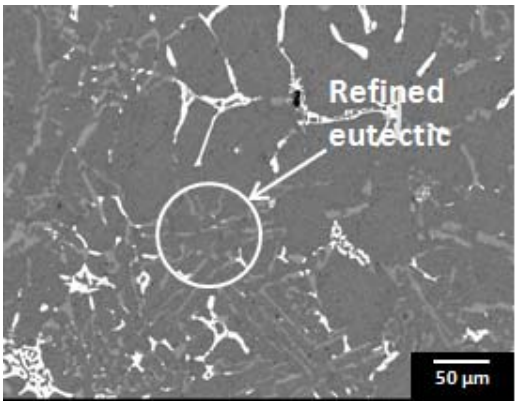

Figure 4.13: SEM micrograph of modified and grain refined Al-7Si-4.5Cu after ageing for 4 h

Deyan Yin et al. (2016) studied the effect of natural ageing and pre-straining on the hardening behaviour and microstructural response during artificial ageing of an Al–Mg–Si–Cu alloy. They suggested that with increased ageing time, the peak ageing hardness of Al–Mg–Si–Cu alloy decreased from 132 HV to 127 HV (3 h ageing), 122 HV (24 h ageing), and 121 HV (18 d ageing), the peak-ageing times are prolonged from 8 h to 12 h and 16 h, respectively. This decrease of peak-ageing strengthening contributed to the formation of clusters / GP zones induced by natural ageing before

artificial ageing (phenomenon of reversion). However, in the present investigation, 20 h ageing time has been considered as the peak ageing where hardness of 138 BHN is obtained.

It can be concluded that aging of Al-Si hypoeutectic alloys with 4.5% Cu additions have led to a good improvement in hardness due to the precipitation of GP zones and others. Beyond 20 hours over ageing effect sets in and hardness begins to decrease at a faster rate. The precipitate size and distribution in case of modified alloy further shows more positive effect on hardness.

4.3 Al-12Si and Al-12Si-4.5Cu Alloys

4.3.1 Combined modification and grain refinement of Al-12Si alloy

The SEM micrographs of as-cast and melt treated Al-12Si alloy are shown in Figure 4.14a and b, respectively. Melt treatment is by combined additions of 0.2% Al-10Sr modifier and 1% of Al-1Ti-3B grain refiner. The microstructure of as-cast Al-12Si alloy shows predominantly eutectic mixture with primary α-Al dendrites. Primary α-Al surrounded by the eutectic Si in the interdendritic region can be seen in the magnified view. It is observed that the addition of Al-10Sr modifier has changed the plate like or lamellar eutectic Si particles to fine distribution of fibrous silicon particles. Under equilibrium cooling conditions, Al-12Si alloy normally should consist of only a eutectic mixture. The presence of α-Al and primary Si particles indicates that the cooling had taken place faster than equilibrium cooling conditions. This phenomenon is attributed to the concept of skewed coupled zone by earlier researchers (Jigajinni et al. 2013). It is strongly believed that Ti acts as grain refiner to aluminium and its alloys, but there is an additional factor that must be considered: the dissolution of $TiAl_3$ particles. The amount of grain refiner added is important, normal addition level of Ti is around 100 ppm (0.01 %Ti). When this amount of Ti is added to relatively pure aluminium at normal casting temperatures, $TiAl_3$ forms and it could refine aluminium grains. But with a small time delay in pouring the melt the $TiAl_3$ will dissolve into the aluminium melt and the grain refining effect fades. In the present

work, the fading effect is practically not visible as significant refinement is visible in the microstructure.

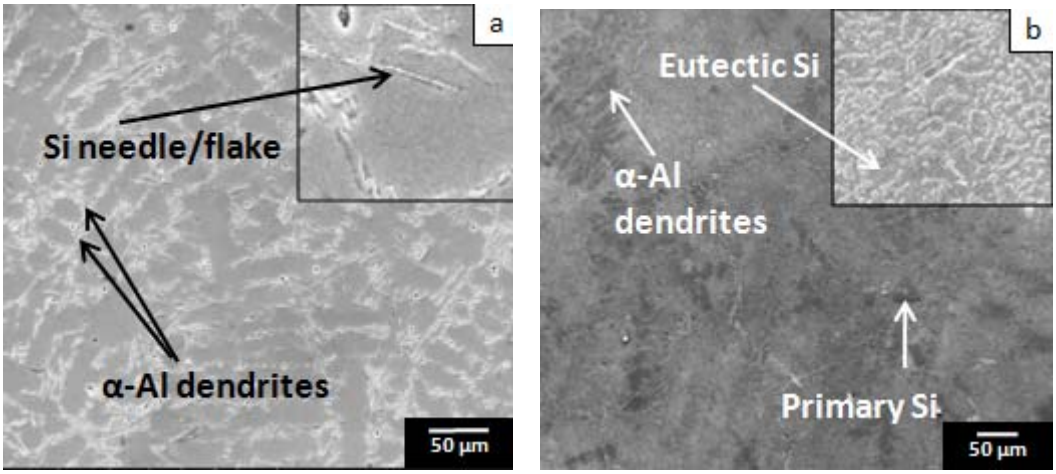

Figure 4.14: SEM micrographs of Al-12Si alloy (a) As-cast (b) Modified and grain refined

Microstructure of as-cast Al-12Si alloy in Figure 4.15a shows primary α-Al grains and eutectic silicon has appeared in the form of large plates with sharp edges and a few primary Si particles. Al-Si eutectic resembles lamellar structure. This is due to the anisotropic growth of Si due to lower interfacial energy between Al and Si. (Yasir and Abdul 2014). The modification of the alloy structure through the addition of Sr leads to the elimination of primary Si and the development of a granular eutectic structure. With this geometry change in primary Si morphology, the stress raisers features are reduced. The surface area of Si per unit volume in the eutectic decreases; this favours the isotropic distribution of the strain in the α-Al phase, both in the eutectic and in the primary phase. The modification of Al–12Si by Sr also accomplishes the development of well distributed eutectics. This helps to confine plastically the progress of the less likely crack tips in the α-Al of the eutectic. Refined microstructural features consisting of fine equiaxed α-Al grains and fine eutectic Si can be seen in Figure 4.15b due to the grain refinement and modification effect.

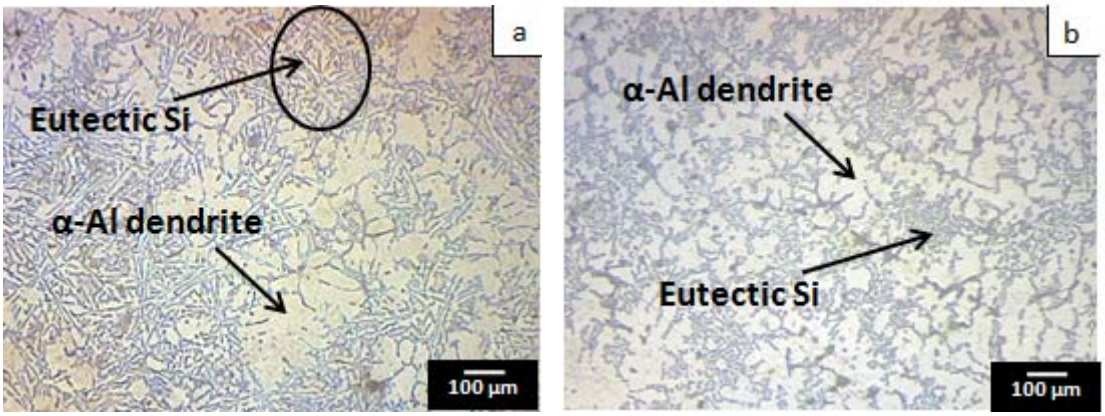

Figure 4.15: Optical images of Al-12Si alloy (a) As-cast (b) Modified and grain refined

4.3.2 Al-12Si alloy with Copper addition

With 4.5 wt% Cu addition, the microstructure shows large primary α-Al grains, needle like eutectic silicon and large $CuAl_2$ particles in the interdendritic region as seen in Figure 4.16a.

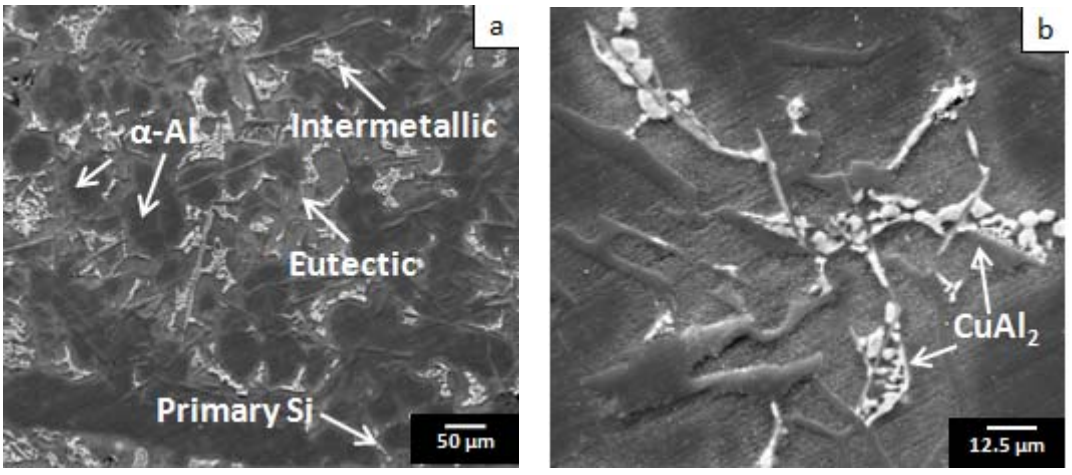

Figure 4.16: SEM micrographs of (a) Al-12Si-4.5Cu alloy (as-cast) (b) $CuAl_2$ intermetallic

At higher magnification shown in Figure 4.16b the as-cast alloy shows Cu intermetallic precipitates appear like white dots and are clearly visible. The $CuAl_2$ precipitates in the α-Al matrix have improved the hardness. Al-Si-Cu alloys usually

contain Cu (2 - 4 %), along with a certain amount of Fe, Mn, Mg and Zn that are either present as impurities or they are added deliberately to obtain desired material properties. These elements partly go into the solid solution and partly form intermetallic particles during solidification. Moreover, the influence of intermetallic phases such as $CuAl_2$ is responsible for improved mechanical properties. The extent of improvement depends on the size, volume and morphology of $CuAl_2$ particles. To understand the effect of copper, hardness of Al-12Si-4.5Cu alloy was measured and it showed a hardness of 78 BHN which is 21.9% higher than that of as-cast Al-12Si alloy that measured 64 BHN. Yasir and Abdul (2014) based on strengthening studies in Al-Si alloys with Cu addition has concluded that the copper content influences the reduction in the grain diameter resulting in increase of strength and hardness.

4.3.3 Combined modification and grain refinement of Al-12Si-4.5Cu alloy

The microstructure of Al-12Si with the addition of 4.5 wt.% Cu under combined modification and grain refinement is presented in Figure 4.17a and b. In Figure 4.17a, the eutectic Si appears to be coarse and morphology of α-Al grains is not uniform. In the inter-dendritic Al region, $CuAl_2$ intermetallic particles are found. Figure 4.17b shows further magnified image of the as-cast Al-12Si-4.5Cu alloy. The point EDS analysis at point 1 and point 2 as shown in Figure 4.17b confirms $CuAl_2$ phase and Si. The EDX spectrums of $CuAl_2$ phase and Si particle are shown as Figure 4.17c and d, respectively.

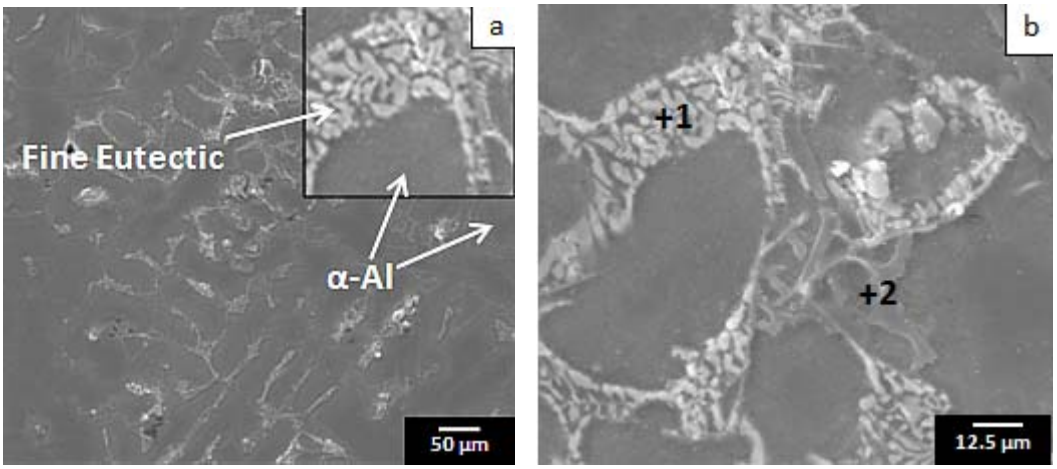

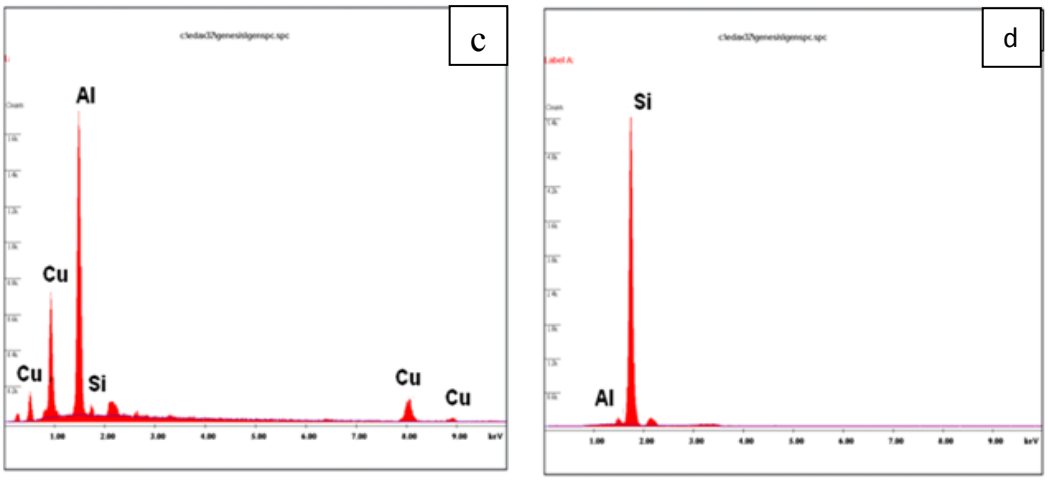

Figure 4.17: SEM micrographs of Al-12Si-4.5Cu alloy (a, b) Modified and grain refined; (c) EDS point wise analysis of marker 1 showing $CuAl_2$ intermetallic; (d) EDS point wise analysis of marker 2 showing Si.

The optical images shown in Figure 4.18a shows plate like eutectic Si and coarse columnar α-Al grains. Figure 4.18b demonstrates that addition of 1 wt.% of Al-1Ti-3B (grain refiner) has significantly refined the coarse columnar α-Al grains to fine equiaxed α-Al grains. This is due to the presence of AlB_2 and TiB_2 particles in the Al-1Ti-3B master alloy, which act as nucleating agents during solidification of α-Al dendrites (Basavakumar et al. 2008).

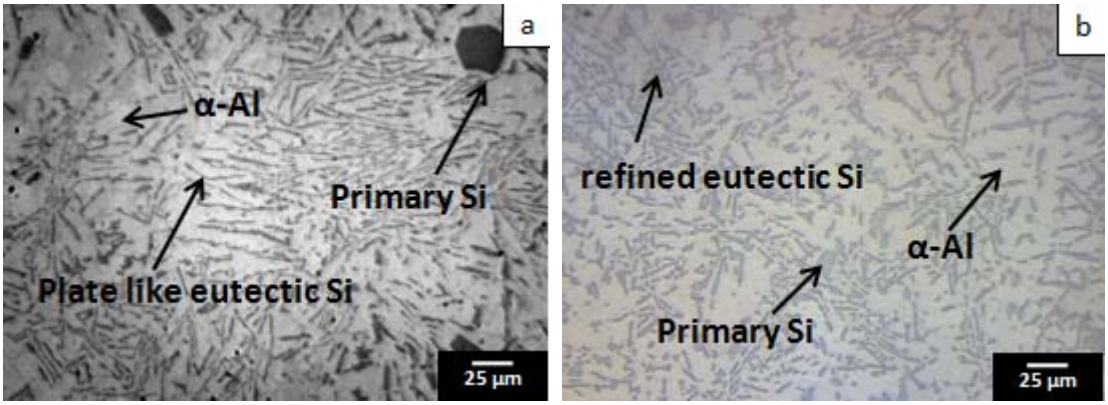

Figure 4.18: Optical images of Al-12Si-4.5Cu alloy
(a) As-cast (b) Modified and grain refined

Also, an addition of 0.2 wt.% of Al-10Sr (modifier) to Al-Si-Cu alloys has changed its plate like eutectic Si to fine eutectic particles and fine $CuAl_2$ particles in the inter dendritic region. The primary α-Al phase has a fully columnar (dendritic) structure in the untreated alloy but transforms to equiaxed morphology with the melt treatment. Mohamed et al. (2009) observed that copper rich blocky $CuAl_2$ phase nucleates on pre-existing coarse Si particles. The addition of Sr results in segregation of $CuAl_2$ intermetallic particles in regions away from the growing Al-Si eutectic colonies. A similar observation is reported by Samuel et al. (1996). The modified and grain refined Al-12Si-4.5Cu alloy exhibited 9% improvement in hardness as compared to 78 BHN of the as-cast alloy. It is evident that the addition of copper has influenced the hardness more than the combined refinement and modification of the alloy. The improvement in hardness of as cast alloy on combined refinement and modification is found to be 12.5%. With copper addition to as cast alloy, the improvement is 22% even without modification and grain refinement. And further improvement in hardness due to combined refinement and modification of Al-12Si-4.5Cu alloy is only 9%. Hence the addition of Cu and subsequent melt treatment has showed an overall increase of 33% in the hardness of as cast Al-12Si alloy

4.3.4 T6 heat treatment of as cast Al-12Si-4.5Cu alloys - Influence on microstructure and hardness

In general, the solution heat treatment causes soluble elements to dissolve into the solid solution. This requires high temperatures and sufficiently long time (enough for phases containing copper and / or magnesium to dissolve completely) to achieve nearly homogenous solid solution. Solution heat treatment is mainly carried out to produce solid solution that is required to take advantage of the precipitation hardening reaction. Figure 4.19 depicts the effect of solution treatment on the microstructure of Al-12Si-4.5Cu alloy.

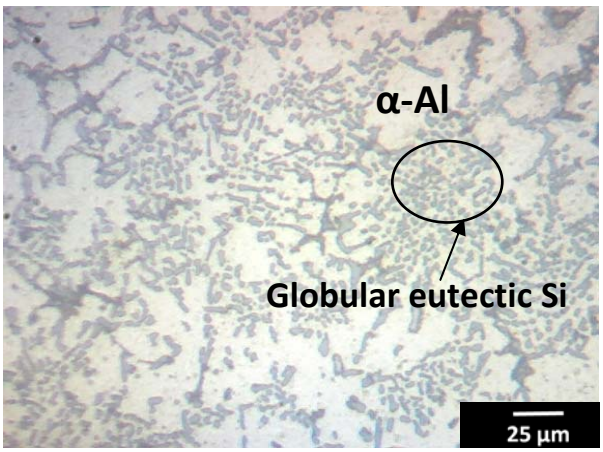

Figure 4.19: Optical microstructure of Al-12Si-4.5Cu (solutionized)

Figure 4.16a presented in earlier section shows the presence of $CuAl_2$ particles at the interdendritic regions. However, after solutionizing, the quantity of $CuAl_2$ phase decreased significantly, indicating dissolution of $CuAl_2$ particles. Mohamed et al. (2009) noticed 90% (highest) dissolution of $CuAl_2$ phase when Al-11.3Si-3.1Cu alloy was solution treated. The dissolution of $CuAl_2$ phase during solutionizing is also attributed to the presence of small quantity of Mg which lowers the temperature of Al-Si-eutectic leading to faster dissolution of $CuAl_2$ particles. In Figure 4.19, solution treatment has resulted in fragmentized smaller spherical eutectic Si particles and Al appears as homogenized structure. In addition, silicon structure is changed from needle to spherical shape which coarsens to decrease the interfacial energy. These microstructural changes along with dissolution of $CuAl_2$ phase led to strengthening of the solid solution with 23.1% increase in hardness value from 78 BHN to 96 BHN. Figure 4.20 presents backscattered image of Al-12Si-4.5Cu alloy (solutionized condition) along with $CuAl_2$ phase and corresponding X-ray mapping of Al, Si and Cu.

Figure 4.20a, shows that the solution treatment has resulted in homogenization of the as-cast structure and the eutectic Si morphology is drastically changed to dot eutectic and Cu particles are dissolved and distributed in solid solution.

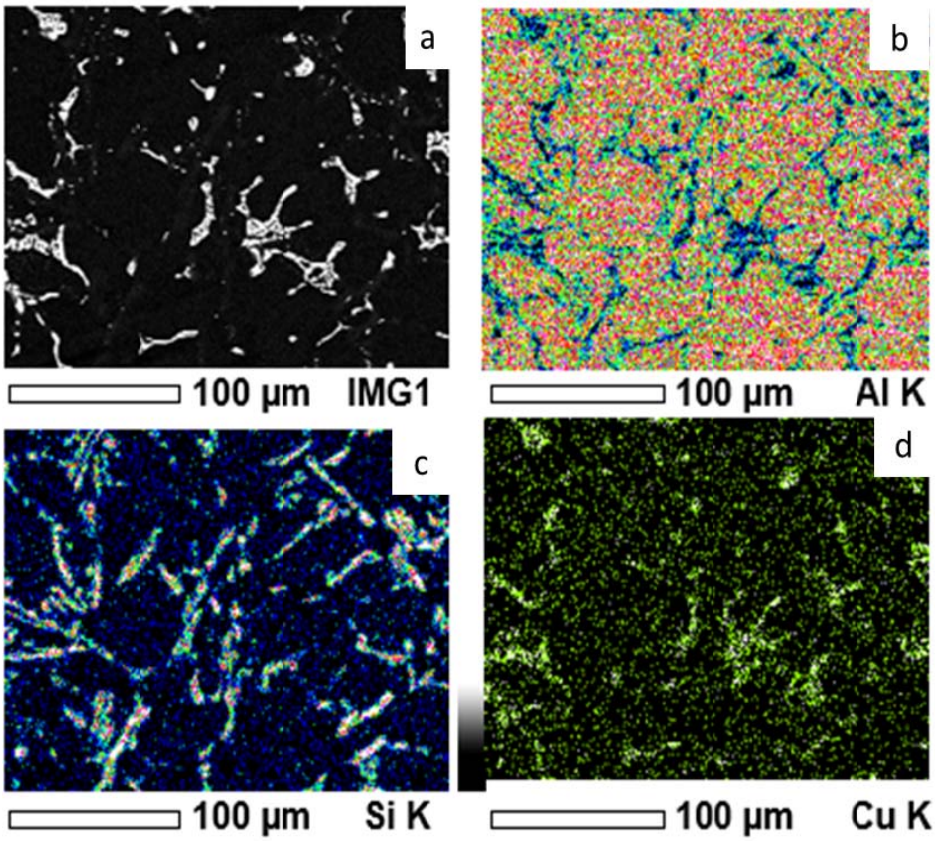

Figure 4.20: Backscattered image of Al-12Si-4.5Cu alloy (solutionized condition) along with $CuAl_2$ phase and corresponding X-ray mapping of Al, Si and Cu

Distribution of Al, Si and Cu particles in the microstructure can be visualized in Figure 4.20. Si particles are seen at the grain boundaries of Al. Presence of Cu in the α-Al matrix confirms good dissolution of Cu in Al matrix.

Figure 4.21 shows the evolution of hardness of Al-12Si-4.5Cu alloy aged at 200 °C up to 48 h. On aging, the hardness of the alloy increased up to 2 h of ageing to 116 BHN. With further increase in ageing time, a reduction in hardness sets in due to stages in aging. After 12 h of ageing, the hardness of the alloy reached a peak of 140 BHN due to the formation of θ′. Further ageing resulted in reduction of hardness as θ $CuAl_2$ starts to form.

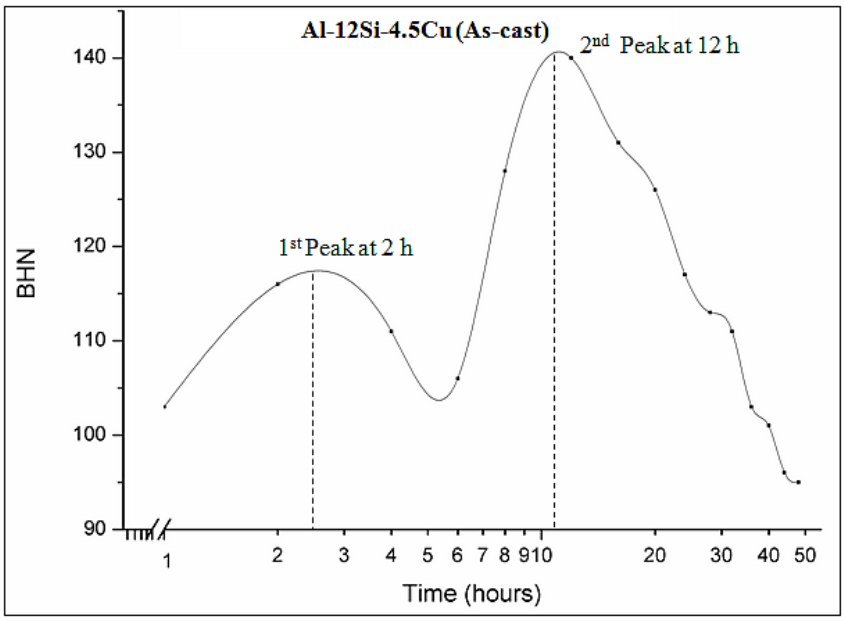

Figure 4.21: Ageing characteristics of as-cast Al-12Si-4.5Cu alloy

The SEM picture of as-cast Al-12Si-4.5Cu shown in Figure 4.17 depicts α-Al solid solution as a major phase (light gray). α-Al phase forms dendritic network usually coarse and precipitates in multi-phase eutectic reactions. The Cu is present in the form of $CuAl_2$ intermetallic phase and after the precipitation of $CuAl_2$ at grain boundaries the microstructure exhibits needle shape.

In as-cast Al-12Si-4.5Cu the intermetallics, particularly $CuAl_2$ present in the alloy dissolves in Al matrix after solution treatment and after 2 h of ageing time, the first stage of aging starts with the GP zone formation. Disk like coherent θ″ leads to the strengthening of material which is indicated by the first peak. Figure 4.22 shows SEM micrograph of the alloy subjected to ageing for 12 h. The bright spots in the SEM micrograph correspond to $CuAl_2$ precipitates while the fragmented Si particles are appearing as clusters of white particles in the matrix.

With increase in ageing time, the θ′ transient semi-coherent precipitate starts forming leading to a peak in hardness. This resulted in an improved hardness value of 140 BHN and 12 h ageing time is considered as a peak aged condition of

Al-12Si-4.5Cu. Beyond this time, equilibrium θ $CuAl_2$ phase starts forming leading to reduction in hardness.

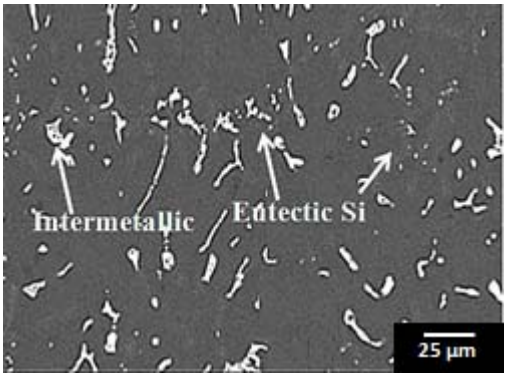

Figure 4.22: SEM micrograph of as-cast Al-12Si-4.5Cu after ageing for 12 h

4.3.5 T6 heat treatment of combined modified and grain refined Al-12Si-4.5Cu alloy - Influence on microstructure and hardness

Earlier in section 4.3.3 the role of Sr in modifying the plate like or lamellar eutectic Si particles into fine distribution of fibrous silicon particles has been discussed. During solution treatment, it is easier for fibrous Si particles to undergo fragmentation, necking, spheroidization and coarsening as compared to plate like eutectic Si particles (Crowell and Shivkumar 1995). The microstructural features resulting from solution heat treatment is outcome of the instability of the interface between two phases. The degree of spheroidization in modified alloy is higher because of lower resistance of fibrous silicon to interfacial instability (Khaled Ragab 2012). The SEM micrograph of the modified and grain refined Al-12Si-4.5Cu alloy shows $CuAl_2$ phase (Figure 4.23a). Samuel et al. (1996) have observed that $CuAl_2$ intermetallic phase is present in as-cast structure as a mixture of both block like $CuAl_2$ phase and as eutectic $CuAl_2$ phase and are either fully or partially soluble. However, Sr modification increases the fraction of blocky $CuAl_2$ phase (Samuel et al. 1996). Figure 4.23b shows the SEM micrograph of Al-12Si-4.5Cu alloy after solution treatment. Solution heat treatment has resulted in modifying the fibrous Si to spheroids. The blocky $CuAl_2$ precipitates have been taken into solution in the matrix

with eutectic $CuAl_2$ still visible in the microstructure. This is justified by the observations of Khaled Ragab (2012) that the amount of undisolved $CuAl_2$ in modified alloy was more than that in the non-modified alloy. Accordingly, the hardness of combined modified and grain refined Al-12Si-4.5Cu alloy has improved by 17.6% from 85 BHN to 100 BHN.

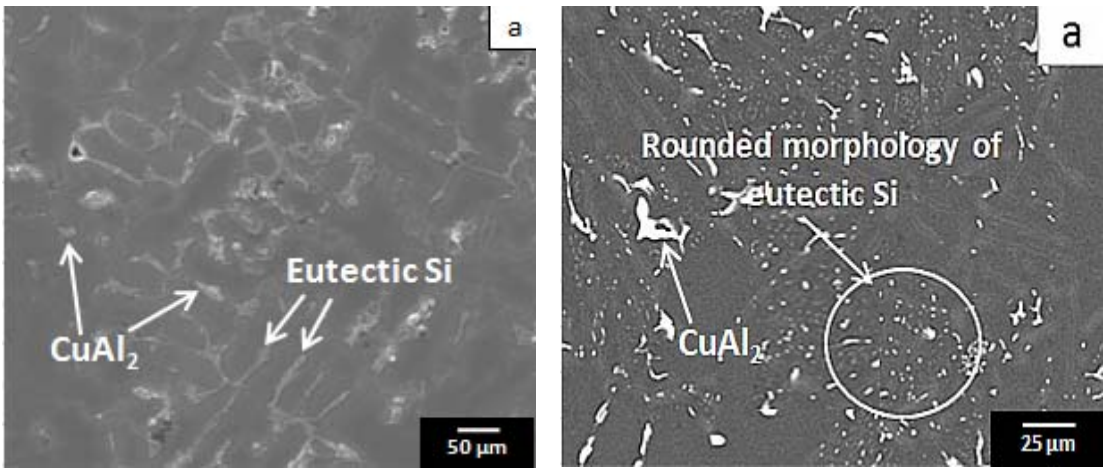

Figure 4.23: (a) SEM micrograph of modified and grain refined Al-12Si-4.5Cu alloy (b) Backscattered SEM micrograph after soultionizing

Figure 4.24 shows the ageing graph of modified and grain refined Al-12Si-4.5Cu alloy subjected to ageing at 200 °C. From the ageing graph it can be seen that hardness of the alloy increased up to 2 h of ageing until it reached a hardness level of 125 BHN. Further increase in ageing duration showed a reduction in hardness up to 6 h after which hardness increases further to attain its highest hardness value of 148 BHN on 12 h ageing. It is reported that the morphology of eutectic Si due to modification is improved further during solution heat treatment and also the increasing solution heat treatment time produces better results (Khaled Ragab 2012). Modification is also significant because as compared to as cast alloy the modified alloy requires approximately 1/10 treatment time to get smallest possible grain size.

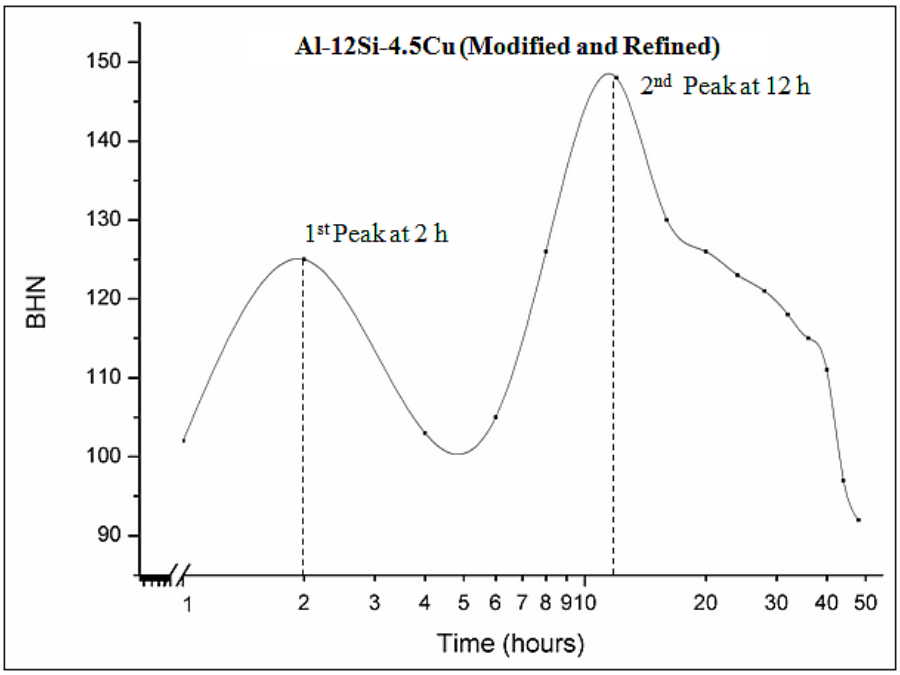

Figure 4.24: Ageing characteristics of Al-12Si-4.5Cu alloy (Modified and Grain refined)

After solution treatment of modified and grain refined alloy, the eutectic Si is refined and precipitates of $CuAl_2$ are nearly dissolved in the Al matrix. Moustafa et al. (2002) found that Sr modification has no marked effect on the precipitation of Cu phases during aging. The hardness values of the Sr-modified A413.1 alloy with 0.88% and 2.6% Cu additions were having the same hardness range as those of the unmodified alloys. It was also reported that Sr does not appreciably affect the age-hardening of Al–Si–Cu alloys (Mondolfo 1976). By observations of hardness of heat treated samples of both as cast and combined modified and refined alloys, it can be interpreted that modification has not significantly contributed while hardness is improved through heat treatment. After ageing for 12 h, peak hardness of 148 BHN is achieved. This is slightly better than for as cast and treated alloy (140 BHN). Age hardening improves hardness of the base alloy.

4.4 Al-15Si and Al-15Si-4.5Cu Alloys

4.4.1 Combined modification and grain refinement of Al-15Si alloy

SEM micrographs of as-cast and modified and grain refined Al-15Si alloy are shown in Figure 4.25a and b. The microstructural characterization in case of hypereutectic as-cast Al–15Si alloy reveals the presence of primary silicon (Si) and acicular eutectic silicon phases. While the eutectic silicon exhibited needle shape morphology, the primary Si exhibited the blocky morphology. The size of the eutectic Si also appears to be large. The morphology of primary Si is like star-shaped, polyhedral and dendritic. The star shaped primary Si crystals grow from the twinned decahedral nucleus, which is an assembly of five silicon crystals in twinned orientation. Previous studies have found that primary Si grows with twin plane re-entrant (TPRE) mechanism, where Si grows parallel to the existing silicon twin plane (Xu et al. 2006). Coarse platelet and polygon morphology of primary Si along with needle shaped eutectic Si have detrimental effects on mechanical properties of hypereutectic Al-Si alloys. Hence these precipitates must be effectively modified and refined.

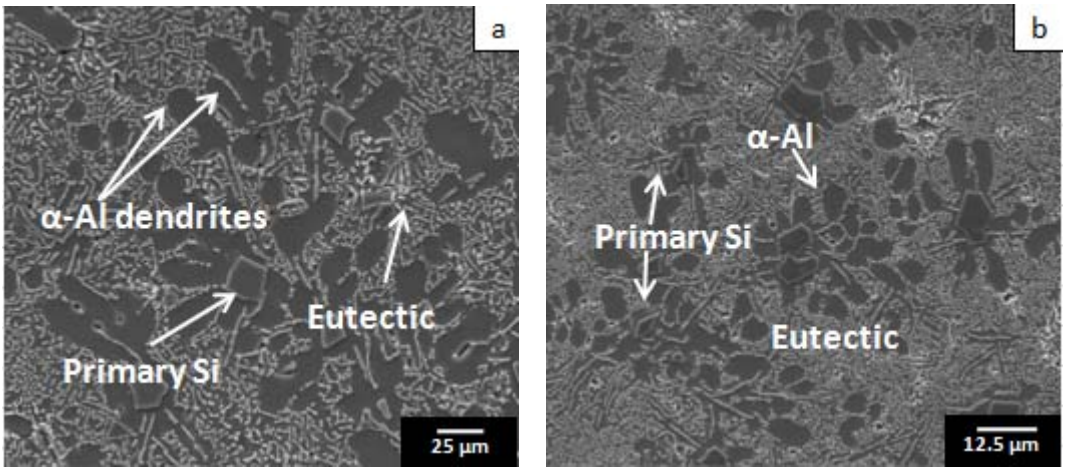

Figure 4.25: SEM micrographs of Al-15Si alloy (a) As-cast (b) Modified and grain refined

Addition of strontium has resulted in transforming the eutectic Si into finely distributed fibres / globules as seen in Figure 4.25b. In addition, treatment of melt with phosphorous master alloy (Al-23P) has led to segmentation of primary Si in to smaller sizes. Refined grain structure due to the addition of Al-1Ti-3B is evident from the microstructure. Lots of Si are observed at the edge of the dendrite as compared to that in hypoeutectic alloy. The eutectic alloy also shows generally coarser microstructures because of higher overall Si concentrations. For the slowly solidified materials, during solidification, the freezing Al dendrites will be pushing excess Si ahead of it that precipitates as a cluster ahead of dendrite.

Figure 4.26a shows the optical microstructure of as-cast Al-15Si alloy. The eutectic Si is coarse acicular or plate type with sharp edges and tends to be nonhomogeneous in distribution. The as-cast alloy exhibited maximum silicon particle size in the range of 110 – 200 μm.

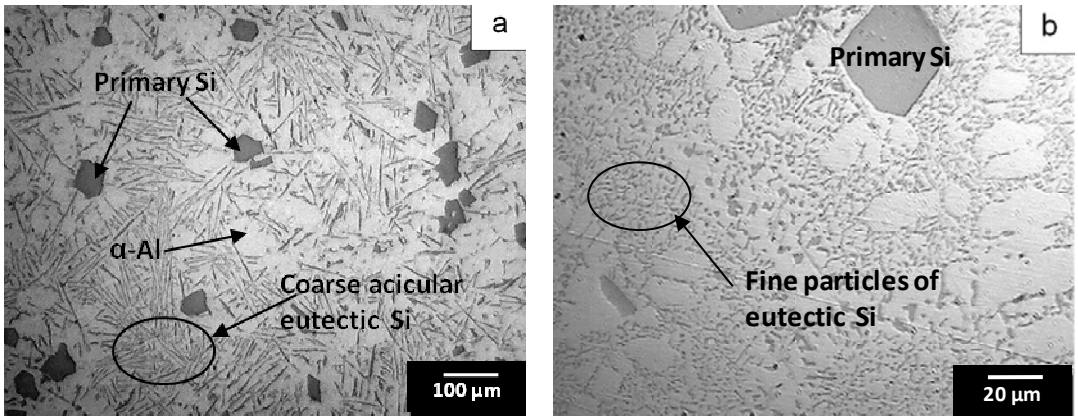

Figure 4.26: Optical images of Al-15Si alloy (a) As-cast (b) Modified and grain refined

Figure 4.26b exhibits the optical microstructure of modified and grain refined Al-15Si alloy. Al-Si alloys containing more than about 12% Si exhibit a hypereutectic microstructure normally containing primary Si phase in a eutectic matrix. Cast eutectic alloys with coarse acicular silicon shows low strength and ductility because of the coarse plate-like nature of the Si phase that leads to premature crack initiation and fracture in tension. Similarly, the primary Si in normal hypereutectic alloys is

usually very coarse and imparts poor properties to these alloys. From the present experimental results it is seen that the addition of phosphorous (AlP) as refiner to Al-15Si alloy has significantly refined the primary Si to fine and uniformly distributed silicon particles (approximately 25-30 μm). AlP acts as heterogeneous nucleant due to structure compatibility with Si (Gruzleski and Closset 1990). The phosphorous addition has favoured higher rate of primary Si particles heterogeneously nucleating on AIP particles with cube-cube orientation i.e. appearing with polyhedral morphology. This is due to increase in the nucleating temperature of primary Si on account of phosphorus addition and probably cooling conditions are also favorable. This indicates that the solidification might have taken place at low undercooling promoting nucleation of silicon by AIP particles. Al-P series master alloy without any impurities is an ideal refiner for hypereutectic Al-Si alloys since it has better wet ability. The effectiveness in refining primary Si uniformly depends on the uniform distribution of AlP compounds in the melt. Based on the findings of earlier researchers the refinement of the silicon obtained in the present work can be justified as due to reduction of the nucleation energy for the formation of primary Si by the AlP particles in the melt and further enhancing the growth in more regular shape with a uniform distribution. Literature also reveals that due to the complexity involved in the foundry practices; solidification conditions such as cooling rate, the presence of impurities and the ease of nucleation the silicon particles grow into different sizes and shapes (Vijeesh and Narayan Prabhu 2014). Zuo et al. (2013) have reported that addition of 2% Al_3P and 0.7% Al-Sr effectively refined hypereutectic alloy with Si as high as 30 wt%. It is observed that primary Si has been refined from 200 μm to 32.8 μm and evenly distributed in the α-Al matrix and also that melt temperature is a critical parameter for combined use of phosphorous and strontium for modification. 770 °C was found to be the optimum temperature as P and Sr does not react at this temperature to form certain intermetallics rather they form AlP and Al_4Sr leading to excellent refinement. In the present study melt temperature is 780 °C. As a result of the microstructural changes caused by combined modification and grain refinement, hardness of the Al-15Si increased by 8.6% from 70 BHN to 76 BHN.

Even though the aluminium-silicon eutectic undergoes change in morphology upon the addition of certain elements e.g. strontium or sodium, the exact mechanism of modification is still not well understood despite of decades of research (Yasir and Abdul 2014).

4.4.2 Al-15Si alloy with Copper addition

The microstructure of Al-15Si alloy with 4.5 wt.% copper addition is shown in Figure 4.27. It shows the presence of primary Si and α-Al dendrite with inter-dendritic regions comprising of eutectic Si and $CuAl_2$ intermetallic phase. The polygonal primary Si particles are dark gray in colour and $CuAl_2$ intermetallics are seen light gray.

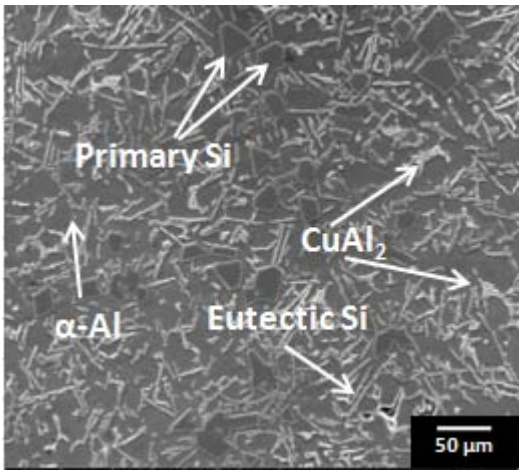

Figure 4.27: SEM micrograph of Al-15Si-4.5Cu alloy (As-cast)

The morphology and size of $CuAl_2$, eutectic Si and primary Si are realized through SEM micrographs (Figure 4.28a, 4.29a, 4.30a and further confirmed from EDX analysis (Figure 4.28b, 4.29b, 4.30b, respectively). Improvement in mechanical properties of these alloys due to similar microstructural features are reported by earlier researchers (Zedan and Alkahtani 2013; Zor et al. 2010; Li et al. 2003; Moustafa et al. 2002).

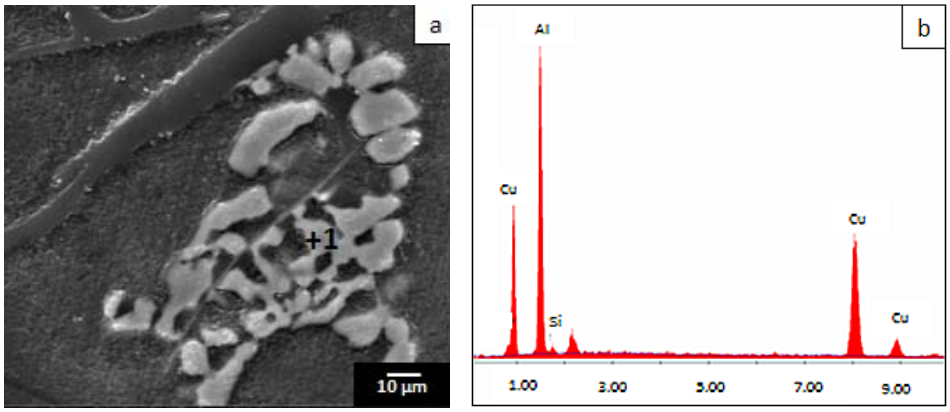

Figure 4.28: (a) SEM micrograph showing $CuAl_2$ intermetallic phase in Al-15Si-4.5Cu alloy (b) EDX point wise analysis at point +1 in Figure (a)

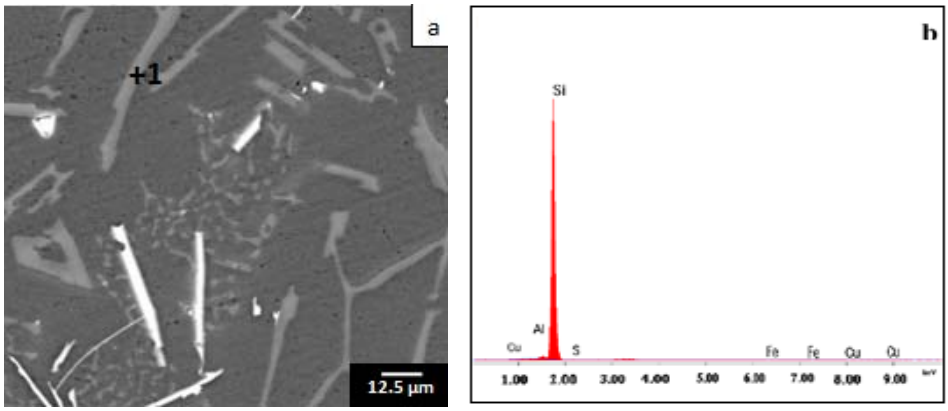

Figure 4.29 (a) SEM micrograph of the eutectic Si (b) EDX point wise analysis (marked as+1)

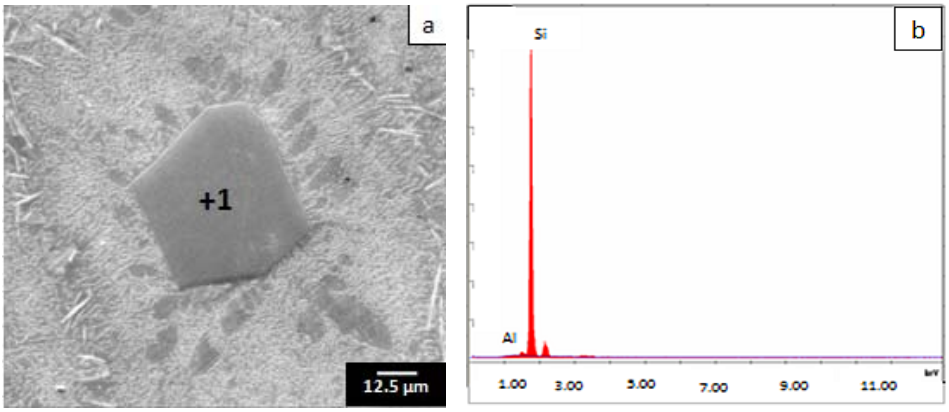

Figure 4.30: (a) SEM micrograph of the primary Si (b) EDX analysis on Si (Marked as +1)

4.4.3 Combined modification and grain refinement of Al-15Si-4.5Cu alloy

The microstructure of Al-15Si-4.5Cu as-cast alloy in Figure 4.27 features needle / plate type silicon particles. Unmodified acicular silicon acts as internal stress riser (Pena and Lozano 2006). In this study, microstructure refinement is achieved by controlling the melt chemistry by addition of 1% Al-1Ti-3B grain refiner, 0.4% Al-10Sr and 0.04% P.

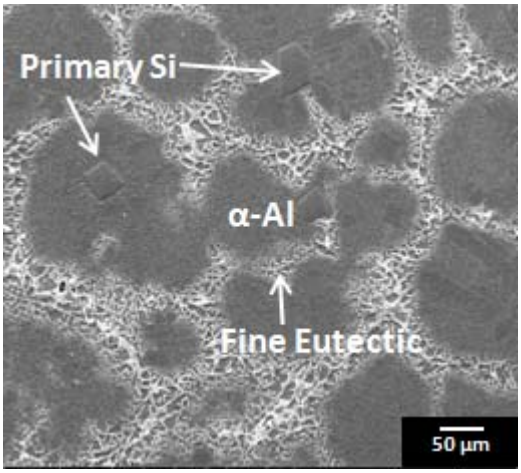

Figure 4.31:SEM micrograph of Al-15Si-4.5Cu alloy (modified and grain refined)

The refined microstructure in Figure 4.31 shows well-distributed primary Si in Al matrix and also the plate like eutectic silicon modified to fine particles. The addition of phosphorus to Al-15Si-4.5Cu alloy significantly refines the coarse platelet, star-like and irregular primary Si to fine and uniformly distributed silicon particles mainly due to aluminium phosphide (AlP) acting as nucleating agent for silicon.

Comparing the hardness values of the Al-15Si (as-cast), Al-15Si-4.5Cu(as-cast) and Al-15Si-4.5Cu (modified and grain refined) which exhibited hardness values of 70 BHN, 82 BHN and 90 BHN respectively, the improvement in hardness of Al-15Si due to copper addition is more significant (17.1%) as compared to combined grain refinement and modification of the base alloy (8.6%). Also observing the values of hardness of combined modified and grain refined Al-15Si-4.5Cu alloy which shows 9.8% improvement over the as cast Al-15Si-4.5Cu alloy, it appears that copper

addition to the base alloy has more influence on its hardness. However with grain refiner and modifier an overall improvement of 28.6 % is achieved.

4.4.4 T6 heat treatment of as cast Al-15Si-4.5Cu alloys - Influence on microstructure and hardness

In the applications where ductility is not of prime importance such as cylinder head, Cu containing variants of these alloy have the distinct advantage of increased strength at high temperatures and therefore are becoming increasingly popular. Hence hypereutectic Al-Si with alloy containing Cu is mainly used in casting engine blocks, cylinder heads, pistons and manifolds.

T6 heat treatment is expected result in roundness of the primary and eutectic silicon due to partial dissolution. Al-15Si-4.5Cu alloy is subjected to solution treatment at 500 °C for 6 h, and quenched in water. Subsequently, ageing is carried out at 200 °C up to 48 h for various time intervals. Plots of hardness against time during ageing for quenched samples are obtained and microstructural studies are carried out for specimens displaying peak hardness. Figure 4.32 shows the microstructure of the alloy after solution treatment. It can be observed that the eutectic silicon is fairly well distributed and the particles thin out, neck, fragment and tend to get spherical shape. The sharp edges of eutectic silicon particles observed in the as-cast state are seen to be rounded. However, complete transformation of the needle-like structure into fine fibrous morphology is not achieved in this alloy as the transformation rate is affected by the size of the particles. The aspect ratio of the eutectic Si decreases with increasing solution time (Kezhun et al. 2011). It is also interesting to observe the tendency silicon segregation in the immediate vicinity of primary Si particles. These microstructural changes led to increased hardness. The hardness of Al-15Si-4.5Cu alloy after solution treatment and quenching improved by 20.7 % from 82 BHN to 99 BHN.

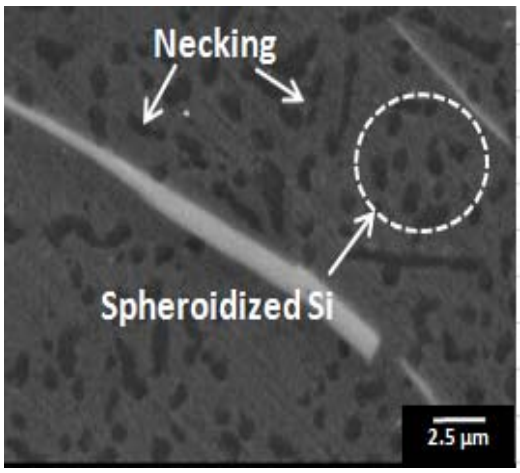

Figure 4.32: Effect of solution treatment on morphology of eutectic Si of Al-15Si-4.5Cu

The features and morphology of primary Si and $CuAl_2$ are shown in the SEM micrograph in Figure 4.33. The $CuAl_2$ phase is present in blocky form. It is observed that blocky $CuAl_2$ phase has not dissolved completely in the solid solution but precipitates on top of the primary Si particles. These observations are in concurrence with published literature (Mondolfo 1976).

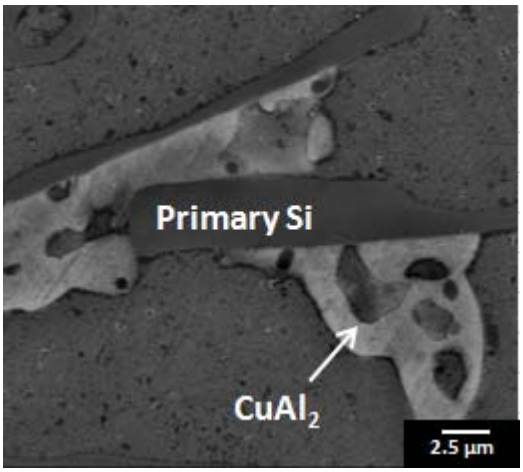

Figure 4.33: SEM micrograph of blocky $CuAl_2$ phase precipitated on top of primary Si particle

Figure 4.34 shows elemental mapping of Al, Si and Cu in Al-15Si-4.5Cu alloy. Some Si is seen at the interdendritic regions. Homogenous distribution of Cu in the α-Al matrix is apparent.

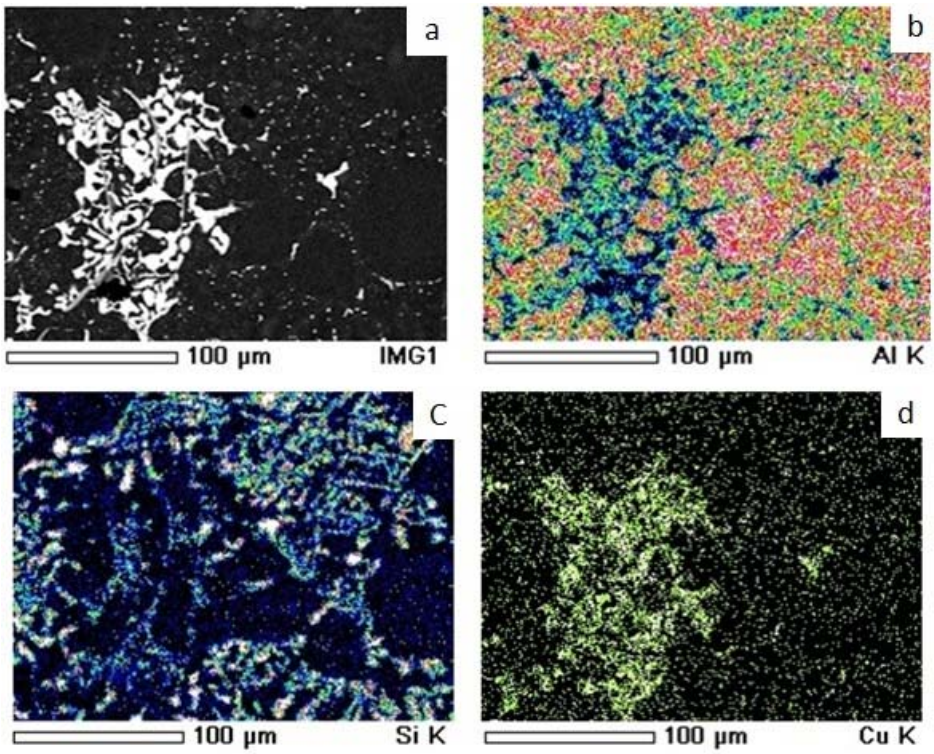

Figure 4.34: Backscattered image of Al-15Si-4.5Cu alloy (solutionized) along with $CuAl_2$ phase and corresponding elemental mapping of Al, Si and Cu

The variation in hardness of Al-15Si-4.5Cu alloy with increase in ageing time is presented in Figure 4.35. The hardness of the Al-15Si-4.5Cu alloy increased and at 8h of ageing a hardness of 120 BHN is observed. Further increase in ageing showed a transition with the hardness decreasing up to 15 hours then again increasing. At 20 h of ageing, peak hardness of 148 BHN was observed. As discussed earlier, the peak hardness is achieved due to the formation of GP zones and metastable phase θ′ phase. Further ageing resulted in reduction of hardness level due to onset of θ equilibrium. The mechanism for increased hardness of the alloy during ageing treatment initially and subsequent reduction in hardness before it reaches peak hardness is documented (Verhoeven 1975; Smith 1981; Porter and Easterling 1981).

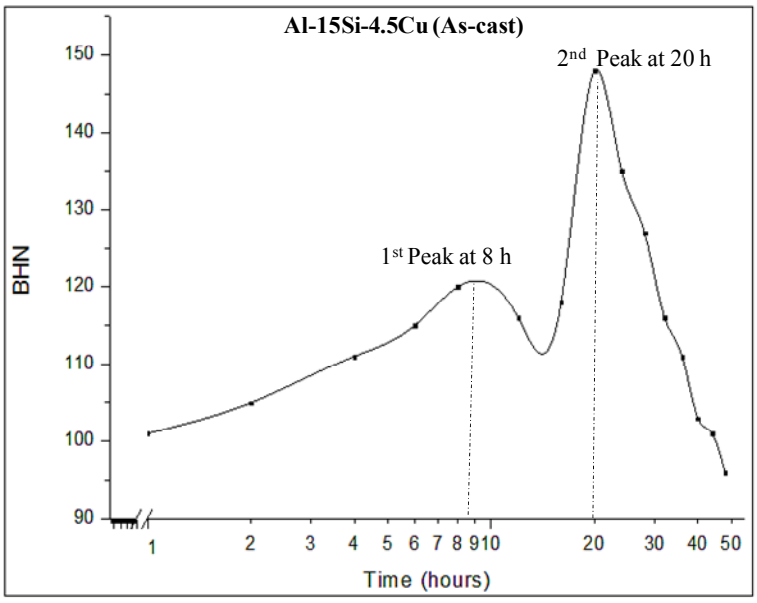

Figure 4.35: Ageing characteristics of as-cast Al-15Si-4.5Cu alloy

Figure 4.36 displays SEM micrograph of the as-cast Al-15Si-4.5Cu alloy subjected to ageing for 4 h. In contrast with the as-cast microstructure of Al-15Si-4.5Cu alloy, the α-Al dendrites are not seen here. However, Cu and eutectic Si are homogenously present in Al matrix. It can be seen in the image that there is a uniform distribution of primary Si particles and eutectic Si particles in Al matrix of the alloy.

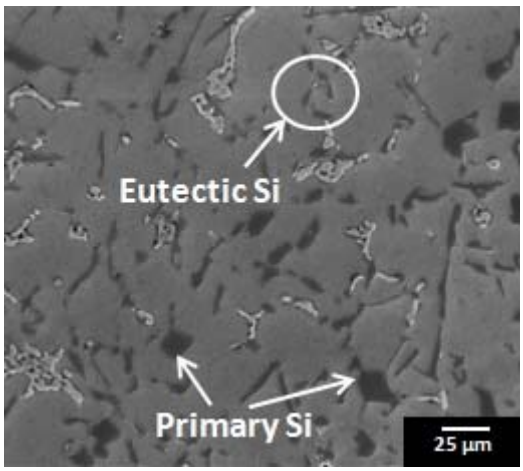

Figure 4.36: SEM micrograph of Al-15Si-4.5Cu after ageing for 8 h

4.4.5 T6 heat treatment of combined modified and grain refined Al-15Si-4.5Cu alloy - Influence on microstructure and hardness

Due to combined grain refinement and modification of as-cast Al-15Si alloy primary Si particles size was reduced and they were uniformly distributed in the matrix. It has been proposed that during solution heat treatment, Si particles undergo spheroidization in two steps. First, eutectic Si branches are fragmented and later spheroidization of separated branches takes place. It is easier for fibrous Si particles found in modified alloys to undergo fragmentation, necking and spheroidization as compared to plate like eutectic Si particles found in as-cast Al-15Si-4.5Cu alloys. This is due to the increased driving force provided by the finer as-cast structure of the modified eutectic Si in the former (Meyers et al. 1992). The SEM micrograph of modified and grain refined Al-15Si-4.5Cu after solution treatment is shown Figure 4.37.

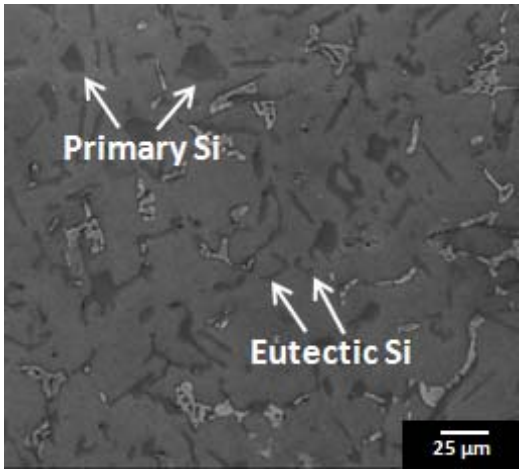

Figure 4.37: SEM micrograph of modified and grain refined Al-15Si-4.5Cu alloy after solutionizing

The variation in hardness of modified and grain refined Al-15Si-4.5Cu alloy with ageing time is shown in Figure 4.38. It can be seen from the Figure 4.38 that hardness of the alloy increased up to 8 h of ageing until it reached a hardness level of 130 BHN. During the initial stages of aging, a redistribution of solute atoms within the lattice takes place to form ordered clusters or GP (Guinier-Preston) zones which

are enriched in solute atoms. GP zones may precipitate in different shapes: rods, needles, spherical clusters; their form depends to a high degree on the specific alloy system (Khaled Ragab 2012).

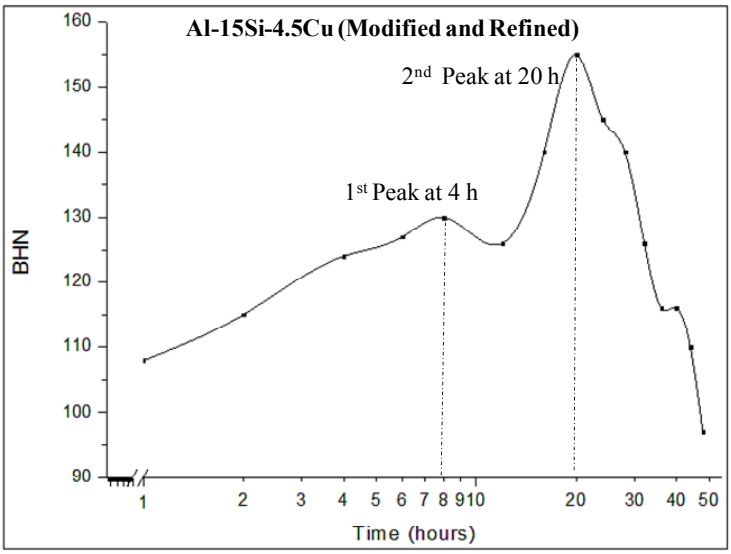

Figure 4.38: Ageing characteristics of Al-15Si-4.5Cu alloy (Modified and Grain refined)

This transforms to θ″ with time up to 8 hours where the first peak is observed. Continued ageing resulted in a reduction in hardness for a short period as GP zones and θ′ get reversed into the solution prior to the formation of meta-stable phase θ′. After 20 h of ageing, peak hardness of 158 BHN was observed due to the presence of meta-stable phase θ′ along with θ″. Further ageing resulted in the formation of non coherent θ precipitate phase leading to over ageing and hardness begins to drop. The behavior is similar to hypoeutectic and eutectic alloys. However, the difference in peak values, time and drop due to over ageing are different in each case. Mondolfo (1976) has reported that aging is fastest in Al-Si eutectic alloy and more or less Si seems to slow down the aging rate..

It is evident from the results that with ageing there is an increase in peak hardness values and this increase is in proportion to the weight percent of silicon. This can be attributed to corresponding volume fraction of harder silicon based phases in the aluminium matrix. In case of hypoeutectic Al–Si alloys the silicon based phases

refer to eutectic silicon and in the case of hypereutectic alloy it is primary and eutectic silicon. The ability of the defect structure to serve as a heterogeneous nucleation site during aging treatment may further be reason for the increased precipitation of the secondary phases and hence the increase in magnitude of age hardening.

In all the three types of alloys, similar pattern of hardness response is evident. The response is faster in eutectic alloys as compared to hypo and hyper eutectic alloys. Referring to Figure 4.39 the first and second peaks have occurred much earlier in case of eutectic alloy. This suggests that silicon content does not proportionately influence the aging kinetics. However, it is observed form ageing studies of all the three types of alloys that with the increase in the weight percentage of silicon, the magnitude of age hardening has increased at both first peak and second peak.

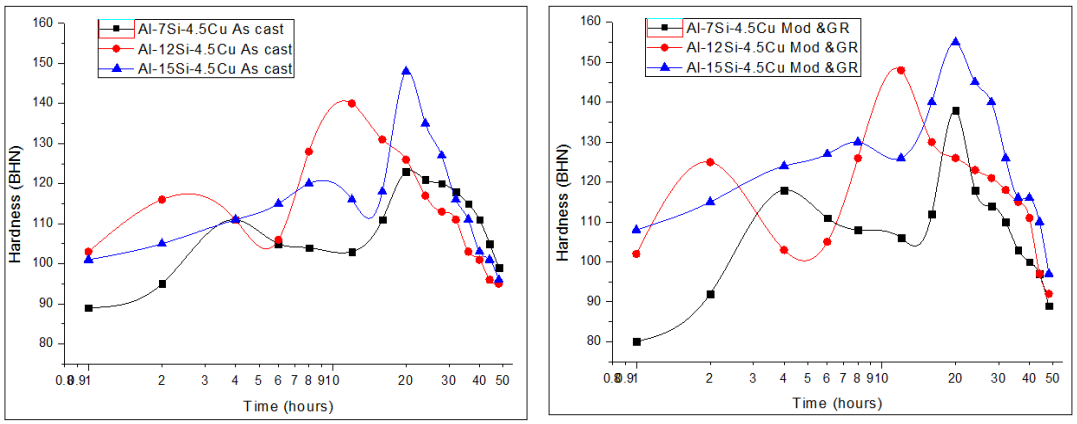

Figure 4.39: Ageing pattern of the three alloys

Gupta and Ling (1999) have reported similar ageing kinetics behavior for hypoeutectic (7% and10% Si) and hypereutectic (19% Si). Si content predominantly influences the hardness owing to its low solubility in aluminium which causes it to precipitate virtually as pure Si. Similar results are evident in this work, however the eutectic composition has yielded both first peak and second peak much faster than other two types.

Chapter 5

Evaluation of Mechanical Properties of Al-Si and Al-Si-Cu alloys

5.1 Introduction

In this chapter, the effect of combined addition of grain refiner and modifier on mechanical properties of Al-7Si, Al-12Si, and Al-15Si with and without Cu is discussed. Mechanical behaviour is studied by evaluating ultimate tensile strength (UTS), yield strength (YS) and % elongation (ductility) of the alloys before and after combined refinement and modification and is related to the microstructural composition. The fractographs of the broken specimen are analyzed to understand the nature of their failure. The effect of T6 heat treatment on all three alloys with Cu in as-cast and combined modified and grain refined condition is also presented.

5.2 Influence of combined modification and grain refinement on mechanical properties of Al-7Si and Al-7Si-4.5Cu Alloys

The tensile test is conducted on Al-7Si and Al-7Si-4.5Cu alloys in as-cast and modified and grain refined conditions to investigate the mechanical properties. Table 5.1 shows UTS, YS and % elongation values of alloys. The improvement in hardness in the grain refined and modified alloys is discussed and justified with reference to microstructure presented in section 4.2.1. The tensile properties of Al-7Si alloy are influenced by the shape and size of α-Al grains and eutectic Si; and in Al-7Si-4.5Cu, it also depends on intermetallics size and distribution. (Flemings 1974; Collins 1972; Hamid 1989). The as-cast Al-7Si and Al-7Si-4.5Cu alloys showed the precipitation of acicular eutectic Si and $CuAl_2$ blocks in the interdendritic region. 11% increase in UTS is observed in as-cast Al-7Si alloy due to modification and refinement with UTS increasing from 154 MPa to 171 MPa.

Table 5.1: Influence of copper addition and combined grain refinement and modification on the mechanical properties of cast Al-7Si alloys

Alloy Composition	**Al-7Si**	**Al-7Si***	**Al-7Si-4.5Cu**	**Al-7Si-4.5Cu***
UTS (MPa)	154	171	180	208
0.2% Proof stress (MPa)	58	67	85	107
% elongation	7.6	11.9	5.9	8.5

*Grain refined and modified

It is well established that hardening of alloys requires inhibiting the motion (glide or climb) of dislocations. Due to melt treatment number of grain boundaries increase. During deformation, dislocations experience resistance for their movement at the grain boundaries. Hence presence of many grain boundaries in turn decreases the extent of uninterrupted movement of dislocations.

Microstructural changes such as fine equiaxed α-Al and rounded fine eutectic Si are caused due to the presence of Al_3Ti particles present in Al-1Ti-3B master alloy which provides heterogeneous nucleating sites during solidification. The Al_4Sr particles present are responsible for modification effect. Jigajinni et al. reported similar trend in UTS, 0.2% proof stress and % elongation when Al-7Si alloy was treated with 0.55% of Al-1Ti-2.2B master alloy and 0.02% Sr (Jigajinni et al. 2013). The addition of 4.5 wt.% Cu to as-cast Al-7Si alloy improved its strength by 16.9% from 154 MPa to 180 MPa. Mechanical properties of Al-7Si-4.5Cu alloys are significantly improved by solid solution and intermetallic compounds of copper. Further modified and grain refined Al-7Si-4.5Cu alloy showed 15.6% improvement in UTS from180 MPa to 208 MPa. A large number of intermetallic particles in the alloys get refined and are responsible for improved tensile strength. The as-cast Al-7Si-4.5Cu alloy is having a coarse microstructure consisting of large primary α-Al

dendrites, interdendritic networks of eutectic silicon plates or needles and intermetallic $CuAl_2$ phase formed along the interdendritic region (Figure 4.3). Unmodified acicular Si structure acts as internal stress riser providing an easy path for fracture and is the primary reason for the low tensile strength of these alloys. We can conclude that breaking up these microstructures and dispersing the eutectic silicon needles uniformly and intermetallic $CuAl_2$ particles to fine particles of $CuAl_2$ phase formed along the interdendritic region, as shown in fig 4.4, would help in improving the mechanical properties of alloys. The increase in 0.2% proof strength after refinement and modification is due to the refinement of the Si rich phase that increases resistance to plastic deformation resulting in higher stress needed to nucleate cracks at the particle matrix interface. The improvements in mechanical properties of Al-7Si and Al-7Si-4.5Cu alloys are due to the microstructural changes between the combined modified and grain refined alloys and as-cast alloys. Basvakumar et al. (2007) have reported similar results in a 2.5% Cu containing Al-7Si alloy. The author has reported that refinement and modification are beneficial for improvement in mechanical properties individually and in combined form. The alloy exhibited an improvement in UTS of 149 MPa and 163 MPa with Cu additions in as-cast. This is about 10% improvement. Further, on combined addition of Al-1Ti-3B and Al-10Sr master alloys UTS was 200 MPa i.e approximately 22% improvements. Comparing these results with UTS values given in Table 5.1, increase in amount of Cu appears to have more significant influence in as-cast condition (163 MPa for 2.5 % Cu and 180 MPa for 4.5% Cu) and further with modification and refinement these alloys showed UTS 200 MPa and 208 MPa respectively indicating not much difference. However the melt treatment provides substantial improvement in ductility as compared to as-cast Al-7Si-4.5Cu alloy.

Figure 5.1a depicts the fracture surface of as-cast Al-7Si alloy, whereas Figure 5.1b shows the fracture surface of grain refined and modified Al-7Si alloy. The SEM observations indicate a large fraction of broken Si particles and relatively flat Al matrix regions. These features suggest the easy crack nucleation and propagation. This results in low strength and hardness values. Figure 5.1b shows lot of dimples suggesting ductile fracture and slow crack movement accompanied by plastic

deformation and the fracture surface does not appear to be brittle type as there is no evidence of cleavage on the fractured surface. As per the Hall Petch relationship, yield strength (YS) for a given material is expressed by $s_s = s_o + K*d^{-1/2}$, where s_o is YS of the single crystal, K is a constant and d is grain diameter. Hence smaller the grain size higher is the YS. With smaller grain sizes grain boundaries (GB) increase and- hinder the dislocation movement.

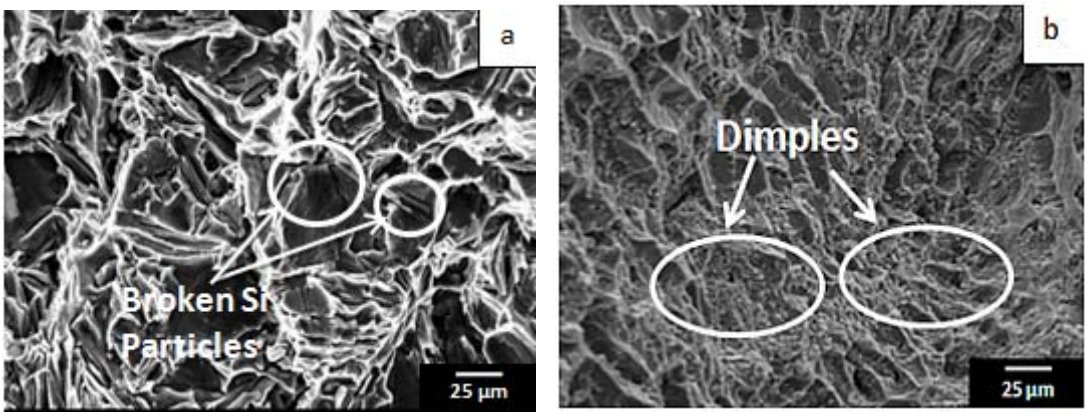

Figure 5.1: SEM images- Fractured surfaces of Al-7Si alloy (a) As-cast (b) Grain Refined and Modified

The fracture surface of the Al-7Si-4.5Cu alloy (as-cast) is shown in Figure 5.2a. Comparing with Figure 5.1a, the Fractograph is showing a number of cleavages with a few dimples, characterizing more of brittle nature of fracture. This may be due to the hard $CuAl_2$ intermetallics in the matrix.

The untreated specimen (Fig 5.2a) shows cleavage features due to its brittle nature. In comparison the fracture surface of grain refined and modified alloy in Figure 5.2b shows a fine and homogenous feature with more number of dimples and less cleavage features representing a typical ductile fracture. Hence the tensile test results show an improvement in ductility from 5.9% to 8.5% after combined refinement and modification.

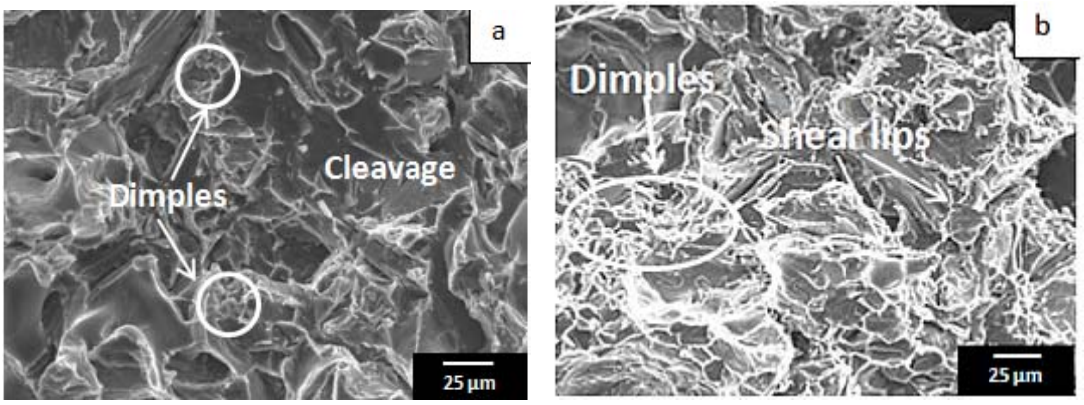

Figure 5.2: SEM images- Fractured surfaces of Al-7Si-4.5Cu alloy (a) As-cast (b) Grain refined and modified

The changes observed in mechanical properties of Al-7Si and Al-7Si-4.5Cu alloys in as-cast condition and after combined addition of modifier and grain refiner are shown in Figure 5.3.

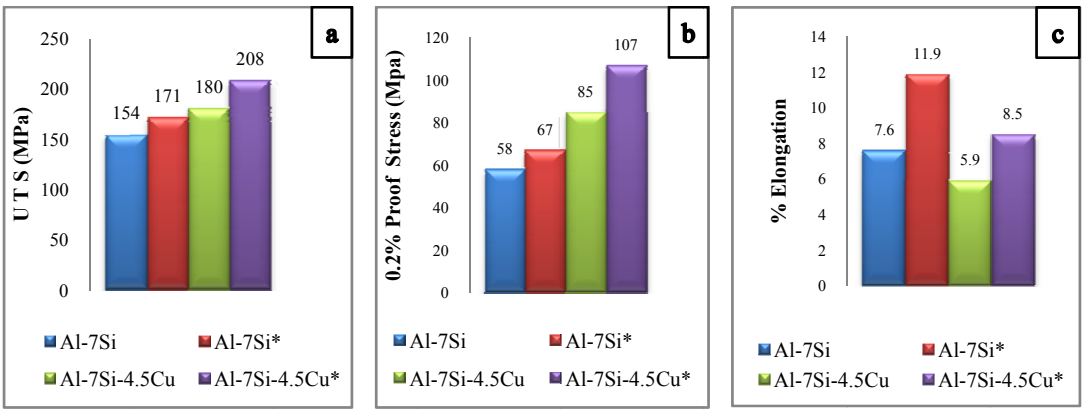

Figure 5.3: Mechanical properties of Al-7Si and Al-7Si-4.5Cu alloys

Modification and grain refinement of Al-7Si alloy has resulted in the improvement of UTS and 0.2% proof stress by 11% and 16%, respectively. Addition of 4.5% copper to Al-7Si alloy has resulted in the improvement of UTS and 0.2% proof stress by 17% and 47%, respectively. Melt treatment of Al-7Si-4.5Cu showed further improvement in UTS and 0.2% proof stress. Overall 35% and 84% increase are observed as compared to as-cast Al-7Si alloy respectively. Also the combined modification and grain refinement of Al-7Si alloy resulted in the substantial

improvement in ductility (57%). The change in morphology to fibrous Si and refined grains enhances ductility because of its profound effect on crack initiation and crack propagation resistance (Samuel et al. 2015). However, addition of 4.5% Cu resulted in the loss of ductility (22%) due to the presence of Cu rich intermetallics located in the grain boundaries. Smallman et al. (2007) have concluded that dislocations pile due to micro-stresses originating at the interface between the second phase particles and the matrix as a result intensify the possibility of micro crack initiation at these interfaces.

Further, the combined effect of modification and grain refinement resulted in improvement in the ductility by 12%. The improved ductility can be attributed to a finer and more abundant proportion of α-Al and to a more refined eutectic. The % change in mechanical properties of Al-7Si alloy due to combined modification and grain refinement and due to addition of 4.5% Cu is presented graphically in Figure 5.4.

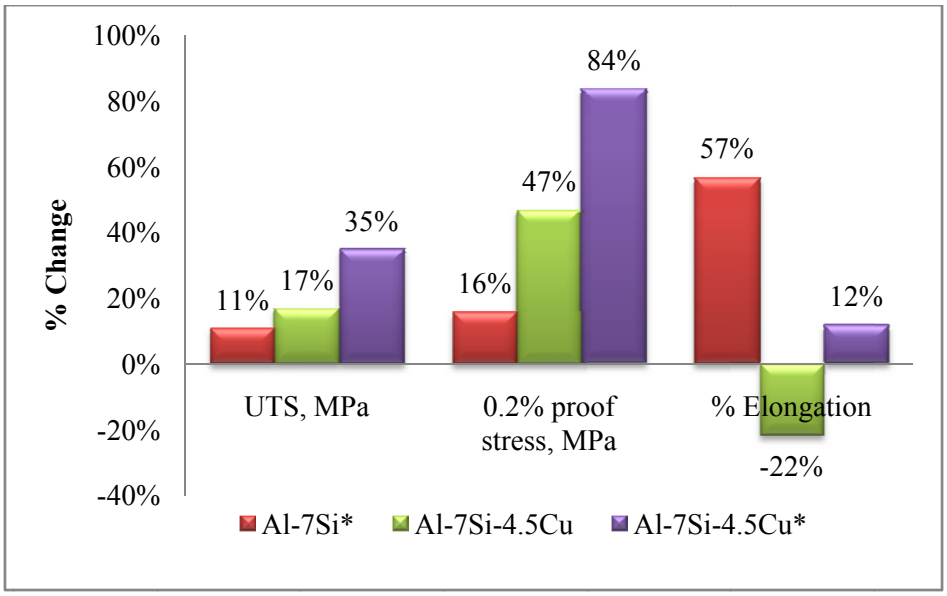

Figure 5.4: Improvement in mechanical properties of as-cast Al−7Si alloys due to combined modification and grain refinement and copper addition

5.3 Influence of combined modification and grain refinement on mechanical properties of Al-12Si and Al-12Si-4.5Cu Alloys

Table 5.2 displays the variations in UTS and yield strength and % elongation in as-cast condition and after combined grain refinement and modification.

Table 5.2: UTS and yield strength of Al-12Si and Al-12Si-4.5Cu alloys

Alloy Composition	**Al-12Si**	**Al-12Si***	**Al-12Si-4.5Cu**	**Al-12Si-4.5Cu***
UTS, Mpa	201	237	276	292
0.2% proof stress, MPa	69	99	129	141
% Elongation	5.8	9.1	4.3	7.6

*Grain refined and modified

It can be observed that after combined refinement and modification, UTS, YS and % elongation are increased. This effect may be attributed to the increase in nucleation sites due to the presence of Al_3Ti and TiB_2 particles in Al-1Ti-3B grain refiner which act as nucleating agents during solidification for the pre-eutectic α-Al phase nucleation during solidification resulting in finer grain size. A finer grain size results in improved tensile properties of the alloy due to the resistance experienced by the dislocations for their movement. The increased number of grain boundaries reduces the extent of uninterrupted movement of dislocations. It can be seen that with the addition of grain refiner and modifier to melt, UTS has increased by 17.9% from 201 MPa to 237 MPa. Similarly, 0.2% proof stress is improved by from 69 MPa to 99 MPa. These results indicate that the combined refinement and modification has similar beneficial effect for the enhancement of mechanical properties just like that in case of Al-7Si alloy. However, on the other hand, for the alloy with 4.5 wt.% of Cu UTS increased by 37% to 276 MPa. Further, after treating Al-12Si-4.5Cu alloy with

modifier and grain refiner UTS improved marginally (5.8%) from 276 MPa to 292 MPa. The as-cast Al-12Si and Al-12Si-4.5Cu alloys displayed the formation of acicular eutectic silicon and $CuAl_2$ particles in the interdendritic region, respectively as shown in Fig 4.14a and 4.16a. The presence of these phases leads to premature crack initiation during tensile load and reduce the strength and ductility of the alloy. When these alloys were treated by the combined addition of grain refiner and modifier in liquid phase the microstructure is refined considerably (average grain size of Al-12Si reduced from 90 μm to 40 μm and that of Al-12Si-4.5Cu 75 μm to 35 μm) leading to improvement in mechanical properties. Jigajinni et al. (2013) while testing near eutectic alloy (Al-11Si) reported similar trend in improvement of mechanical properties for alloy treated with 0.65% of Al-1Ti-2.2B master alloy and 0.03% Sr. Combined addition of 1% Al-1Ti-3B grain refiner and 0.4% Al-10Sr to Al-12Si-3Cu alloy has resulted in improved mechanical properties. UTS increased from 215 MPa to 275 MPa and 0.2% proof stress increased to 121 MPa from 90 MPa after grain refinement and modification (Basavakumar et al. 2007). From the above discussions it can be inferred that Cu content, % of modifier or / and refiner together influences the improvement in mechanical properties of the Al-Si alloy.

The SEM micrograph showing the fracture surfaces of Al-12Si alloy in as-cast condition is presented in Figure 5.5.

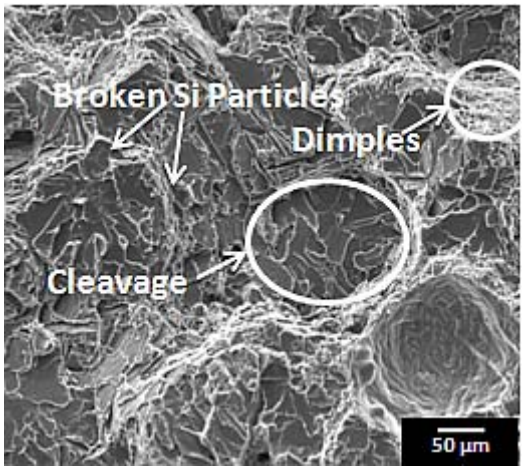

Figure 5.5: Fractured surface of as-cast Al-12Si alloy

The fracture surfaces are perpendicular to tensile direction and show fractured / broken primary Si particles. It may be observed that the failure is dominated by quasi cleavage fracture. Flat surfaces formed by the fracture of acicular Si are also reported by Yudong Sui et al. (2015) suggesting that the brittle fracture is more dominant. However, in the case of grain refined and modified Al-12Si alloy, the modified Si morphology is more resistant to fracture. As seen in Figure 5.6 dimples are more predominant than cleavage in the Fractograph. Due to modification there may be decrease in the total area of cleavage planes with the smooth flat areas are appearing smaller. The refinement of α-Al is also responsible for offering more resistance to deformation during a tensile test and thus responsible for increasing the UTS to 237 MPa. More grain boundaries are available due to more number of small size grains, causing a significant change in flow behaviour.

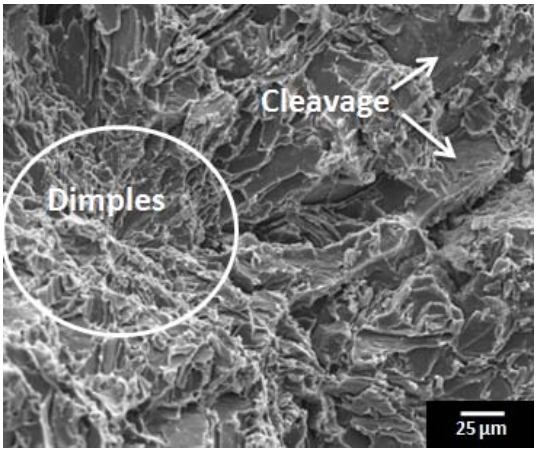

Figure 5.6: SEM micrograph of fractured surface of Al-12Si modified and grain refined alloy

Solid solution formation and presence of copper rich precipitates in Al-12Si-4.5 Cu contribute to increase the tensile strength. Figure 5.7 displays the SEM micrograph of fractured surface of as-cast Al-12Si-4.5Cu alloy mainly exhibiting cleavage facets. As compared to the fractured surface of the base alloy in Figure 5.5, the micrograph demonstrates a brittle fracture with limited evidence of ductility. The observed cleavage features suggest that the extent of brittle failure is comparatively more severe than Al-7Si-4.5Cu alloy. This is mainly due to the increase in hard Si

phase in addition to $CuAl_2$ intermetallics. Accordingly the strength has increased substantially while % of elongation has further decreased to 4.3 as compared to 5.9 in case of Al-7Si-4.5Cu alloy.

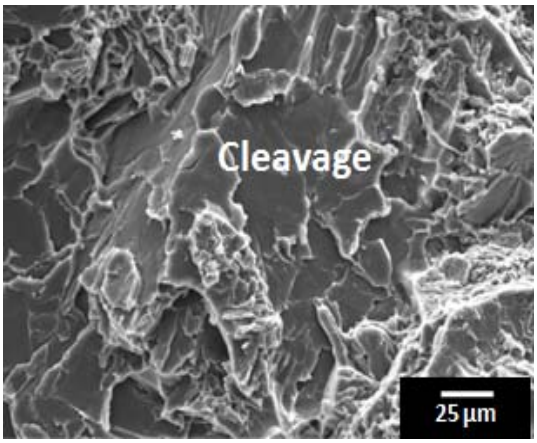

Figure 5.7: SEM micrograph of fractured surface of as-cast Al-12Si -4.5 Cu alloy

The microstructure of fractured surface of Al-12Si-4.5Cu with the addition of modifier and grain refiner is shown in Figures 5.8. It shows typical features failure of a material possessing good ductility. The fibrous appearance is an evidence for improved ductility.

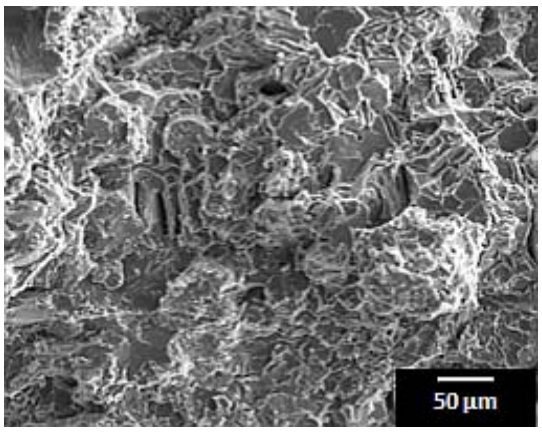

Figure 5.8: SEM micrograph of fractured surface of Al-12Si-4.5Cu modified and grain refined alloy

With modification and refinement the eutectic silicon grains fragment into smaller spheroids and more in number as shown in Fig 4.18b. Also the $CuAl_2$

precipitates become finer. The material undergoes deformation to some extent and the crack ahead of this propagates along the grain boundaries. Since grain boundaries effectively act as obstacles for slip dislocations, the strength and ductility improves. As suggested by Brechet et al. (1991), the degree of additional plastic flow around the particle depends on the particle size and its aspect ratio. According to their model the damage initiating process will affect the tensile strain. The second phase particles give rise to the internal stresses in the matrix material which in-turn affects the flow stress. The changes observed in the mechanical properties of Al-12Si and Al-12Si-4.5Cu alloys in as-cast condition and after combined addition of modifier and grain refiner are shown in Figure 5.9.

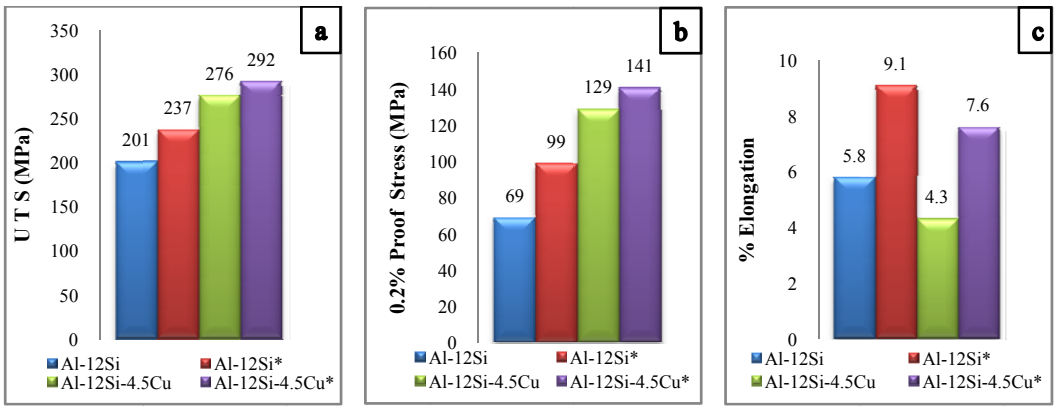

*Grain refined and modified

Figure 5.9: Mechanical properties of Al-12Si and Al-12Si-4.5Cu alloys

Modification and grain refinement of Al-12Si alloy improved UTS and 0.2% proof stress by 18% and 43%. This is mainly due to the conversion of large α-Al grains into fine equiaxed α-Al grains, plate like eutectic Si into fine particles. With an addition of 4.5% copper, precipitation of Cu rich intermetallics resulted in improved UTS and 0.2% proof stress by 37% and 75% respectively. However, the addition of 4.5% Cu and modifier and grain refiner together improved the UTS and 0.2% proof stress by 45% and 104%, respectively as compared to as-cast Al-12Si alloy. Improvement in mechanical properties is on account of the change of Si eutectic morphology from acicular and needle type to fibrous and globular. Combined modification and grain refinement of Al-12Si alloy resulted in substantial

improvement in ductility (57%). On the other hand, addition of 4.5% Cu resulted in the loss of ductility (26%). This is due to $CuAl_2$ intermetallics formed along the interdendritic region which act as crack initiation sites. The finer cracks initiated at these crack initiation sites get propagated through grain boundaries present in as-cast alloys. Further, by combined modification and grain refinement, the ductility is improved by 31%. The % change in mechanical properties of Al-12Si alloy due to combined modification and grain refinement and due to addition of 4.5% Cu is presented graphically in Figure 5.10.

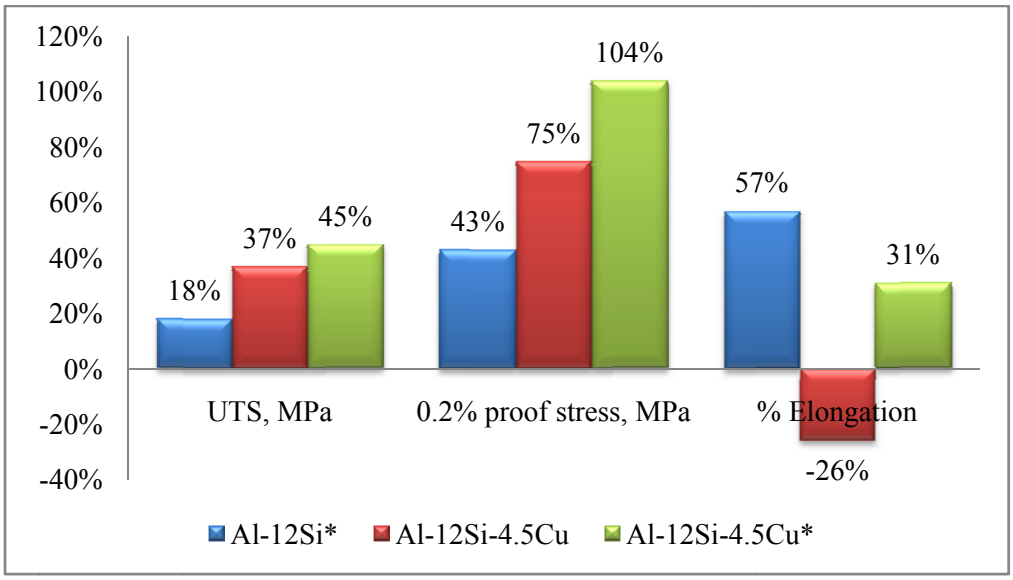

*Grain refined and modified

Figure 5.10: Improvement in mechanical properties of as-cast Al−12Si alloys due to combined modification and grain refinement and copper addition

5.4 Influence of combined modification and grain refinement on mechanical properties of Al-15Si and Al-15Si-4.5Cu alloys

Influence of combined modification and grain refinement on mechanical properties of Al-15Si and Al-15Si-4.5Cu Alloys was investigated and compared with those of the as-cast condition.. Table 5.3 presents the variations in UTS and yield strength and % elongation alloys in as-cast condition and after combined grain

refinement and modification. With combined addition of modifier and grain refiner the tensile strength of as-cast alloy increased from 186 MPa to 227 MPa. Similarly, 0.2% proof stress is improved from 76 MPa to 102 MPa. The microstructure of Al-15Si alloy (Fig 4.25a) consisted of coarse platelet and star like primary Si particles together with widely distributed eutectic silicon needles and few elongated α-Al dendrites resulting in poor ductility. Breaking up of these microstructures and dispersing the primary silicon and eutectic Si uniformly throughout the matrix as shown in Figure 4.25b, resulted in improved mechanical properties of the alloy. The as-cast Al-15Si alloy containing 4.5 wt.% of Cu showed a UTS value of 253 MPa.

Table 5.3: UTS and yield strength of Al-15Si and Al-15Si-4.5Cu alloys

Alloy Composition	**Al-15Si**	**Al-15Si***	**Al-15Si-4.5Cu**	**Al-15Si-4.5Cu***
UTS, MPa	186	227	253	271
0.2% proof stress, MPa	76	102	117	128
% Elongation	6.0	7.7	4.1	7.2

*Grain refined and modified

Further, UTS is improved to 271 MPa on treating Al-15Si-4.5Cu alloy with modifier and grain refiner. The microstructure of Al-15Si-4.5Cu cast alloys treated with the combined addition of refiner and modifier reveals fine and homogeneous primary Si particles together with fine modified eutectic silicon and fine intermetallic $CuAl_2$ phase formed along the interdendritic region, (Figure 4.31) which further enhances the tensile strength. However the effect of melt treatment in Al-15Si-4.5Cu is not as significant as in Al-15Si alloy, but there is a marked improvement in % elongation of Al-15Si-4.5Cu alloy.

The fracture surface of Al-15Si alloy in condition after tensile test is shown in Figure 5.11a. The structure features cracks and cleavage facets with less number of

dimples. This suggests that the specimen has undergone predominantly a cleavage fracture with minimum evidence of plastic deformation in the α-Al matrix. In this alloy the number of Si (hard phase) particles in α-Al (soft phase) matrix are relatively more. The dislocations pile up at α-Al / Si interfaces and result in larger number cleavage micro cracks at these sites. The brittle phases are smashed under stress concentration and act as crack initiators. As a result, as-cast Al-15Si alloy exhibited low tensile properties. Moreover, it can be seen that the cracks are initiated at Si particles. These observations, further suggest that in as-cast Al-15Si alloy, fracture is initiated and propagated through Si particles that have coarse plate like structures. M Gupta et al. (1999) have reported much higher rate of drop in ductility for higher Si percentages.

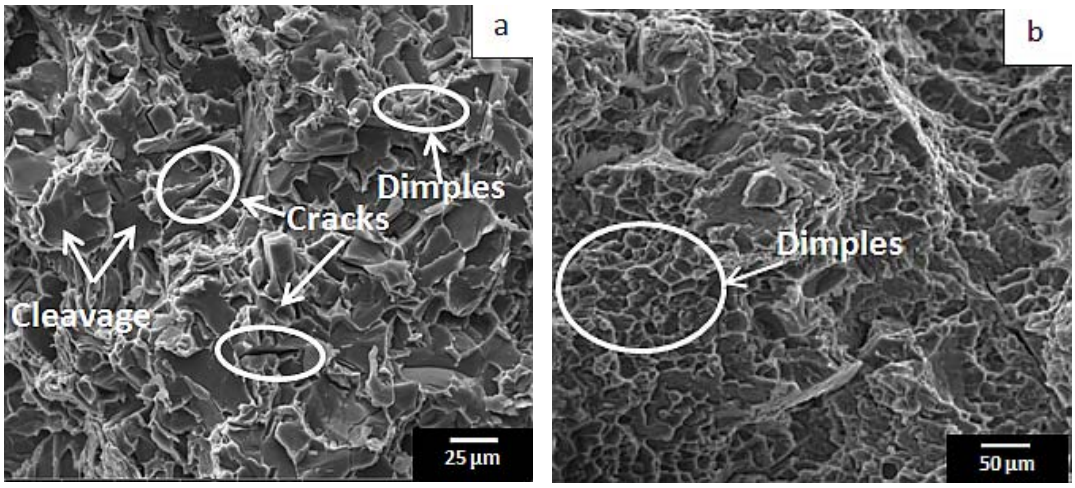

Figure 5.11: SEM micrographs of fractured surfaces of Al-15Si alloy (a) As-cast (b) Modified and grain refined

Figure 5.11b reveals predominantly dimples and very few cleavage facets indicating the ductile nature of fracture in Al-15Si alloy that is grain refined using Al-1Ti-3B and modified using P and Sr. This suggests that modification of eutectic Si morphology has influenced significantly. The change in fracture mechanism from brittle to ductile is basically due to changes in morphology of Si particles and a close observation of microstructures of as-cast Al-15Si and melt treated Al-15Si alloys presented in chapter 4 suggests that needle / plate like Si particles have changed to fibrous type. Moreover, dimples observed in Figure 5.11b evidently exhibit a plastic

deformation had occurred before the fracture took place. These microstructural results are in support of the improved tensile properties from 186 MPa to 227 MPa and ductility from 6.0% to 7.7%. Observations on the effect of Si content reveals that up to eutectic composition the strength of the alloy increases and further it begins to decline. In comparison to strength, the hardness continuously increases with Si content while % elongation continuously decreases with increasing Si content. This is mainly attributed to Si appearing as fine particles distributed uniformly in the matrix up to eutectic composition and beyond eutectic composition the primary silicon appears as coarse polyhedral particles aiding the easy crack propagation.

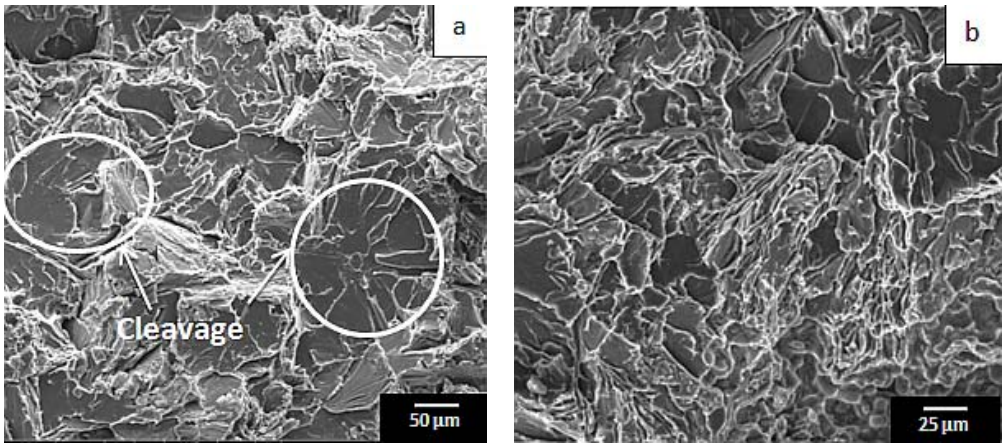

Figure 5.12: SEM micrographs of fractured surfaces of Al-15Si-4.5Cu alloy
(a) As-cast (b) Modified and grain refined

Figure 5.12a shows the fractured surface of Al-15Si-4.5Cu as-cast alloy. Cleavage facets are predominant revealing that the alloy has undergone brittle fracture. Figure 5.12b shows the fractured surface of Al-15Si-4.5Cu alloy which is grain refined and modified. A close observation of the fractured surface reveals that dimples are more predominant than cleavage planes. Melt treatment has resulted in decrease in the total area of cleavage planes. Al-15Si-4.5Cu alloy exhibits high tensile strength as compared to as-cast Al-15Si and melt treated Al-15Si alloys.

The changes observed in mechanical properties of Al-15Si and Al-15Si-4.5Cu alloys in as-cast condition and after combined addition of modifier and grain refiner are shown in Figure 5.13.

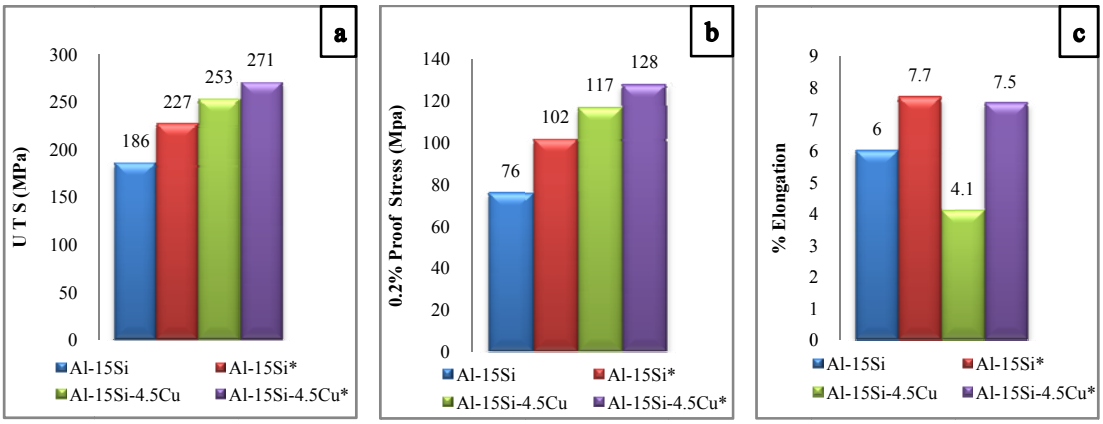

*Grain refined and modified

Figure 5.13: Mechanical properties of Al-15Si and Al-15Si-4.5Cu alloys

The % change in mechanical properties of Al-15Si alloy due to combined modification and grain refinement and due to addition of 4.5% Cu is presented graphically in Figure 5.14. While combined modification and grain refinement of Al-15Si resulted in substantial improvement in ductility (28%), addition of 4.5% Cu resulted in the loss of ductility (32%). Addition of Cu leads to the formation of hard Cu rich intermetallics, which act as reinforcing agents increasing the hardness, UTS and yield strength of the material. On the other hand, Cu addition results in reduction in elongation based on segregation of intermetallics in grain boundaries. Further, by combined modification and grain refinement, the ductility could be improved by 22%. A steady improvement of 9%, 17% and 29% was observed in hardness values, after melt treatment, 4.5% copper addition and after both copper addition and combined modification and grain refinement.

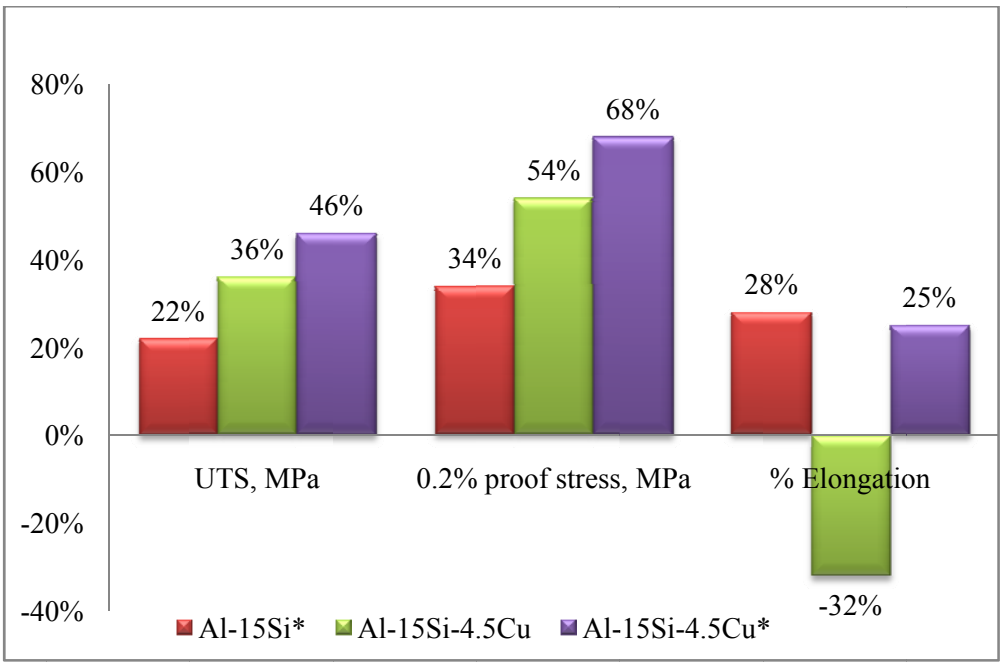

*Grain refined and modified

Figure 5.14: Improvement in mechanical properties of as-cast Al−15Si alloys due to combined modification and grain refinement and copper addition

5.5 Influence of Ageing on Mechanical properties

As discussed in sections chapter 4, T6 heat treatment produces considerable improvements in the microstructure of all the three alloys with 4.5% Cu both in as-cast as well as modified and refined condition. The addition of copper to Al-Si alloys improves their tensile strength due to precipitation of hard $CuAl_2$ precipitates. However the ductility reduces due to this. Based on the observations of earlier researchers (Mohamed and Samuel 2012; Sjolander and Seifeddine 2010) T6 heat treatment is employed to envisage further improvement in strength with decrease in ductility. In the present work, the material is subjected to solution treatment 500 °C for 6 hours, quenching and ageing at 200 °C up to 48 hours. It is reported by earlier researchers that 500 °C and up to 20 h of solutionizing are favorable for dissolution of $CuAl_2$ precipitates. The amount of dissolved Cu or super saturation of solute atom in Al matrix and the number of vacancies (that act as potential sites for precipitation)

created during solutionizing correspond to selected temperature and time and this in turn controls dispersion of the particles and the typical distance between them.

5.6 Effect of Ageing on Mechanical properties of Al-7Si-4.5Cu alloy

Table 5.4 shows the variations in UTS, yield strength and % elongation of the alloy before and after combined modification and grain refinement in as-cast and aged conditions. A significant improvement is achieved in the mechanical properties due to heat treatment but at the expense of ductility.

Table 5.4: Mechanical properties of as-cast and age hardened Al-7Si-4.5Cu alloy

Alloy`	Heat treatment	Time (h)	UTS (MPa)	0.2% Proof Stress (MPa)	% Elongation
Al-7Si-4.5Cu	As-cast	--	180	85	5.9
	Aged	4	195	115	5.5
		20	240	125	4.6
Al-7Si-4.5Cu (Modified and Grain Refined)	As-cast	--	208	107	8.5
	Aged	4	210	122	7.5
		20	262	137	7.0

As-cast Al-7Si-4.5Cu alloy exhibited UTS of 180 MPa and with T6 heat treatment it improved up to 240 MPa. However, the elongation is reduced from 5.9% to 4.6% when samples were aged for 20 h. Similarly, modified and grain refined alloy exhibited 208 MPa and after heat treatment, it achieved a tensile strength of 262 MPa while ductility reduced from 8.5% to 7.0%. The increase in strength is attributed to the precipitation hardening due to intermetallic compounds wherein Cu precipitates inside the grains in the form of fine zones and transition precipitates during ageing stage to harden the alloy. Also, the spheroidization of eutectic Si phase retards the

crack initiation. These fine transition precipitates play a significant role in impeding the dislocation motion. The strength values of grain refined and modified alloy are comparatively higher than the as-cast Al-7Si-4.5 Cu alloys in cast and aged conditions because higher grain refinement of Al matrix and modified structure of Si morphology. In the as-cast alloy the solute atoms show a tendency to segregate into networks of eutectic constituents. On heat treatment due to dissolution, the redistribution of elements occurs in the constituent phases. This minimizes the segregation and this is one of the causes for improvement in strength.

The increase in strength and hardness due to precipitation hardening is balanced out by corresponding decrease in ductility as is observed in Table 5.4.

The decrease in ductility due to solution treatment and aging results in enhanced internal stress generation. This lowers the ductility. Also the Cu in the alloy forms Al-Cu-Sr compound thus reducing the amount of Sr for modification of acicular Si. Hailin Yang et al. (2015) have reported that even sufficiently high solute contents can be detrimental to ductility as they can result in overwhelming precipitates. $CuAl_2$ may also hinder the Si from diffusing into Al matrix resulting in larger size Si particles after solidification. Parelastic interaction (coherency stresses between the particle and the matrix) is one of the mechanisms by which precipitated particles can effectively obstruct the motion of dislocations in the matrix. The maximum strength is obtained after 20 h of ageing (corresponding to peak hardness). This may be the stage where the coherent (θ'') and semi coherent (θ') precipitates co exist in the microstructure. As reported by Khaled Ragab (2012), highest strength is obtained in transition as this result in extensive coherency strains. The precipitate particle shape and size also contribute to strength. Spherical particles and small sizes result in fine dispersion in matrix minimizing inter particle distance.

Fractograph in Figure 5.15 a shows the fractured surface of the Al-7Si-4.5Cu alloy aged for 4 h. Microcracks are visible indicating brittle nature of failure. This hardening due to $GP_{(2)}$ zones is responsible for reduction in ductility from 5.9% to 5.5%. Micro mechanisms governing fracture characteristics of such alloys depend on

coherency and distribution of precipitates, grain size and shape, grain boundary precipitates, presence of other second phase particles which result from impurities (Kezhun et al. 2011). Figure 5.15b presents the fractured surface of the Al-7Si-4.5Cu alloy aged for 20 h. The surface displays cleavage fracture suggesting presence of large number of hard $CuAl_2$ precipitates. This is justified by the corresponding peak hardness and strength values and further drop in the ductility value to 4.6%.

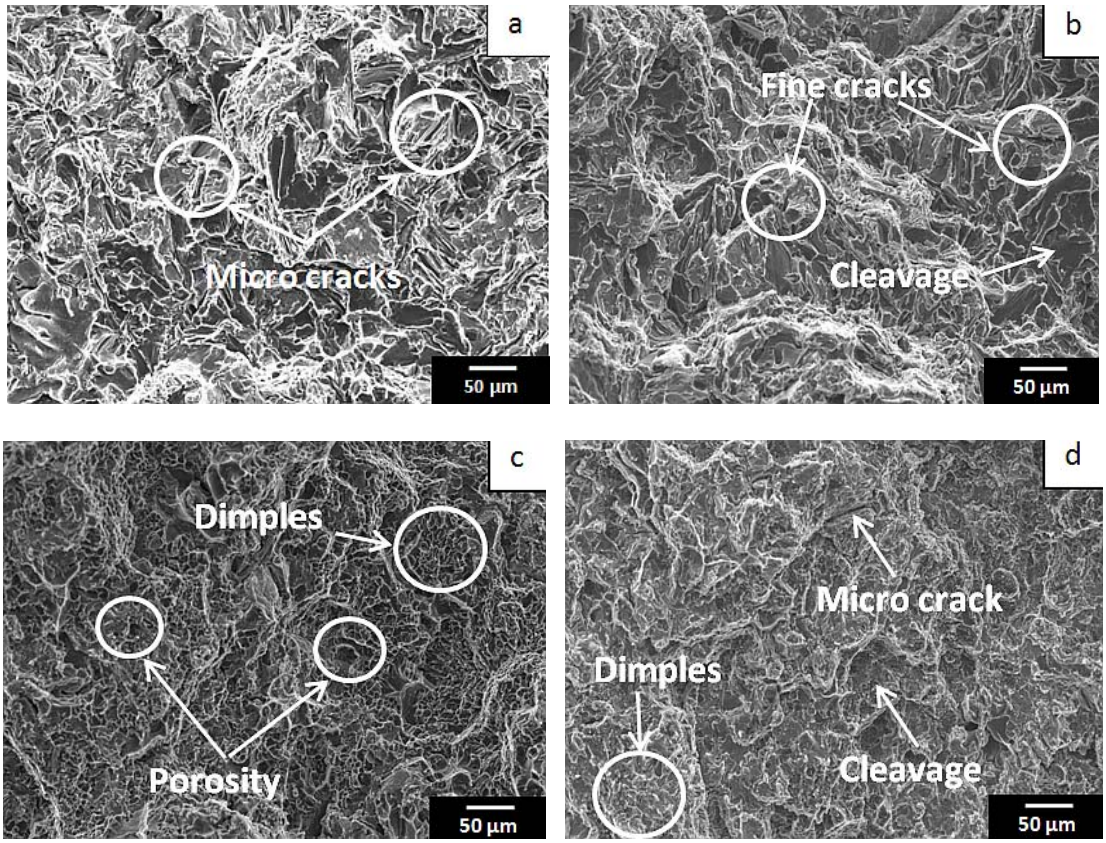

Figure 5.15: Fractured surfaces of Al-7Si-4.5Cu alloy: (a) aged for 4 h (b) aged for 20 h and Al-7Si-4.5Cu (modified and grain refined): (c) aged for 4 h (d) aged for 20 h

Figure 5.15 c and d shows the fractured surface of melt treated alloy aged for 4 h and 20 h. Both fractographs exhibit fibrous appearance and dimples suggesting evidence of ductile fracture. However, fractured surfaces also show presence of porosity and micro cracks indicating brittle failure to a certain extent. Considering these aspects, the nature of fracture can be considered as quasi-ductile. % elongation observed for the alloy aged for 4 h is 7.5% whereas the alloy aged for 20 h is 7%.

Li et al. (2004) have made the following observations. Due to the Sr-modification, the eutectic Si precipitates in fibrous form and the T6 heat treatment causes redistribution of copper into the aluminium matrix. Both factors contribute in enhancing the UTS. Sr addition also leads to segregation of blocky $CuAl_2$ phase, in the areas away from the Al-Si eutectic regions. Blocky $CuAl_2$ phase is harder to dissolve in the aluminium matrix. Thus the benefits of having Cu as a strengthening agent are reduced. This results in reducing the tensile properties. However, dissolution of $CuAl_2$ particles after T6 heat treatment can minimize this kind of negative effect.

5.7 Effect of Ageing on Mechanical properties of Al-12Si-4.5Cu alloy

Table 5.5 presents the variations in UTS, yield strength and % elongation of Al-12Si-4.5Cu alloy before and after combined modification and grain refinement in as-cast and aged conditions.

Table 5.5: Effect of Ageing on Mechanical properties of Al-12Si-4.5Cu alloy

Alloy	Heat treatment	Time (h)	UTS (MPa)	0.2% Proof Stress (MPa)	% Elongation
Al-12Si-4.5Cu	As-cast	--	276	129	4.3
	Ageing	2	290	137	4.1
		12	312	155	3.6
Al-12Si-4.5Cu (Modified and Grain Refined)	As-cast	--	292	141	7.6
	Ageing	2	320	149	7.3
		12	344	170	6.8

During T6 heat treatment, the α-Al phase super saturated with Cu precipitates as GP zones, transition precipitates and finally as equilibrium $CuAl_2$. Wang et al.

(2011) have reported that the GP zones keep coherencey with the matrix, and form coherence strain zone, resulting in improved matrix strength leading to significant improvement in the mechanical properties after heat treatment. As-cast alloy exhibited initially 276 MPa and after heat treatment, a tensile strength of 312 MPa was achieved. However, elongation is reduced from 4.3% to 3.6%. Similarly, modified and grain refined alloy exhibited initially 292 MPa and after heat treatment, a tensile strength of 344 MPa was achieved. In this case elongation is reduced from 7.6% to 6.8%. Figure 5.16a shows the fractured surface of the Al-12Si-4.5Cu alloy aged for 2 h. The features of SEM indicate cleavage facets and broken Si particles suggest that the specimen has undergone brittle fracture.

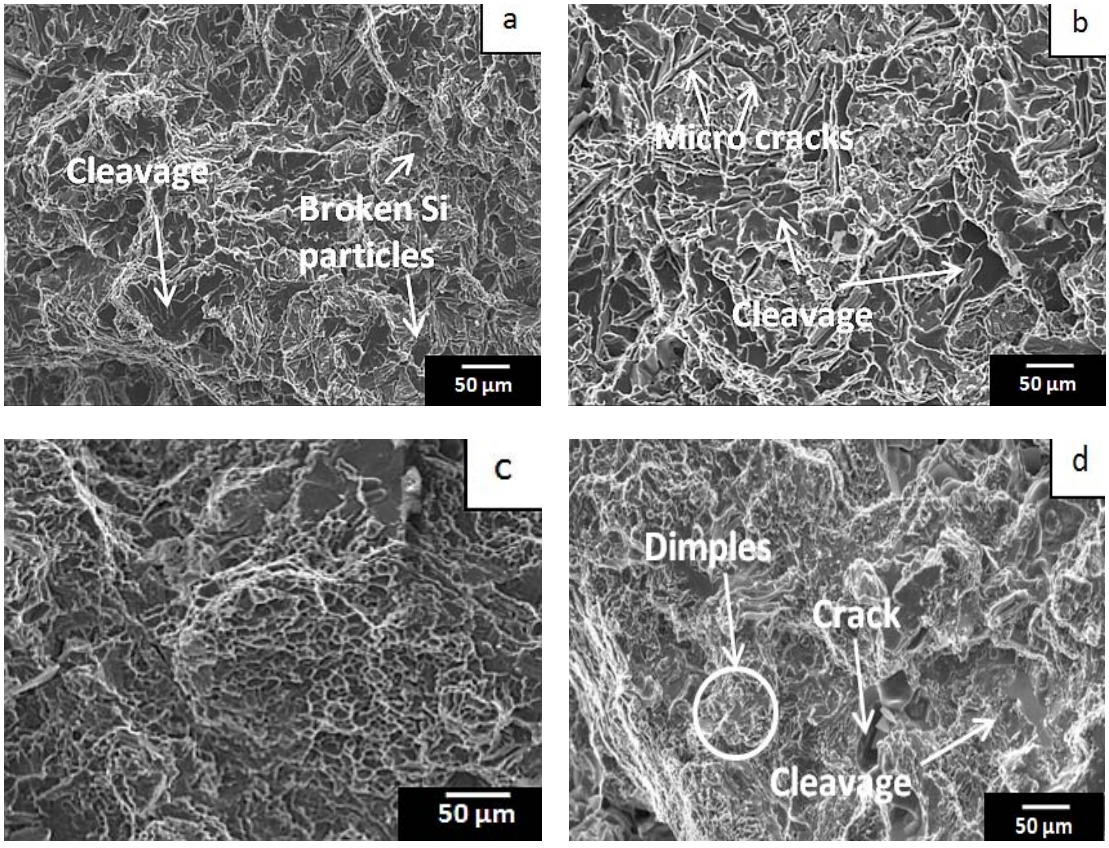

Figure 5.16: Fractured surface of Al-12Si-4.5Cu alloy: (a) aged for 2 h (b) aged for 12 h and Al-12Si-4.5Cu (modified and refined): (c) aged for 2 h (d) aged for 12 h

Fractured surface shown in Figure 5.16b is of Al-12Si-4.5Cu alloy aged for 12 h. The fracture surface exhibits cleavage fracture, confirming lowering the ductility to

3.6% from 4.3% of that of the as-cast alloy. Figure 5.16c exhibits the fractured surface of the modified and grain refined alloy. Cleavage facets along with dimples covering large area of the fractured surface, indicating both ductile and brittle characteristics yielding a elongation of 7.3%. Figure 5.16d is the fracture surface of melt treated Al-7Si-4.5Cu. The presence of some cracks and cleavage can be seen in this fracture. This is the reason for minor reduction in ductility from 7.3 to 6.8%. In both the cases reduction in % elongation is observed on ageing. However in case of modified and refined alloy the ductility levels are higher and also the % reduction on ageing is lesser. A more refined structure is less affected by internal stresses from T6 treatment.

5.8 Effect of Ageing on Mechanical properties of Al-15Si-4.5Cu alloy

Table 5.6 shows the variations in UTS, yield strength and % elongation of Al-15Si-4.5Cu alloy before and after combined modification and grain refinement in as-cast and aged conditions.

Table 5.6: Effect of Ageing on Mechanical properties of Al-15Si-4.5Cu alloy

Alloy`	Heat treatment	Time (h)	UTS (MPa)	0.2% Proof Stress (MPa)	% Elongation
Al-15Si-4.5Cu	As-cast	--	253	117	4.1
	Ageing	8	272	130	3.9
		20	290	135	3.2
Al-15Si-4.5Cu (Modified and Grain Refined)	As-cast	--	271	128	7.2
	Ageing	8	285	140	6.8
		20	300	144	6.3

Significant improvement is achieved in the mechanical properties by heat treatment. As-cast alloy exhibited initially 253 MPa and after heat treatment, a tensile strength of 290 MPa was achieved. However, elongation is reduced from 4.1% to 3.2%. Similarly, modified and grain refined Al-12Si-4.5Cu alloy exhibited initially 271 MPa and after heat treatment, a tensile strength of 300 MPa was achieved. In this case elongation is reduced from 7.2% to 6.3%.

Figure 5.17a displays the SEM micrograph of fractured surface of the Al-15Si-4.5Cu alloy aged for 4 h. The features of SEM show cleavage facets with less number of dimples. This suggests that the specimen has undergone predominantly a brittle fracture with little ductility. Micro cracks also can be observed which usually stem from primary Si crystals in hypereutectic alloys.

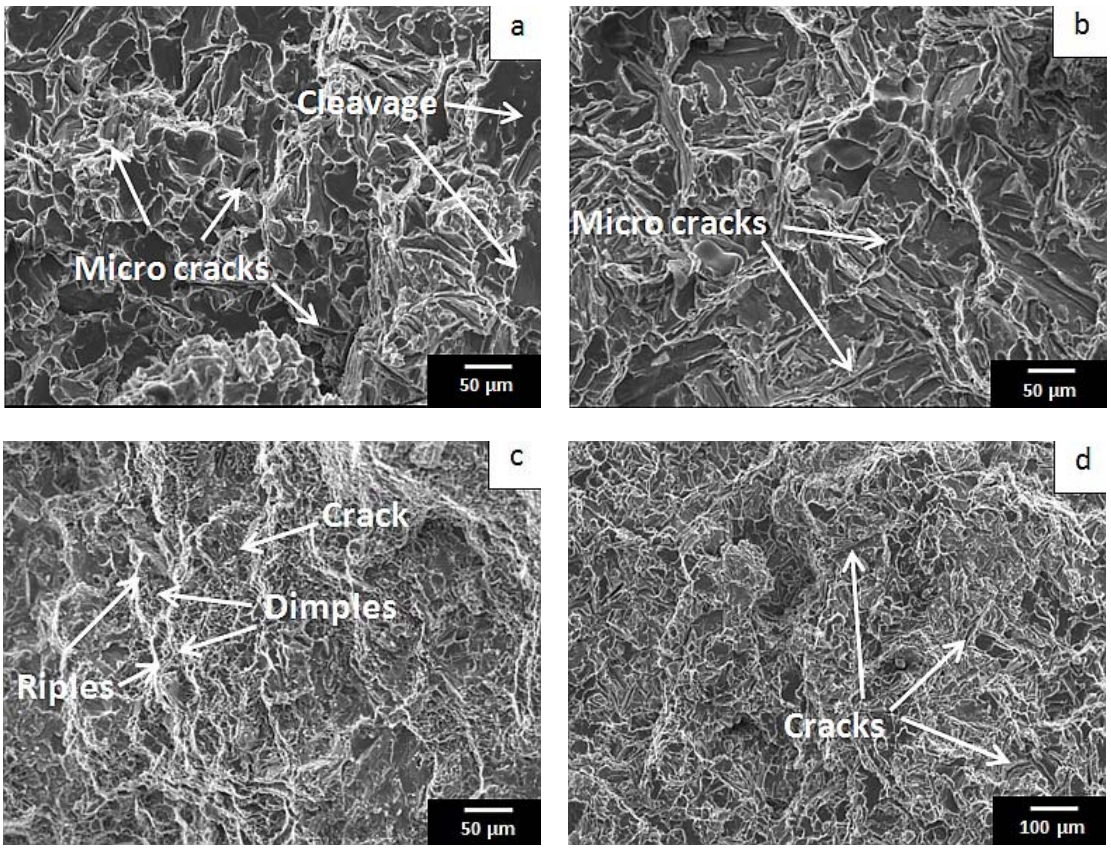

Figure 5.17: Fractured surface of Al-15Si-4.5Cu alloy: (a) aged for 8 h (b) aged for 20 h and Al-15Si-4.5Cu (modified and refined): (c) aged for 8 h (d) aged for 20 h

Figure 5.17b exhibits the SEM micrograph of fractured surface of the Al-15Si-4.5Cu alloy aged for 20 h. The cracks are mainly localized in interdendritic region. The T6 heat treatment has accelerated the precipitation of ultra-fine phases that take the alloy to its peak strength of 240 MPa. In Figure 5.17c, it can be seen that a dimple-like pattern on the eutectic regions and smooth ripple pattern on the α-phase region is observed. The SEM fractograph of Al-15Si-4.5Cu alloy aged for 8 h exhibited a smooth ripple pattern along with fine cracks in the fracture surface. This type of fracture results in low ductility. In addition, Al-15Si4.5Cu alloy aged at 20 h showed more number of cracks resulting in further reduction in ductility levels.

5.9 Effect of Ageing on Mechanical properties of Al-7Si-4.5Cu, Al-12Si-4.5Cu and Al-15Si-4.5Cu alloy – A comparative Analysis

In earlier sections it is observed that addition of copper to Al-Si alloys influences mechanical properties and hardness. In this section a comparative illustration is given to understand the effect of modification and ageing on the three types of Al-Si alloys with same amount of copper addition.

5.9.1 Hardness

As compared to Al-7Si and Al-12Si alloys, addition of copper to Al-15Si resulted in achieving highest hardness of 82 BHN. This is due to higher Si content and $CuAl_2$ precipitates present in Al-15Si-4.5Cu alloy. Combined modification and refinement further improved the hardness to 90 BHN. Figure 5.18 shows the hardness behaviour of the 3 alloys with 4.5 wt% Cu considered in this work in as-cast and modified and refined conditions and further in both cases aged alloys were also evaluated. It can be seen from this figure that the as-cast Al-7Si-4.5Cu alloy exhibited a hardness of 65 BHN, which is substantially increased to 78 BHN (20% increase) and to 82 BHN (26.2% increase) due to increase in silicon content to 12 wt.% and 15% wt.% respectively. The imporvemnt of hardness in these alloys is basiclaly due to the higher silicon content and its size, shape and distribution in the matrix. As the silicon content is increased from 7 wt.% to 15 wt.% Si, a gradual increase in hardness

is noticed in this work. When these alloys are modfied and grain refined, they exhibited further improvemnt in hardness values due to the modfictaion of of Si partciles and grain refinemnt of Al phase. These grain refined and modified microstructural changes led to imporved hardness values. Another interesting aspect to note is that the % increase in hardness due to modification and refinement for both as-cast and aged Al-Si-Cu alloys is not proportional to their corresponding Si content. From this observation it may be inferrred that the $CuAl_2$ precipitates formed due to addition of Cu (which is 4.5 wt% for all the three alloys) contributes more significantly to their hardness.

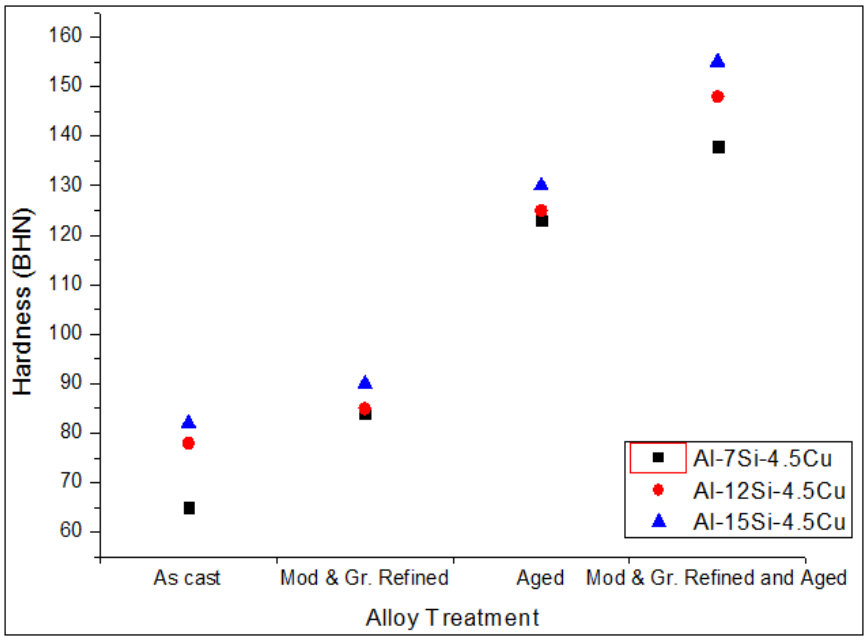

Figure 5.18: Effect of alloy treatment on Hardness

5.9.2 Ultimate Tensile Strength and Proof Stress

Among the three alloys, the maximum tensile strength of 276 MPa is achieved by Al-12Si-4.5Cu alloy. Tensile strength further improved to 292 MPa with combined modification and grain refinement. Figure 5.19 and 5.20 shows the variation in UTS and YS under different conditions of the three alloy variations. This may be attributed to the presense of both α-Al and Si in eutectic form.

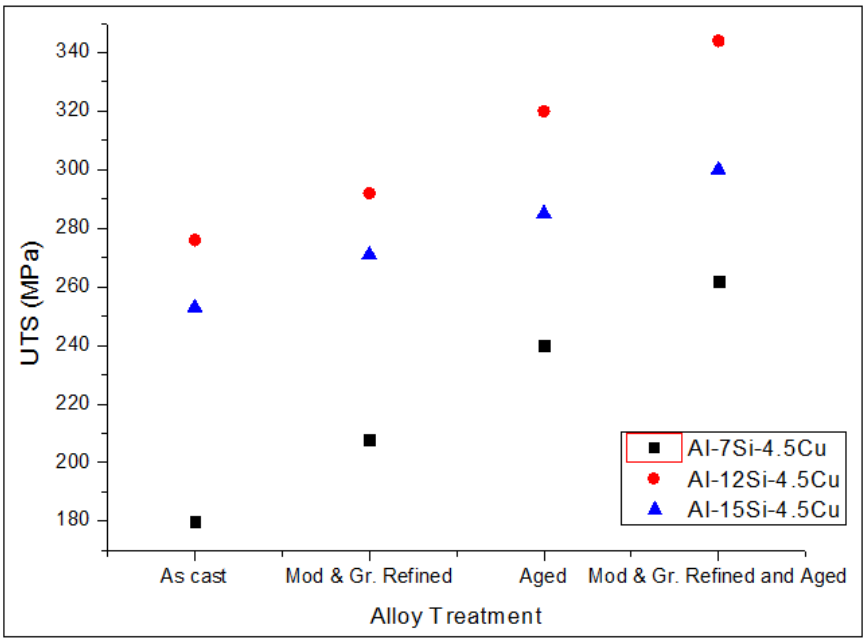

Figure 5.19: Effect of alloy treatment on Ultimate Tensile Strength

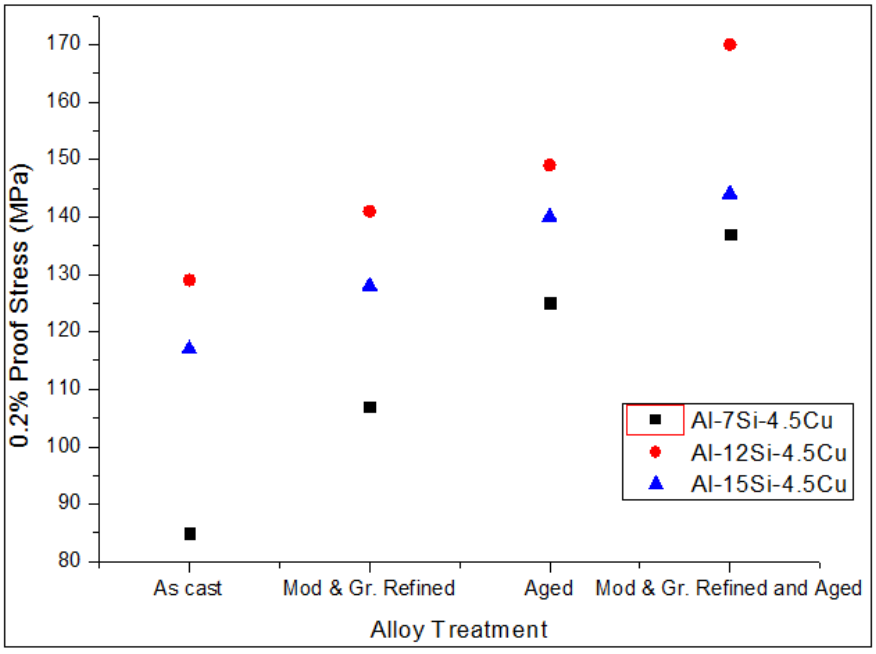

Figure 5.20: Effect of alloy treatment on Proof Stress

In addition to Sr the heating to solutionizing has also contributed appreciably in modifying accicular Si to fibrous form. The rate of spheroidization is proportional

to extent of modification. Hence in this case we can assume that nearly all the eutetcic silicon is spheroiidzed and further refined in to small particles, distributed uniformly in the matrix. This effect together with refinement of $CuAl_2$ precipitates and Al grains could be the probable reason for eutectic alloy exhibiting the highest strength values. Also in case of hypereutectic alloy the % Si, its shape and size and corresponding lower response to modification lowers its strength values, however the increased hard phase provides higher hardness under all conditions as shown in Figure 5.18.

5.9.3 Elongation

The % elongation values of modified and grain refined as-cast alloys, heat treated as-cast alloys and also modified and grain refined and heat treated alloys are plotted in Figure 5.21.

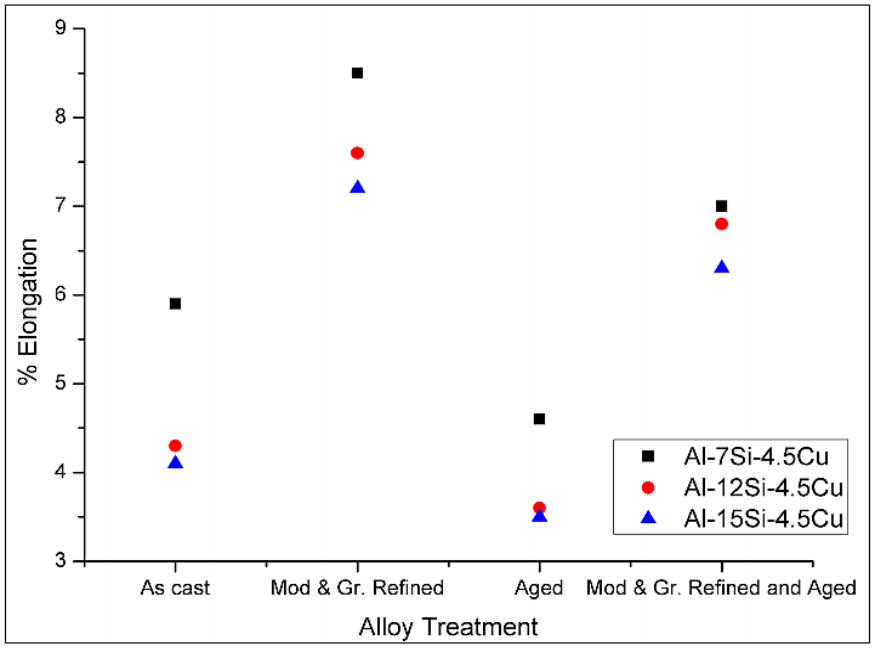

Figure 5.21: Effect of alloy treatment on Elongation

Combined modification and grain refinement resulted in improved elongation property of all experimental alloys. Highest elongation of 8.5% is achieved by Al-7Si-4.5Cu alloy after modification and grain refinement. However, Al-12Si-4.5Cu alloy

witnessed highest improvement in elongation as compared to it's as-cast condition. This is due to refinement of any primary Si particles which are detrimental to ductility as they act as crack initiating points.

In contrast to the effect produced by grain refinement and modification. precipitation hardening resulted in reduction of % elongation values. The decrease in elongation observed in this study is in good agreement with other researchers (Caceres et al. 1999; Sjolander & Seifeddine 2010).

Another possible reason could be coarsening of Si particles due to longer solutionizing time Literature reveals solutionizing times of up to 2 hours but in the present work it is done for 6 hours to ensure complete dissolution of solute atoms. The rate of spherodoization is rapid in modified alloys. Since the Si content in hypereutectic alloy is higher, modified and heat treated hypereutectic alloy can be a suitable material for components requiring high hardness and hence good wear resistance with reasonable strength and ductility. For applications requiring superior mechanical properties modified and heat treated eutectic alloy is a suitable material.

Chapter 6

Dry Sliding wear behavior of Al-Si alloys

6.1 Introduction

Dry sliding wear behaviour of pure metals has been extensively studied and attempts are made to study the sliding wear behaviour in polycrystalline materials. As far as the mechanism of wear is concerned, the pure metal exhibits same phenomena. However, the wear mechanism in alloys and compounds is different and complex in nature. It is reported in literature that several mechanisms play vital role in dry sliding wear behaviour of Al-Si alloys. The objective of the present investigation is to study the dry sliding wear behavior of Al-Si alloys in terms of Si content, combined addition of modifier and grain refiner with and without the addition of copper and also to evaluate the effect of ageing on dry sliding wear characteristics of Al-7Si-4.5Cu, Al-12Si-4.5Cu, and Al-15Si-4.5Cu alloys.

6.2 Influence of combined modification and grain refinement on dry sliding wear of Al-7Si and Al-7Si-4.5Cu alloys

In earlier chapters, the effect of addition of 4.5 wt.% Cu on microstructure and mechanical properties of Al-Si alloys and the effect of combined addition of grain refiner (Al-1Ti-3B) and modifier (Al-10Sr) on Al-7Si and Al-7Si-4.5Cu alloys have been discussed. Dry sliding wear behaviour of Al-Si cast alloys mainly depends on the shape, type, size and distribution of the α-Al grains, eutectic morphology (as a function of percentage Si) and $CuAl_2$ particles in the interdendritic region. The microstructure of Al-7Si and Al-7Si-4.5Cu cast alloys shown in Figure 4.1a and 4.4 consists of large primary α-Al grains, plate and needle-like eutectic Si and $CuAl_2$ particles in the interdendritic region. The unmodified acicular Si acts as internal stress risers (Casari et al. 2013). The combined addition of modifier and grain refiner

converts large elongated α-Al grains into finer grains and fine $CuAl_2$ particles in the interdendritic region as shown in Figure 4.1b and 4.5.

Figure 6.1 shows the volume loss at different load conditions of 10 N, 30 N and 50 N with constant sliding speed (2m/s) and sliding distance (1500 m).

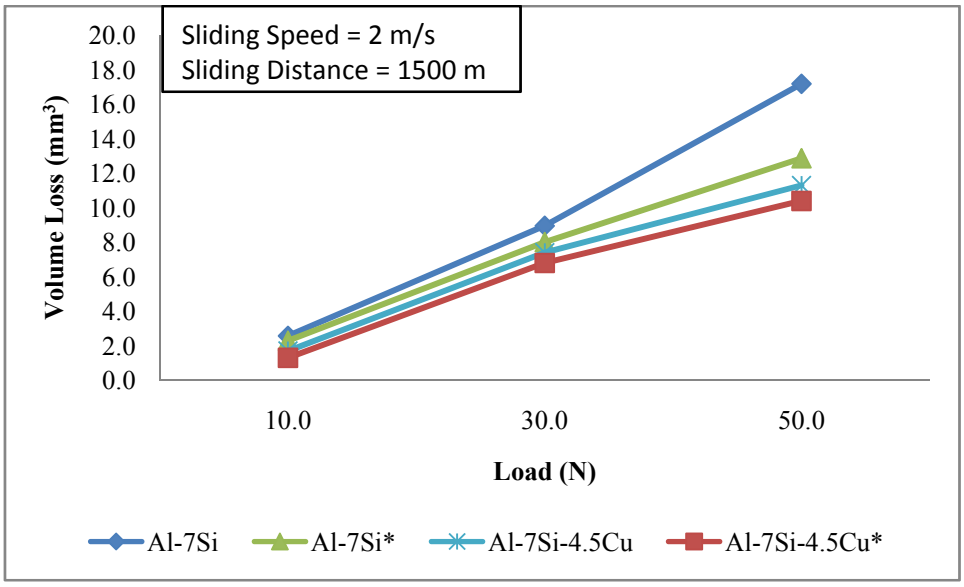

*Modified and grain refined

Figure 6.1: Variation of volume loss vs. normal loads of Al-7Si (as-cast and combined modified and grain refined) and Al-7Si-4.5Cu (as-cast and combined modified and grain refined) alloys

The combined addition of 1 wt.% of Al-1Ti-3B and 0.2 wt.% of Al-10Sr to Al-7Si and Al-7Si-4.5Cu alloys resulted in improved wear properties. The as-cast Al-7Si-4.5Cu alloys exhibited lower wear loss compared to as-cast Al-7Si alloy. Also, the combined modified and grain refined alloys showed improved wear resistance properties over the untreated alloys. The reduced wear loss can be attributed for the grain refined and modified Si particles which share the load more effectively and thereby protecting the matrix. In as-cast Al-7Si-4.5Cu alloy, needle type particles are more prone to cracking at high loads and results in greater wear loss. In addition, the hardness of Al-7Si-4.5Cu alloy with grain refinement and modification is comparatively higher than the as-cast alloy. This may be due to the solid solution

strengthening by Cu in presence of $CuAl_2$ intermetallics. (Garcia et al. 2003). The results demonstrate a gradual increase in wear volume loss with increase in load for all the investigated samples.

During sliding wear test, the pin experiences increased frictional force as the actual area of contact is increased. The increased frictional force and increased area of contact results in high wear loss. As seen in Figure 6.1 the decrease in volume loss for modified and refined alloys are comparatively much lesser at lower loads (30 N and 10N) in that order whereas it is quite appreciable at 50 N.

Prasad Rao et al. (2004) studied the wear behavior of Al-7Si alloy with varying load conditions and observed seizure of the specimen when the load is increased from 50 N to 70 N due to severe wear. In contrast, grain refined Al-7Si alloy did not seize at 70 N load due to lower wear loss. Basavakumar et al. (2007) studied the wear properties of Al-7Si alloy at higher loads and noticed occurrence of seizure at 100 N load. This is explained by the mechanism proposed by Lim and Ashby (1987). During sliding, a large pressure is experienced between the pin and counter surface and the asperities of both surfaces experiences many contact forces. As the load is increased, the area of contact also increases and equals to the normal area of the pin and results in seizure, referred as seizure pressure.

Figure 6.2 shows the variation of coefficient of friction (COF) vs. normal load for Al-7Si and Al-7Si-4.5Cu alloys. The coefficient of friction (μ) is more at higher loads for as-cast samples. It is clear that COF is decreased when Al-7Si alloy is modified and refined also with copper additions to Al-7Si alloy. Refinement of Al-Si-Cu showed lowest COF results when compared to those of other experimental alloys.

On comparing the COF values of Al-7Si-4.5Cu alloy with modified and grain refined alloy, it is observed that the COF values are reduced from ~0.55 to ~0.35. From these studies, it can be inferred that addition of 4.5% copper to Al-7Si alloy along with combined modification and refinement results in reduced COF and better wear resistance making these alloys suitable for various engineering applications requiring simplified lubrication, and quieter operation. Similar microstructural

observations in case of copper additions and grain refinement for Al-7Si alloy and corresponding reduction in COF values are observed by Alemdag and Savaşkan, (2009).

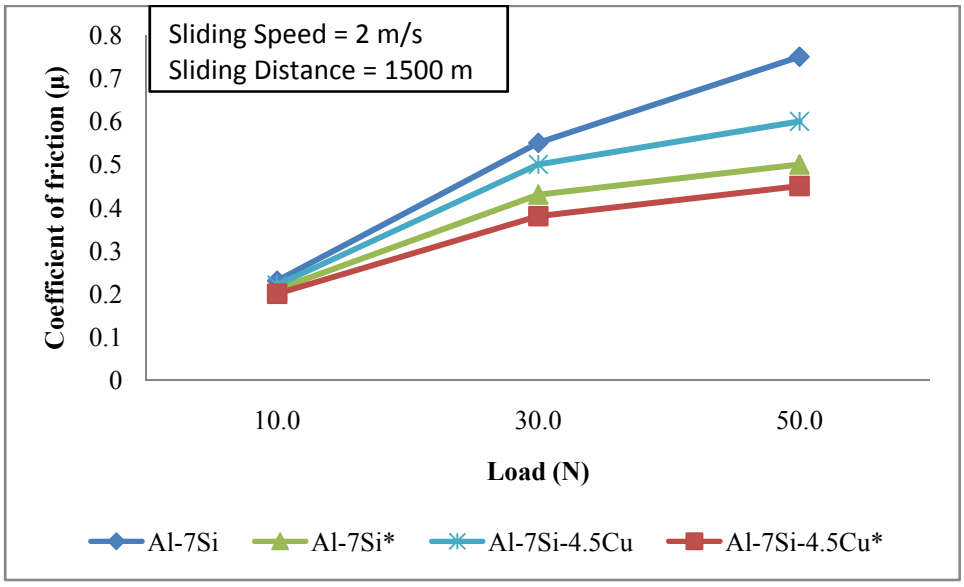

*Modified and grain refined

Figure 6.2: Variation of coefficient of friction vs. normal loads of Al-7Si as-cast and combined modified and grain refined) and Al-7Si-4.5Cu (as-cast and combined modified and grain refined) alloys

The SEM micrograph of worn surface of as-cast Al-7Si alloy at 50 N load is shown in Figure 6.3a. The SEM micrograph shows presence of ploughing. The ploughing marks are longer and continuous as compared to SEM of worn surface of Al-Si alloy with 4.5% Cu shown in Figure 6.3b. These results suggest significant material removal for as-cast Al-7Si alloy. This may be mostly due to low hardness of the alloy. Extensive plastic flow can also be seen. Cracks are generally initiated at the work hardened layer. These cracks grow and get interconnected in later stages. This leads to removal of layer of material which is referred as adhesive mechanism.

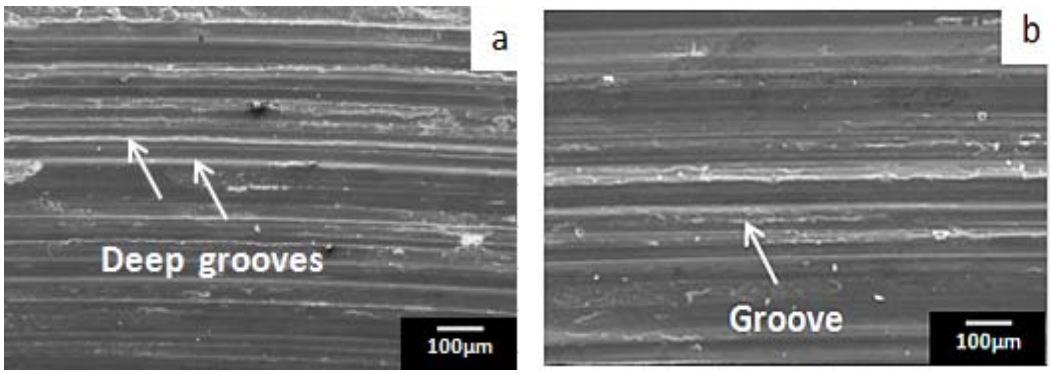

Figure 6.3: SEM micrographs of worn surfaces of as-cast alloys: at 50 N load (a) Al-7Si;(b) Al-7Si-4.5Cu

Figure 6.3b shows the worn surface of as-cast Al-7Si-4.5Cu alloy under dry wear conditions. The deep grooves are less in the case of Al-7Si-4.5Cu alloy as compared to that of Al-7Si alloy. The groves must have been created due to the presence of hard dispersoid particles or fractured debris. This genarally occurr during abrasion by entrapped debris, hard asperities on the hardened steel counter face or work hardened deposits on the counterface. As the copper additions have significant changes in microstructure and the needle like Si morphology also changed, the deep separated grooves into smooth grooves indicating increase in wear resistance.

The worn surface of modified and grain refined Al-7Si and Al-7Si-4.5Cu alloy under dry sliding wear conditions are shown in Figure 6.4a and b, respectively. Even though some sliding wear grooves are observed, the depth and width of these grooves are less as compared to those on the worn surfaces of Al-7Si, Al-7Si-4.5Cu as-cast alloys. Wear loss is inversely proportional to material hardness and tensile strength (Halling 1989). Both copper additions and Al-1Ti-3B grain refiner and Al-10Sr modification are responsible for high strength of the Al matrix. Refined Si and fine grain size of Al is responsible for good sliding wear resistance. As a result, the grain refined and modified Al-7Si alloy exhibited good wear resistance and low surface damage features.

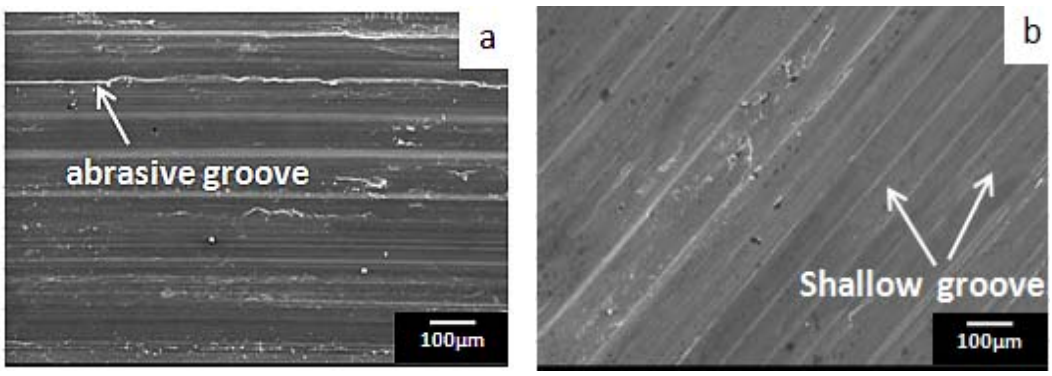

Figure 6.4: SEM micrographs of worn surfaces of modified and grain refined alloys: at 50 N load (a) Al-7Si (b) Al-7Si-4.5Cu

The studies conducted to understand the wear behaviour of hypoeutectic as-cast alloy before and after modification and grain refinement using Sr and Al-Ti-B respectively, reported improved wear resistance after melt treatment due to the changes in microstructure. Delaminated wear was reported for as cast Al-7Si alloy and the alloy treated with modifier and refiner exhibited abrasive / oxidative wear (Kori and Chandrashekharaiah 2007).

6.3 Influence of melt treatment on dry sliding wear of Al-12Si and Al-12Si-4.5Cu alloys

The influence of combined addition of modifier and grain refiner to eutectic Al-Si alloy with and without the addition of 4.5% Cu on the dry sliding wear behavior is studied. The volume loss variation at different applied loads for a constant sliding speed of 2m/s for a sliding distance of 1500 m is shown in Figure 6.5. Figure 6.6 shows variation of COF with load. It is noticeable from Figure 6.5 and 6.6 that the volume loss (mm^3) and COF are more at higher normal loads for as-cast samples. However, Al-12Si-4.5Cu cast alloy treated with the combined addition of grain refiner and modifier shows less volume loss (mm^3) and COF with increasing normal load. The addition of 4.5% Cu to Al-12Si alloy shows lower wear rate when compared to Al-12Si alloy.

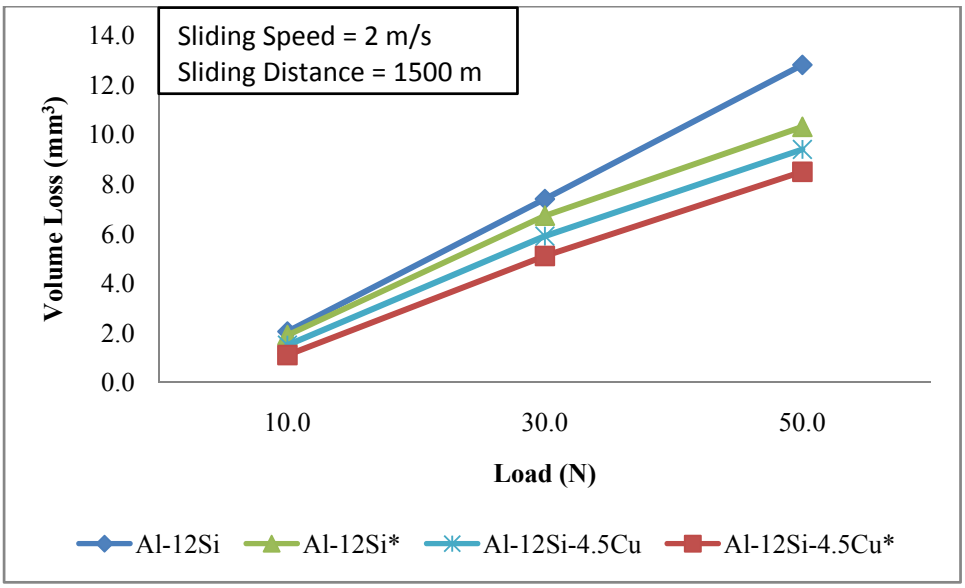

*Modified and grain refined

Figure 6.5: Variation of volume loss vs. normal loads of Al-12Si (as-cast and combined modified and grain refined) and Al-12Si-4.5Cu (as-cast and combined modified and grain refined) alloys

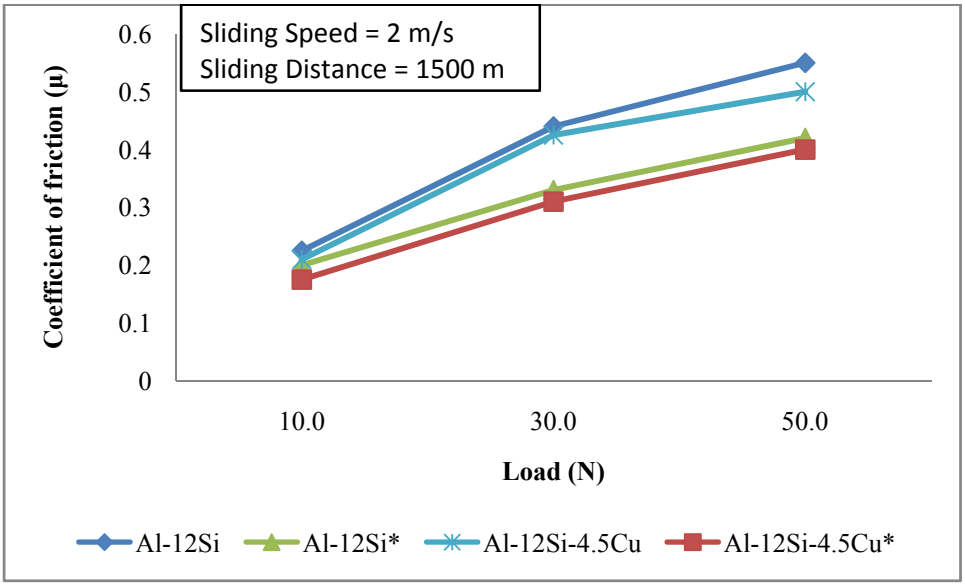

*Modified and grain refined

Figure 6.6: Variation of coefficient of friction vs. normal loads of Al-12Si (as-cast and combined modified and grain refined) and Al-12Si-4.5Cu (as-cast and combined modified and grain refined) alloys

Further, it is clear from the EDX studies on worn surfaces that the copper addition in general is responsible for improved wear resistance. Moreover, applied load and its increase are also responsible for high wear, as expected. These observations are similar to those of hypoeutectic Al-Si and Al-Si-Cu alloy that has been discussed earlier in section 6.2. Similar improvement in wear resistance of Al-Si eutectic alloy is noticed with addition of pure Ti as modifier (Saheb et al. 2001).

Figure 6.7a shows the worn surface of Al-12Si alloy where deep and wide grooves are seen. A number of long, deep unidirectional ploughing grooves can be observed. However, these grooves are less in number and shallow as compared to the grooves observed in Figure 6.3 for as-cast Al-7Si alloy. The improved wear resistance of Al-12Si as-cast alloy compared to Al-7Si cast-alloy is mainly due to higher hardness of the alloy. A close observation of worn surface of copper containing alloy in Figure 6.7b shows surface damages, like micro-grooves and delamination. Oxidation of delaminated area can also be clearly seen.

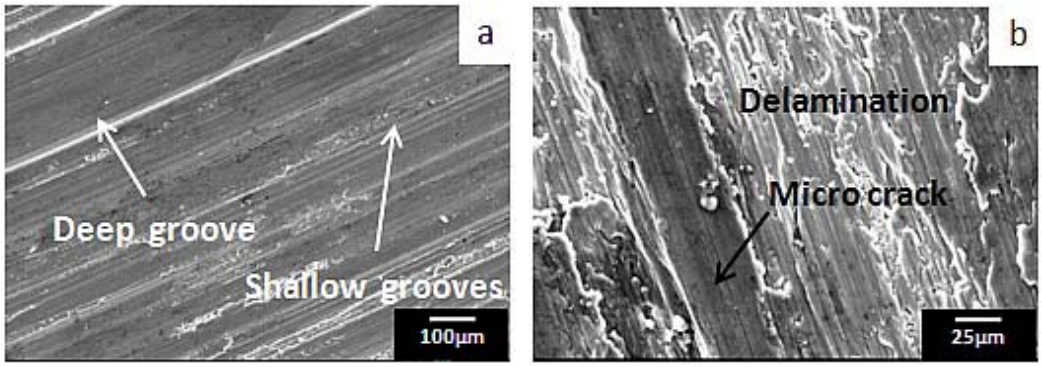

Figure 6.7: SEM micrographs of the worn surfaces as-cast alloys: at 50 N load (a) Al-12Si (b) Al-12Si-4.5Cu

The abrasive mechanism during sliding action of engineering materials is governed by processing parameters such as normal applied load and abrasive medium. Copper containing Al-12Si alloy does not show deep craters. This suggests the copper addition improves strength that resists the abrasive mechanism which is indirectly responsible for low wear rate and COF. The worn surface of the Al-12Si alloy at 50 N applied load showed deep grooves as compared to those of grain refined and modified

Al–12Si–4.5Cu cast alloys. The wear resistance of Al-12Si-4.5Cu alloy is due to higher strength.

Figure 6.8a and b shows the wear track observed for modified and grain refined Al-12Si alloy and Al-12Si-4.5Cu alloy, respectively. It can be observed that the wear grooves are shallow and are very few in number as compared to Figure 6.7a. This clearly demonstrates that the combined addition of modifier and grain refiner to the Al-12Si alloy leads to better sliding wear performance. Further, the presence of copper in Al-12Si makes the material hard (85 HB) and as a result, the grooves are shallow in Figure 6.8b for Al-12Si-4.5Cu alloy. However, the signs of delamination mechanism are observed in modified and grain refined Al-12Si-4.5Cu alloy, which may be attributed to the improvement of metal resistance to cracks nucleation and growth.

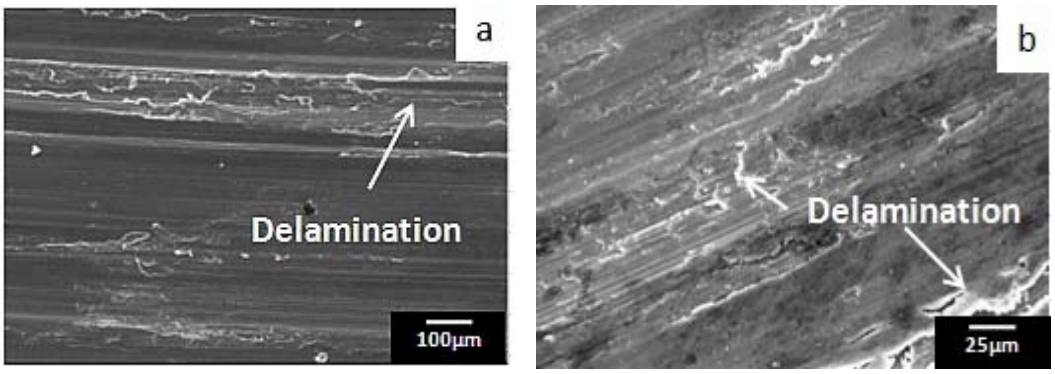

Figure 6.8: SEM micrographs of the worn surfaces of modified and grain refined alloys: at 50 N load (a) Al-12Si; (b) Al-12Si-4.5Cu

Extensive plastic flow and cracking is witnessed in the worn surfaces of the samples taken at high magnification. A crack initiation and propagation is clearly noticed. Cracks are initiated at highly work hardened layer and mostly observed in sub surface area. These are the two likely modes of crack initiation and propagation. Cracks may initiate in the highly work-hardened layer, particularly in the subsurface region. When cracks grow and interconnected, a layer of metal is removed leading to delamination wear (Jahanmir and Suh 1977). During sliding wear, the hard discrete particles and/or fractured pieces are mechanically dislodged. Based on the analysis it is reasoned that the small holes formed act as potential sites for the nucleation and

growth of cracks, and responsible for delamination. In Al-12Si-4.5Cu alloys the dispersoid particles act as asperities and responsible to experience the applied load. Eventually these asperities fracture and levelled off. In addition, as the degree of grain refinement and modification is increased the work hardening behaviour is also increased. These results further suggest that finer dispersoid particles present in grain refined and modified alloys experiences a low plastic deformation as seen in Figure 6.8a and b. The delaminated wear debris particles are so severely hardened, fractured and oxidized that they do not stick to the sliding surface any further and moved away from the interface zone. In the present study, abrasive wear is observed in case of as-cast Al-12Si alloy and delamination type of wear predominated for modified and refined alloy. Chandrashekharaiah and Kori (2009) have observed abrasive wear of Al-12Si as-cast alloy and abrasive and oxidative type of wear was found in case of alloy treated with grain refiner and modifier.

6.4 Influence of melt treatment on dry sliding wear of Al-15Si and Al-15Si-4.5Cu alloys

In chapter 4 it is discussed that the microstructure of Al-15Si and Al-15Si-4.5Cu cast alloys consists of coarse, platelet and star like primary silicon particles together with widely distributed eutectic silicon needles and elongated α-Al dendrites. It shows poor ductility. The combined addition of Al-10Sr modifier and Al-1Ti-3B grain refiner is responsible for converting large α-Al dendrites to fine α-Al dendrites and needle shaped eutectic silicon and $CuAl_2$ particles into fine and homogenous discretes at the interdendritic region that results improved wear resistance of the Al-Si alloys. The improvement in wear performance can be attributed to refined and strengthened microstructure.

Figure 6.9 shows the dry sliding wear behaviour of as-cast and melt treated Al-15Si and Al-15Si-4.5Cu alloys. It is noticeable that the volume loss (mm^3)is substantial at higher normal loads for as-cast samples. However, Al-15Si-4.5Cu cast alloy treated with the combined addition of grain refiner and modifier shows significantly less volume loss (mm^3) particularly at higher normal load. The addition

of 4.5% Cu to Al-15i alloy shows lower wear rate when compared to Al-15Si alloy. The influence of refined microstructure is better demonstrated at higher loads.

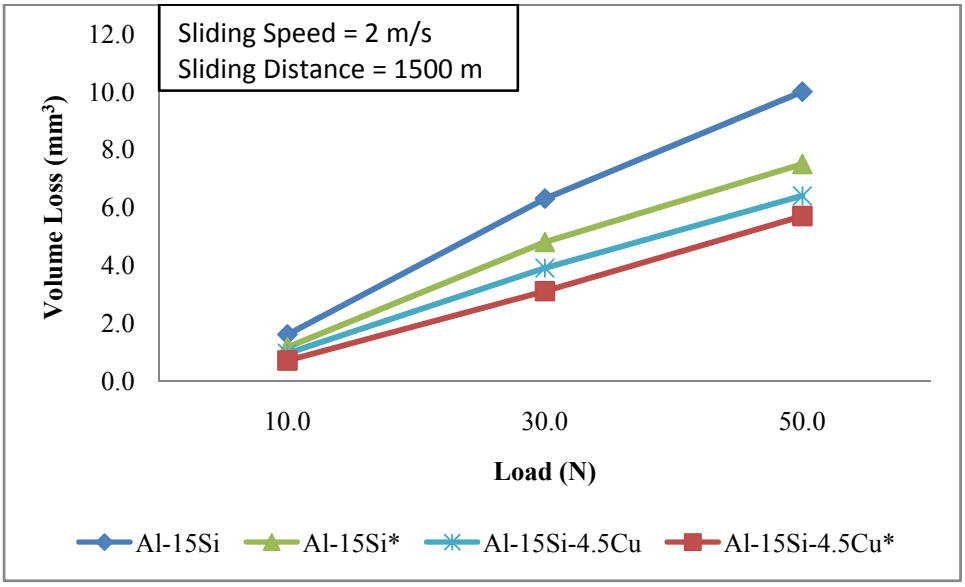

*Modified and grain refined

Figure 6.9: Variation of volume loss Vs loads for Al-15Si (as-cast and combined modified and grain refined) and Al-15Si-4.5Cu (as-cast and combined modified and grain refined)

It is observed that, for any particular composition, the amount of wear is more in as-cast sample. It could be seen that at lower silicon content (hypoeutectic) the wear loss is more than that for the higher silicon content (hypereutectic). This is basically due to load absorbing capabilities of the refined Si particles in the grain refined Al matrix.

The refinement of the microstructure and modification of Si in Al-15Si alloy is attributed for the lower wear as compared to as-cast Al-15Si alloy. In Al-15Si-4.5Cu alloy, the reduced wear loss can be attributed for the grain refinement and modification of Si particles which absorb the load more effectively. (Yasin and Savaskan 2009). Needle type particles are more prone to cracking at high loads and results in greater wear loss. In addition, the hardness of Al-15Si-4.5Cu alloy with grain refinement and modification is comparatively higher than the as-cast alloy. This may be due to solid solution strengthening and intermetallics that are present.

Figure 6.10 shows the COF of Al-15Si alloy and Al-15Si-4.5Cu alloys in as-cast, modified and refined conditions. Similar to hypoeutectic and eutectic alloys discussed in earlier sections, it is observed that as the load is increased from 10 to 50 N, the COF is also increased. The as-cast Al-15Si alloy exhibited high COF as compared to the combined grain refined and modified Al-15Si alloy with copper. The grain refined and modified Al-15Si-4.5Cu alloy exhibited lower COF.

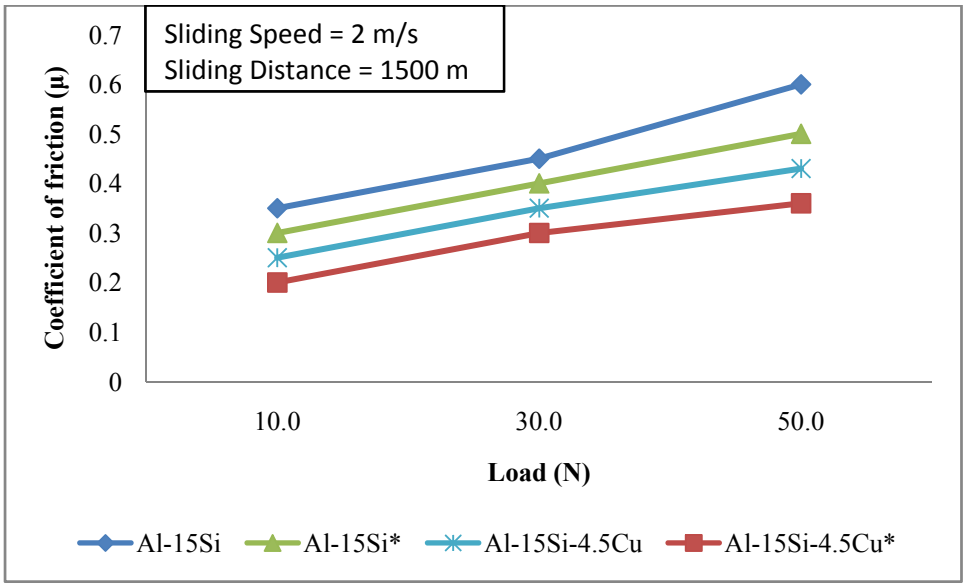

*Modified and grain refined

Figure 6.10: Variation of coefficient of friction vs. normal loads of Al-15Si (as-cast and combined modified and grain refined) and Al-15Si-4.5Cu (as-cast and combined modified and grain refined) alloys

When specimen surfaces are loaded against rotating base plate, the contacts are made through the tips of asperities. The higher friction coefficient at the beginning of the test is attributed to a direct metal on metal contact, which is due to adhesion. The COF is found to reduce in case of copper containing grain refined and modified alloy. Such a reduction in COF is associated with improved mechanical properties of melt treated alloy. The COF of Al-15Si-4.5Cu alloy with melt treatment is found to be the lowest among all the alloys.

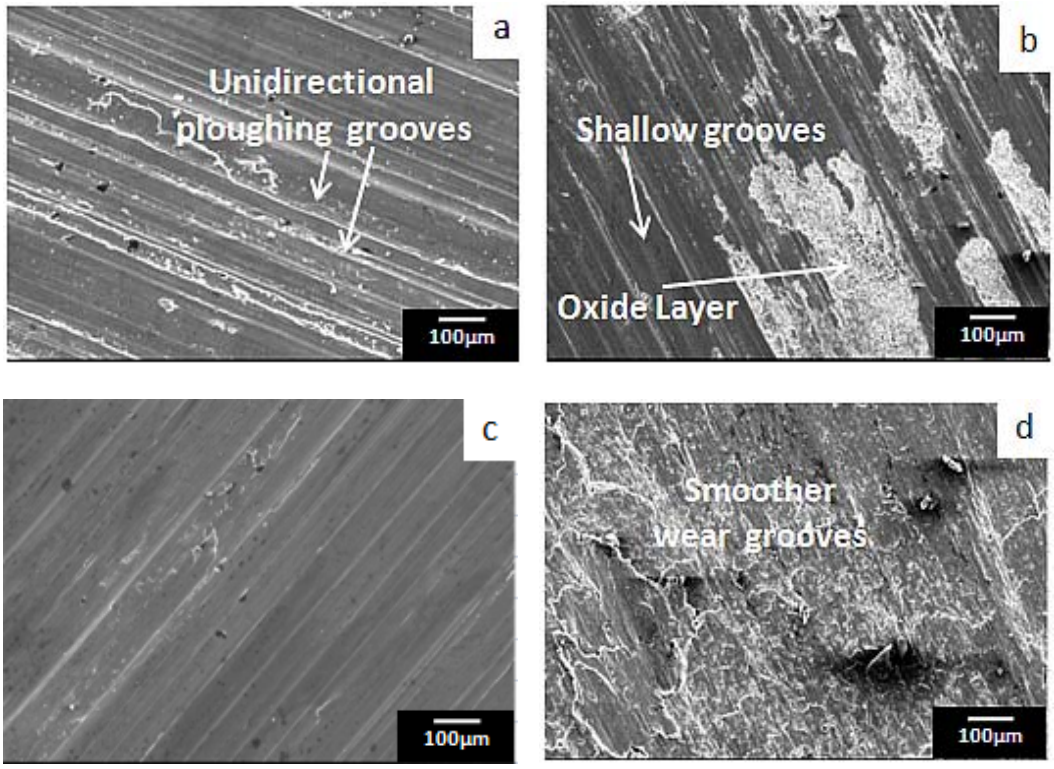

Figure 6.11: SEM micrographs of the worn surface of (a) Al-15Si (as-cast) (b) Al-15Si (combined modified and grain refined) and Al-15Si-4.5Cu (as-cast) and Al-15Si-4.5Cu (combined modified and grain refined) alloys at 50 N load

Figure 6.11a shows SEM image of a worn surface of as-cast Al-15Si alloy. Features such as metallic grooves and to certain extent wear track depicting adhesive wear phenomenon with plastic deformation are visible. A number of long, deep unidirectional ploughing grooves can be observed. Unidirectional action during sliding takes place and fragments come out of its surface and form debris. This depends on the critical shear stress of both mating surfaces. Figure 6.11b shows oxide layers on the worn surface of modified and grain refined Al-15Si alloy. With the addition of grain refiner and modifier, the hardness and strength of the material increased and resisted the yield of asperities leading to plastic deformation at the surface. This makes the oxide film more stable and as a result, mild wear has been observed. Figure 6.11c shows the wear track for Al-15Si-4.5Cu alloy. It can be observed that the wear grooves are smooth and not much deeper as compared to Figure 6.11a. These results can be compared with Figure 6.9a and b where the wear

loss for the Al-15Si-4.5Cu alloy exhibits low wear rates as compared to the Al-15Si base alloy and grain refined and modified Al-15Si alloy. Figure 6.11d shows the wear track of the grain refined and modified Al-15Si-4.5Cu alloy. These results further suggest that the presence of copper enhances the matrix strength and the presence of intermetallics protects against the cutting action of asperities in the counter surface and as a result grain refined and modified Al-15Si-4.5Cu alloy exhibits superior sliding wear resistance properties. The Cu addition in Al-Si is responsible for improved strength properties and this is basically due to redistribution of precipitating particles during ageing studies. The strength is mainly contributed from the precipitation of particle sizes and its distribution (Zeren and Karakulak 2009). Further the presence of Al_4Sr intermetallics in modified and refined alloy may also be responsible for improvement (Dwivedi 2010). The effect of 1-5% Cu addition on sliding wear behaviour of hypereutectic Al-Si alloy as a function of sliding speed (2 m/s) at constant load (50 N load) showed decrease in wear rate with increase in copper content. Increase in transition load of hypereutectic alloy is noticed with the addition of Cu (Dwivedi 2004).

6.5 Effect of modification and refinement, copper addition on wear properties– A comparative analysis.

The effect of combined addition of modifier, grain refiner and 4.5 wt.% of copper addition on wear behavior of Al-7Si, Al-12Si and Al-15Si alloys is presented in sections 6.2, 6.3 and 6.4, respectively. Comparative analyses of the findings are presented in subsequent sections.

6.5.1 Effect of Si, combined modification and refinement on Al-Si alloys

Figure 6.12 presents the volumetric wear loss observed for Al-Si alloys with and without combined modification and refinement.

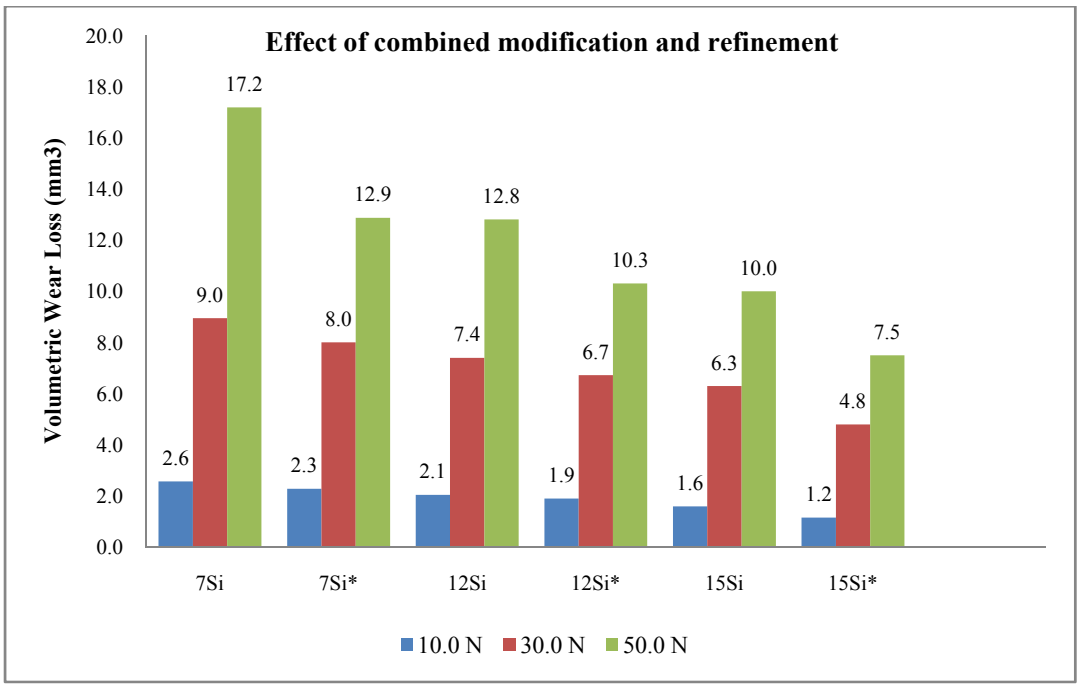

*Modified and grain refined

Figure 6.12: Volumetric wear loss for as-cast Vs modified and refined Al-Si alloys

From these results, it is clearly observed that the increase in Si content resulted in better wear resistance. Hypereutectic alloy showed the lowest wear loss and hypoeutectic alloy showed highest wear loss at each load investigated. Analyzing the melt treatment impact, at 10 N and 30 N loads, the effect of melt treatment had less impact on volumetric wear loss for Al-12Si alloy with 7% and 9% reduction respectively, while for Al-7Si alloy the reduction was 11% at both loads and Al-15Si alloy showed 27% reduction in volumetric wear loss. However at higher load of 50 N, all the three alloys showed almost equal improvement (24% – 27%) in wear resistance after modification and refinement. In general, silicon being a hard material, the wear rate of Al- Si alloys is predominantly dependent on Si content (the volume fraction of harder phase in Al matrix) and it decreases substantially with the increase in Si content up to 15 % (Torabian et al. 1994). The low solubility of silicon in aluminium causes it to precipitate as virtually pure Si. It is reported that the load bearing ability of the alloy under compression is increased as the Si content is increased and the signatures of seizure is reduced (Torabian et al. 1994). However, present study is carried out at up to 50 N load and seizure is not noticed in any of the alloys studied.

The silicon particles get embedded in Al matrix and under load the matrix deforms causing pile up of Al adjacent to embedded Si. With more silicon particles in case of Al-15Si alloy, the resistance for pull out of these particle increases. The wear performance of Al-Si alloy is improved due to the combined addition of Al-1Ti-3B grain refiner and Al-10Sr modifier. This is attributed to the fact that embrittlement effect and micro cracking tendency of the coarse Si particles are minimized due to conversion to fine particles and modified morphology. Vijeesh and Narayan Prabhu (2014) who have reviewed microstructure evolution in hypereutectic Al–Si alloys and its effect on wear properties reported similar findings. Kori and Chandrashekharaiah (2007) reported that higher Si restricts dislodging of material and also have cited refinement of coarse Al dendrites into fine equiaxed dendrites as a possible reason for better wear resistance as it improves strength and toughness which in turn leads to lesser material dislodging during wear test.

6.5.2 Effect of copper addition on Al-Si alloys

The volumetric wear loss incurred by Al-Si alloys with and without the addition of 4.5 wt.% Cu is shown in Figure 6.13.

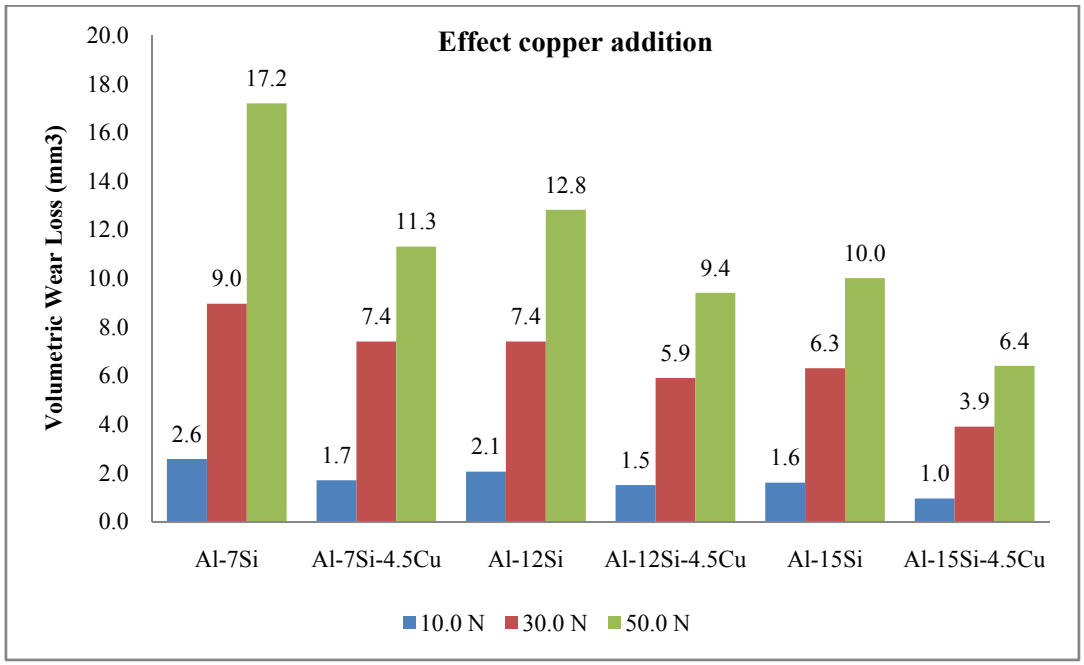

*Modified and grain refined

Figure 6.13: Volumetric wear loss for Al-Si Vs Al-Si-Cu alloys

At all working load conditions, copper containing alloys showed lesser volumetric wear loss as compared to modified and refined alloys. Least wear loss is witnessed by Al-15Si-4.5Cu alloy. The main reason for the improved wear behavior of alloys with copper addition is the formation of hard second phase particles $CuAl_2$ at the interdendritic region and the copper in solution acts as strengthening agent in the Al Matrix. It is also reported copper also influences the reduction in the grain size thus enabling further strengthening (Yasir and Abdul 2014). Both of these effects reduce the tendency of material removal during wear test. Further it is also reported that the effect of copper does not change significantly beyond 4.5% particularly in case of hypereutectic alloy (Dwivedi 2010).

6.5.3 Effect of modification and grain refinement on Al-Si-Cu alloys

The volumetric wear loss in Al-Si-Cu alloys in as cast condition and after modification and refinement is shown in Figure 6.14.

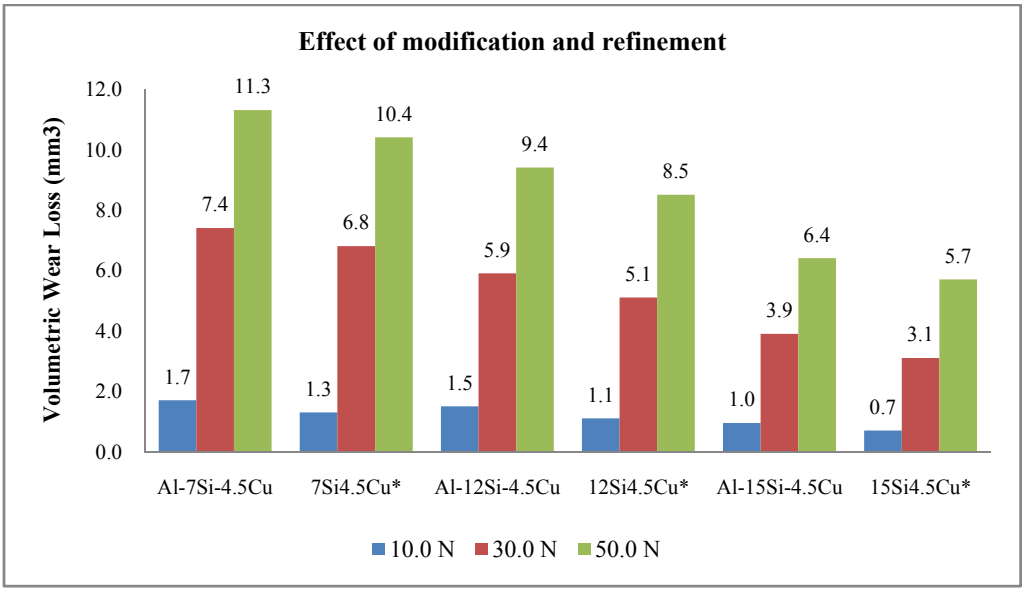

*Modified and grain refined

Figure 6.14: Volumetric wear loss for as-cast Vs modified and refined Al-Si-Cu alloys

Al-15Si-4.5Cu alloy exhibited least volume loss among all the alloy systems tested. At 50 N load, after copper addition to Al-15Si, wear volume loss is reduced by 36% and further 7% reduction in wear loss is attained by modification and grain refinement of Al-15Si-4.5Cu alloy. Fine equiaxed Al grains and uniform distribution of second phase particles are reasons for improvement in wear resistance. Observations by Basavakumar et al. (2007) have indicated that the conversion of blocky $CuAl_2$ into fine particles resulted in a significant improvement in hypoeutectic alloy containing 7% Si and 2.5 Cu. Similar results are obtained in this work with better wear performance for higher Si and Cu content. It may be inferred that the contribution of more number of fine $CuAl_2$ particles and more number of fine hard Si particles have contributed towards further improvement as per Basavakumar et al. (2007).

6.6 Influence of ageing on dry sliding wear of Al-Si-Cu alloys

The microstructural modifications in hypoeutectic, eutectic and hypereutectic alloys in the as-cast, modified and grain refined conditions obtained during heat treatment are discussed earlier in chapter 4. The changes obtained through heat treatment (solutionizing and ageing) occur mainly during solution treatment. The needle like eutectic Si morphology of the as-cast alloys gets rounded during solutionizing. The aim of this study is to understand the influence of ageing on dry wear behaviour of Al-Si-Cu alloys. Wear test specimens were subjected to T6 heat treatment as detailed in experimental procedure and dry sliding tests were conducted after ageing the specimen for times at which peak hardness were obtained. The aim of the study is to find the volume loss under different loads. The wear mechanism causing the loss of material during dry sliding wear of Al-7Si-4.5Cu, Al-12Si-4.5Cu and Al-15Si-4.5Cu are the key points of this study.

6.7 Influence of ageing on dry sliding wear of Al-7Si-4.5Cu alloys

Figure 6.15 shows the sliding wear performance of hypo eutectic alloys with copper additions in as cast and modified and grain refined conditions subjected to

ageing for 48 h(Figure 4.10 and 4.12). The first peak was obtained at 4 h whereas second peak was at 20 h.

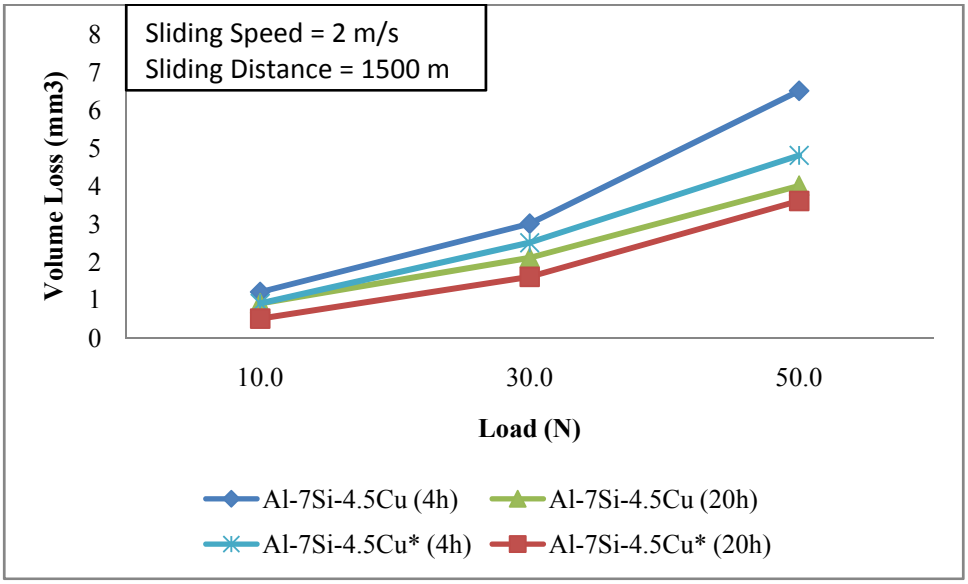

*Modified and grain refined

Figure 6.15: Variation of volume loss vs. normal loads of Al-7Si-4.5Cu (as-cast) and Al-7Si-4.5Cu (modified and grain refined) alloys at 4h and 20h

A close observation of Figure 6.15 suggests that the alloys that are aged for 20 h exhibited lower wear loss as compared to samples aged for 4 h. This response is seen for both Al-7Si-4.5Cu and Al-7Si-4.5Cu (grain refined and modified) alloys. Further, these results suggest that 4 h ageing is responsible for improved wear results due to formation of GP Zones. Further increase in ageing time for 20 h suggests that peak ageing has been achieved and resulted in highest yield strength. These results are ascribed to the strengthening of Al matrix that offers good resistance during the sliding action and can be further clarified from the wear track observations as seen in Figure 6.16. These observations are in agreement with other investigators who demonstrated similar results (Sjolander and Seifeddine 2010).

In case of Al-7Si-4.5Cu alloy with 4 h ageing, the wear tracks produced are deep (Figure 6.16a). Long ploughing grooves on the wear surface are observed along the sliding direction. These features are indicative of abrasive wear and are caused by

material being removed from the pin surface by hard particles or protuberances on the counterface, forcing against and cutting or ploughing into the surface. As compared to this the wear tracks seen in Figure 6.16b (Al-7Si-4.5Cu alloy 20 h aged) shows wear tracks that look comparatively smooth and also the groove depths are appearing to be shallower. The features of worn surface suggest that the main mechanism operative is oxidation wear. Oxidative wear is caused by frictional heating during sliding, causing the pin surface to oxidize; oxide fragments are removed upon subsequent sliding, resulting in wear. Low wear rates are observed when oxidation is dominant. This is because of the oxide layer covering the pin surface and it minimizes metallic contact with the disc and acts as a protective layer inhibiting severe wear.

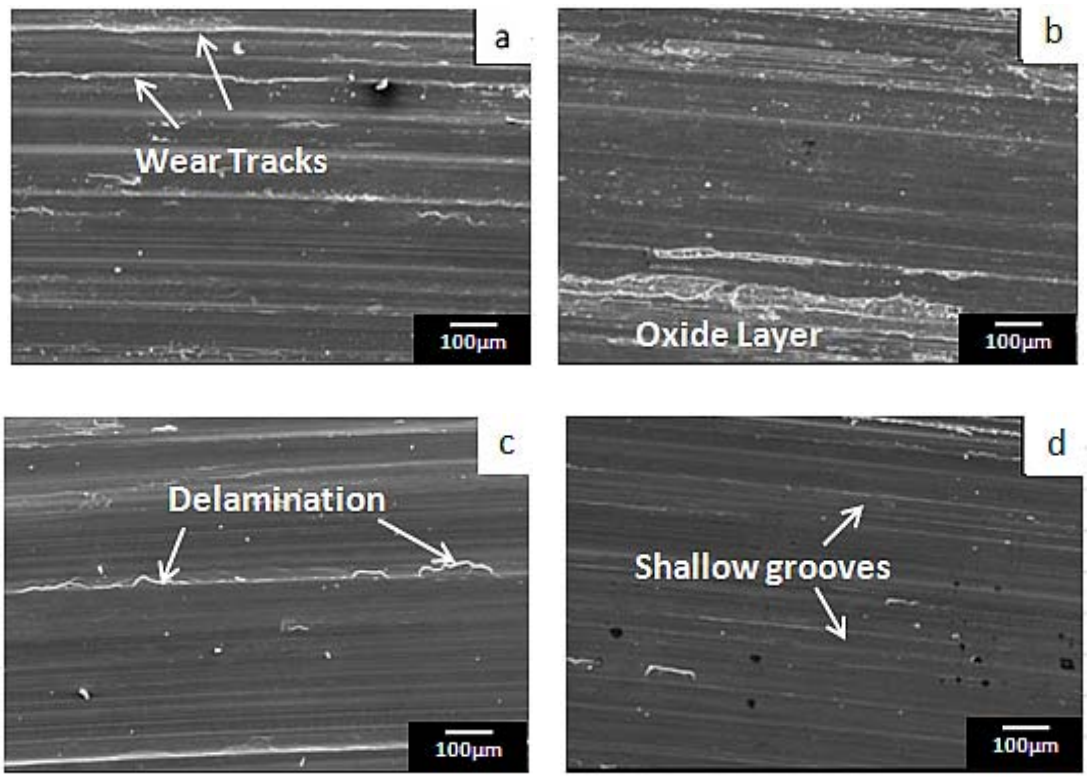

Figure 6.16: SEM micrographs of the worn surfaces of aged samples at 50 N load (a) Al-7Si-4.5Cu (4 h); (b) Al-7Si-4.5Cu (20 h); (c) Al-7Si-4.5Cu* (4 h); (d) Al-7Si-4.5Cu* (20 h)

*Modified and refined

Figure 6.16c and d wear track analysis also exhibit similar results as can be correlated with Figure 6.16a and b. The lesser number of grooves in Figure 6.16c explain their better wear resistance. The wear surface in Figure 6.16d is practically free from grooves. As a result, modified and grain refined Al-7Si-4.5Cu alloy with 20 h ageing, exhibited highest sliding wear properties as compared to all other experimental alloys. Eshaghi et al. (2010) investigated the influence of T6 heat treatment on the wear performance of Al-9.4Si with minor additions of iron. It is observed that aged samples exhibited better wear surface features such as small craters and mild oxide layers as compared to the non-aged samples under all applied loads (20-40 N). It is observed that due to T6 heat treatment the eutectic Si particles became round and also having a low length and aspect ratio. Moreover, the heat treatment is also responsible for modifying the geometry at the tip of the plates. Similar changes in Si morphology namely spheroidizing and reduction in length and aspect ratio can be observed in microstructures presented in Figure 4.5b and 4.8b. These microstructural changes of the heat treated samples experiences a tendency to initiate subsurface cracks thereby improving the sliding wear resistance properties.

6.8 Influence of ageing on dry sliding wear of Al-12Si-4.5Cu alloys

The increased Si content in eutectic alloy has accelerated the ageing response and the 1st peak was at 2 h and 2nd peak was at 12 h as compared to 4 h and 20 h for corresponding peaks of hypoeutectic alloys. Figure 6.17 exhibits the sliding wear performance of Al-12Si-4.5Cu (as-cast and grain refined and modified) alloys at ageing time of 2 h and 12 h. The results are very similar to hypoeutectic alloys with copper additions but wear volumes are lower due to additional Si content compared to that of Al-7Si. 12 h aged samples exhibited better wear resistance compared to 2 h aged alloys due to their improved hardness. As indicated earlier, the 2 h aged alloy having GP zones show more wear volume compared to those of 12 h aged alloy possibly having θ′ phase.

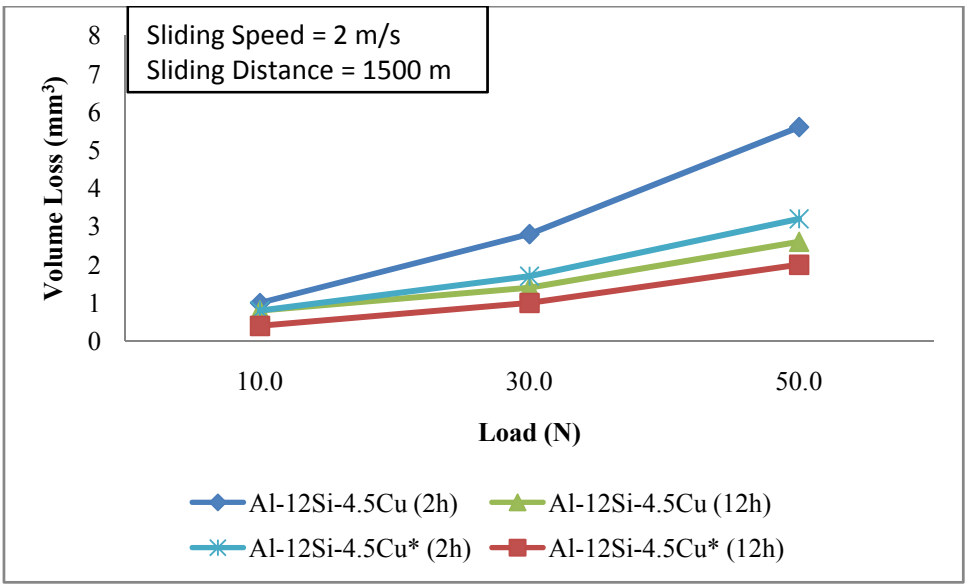

*Modified and grain refined

Figure 6.17: Variation of volume loss vs. normal loads of Al-12Si-4.5Cu (as-cast) and Al-12Si-4.5Cu (modified and grain refined) alloys aged for 2 h and 12 h

Figure 6.18a shows SEM micrograph of the worn surface of slightly higher hardness (116 BHN) Al-12Si-4.5Cu alloy aged for 2 h. Wear surface displays numerous grooves and scouring marks on the pin surface. The microstructure also shows very minimal plastic deformation in the worn surfaces and a few unidirectional ploughing grooves can also be observed. These features are very much indicative of abrasive wear. Figure 6.18b shows SEM image of the worn surface of Al-12Si-4.5Cu alloy aged for 12 h. The surface seems to be more wear resistant with very shallow grooves. Figure 6.18c shows SEM micrograph of the worn surface of modified and grain refined Al-12Si-4.5Cu alloy aged for 2 h. The scouring may be due to abrasion by entrapped debris and work hardened deposits on the hardened steel counter face. Figure 6.18d shows SEM image of the worn surface of modified and grain refined Al-12Si-4.5Cu alloy aged for 12 h. Typical surface damage like, craters are observed. Elmadagli et al. (2007) have made similar observations on wear behavior of heat treated Al-Si alloys. Heat treated alloys showed higher hardness values not only because of precipitation hardening but also due to morphological changes of

intermetallics and Si particles. This results in mechanically stable structure that contributes to improved wear resistance properties.

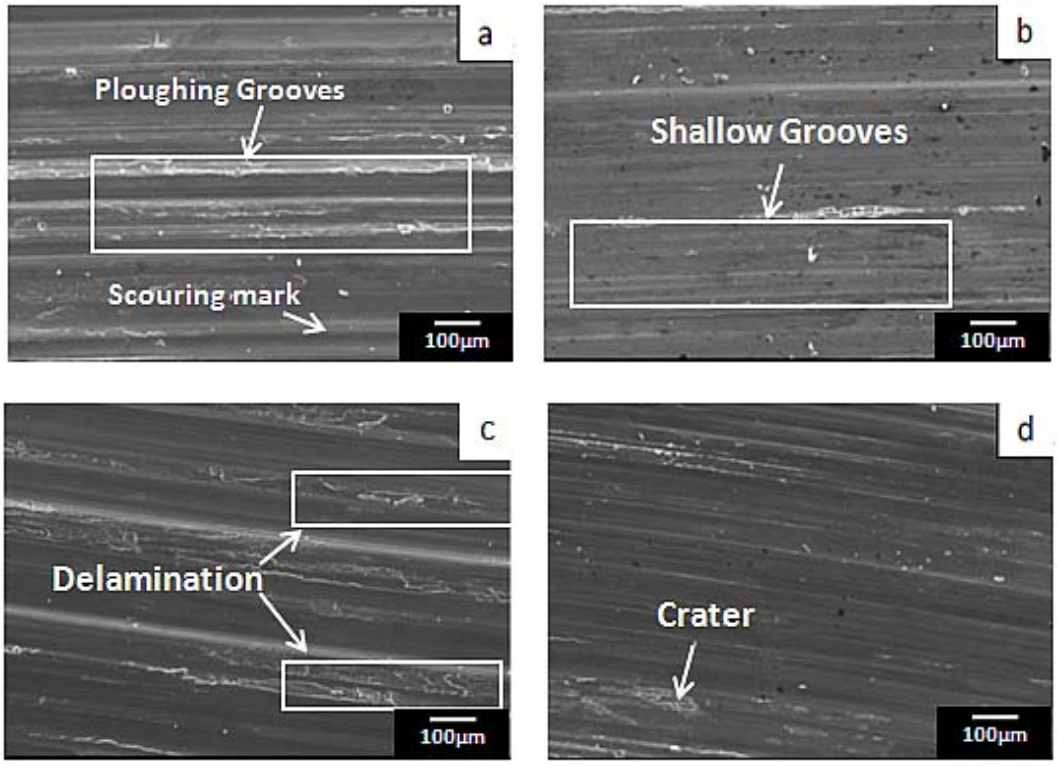

Figure 6.18: SEM micrographs of the worn surfaces of aged samples at 50 N load (a) Al-12Si-4.5Cu (2 h) (b) Al-12Si-4.5Cu (12 h) (c) Al-12Si-4.5Cu* (2 h); (d) Al-12Si-4.5Cu* (12 h)

*Modified and grain refined

Basavakumar et al.(2008) also showed similar results suggesting that the worn surfaces of the as-cast Al–12Si and Al–12Si–3Cu alloys undergoes plastic flow and cracking. The worn surface of the as-cast alloy, on the other hand, showed the presence of distinct grooves, suggesting ploughing of the pin surface. They also showed the plastic flow of the matrix, crack nucleation and propagation in the Sr treated and combined grain refined and modified Al–12Si–3Cu cast alloys. At higher applied loads during sliding wear a severe wear is observed. As a result, the failure of the pin material is observed at the interface and responsible for the formation of metallic debris. Further increase in loads resulted in seizure. This is basically due to exceeding the yield strength values of the pin material that caused severe surface

deformation. The deformation of the surface occurred on a fairly massive scale as the yield strength of the pin material was exceeded. In the present study, no seizure is reported until 50 N applied load. However, it is possible to notice such type of seizure after long sliding distances.

6.9 Influence of ageing on dry sliding wear of Al-15Si-4.5Cu alloys

Hardness vs ageing time of Al-15Si-4.5Cu alloy is discussed in section 4.4.4 Compared to eutectic alloy, the ageing time for achieving peak hardness of hypereutectic alloys is longer due to the presence of primary Si in the eutectic matrix. Dry sliding tests were conducted after ageing the specimen for time periods at which 1st peak hardness (8 h) and 2nd peak hardness (20 h) were obtained. Figure 6.19 shows the sliding wear performance of hypereutectic alloys with copper additions and with and without modification and grain refinement after subjected to ageing for 8 h and 20 h.

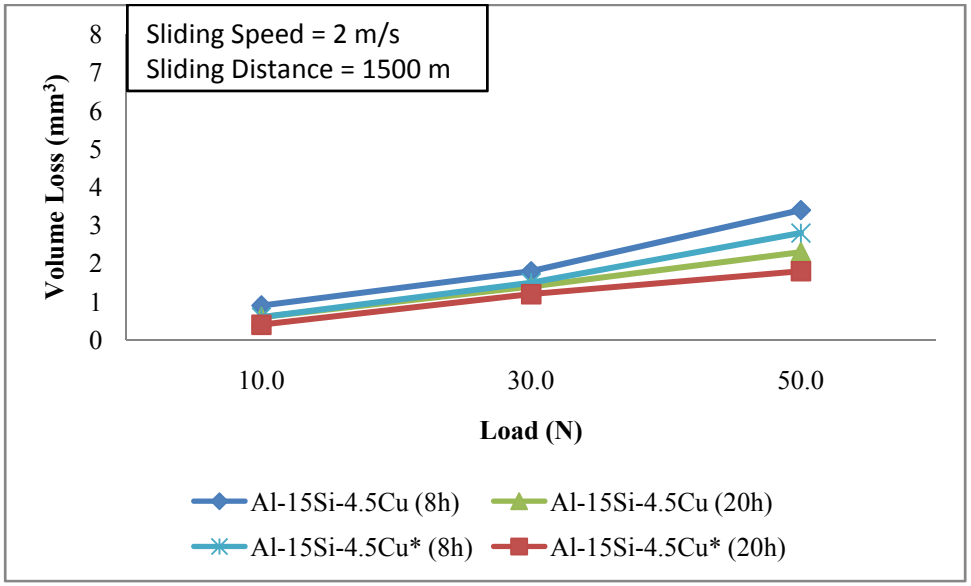

*Modified and grain refined

Figure 6.19: Variation of volume loss vs. normal loads of Al-15Si-4.5Cu (as-cast) and Al-15Si-4.5Cu (modified and grain refined) alloys aged for 8 h and 20 h

The alloys showed higher wear resistance compared to hypoeutectic and eutectic alloys similarly treated at peak ageing temperatures due to higher hardness of

hypereutectic alloys. Modified and grain refined Al-15Si-4.5Cu alloy subjected to ageing for 20 h exhibited the lower wear loss.

SEM micrographs of the worn surfaces of heat treated Al-15Si-4.5Cu alloy samples are shown in Figure 6.20.

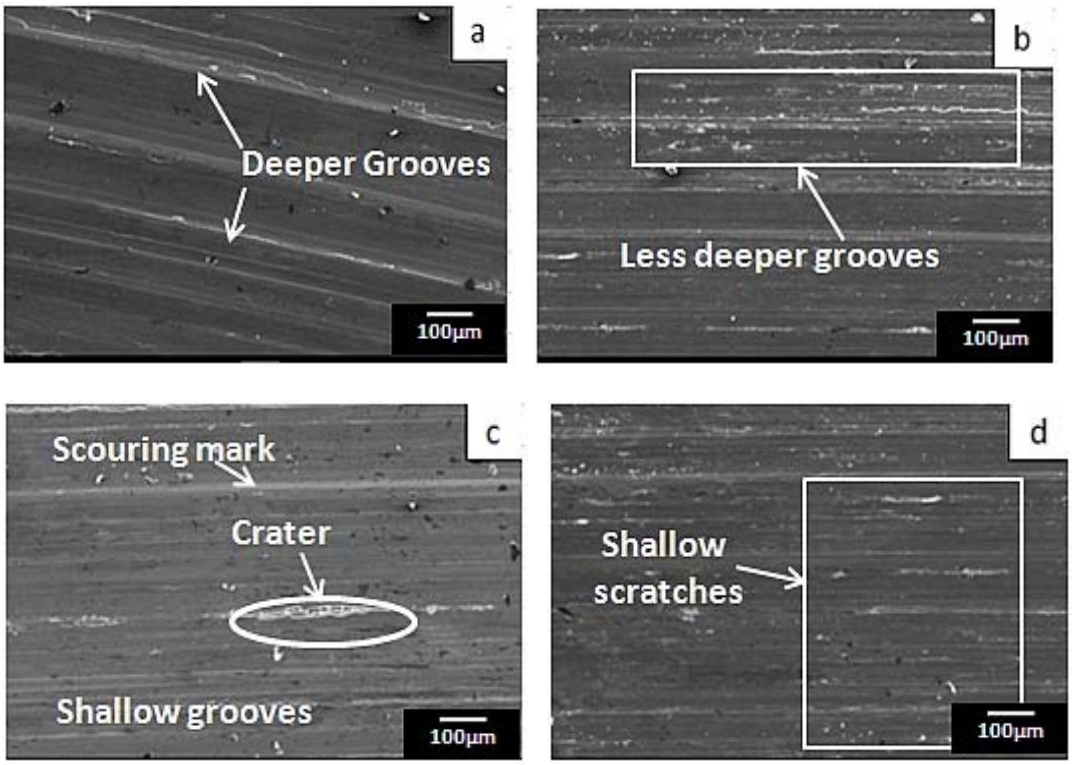

Figure 6.20: SEM micrographs of the worn surfaces of aged samples at 50 N load (a) Al-15Si-4.5Cu (8 h) (b) Al-15Si-4.5Cu (20 h) (c) Al-15Si-4.5Cu* (8 h); (d) Al-15Si-4.5Cu* (20 h)

*Modified and grain refined

The wear tracks of Al-15Si-4.5Cu alloy with 8 h ageing shown in Figure 6.20a are deeper as compared to presence of the wear tracks of Al-15Si-4.5Cu alloy aged for 20 h seen in Figure 6.20b. This wear track suggests that Al-15Si-4.5Cu aged for 20 h offered much sliding wear resistance as compared to Al-15Si-4.5Cu alloy aged for 4 h. After 20 h ageing, the alloy should have θ′ precipitates that are uniformly distributed in Al matrix offered highest yield strength and offered good sliding wear performance. As a result, the wear tracks are looking smooth and also the depth of

grooves appears to be shallow. The worn surface of modified and grain refined Al-15Si-4.5Cu alloy in Figure 6.20 c and shows least surafce damge and suggests that this offered much load bearing capacity and is also responsible for good wear results. The fine θ′ precipitates present in the alloy is also responsible for better sliding wear resistance results.

A significant change in eutectic Si from plate like morphology to nearly spherical shape is observed due to heat treatment and results in the uniform dispersion of silicon particles (Figure 4.32). The wear response is significantly changed basically due to crack initiation at the interface between Si particle and Al matrix. It is well understood that the morphology and distribution of primary silicon in the matrix affects the wear properties of the alloy considerably. This is attributed to a pre-dominating embrittling effect and micro-cracking tendency brought about by the presence of coarse particles. Hence finer particles and modified morphology of primary and eutectic silicon (which are in different proportions in the three types of alloys) have improved the wear resistance of these alloys to different extent based on amount of refinement and modification and also due to solutionizing and ageing (in case of alloys with copper addition). Studies have revealed that the primary silicon in modified alloy was well bounded to the matrix to improve wear resistance and the mechanism of wear for unmodified and modified alloys was different (Vijeesh and Narayan Prabhu 2014). Dwivedi (2001) also has reported improvements in wear resistance after heat treatment of as cast eutectic and hypereutectic alloys.

6.10 Influence of ageing on dry sliding wear of Al-Si-Cu alloys – A comparative analysis

Effect of ageing on Al-Si-Cu cast alloys with and without melt treatment are discussed in this section. The wear testing of aged alloys are conducted for the samples at peak aged condition. Graphical representation of volumetric wear loss of Al-7Si-4.5Cu, Al-12Si-4.5Cu and Al-15Si-4.5Cu with melt treatment and ageing are presented in Figure 6.21-6.23.

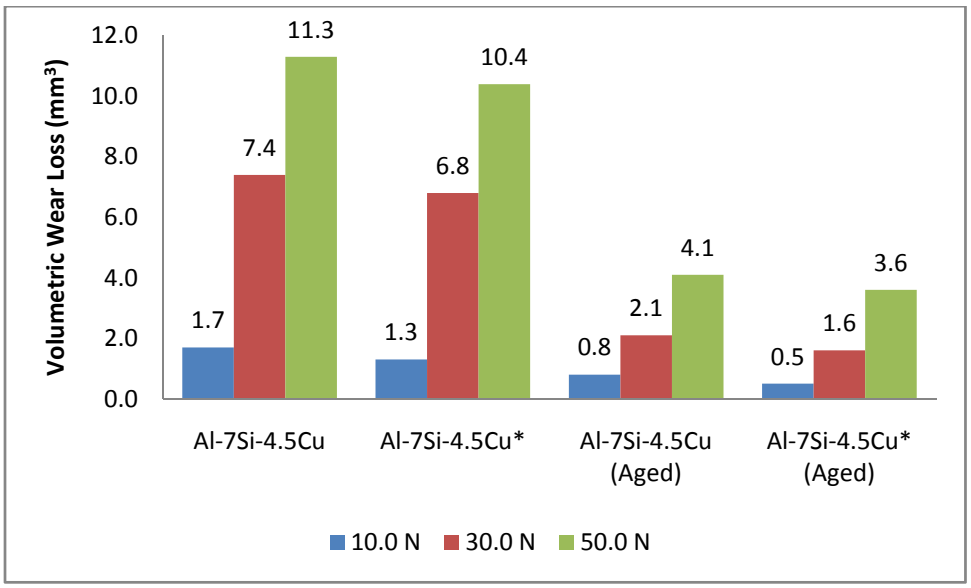

*Modified and grain refined

Figure 6.21: Volumetric wear loss of Al-7Si-4.5Cu alloy (with and without ageing)

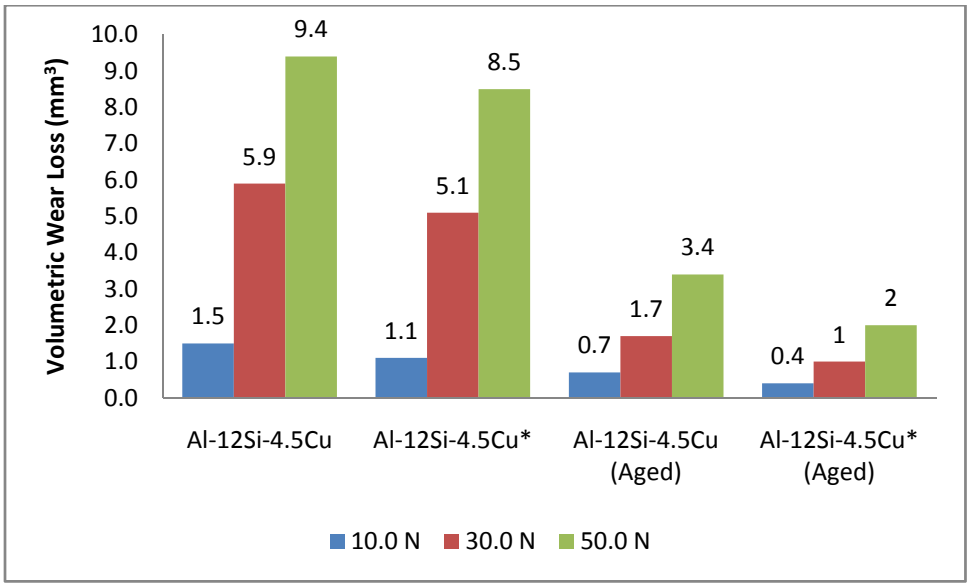

*Modified and grain refined

Figure 6.22:Volumetric wear loss of Al-12Si-4.5Cu alloy (with and without ageing)

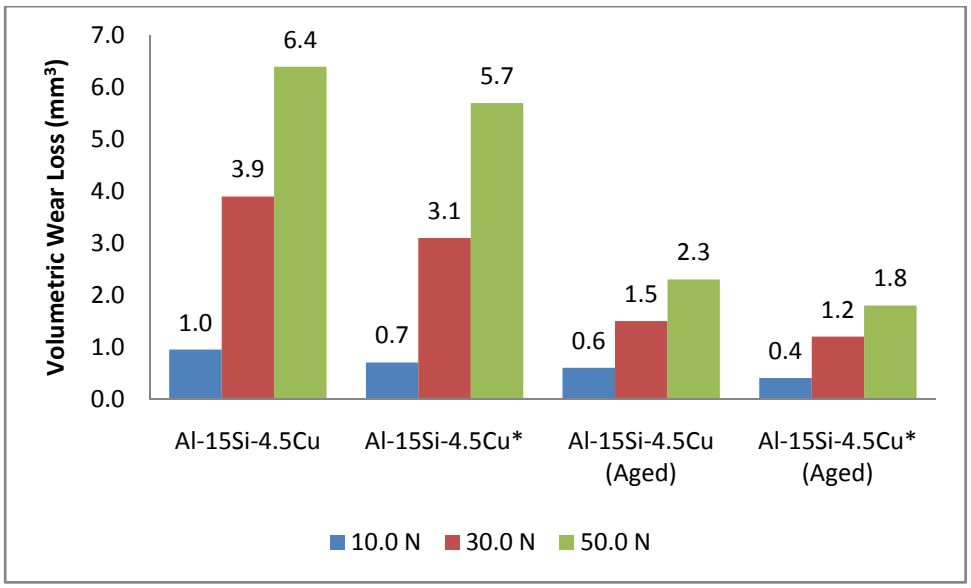

*Modified and grain refined

Figure 6.23: Volumetric wear loss of Al-15Si-4.5Cu alloy (with and without ageing)

The heat treated samples showed better wear resistance compared to non-heat treated samples under all load conditions. This may be due to the rounding of eutectic Si particles caused during heat treatment. Earlier studies have found that heat treatment causes the change in morphology of the tip of the plates to more blunt geometry (Narayan et al. 1999). These structural changes could lower the stress concentration at the interface of the particle and the matrix and hence could lower the tendency to initiate the cracks. Sharma and Dwivedi (2007) have found an increase in bonding between secondary phases and matrix due to diffusion.

The wear results of all the three types of Al-Si alloys with copper addition subjected to ageing suggests the following.

Corresponding to 2nd peak hardness on ageing cycle, the as cast alloy displayed considerable improvement in volumetric wear loss reduction as compared to as-cast alloy without heat treatment. Whereas in case of melt treated alloys the corresponding reduction in volumetric wear loss is not significant. This appears to be an interesting observation because without subjecting to T6 cycle, the melt treated alloy shows reasonable improvement in volumetric wear loss reduction over the as

cast alloy. Thus it can be inferred that T6 cycle has a more significance for as cast alloy over melt treated alloys when it comes to improving wear behavior.

An addition of Ti in the form of grain refiner in Al-12Si alloy is responsible for improved hardness. This is due to the nucleation of a large number of Al_3Ti particles during solidification. Saheb et al. (2001) have reported that Ti is responsible for higher wear resistance values. This is due to the improved micro hardness by the presence of fine disporsoid Al_3Ti particles. Among all the alloys considered in this work, Al-15Si-4.5Cu alloy melt treated and aged for 20 h displayed the best wear behaviour. There is a reduction of 72% in volumetric wear loss in Al-15Si-4.5Cu alloy melt treated and aged alloy as compared to as cast one.

Further considering the three types of Al-Si alloys in the present work, it may be in general inferred that:

Under constant speed and sliding distance the sliding wear rate is influenced by its composition and applied load. As the Si content is increased, the load-bearing capacity of the material also increased and resulted in low wear rate. Moreover, the alloy composition also plays significant role during sliding wear process.

The fineness of the fragmented silicon and its spheroidization are important in determining the extent of plastic deformation. The plastic deformation is comparatively mild in eutectic and hypereutectic alloys. Depending upon the silicon pull out, proportion of modification of Si morphology due to melt treatment and T6 cycle, the extent to which the abrasive wear predominates in these alloys can be controlled. In addition to this, these alloys have shown oxidative wear loss. Kori and Chandrashekharaiah (2007) while using different combinations of refiner with Al-10Sr modifier have also concluded the improvement in wear resistance of Al-12Si alloys due to simultaneous refinement and modification citing change in microstructure from coarse columnar dendrites to fine equiaxed dendrites and plate like eutectic Si to fine particles as the reason. However in the present work Al-1Ti-3B with Al–10Sr has shown similar refinement of matrix and silicon along with modification of eutectic silicon in case of Al-12Si alloy. Prasad Rao et al. (2006) have

concluded that grain refinement and modification can take place together resulting in finer dendrites as well as finer eutectic Si.

In case of alloys with copper addition the hard intermetallic phases resulted in better mechanical properties, while the effect of delamination along with abrasive wear also increased thus causing increased wear loss. The combined modified and refined alloys with T6 cycle heat treatment showed controlled wear rate due to improved strength.

Chapter 7

Conclusions

The objectives of the current research work were to investigate the effect of 4.5 wt.% Cu addition to Al-Si alloys and further study the microstructural changes in Al-Si and Al-Si-Cu alloys due to combined modification and grain refinement and heat treatment and its influence on hardness, mechanical properties and wear resistance of the alloys. From the analysis and discussion presented in Chapters 4 to 6, the following conclusions are drawn.

1. Combined addition of grain refiner (Al-1Ti-3B) and modifier (Al-10Sr) on hypoeutectic, eutectic and hypereutectic Al-Si alloys resulted in refinement of the columnar dendritic structure and coarse eutectic / primary Si particles them to changing to equiaxed fine α-Al and fragmented and spherodoized particles of Si. In case of Al-15Si alloys, Al-23P is used for refinement of primary Si. These microstructural changes improved the mechanical properties of Al-Si alloys. Melt treated Al-15Si exhibited the highest hardness (76 BHN) among the three types of Al-Si binary alloys. This is due to large number of primary Si particles uniformly distributed in the matrix. However, primary Si particles also acted as stress raisers and limited the tensile strength of Al-15Si to 186 MPa which further improved to 227 MPa after melt treatment. The highest value for strengthwas observed in refined and modified Al-12Si (237 MPa) among the three alloys while Al-7Si showed the very good ductility with % elongation values of 11.9%.

2. Addition of copper to Al–Si alloys resulted in forming hard $CuAl_2$ phases contributing to increased strength. The improvement in mechanical properties of as-cast Al-Si due to Cu addition is found to be superior to improvement due to melt treatment these alloys. However, while addition of Cu showed a

favourable increase in hardness, UTS and proof stress, the elongation property of the alloys reduced due to precipitation of $CuAl_2$ particles in the interdendritic region. The loss in ductility is recovered to a certain extent by melt treatment of Al-Si-Cu alloys. Change in Si morphology and refinement of α-Al and eutectic / primary Si are the main reasons for this improvement along with refinement of hard phase precipitate. Among copper added and melt treated Al-Si-Cu alloys, highest values of hardness (90 BHN), strength (292 MPa), and elongation (8.5%) were exhibited by Al-15Si-4.5Cu alloy, Al-12Si-4.5Cu alloy and Al-7Si-4.5Cu alloy, respectively.

3. Generally Al-Si structures are heterogeneous on account of % Si. Solution treatment at 500 ^{0} C and for 6 h has resulted in sufficient dissolution of solute atoms to form homogeneous super saturated α-Al solid solution enriched with Cu. During subsequent ageing large number of fine $CuAl_2$ particles is precipitated replacing the block $CuAl_2$.

4. The ageing graph for hardness typically showed two hardness peaks in all the alloys even though the peak hardness varied among them. As-cast Al-7Si-4.5Cu and Al-15Si-4.5Cu alloys exhibited 1st peak hardness after 4 h of ageing and 2nd peak hardness after 20 h. In Al-12Si-4.5Cu alloy 1st hardness peak (116 BHN) was achieved at 2 h and 2nd hardness peak (140 BHN) at 8 h. This shows ageing kinetics to be faster in this alloy.

5. Among the as-cast Al-Si-Cu alloys subjected to T6 heat treatment, Al-15Si-4.5Cu alloy exhibited highest hardness (148 BHN) and Al-12Si-4.5Cu alloy showed the highest strength (312 MPa). However, elongation of this alloywas low at 3.6%. Modified and refined Al-Si-Cu alloys when subjected to T6 heat treatment showed improved strength among all alloy categories. Modified Al-12Si-4.5Cu alloy exhibited further improved strength of 344MPa with 6.2% elongation.

6. The results of wear test under constant speed and sliding distance conditions indicate that alloys with increasing Si content depicted more of abrasive wear phenomena and also better wear resistance property of Al-Si alloys. The volumetric wear loss was lowest for hypereutectic alloy at all the 3 loads and highest for hypoeutectic alloy which mainly showed adhesive wear phenomena. Further, micro structural changes due to combined melt treatment resulted in improved wear properties. All melt treated Al-Si alloys exhibited almost equal improvement (24% – 27%) in wear resistance. Cu additions to Al-Si alloys resulted in improved hardness and wear properties due to the formation of hard second phase $CuAl_2$ particles and copper acted as strengthening agent in the Al matrix. The combined modified and refined alloys with T6 cycle heat treatment showed controlled wear rate due to improved strength.

7. The as-cast Al-S-Cu alloys aged up to 2^{nd} peak hardness on ageing cycle displayed considerable improvement in volumetric wear loss as compared to as-cast alloy without heat treatment. In case of melt treated alloys, the corresponding reduction in volumetric wear loss at corresponding point was not that significant. So solution treatment followed by ageing is good option for improving the wear resistance of as-cast alloys, however melt treatment of alloys even though improve the wear resistance further only marginally, is a good option as it also improves the mechanical properties of the alloy.

8. Melt treated Al-15Si-4.5Cu alloy aged for 20 h displayed the best wear behaviour among all the different alloy types considered in this work. Volumetric wear loss reduction as high as 72% is observed in melt treated and aged Al-15Si-4.5Cu alloy as compared to as-cast alloy.

REFERENCES

Alemdag, Y. and Beder, M. (2014). "Mechanical and tribological properties of Al–7Si–(0–5) Zn alloys." *Mater. Des.,* 63, 159–167.

Alemdag, Y. and Savaşkan, T. (2009). "Mechanical and tribological properties of Al-40Zn-3Cu alloys." *Tribol. Int.*, 42, 176-182.

Alireza, H.A., Frank, A. (2010). "Effect of conventional and rheocasting processes on microstructural characteristics of hypereutectic Al–Si–Cu–Mg alloy with variable Mg content." *J. Mater. Process. Technol.*, 210(5):767-775.

Andrews, J.B., Seneviratne, M.V., Zier, K.P. and Jett, T.R. (1985). "The influence of silicon content on the wear characteristics of hypereutectic Al-Si alloys." *ASME Int. Conf. on wear of materials*, 180-186.

Apelian, D. (2009). *Aluminum Cast Alloys: Enabling Tools for Improved Performance.* North American Die Casting Association (NADCA).

Apelian, D., Shivkumar, S. and Sigworth, G. (1989). "Fundamental Aspects of Heat Treatment of Cast Al-Si-Mg Alloys." *AFS Transactions*, 97, 727-742.

Backerud, L., Chai, G. and Tamminen, J. (1990). Solidification Characteristics of Aluminum Alloys. Vol. 2, Foundry Alloys. The American Foundrymen's Society.

Balu, P.J. (1981). "Interpretations of the friction and wear break-in behavior of metals in sliding contact." *Wear,* 71 (1), 29.

Barwell, F.T. (1957). "Theories of Wear and Their Significance for Engineering Practice, Treatise on material science and technology." Ed., Douglass Scott, Academic Press, 674-681.

Basavakumar, K.G., Mukunda, P.G. and Chakraborty, M. (2007). "Influence of melt treatments on sliding wear behavior of Al-7Si and Al-7Si-2.5Cu cast alloys." *J. Mater. Sci.*, 42, 7882-7893.

Basavakumar, K.G., Mukunda, P.G. and Chakraborty, M. (2008). "Impact toughness in Al-12Si and Al-12Si-3Cu cast alloys - Effect of process variables and microstructure." *Int. J. Imp. Engg.,* 35, 199-205.

Basavakumar, K.G., Mukunda, P.G. and Chakraborty, M. (2008). "Influence of grain refinement and modification on dry sliding wear behavior of Al-12Si and Al-12Si-3Cu cast alloys." *Int. J. Mater. Res*, 99, 900-906.

Basavakumar, K.G., Mukunda, P.G. and Chakraborty, M. (2008). "Influence of grain refinement and modification on microstructure and mechanical properties of Al-7Si and Al-7Si-2.5Cu cast alloys." *Mater. Charact.*, 59, 283-289.

Basavakumar, K.G., Mukunda, P.G. and Chakraborty, M. (2009). "Dry sliding wear behaviour of Al–12Si and Al–12Si–3Cu cast alloys." *Mater. Des*. 30, 1258–1267.

Belov, N.A., Aksenov, A.A. and Eskin, D.G. (2002). *Iron in aluminium alloys – Impurity and alloying element*. Taylor and Francis, London.

Boileau, J.M., Zindel, J.W. and Allison, J.E. (1997). "The effect of solidification time on the mechanical properties in a cast A356-T6 aluminum alloy." *SAE Transactions*, 106(5), 63-74.

Bowden, F.P. and Tabor, D. (1954). *The friction and lubrication of solids.* Clarendon press, Oxford.

Brechet, Y., Embury, J.D., Tao, S., and Luo, L. (1991). "Damage initiation in metal matrix composites." *Acta Metallurgica*, 39(8), 1781-1786.

Brooks, C.R. (1991). "Heat treating of nonferrous alloys, in ASM Handbook." Vol. 4: Heat Treatment, *ASM International,* 1826-2124.

Burwell, J.T. and Strang, C. D. (1952). "On the Empirical Law of Adhesive Wear." J. Appl. Phys. 23, 18.

Byczynski, G.E., Kierkus, W., Northwood, D.O., Penrod, D., Sokolowski, J.H., Esseltine, W. A., Oswald, J. and Thomas, R. (1996). "The Effect of Quench Rate on Mechanical Properties of 319 Aluminum Alloy Castings." *Materials Science Forum*, 217, 783-788.

Caceres, C.H., Svensson, I.L. and Taylor, J.A. (2003). "Strength-ductility behaviour of Al-Si-Cu-Mg casting alloys in T6 temper." *Int. J. Cast. Met. Res.*, 15, 531–543.

Campbell, J. (1991). *Castings*. Burlington-Heinemann, Butterworth.

Casari, D., Fortini, A. and Merlin, M. (2013). "Fracture behaviour of grain refined A356 cast aluminium alloy: tensile and charpy impact specimens." Convegni Nazionale., *IGF XXII*, 1-3, 314-321.

Chandra Sekhar Rao, P.V., Satya Devi, A. and Basavakumar, K.G. (2012). "Influence of Melt Treatments on Dry Sliding Wear Behavior of Hypereutectic Al-15Si-4Cu Cast Alloys." Jordan *J. of Mech. and Ind. Engg.*, 6 (1), 55-61.

Chandrashekharaiah, T.M. and Kori, S.A. (2009). "Effect of grain refinement and modification on the dry sliding wear behaviour of eutectic Al– Si alloys." *Tribol. Int.*, 42, 59– 65.

Chaudhury, S.K. and Apelian, D. (2006). "Fluidized bed heat treatment of cast Al-Si-Cu-Mg alloy." *Metall. Mater. Trans. A*, 37, 2295-2311.

Chen, L.H. and Rigney, D.A. (1985). "Transfer During Unlubricated Sliding Wear of Selected Metal Systems." *Wear*, 105, 47.

Chen, S., Wang, Z., Yi, S. and Jia, S. (1981). "Studies on the modification mechanism of Al-Si alloys with antimony." Jixie Goncheng Xuebao, 17, 68-77.

Chirita, G., Stefanescu, I., Soares, D. and Silva, F.S. (2009). "Influence of vibration on the solidification behavior and tensile properties of an Al-18 wt.% Si alloy." *Mater. Des.*, 30, 1575–1580.

Cibula (1950). "The mechanism of grain refinement of sand castings in Al alloys." *J. Inst. Metals*, 1949-1950, 76, 321-360.

Clarke, J. and Sarkar, A.D. (1981). "Topographical features observed in a scanning electron microscopy study of aluminium alloy surfaces in sliding wear." *Wear*, 69, 1-23.

Collins, D.L.W. (1972). "Discussions of grain refinement in Al alloyed with Ti and B." *Metall. Trans.*, 3, 2290-2292.

Cook, R., Cooper, P.S. and Kearns, M.A. (1996). "Benefits of master alloy melt treatments in the aluminium foundry industry." *TMS Light metals, Ed. Wayne Hale,* 647-654.

Crowell, N. and Shivkumar, S. (1995). "Solution Treatment Effects In Cast Al-Si-Cu Alloys." *AFS Trans.*, 107, 721–726.

Cupini, N.L., Galiza, J.A., Robert, M.H. and Pontes, P.S. (1980). "Ultimate tensile strength of as cast commercial aluminium refined by volatile mould coating process." Solidification Technology in the Foundry and Cast House, Univ. of Warwick, 65-69.

Das, S., Prasad, S.V. and Ramchandran, T.R. (1989). "Microstructure and wear of cast (Al–Si alloy)–graphite composites." *Wear*, 133(1), 173–187.

Dasgupta, R. (1997). "Property Improvement in Al-Si Alloys through Rapid Solidification Processing." *J. Mater. Process. Technol.,* 72, 380-384.

Davies, R. (1953). *Friction and Wear*. Elsevier, Amsterdam.

Davis, J.R. (2001). *Copper and copper alloys*. ASM International, Materials Park, OH.

Djurdjevic, M., Stockwell, T. and Sokolowski, J. (1999). "The effect of strontium on the microstructure of the aluminium-silicon and aluminium-copper eutectics in the 319 aluminium alloy." *Int. J. Cast. Metal. Resea.*, 12, 67-73.

Dobrzanski, L.A., Maniara, R., Krupinski, M. and Sokolowski, J.H. (2007). "The effect of cooling rate on microstructure and mechanical properties of AC AlSi9Cu alloy." *Archives of materials science and engg.,* 24, 51-57.

Drouzy, M. Jacob, S. and Richard, M. (1980). "Interpretation of tensile results by means of quality index and probable yield strength." *AFS Int. Cast Metals Journal*, Vol. 5, 43-50.

Du, X.F., Gao, T., Wu, Y. and Liu, X. (2014). "Effects of copper addition on the in-situ synthesis of SiC particles in Al–Si–Cu system." *Mater. Des*., 63, 194–199.

Dwivedi, D.K. (2001). "Transitions in wear-friction behaviour under dry sliding conditions of cast Al–Si base alloys." *Inst. Eng. (India)*, 82, 69–74.

Dwivedi, D.K. (2004). “Sliding temperature and wear behaviour of cast Al-Si-Mg alloys.” *Mat. Sci. Eng. a-Struct.*, 382, 328-334.

Dwivedi, D.K. (2010). “Adhesive wear behavior of cast aluminium-silicon alloys: Overview.” *Mat. and Des*., 31, 2517-2531.

Elmadagli, M., Perry, T. and Alpas, A.T. (2007). “A parametric study of the relationship between microstructure and wear resistance of Al–Si alloys.” *Wear*, 262, 79–92.

Elsebaie, O., Samuel, A.M. and Samuel, F.H. (2010). “Effects of Sr-modification, iron-based intermetallics and aging treatment on the impact toughness of 356 Al–Si–Mg alloy.” *J. Mater. Sci.*, 46, 3027-3045.

Elsebaie, O., Samuel, A.M, Samuel, F.H. and Doty, H.W. (2014). “Impact toughness of Al-Si-Cu-Mg-Fe cast alloys: Effects of minor additives and ageing conditions.” *Mater. Des*., 60, 496-509.

Eskin, D.G. (2003). “Decomposition of Supersaturated Solid Solutions in Al-Cu-Mg-Si Alloys.” *J. Mater. Sci.*, Vol. 38, 279-290.

Faraji, M. and Katgerman, L. (2009). “Microstructural analysis of modification and grain refinement in a hypoeutectic Al–Si alloy.” *Int. J. Cast Metal Res.*, 22 (1-4), 108-110.

Feurer, U. (1997). “Quality Control of Engineering - Alloys and the Role of Metals Science.” Nieswaag, H. and Schut, J.W. eds., Delft University of Technology, Delft, The Netherlands, 131-145.

Flemings, M.C. (1974). *Solidification processing*, Mc Graw-Hill book company, New York, 341-344.

Garcia-Hinojosa, J.A., Gonzalez, C.R., Gonzalez, G.M. and Houbaert, Y. (2003). “Structure and properties of Al-7Si-Ni and Al-7Si-Cu cast alloys nonmodified and modified with Sr.” *J. of Mater. Proc. Tech.*, 143-144, 306-310.

Glasson, E. L. and Emely, F. E. (1968). “Heterogeneous nucleation in the solidification of aluminium and magnesium alloys.” *The Solidification of metals*, London, The iron and Steel Institute, 1-9.

Grosselle, F., Timelli, G. and Bonollo, F. (2010). “Doe applied to microstructural and mechanical properties of Al-Si-Cu-Mg casting alloys for automotive applications.” *Mater. Sci. Eng. A*, 527, 3536-3545.

Gruzleski, J.E. and Closset, B.M. (1990). “The treatment of liquid aluminium-silicon alloys.” *AFS, Illinois*, 127-143.

Gupta, M. and Ling, S. (1999). “Microstructure and mechanical properties of hypo/ hyper-eutectic Al–Si alloys synthesized using a near-net shape forming technique.” *Journal of Alloys and Compounds,* 287, 284–294.

Halling, J. (1989). *Principle of Tribology*, Great Britain: Macmillan Education Ltd.

Hamid, A.A.A. (1989). “Effect of other elements on the grain refinement of Al by Ti or Ti and B: Part-1 a critical review.”*Metallkde.,* 80, 566-569.

Han, Y.M., Samuel, A.M., Samuel, F.H. and Doty, H.W. (2008). “Dissolution of Al_2Cu phase in nonmodified and Sr modified 319 type alloys.” *Int. J. Cast Met. Res.*, 21, 387-393.

Haque, M.M. and Sharif, A. (2004). “Study on wear properties of aluminium-silicon piston alloy.” *Mat. Proc. Tech.,* 153-154, 833-838.

Hatch, J.E. (Ed.) (1984). *Aluminum: Properties and Physical Metallurgy*, American Society for Metals, Metals Park, OH, U.S.A.

Hatch, J.E. (Ed.) (1988). *Aluminum: Properties and Physical Metallurgy,* 1st Edition, American Society for Metals, Metals Park, OH.

Hegde, S. and Prabhu, K.N. (2008). “Modification of eutectic Silicon in Al-Si alloys.” *J. Mater. Sci.*, 43, 3009-3027.

Hu, X., Jiang, F., Ai, F. and Yan, H. (2012). “Effects of rare earth Er additions on microstructure development and mechanical properties of die-cast ADC12 aluminum alloy.” *J. Alloys Compd*. 538, 21-27.

Jahanmir, S. and Suh, N. P. (1977). “Mechanics of subsurface void nucleation in delamination wear.” *Wear* 44, 17–38.

Ji, S., Watson, D., Fan, Z. and White, M. (2012). "Development of a super ductile die cast Al-Mg-Si alloy." *Mater. Sci. Eng. A,* 556, 824-833.

Jigajinni, S. M., Venkateswarlu, K. and Kori, S. A. (2013). "Effect of a grain refiner cum modifier on mechanical properties of Al-7Si and Al-11Si alloys." *Met. Mater. Int.,* 19, 2, 171-181.

Kashyap, K.T. and Chandrashekar, T. (2001). "Effects and mechanisms of grain refinement in aluminium alloys."*Bull. Mater. Sci.*, 24-4, 345-353.

Kaufman, J.G. and Rooy, E. L. (2004). *Aluminum Alloy Castings: Properties, Processing, and Applications*, ASM International, Materials Park, Ohio, U.S.A.

Kezhun, H., Fuxiao, Y., Dazhi, Z. and Liang, Z. (2011). "Microstructural evoluation of direct chill cast Al-15.5Si-4Cu-1Mg-1Ni-0.5Cr alloy during solution treatment." *China foundry*, 8, 3, 264-268.

Kezhun, H., Fuxiao, Y., Dazhi, Z. and Liang, Z. (2012). "Characterization of precipitates in a hot-deformed hypereutectic Al–Si alloy." *J. Alloys Compd*. 539, 74-81.

Khaled Ragab (2012). "The use of fluidized sand bed as an innovative technique for heat treating aluminium based castings." PhD Thesis, *University of Quebec*, Chicoutimi, Canada.

Kimura, Y. (1981). "Fundamentals of friction and wear of materials." ASM Materials Science Seminar, Pennsylvania.

Kori, S.A. and Chandrashekharaiah, T.M. (2007). "Studies on the dry sliding wear behaviour of hypoeutectic and eutectic Al-Si alloys." *Wear*, 263, 745-755.

Kori, S.A., Murty, B.S. and Chakraborty, M. (2000). "Development of an efficient grain refiner for Al-7Si alloy and its modification with strontium."*Materials Sc. and Engg. A*283, 94-104.

Kori, S.A., Murty, B.S. and Chakraborty, M. (2000). "Development an efficient grain refiner for Al-7Si alloy." *Materials Sc. and Engg. A,* 280, 58-61.

Kragelskii, I.V. (1965). *Friction and Wear*, Butterworths, London.

Krishna Kanth, V., Pramila Bai, B.N. and Biswas, S.K. (1990). "Wear mechanisms in hypoeutectic aluminium-silicon alloys sliding against steel." *Scr. Metall.*, 24, 267-272.

Kumar, R.(1972). "A study of grain size control in aluminium alloys ingots and castings." *The British Foundryman*, 65(2), 56-72.

Li, J.G., Jhang, B.Q, Wang, L., Yang, W.Y. and Ma, H.T. (2002). "Combined effect and its mechanism of Al-3 wt.% Ti-4 wt.% B and Al-10wt.% Sr master alloy on microstructures of Al-Si-Cu alloy." *Materials Sc. and Engg. A,* 328, 169-176.

Li, Z., Samuel, A.M., Samuel, F.H., Ravindran, C. and Valtierra S. (2003). "Effect of Alloying Elements on the Segregation and Dissolution of $CuAl_2$ Phase in Al-Si-Cu 319 Alloys." *J. Mater. Sci.,* 38, 1203-1218.

Li, Z., Samuel, A.M., Samuel, F.H., Ravindran, C., Valtierra, S. and Doty, H.W. (2004). "Parameters controlling the performance of AA319-type alloys Part I. Tensile properties." *Materials Sc. and Engg. A,* 367, 96–110.

Liao, H., Dong, G. and Sun, G. (2007). "Investigation on Influence of sodium- or strontium modification on corrosion resistance of Al-11.7% Si alloy." *J. Mater. Sci.,* 42, 5175–5181.

Liao, H., Sun, Y. and Sun, G. (2002). "Effect of Al-5Ti-1B on the microstructure of near eutectic Al-13Si alloys." *J. Mater. Sci.,* 37, 3489-95.

Liao, H., Sun, Y. and Sun, G. (2002). "Correlation between mechanical properties and the amount of dendritic α-Al phase in as cast near eutectic Al-11.6% Si alloys modified with strontium." *Mater. Sci. Eng., A*335, 62-68.

Liao, H., Zhang, M., Wu, Q., Wang, H. and Sun, G. (2007). "Refinement of eutectic grains by combined addition of strontium and boron in near eutectic Al-Si alloys." *Scripta Materialia*, 57, 1121-1124.

Lim, Y.P. (2009). "Evaluation of Al-5Ti-1B and Al-10Sr in LM6 sand castings." *J. Ach. Mater. Mfg. Engg.,* 34 (1), 71-78.

Lim, S.P. and Ashby, M.F. (1987). "Wear mechanism maps", *Acta. Metall.*, 35(1), 1987, 1-24.

Lozano, D.E., Mercado-Solis, R.D., Perez, A.J., Talamantes, J., Morales, F. and Hernandez-Rodriguez, M.A.L. (2009). "Tribological behaviour of cast hypereutectic Al–Si–Cu alloy subjected to sliding wear." *Wear*, 267, 545–549.

Lozano, J. A., Pena, B. and Suarez (2006). "Effect of the Addition of Refiners and/or Modifiers on the Microstructure of Die Cast AÎ-12SÎ Alloys." *Scripta Materialia*, 54, 943-947.

Lu, T., Wu, J., Pan, Y., Tao, S. and Chen, Y. (2015). "Optimizing the tensile properties of Al-11Si-0.3Mg alloys: Role of Cu addition." *J. Alloys Compd*., 631, 276-282.

Ma, Z., Samuel, E., Mohamed, A.M.A., Samuel, A.M., Samuel, F.H. and Doty, H.W. (2010). "Influence of aging treatments and alloying additives on the hardness of Al–11Si–2.5Cu–Mg alloys." *Mater. Des.,* 31, 3791-3803.

Ma, Z., Samuel, E., Mohamed, A.M.A., Samuel, A.M., Samuel, F.H. and Doty, H.W. (2010). "Parameters controlling the microstructure of Al–11Si–2.5Cu–Mg alloys." *Mater. Des.*, 31 (2), 902-912.

Mahanti, R.K., Lal, K., Sinha, A.N. and Sivaramakrishnan, C.S. (1993). "A Novel Technique for Hyper Eutectic Al-Si Alloy Melt Treatment." *Mater.Trans., J.I.M.*, 34, 1207-1211.

Mandal, A., Murty, B.S. and Chakraborty, M. (2009). "Wear behaviour of near eutectic Al–Si alloy reinforced with in-situ TiB_2 particles." *Materials Sc. and Engg. A.,* 506, 27-33.

Martin, J.W. (1998). *Precipitation hardening*. Oxford, UK, Butterworth-Heinemann. 79-105.

Massalsski, T.B. (1990). *Binary alloy phase diagrams*, ASM International, Ohio, 2nd edition, 225-227.

McCartney, D.G. (1989). "Grain refining of aluminium and its alloys using inoculants." *Int. Mater. Rev.*, 34, 247-260.

Metan, V. and Eigenfeld, K. (2013). ”Controlling mechanical and physical properties of Al-Si alloys by controlling grain size through grain refinement and electromagnetic stirring.” *Eur Phys. J. Spec. Top.*, 220, 139-150.

Meyers, C.W., Hinton, K.H. and Chou, J. (1992). “Toward the optimization of heat treatment in aluminum alloys.” *Mater. Sci. Forum,* 102–104, 75–84.

Miller, W.S., Zhuang, L., Bottema, J., Witterbrood, A.J., Smet, P.D., Hazler, A. and Vieregge, A. (2000). “Recent Development in Aluminium Alloys for the Automotive Industry.” *Mater. Science. Eng. A.,* 280, 37-49.

Mohamed, A.M.A. and Samuel, F.H. (2012), “A Review on the Heat Treatment of Al-Si-Cu/Mg Casting Alloy.” *InTech Science*, 229-246.

Mohamed, A.M.A., Samuel, A.M., Samuel, F.H. and Doty, H.W. (2009). “Influence of additives on the microstructure and tensile properties of near-eutectic Al-10.8%Si cast alloy.”*Mater Des*, 30, 3943-3957.

Moldovan, P. Popescu, G. and Cuhutencu, M. (2006). “The combined effect of modifier and grain refiner AlTiBSr master alloy on microstructure and porosity of aluminum Alloys.” *Mater. Sci. Forum.,*526, 223-228.

Mondolfo, L. F. (1976). *Al alloys- Structure and properties*, Butterworths, London, 249-250.

Morgeneyer, T.F., Starink, M.J., Wang, S.C. and Sinclair, I. (2008). “Quench sensitivity of toughness in an Al alloy: Direct observation and analysis of failure initiation at the precipitate-free zone.” *Acta Materialia,* 56 (12), 2872–2884.

Moustafa, M.A., Samuel, F.H., Doty, H.W. and Valtierra, S. (2002). “Effect of Mg and Cu additions on the microstructural characteristics and tensile properties of Sr-modified Al–Si eutectic alloys.” *Int. J. Cast Metals Res.*, 14, 235–53.

Mulazimoglu, M.H, (1988) . "Electrical Conductivity Studies of Cast Al-Si and Al-Si-Mg alloys. Ph.D. Thesis, McGill University, Montreal, PQ, Canada

Murray, J. (1992). *Alloy Phase Diagrams.* ASM Hand Book. ASM International.

Narayan, S.C., Girish, B.M., Somashekar, D.R., Satish, B.M. and Kamath, R. (1999). "Sliding wear behaviour of zircon particles reinforced ZA-27 alloy composite materials." *Wear,* 224, 89–94.

Nikanorov, S.P., Volkov, M.P., Gurin, V.N., Burenkov, Yu.A., Derkachenko, L.I., Kardashev, B.K., Regel, L.L. and Wilcox, W.R. (2005). "Structural and mechanical properties of Al-Si alloys obtained by fast cooling of a levitated melt." *Materials Sc. and Engg. A,* 390, 63-69.

Okabayashi, K. and Kawamoto, M. (1968). "Influence of silicon content and grain size of primary silicon crystals on the wear of high silicon aluminium alloys." *Bull. of the Univ. of Osaka Perfecture A*, 17, 199-216.

Palazzo, F. (1977). "The Future of Aluminium in the Automotive Industry." *Aluminio*, 46(9), 323-334.

Palta, A., Sun, Y.and Ahlatci, H. (2012). "Effect of copper addition on wear and corrosion behaviour of Mg_2Si particle reinforced composites." *Mater. Des.,*36, 451–458.

Paray, F and Gruzleski, J.E. (1994). "Factors to consider in modification."*AFS Transactions,* 102, 833-842.

Patel, V.P. and Prajapathi, H.R. (2012). "Microstructural and mechanical properties of eutectic Al–Si alloy with grain refined and modified using gravity-die and sand casting." *Int. J. of Eng. Res. and Apps*., 2, 147-150 147.

Pena, B.S, Lozano, J. A. (2006). "Microstructure and mechanical property developments in Al-12Si gravity die castings after Ti and/or Sr additions." *Materials Characterization*, 57, 218-226.

Peng, J. H., Tang, X. L., He, J. T. and Xu, D. Y. (2011). "Effect of heat treatment on microstructure and tensile properties of A356 alloys." *Trans. Non ferrous Met. Soc. China,* 21(9), 1950-1956.

Polmear, I.J. (2006). *Light Alloys: From Traditional Alloys to Nano crystals*, 4th ed., Oxford: Butterworth-Heinemann.

Porter, A.D. and Easterling, K.E. (1981). Phase Transformations in Metals and Alloys, Van Nostrand Reinhold, Berkshire, England.

Pramila Bai, B.N. and Biswas, S.K. (1987). "Characterization of dry sliding wear of Al-Si alloys." *Wear*, 120, 61-74.

Prasad, B.K. (1994). "Structure-property related changes in a hypoeutectic aluminium-silicon alloy induced by solutionizing." *Mat. Trans.*, 35(12). 873-878.

Prasad, B.K, Venkateswarlu, K., Modi, O.P, Jha, A.K., Das, S., Dasgupta, R. and Yegneswaran, A.H. (1998). "Sliding wear behavior of some Al-Si alloys: Role of shape and size of Si particles and test conditions." *Metall. Mater. Trans. A,* 29A, 2747-2752.

Prasada Rao, A.K., Karabi Das, Murty, B.S. and Chakraborty, M. (2004). "Effect of grain refinement on wear properties of Al and Al-7Si alloy." *Wear*, 257, 148-153.

Prasada Rao, A.K., Chakraborty, M., Karabi Das and Murty, B.S. (2006). "Microstructure and wear behavior." *Wear*, 261, 133-139.

Radjai, A., Miwa, K. and Nishio, T. (1998). "An Investigation of the Effects Caused by Electromagnetic Vibrations in a Hypereutectic Al-Si Alloy Melt." *Metall. Mater. Trans. A,* 29A, 1477-1484.

Rigney, D.A. and Glaeser, W.A. (1978). *Book on wear control technology*, American Society of Metals.

Robles Hernándeza, F.C. and Sokolowski, J.H. (2006). "Comparison among chemical and electromagnetic stirring and vibration melt treatments for Al–Si hypereutectic alloys." J. Alloy Compd., 426, 205-212.

Rodriguez, S.H., Goytia-Reyes, R.E., Dwivedi, D.K., Víctor, H., Baltazar, H., Horacio, F.Z., and María, J. and Pérez, L. (2011). "On influence of Ti and Sr on microstructure, mechanical properties and quality index of cast eutectic Al–Si–Mg alloy." *Mater. Des.* 32, 1865–1871.

Rooy, E.L. (1992). *Aluminum and Aluminum Alloys: Chemical Compositions*. ASM Handbook Vol. 15: Castings, ASM International, 1622-1631.

Saheb, N., Laoui, T., Daud, A.R., Harun, M., Radiman, S. and Yahaya, R. (2001). "Influence of Ti additions on wear properties of Al-Si eutectic alloys". *Wear*, 249, 656-662

Samuel, A.M., Gauththier, J. and Samuel, F.H. (1996). "Microstructural aspects of the dissolution and melting of Al_2Cu phase in Al-Si alloys during solution heat treatment." *Metall. Mater. Trans. A,* 27A, 1785-98.

Samuel, A.M. Doty, H.W., Valtierra, S. and Samuel, F.H. (2013). "Defects related to incipient melting in Al–Si–Cu–Mg alloys." *Mater. Des*., 52, 947-956.

Samuel, A.M., Doty, H.W., Valtierra, S. and Samuel, F.H. (2014). "Effect of grain refining and Sr-modification interactions on the impact toughness of Al–Si–Mg cast alloys." *Mater. Des.*, 56, 2014, 264–273.

Samuel, A.M., Garza-Elizondo, G.H., Doty, H.W. and Samuel, F.H. (2015). "Role of modification and melt thermal treatment processes on the microstructure and tensile properties of Al–Si alloys." *Mater. Des.*, 80, 99–108.

Samuel, F.H. (1998). "Incipient melting of $Al_5Mg_8Si_6Cu_2$ and Al_2Cu intermetallics in unmodified and strontium modified Al-Si-Cu-Mg (319) alloys during solution heat treatment." *J. Mater. Sc.* 33, 2283-2297.

Samuel, F.H., Samuel, A.M. and Doty, H.W. (1996). "Factors controlling the type of morphology of Cu containing phases in 319 Al alloy." *AFS Transactions,* 30, 893-901.

Sarkar, A.D (1975). "Wear of aluminium-silicon alloys." *Wear,* 31, 331-343.

Sarakar, A.D. and Clarke, J. (1982). "Wear Characteristics, friction and surface topography observed in the dry sliding of as cast and age hardening Al-Si alloys." *Wear,* 75, 71-75.

Santnam, N. (1983). "Effect of wear debris on wear in rolling-sliding motion." *Wear,* 90(2), 261–267.

Seifeddine, S., Timelli, G. and Svensson, I.L. (2007). "Influence of quench rate on the microstructure and mechanical properties of aluminium alloys A356 and A354." *Int. Foun. Res.*, 2-10.

Shabestari, S.G. and Shahri, F. (2004). "Influences of Modification, Solidification Conditions and Heat Treatment on the Microstructure and Mechanical Properties of A356 Aluminum Alloy." *J. Mater. Sci.*, 39, 2023-2032.

Sharma, R. and Dwivedi, D. K. (2007). "Solutionizing temperature and abrasive wear behavior of cast Al- Si-Mg alloys." *Mater. and Des.*, 28, 975–1981.

Shivkumar, S., Ricci, Jr., Keller, C. and Apelian, D. (1990). "Effect of solution treatment parameters on tensile properties of cast aluminium alloys." *J. Heat Treating.,* 8, 63-70.

Shivnath, R., Senguota, P.K. and Eyre, T.S. (1977). "Wear of aluminium-silicon alloys." *Br. Foundryman*, 70, 349-356.

Sigworth, G.K. (1983). "Theoretical and practical aspects of the modification of Al-Si alloys." *AFS Trans.*, 83, 7-16.

Sigworth, G.K. (2008). "The modification of Al-Si casting alloys: Important practical and theoretical aspects." *Int. J. Metal casting*, 19-40.

Sigworth, G. K. and Kuhn,T. A. (2007). "Grain refinement of aluminium casting alloys", *AFS Transactions*, 67(2), 1-12.

Sjolander, E. and Seifeddine, S. (2010). "Optimisation of solution treatment of cast Al–Si–Cu alloys." *Mater. Des.*, 31, S44-S49.

Sjolander, E. and Seifeddine, S. (2010). "The heat treatment of Al-Si-Cu-Mg casting alloys." *J. Mater. Process Tech.,* 210, 1249-1259.

Smallman, R. E. and Ngan, A. H. W. (2007). *Physical Metallurgy and Advanced Materials*, 7thEdition, Butterworth Heinemann, Boston, 385-404.

Smith, W.F. (1981). *Structure and Properties of Engineering Alloys*, McGraw-Hill, N.Y.

Sokolowski, J.H., Sun, X.C., Byczynski, G., Northwood, D.O., Penrod, D.E., Thomas, R. and Esseltine, A. (1995). "Removal of copper-phase segregation and the subsequent improvement in mechanical properties of cast 319 aluminium alloys by a two-stage solution heat treatment." *J. Mater. Process Tech*., 53, 385-392.

Son, S.K., Takeda, M., Mitome, M., Bando, Y. and Endo, T. (2005). "Precipitation Behaviour of an Al-Cu Alloy during Isothermal Aging at Low Temperatures." *Mater. Letters*, 75, 629-632.

Spada, A.T. (2002). "In Search of Light-Weight Components: Automotive's Cast Aluminium Conversion." *Engineered Casting Solutions,* 4(2), 28-31.

Spittle, A., Keeble, J.M. and Meshhedani, M. A. (1997) "The grain refinement of Al-Si foundry alloys." *TMS light metals,* Ed. Redar Hugles, 795-800.

Srivastava, V.C., Mandal, R.K. and Ojha, S.N. (2004). "Evolution of Microstructure in Spray Formed Al-18%Si Alloy." *Mater. Sci. Eng. A*, 383, 14-20.

Staley, J.T. (1987). "Quench factor analysis of aluminum alloys." *Mater. Sci. Tech.* 3, 923-935.

Stonebrook, E. E., (1960). "Aluminium alloy with silicon content." Mod, Cast., 38, 111-114.

Suh, N.P. (1978). *Proc. Int. Conf. on Fundamentals of tribology*, MIT press, 443.

Sui, Y., Wang Q., Wang G. and Liu T. (2015). "Effects of Sr content on the microstructure and mechanical properties of cast Al–12Si–4Cu–2Ni–0.8Mg alloys." *J. Alloy Compd.,* 622, 572-579.

Tao, L., Jili, W., Ye, P., Shiwen, T. and Yu, C. (2014). "Optimizing the tensile properties of Al–11Si–0.3Mg alloys: Role of Cu addition." *J. Alloys Compd.*, 631,276-282.

Tash, M., Samuel, F.H., Mucciardi, F.and Doty, H.W. (2007). "Effect of metallurgical Parameters on the hardness and microstructural characterization of as-cast and heat treated 356 and 319 Aluminium alloys." *Mater. Sci.. Eng. A,* 443, 185-201.

Torabian, H., Pathak, J.P. and Tiwari, S.N. (1994). "Wear characteristics of Al-Si alloys." *Wear*, 172, 49-58.

Verhoeven, J.D. (1975). *Fundamentals of Physical Metallurgy*, J. Wiley and Sons, New York.

Vijeesh, V. and Narayan Prabhu, K. (2014). “Review of Microstructure Evolution in Hypereutectic Al–Si Alloys and its Effect on Wear Properties” *Trans. Indian Inst. Met.*, 67(1), 1–18.

Wang, E.R, Hui, X.D., Wang, S.S., Zhao, Y.F. and Chen, G.L. (2010). “Improved mechanical properties in cast Al-Si alloys by combined alloying of Fe and Cu.” *Mater. Sci. Eng. A.*, 527, 7878-7884.

Wang, E.R., Hui, X.D. and Chen, G.L. (2011). “Eutectic Al-Si-Cu-Fe-Mn alloys with enhance mechanical properties at room and elevated temperature.” *Mater. Des.*, 32, 4333-434.

Wang, E.R., Hui, X.D. and Chen, G.L. (2013). “Eutectic Al–Si–Cu–Fe–Mn alloys with enhanced mechanical properties at room and elevated temperature.” *Mater. Des*. 47, 857-864.

Wang, G., Bain, X., Wang, W. and Zhang, J. (2003). “Influence of Cu and minor elements on solution treatment of Al-Si-Mg-Cu cast alloys.” *Mater. Lett.*, 57, 4083-4087.

Whisler, N. J. and Kattamis, T. Z. (1972). “Dendritic Coarsening during Solidification.” *Journal of Crystal Growth.* 15, 20-24.

William, D. and Callister Jr. (2004). *Materials Science and Engineering – An introduction*, sixth edition, John Wiley & Sons, Inc.

Wislei, R.O., Daniel, J.M., Leandro, C.P., Ivaldo, L.F., and Amauri, G. (2011). “Microsegregation and microstructure dendritic array affecting the electrochemical behavior of ternary Al-Cu-Si alloys.” *Electrochemical Acta,* 56, 8412-8421.

Wu, C.T., Lee. S.L., Hsieh, M.H. and Lin, J.C. (2010). “Effects of Cu content on microstructure and mechanical properties of Al-14.5Si-0.5Mg alloy.” *Materials Characterization*, 61, 1074-1079.

Xu, C.L., Wang, H. Y., Liu, C. and Jiang, Q.C. (2006). “Growth of Octahedral Primary Silicon in cast hypereutectic Al-Si alloys.” *J. Cryst. Growth,* 291, 2006, 540-547.

Yang, H., Ji, S. and Fan, Z. (2015). “Effect of heat treatment and Fe content on the microstructure and mechanical properties of die cast Al-Si-Cu alloys.” *Mater. Des.*, 823-832.

Yang, Y., Li, Y., Wu, W., Zhao, D.and Liu, X. (2011). “Effect of existing form of alloying elements on the micro hardness of Al-Si-Cu-Ni-Mg piston alloy.” *Mater. Sci. Eng. A.*, 528, 5723-5728.

Yasir, M and Abdul, S. (2014). “Effect of Cu addition on the microstructure and mechanical properties of Al-Si alloy.” *Al-Qadisiya J. for Engg. and Sc*., 7, 4, 366-381.

Yasmin, T., Khalid, A.A. and Haque, M.M. (2004). “Tribological (wear) properties of aluminium-silicon eutectic base alloy under dry sliding condition.” *J. Mater. Process Tech.*, 153-154, 833-83.

Yin, D., Xiao, Q., Chen, Y., Liu, H., Yi, D., Wang, B. and Pan, S. (2016). “Effect of natural ageing and pre-staining on the hardening behaviour and microstructural response during artificial ageing of an Al-Mg-Si-Cu alloy.” Mater. & Des., Volume 95, 329-339.

Ying, Z., Dan-Qing, Y., Wang-Xing, L., Zhi-Sen, R., Qun, Z. and Jung-Hong, Z. (2007). “Transformation of Microstructure after Modification of A390 Alloy.” *Trans. Nonferrous Met. Soc. China*, 17, 413-417.

Zedan, Y. and Alkahtani, S. (2013). “Influence of the microstructure on the machinability of heat-treated Al–10.8% Si cast alloys: Role of copper-rich intermetallics.” *J. Mater. Process Tech*. 213, 167-179.

Zeren, M. (2005). “Effect of copper and silicon content on mechanical properties of Al-Cu-Si-Mg alloys.” *J. Mater. Process Tech.,* 169, 292-29.

Zeren, M. (2007). “The effect of heat treatment on aluminium based piston alloys.” *Mater. Des.*, 28, 2511-2517.

Zeren, M. and Karakulak, E. (2008). “Influence of Ti addition on the microstructure and hardness properties of near eutectic Al-Si alloys.” *J. Alloy Compd.*, 450, 255-259.

Zeren, M. and Karakulak, E. (2009). “A study on hardness and microstructural characteristics of sand cast Al-Si-Cu alloys.” *Bull. Mater. Sci.,* 32/6, 1-4.

Zeren, M., Karakulak, E. and Gumus, S. (2011). “Influence of Cu addition on microstructure and hardness of near-eutectic Al-Si-xCu-alloys.” *Trans. Nonferrous Met. Soc. China*, 21, 1698-1702.

Zhang, D.L. and Zheng, L. (1996). “The quench sensitivity of cast Al–7Wt Pet Si–0.4 Wt pct Mg alloy.” *Metall. Mater. Trans. A,* 27, 3983–3991.

Zhang, X.H., Su G.C., Ju, C.W., Wang, W.C. and Yan, W.L.(2010). “Effect of modification treatment on the microstructure and mechanical properties of Al-0.35%Mg-7.0%Si cast alloy.” *Mater. Des.*, 31, 4408-4413.

Zor, S., Zeren, M., Ozkazanc, H. and Karakulak, E. (2010). “Effect of Cu content on the corrosion of Al-Si eutectic alloys in acidic solutions, Anti-Corros Methods.” *Mater.* 57, 185-191.

Zuo, M., Jiang, K. and Liu, X. (2010). “Refinement of hypereutectic Al–Si alloy by a new Al–Zr–P master alloy.” *J. Alloy Compd.*, 503, 26–30.

Zuo, M., Liu, X. and Sun, Q. (2009). “Effects of Processing Parameters on the Refinement of Primary Si in A390 Alloys with A New Al-Si-P Master Alloy.” *J. Mater. Sci.*, 44, 1952-1958.

Zuo, M., Zhao, D., Teng, X., Geng, H. and Zhang, Z. (2013). “Effect of P and Sr complex modification on Si phase in hypereutectic Al–30Si alloys.” *Mater. Des.*, 47, 857-864.